

Vol. 55, No. 3, pp. 189 – 286, 2011

INTERNATIONAL JOURNAL



BRATISLAVA

Heat-shock protein 70 is associated with the entry of Marek's disease virus into fibroblast

XIAO-JIA WANG

College of Veterinary Medicine, Key Laboratory of Zoonosis of Ministry of Agriculture, China Agricultural University, No. 2, Yuan Ming Yuan West Road, Haidian District, Beijing 100193, P.R. China

Received December 16, 2010; accepted June 27, 2011

Summary. – Literature pertaining to the interactions between Marek's disease virus (MDV) entry-related glycoproteins and corresponding receptors is still limited. Results from a Western blot analysis of cellular proteins for virus receptors and co-immunoprecipitation suggest that heat shock protein 70 (HSP70) is a potential cellular receptor for MDV glycoprotein gH. Plaque inhibition assays confirm the involvement of HSP70 in the early stages of MDV entry into chicken embryo fibroblasts (CEF). The present work supports that HSP70 is implicated in the MDV entry process by binding to gH, and enhances the understanding of multifunctional HSP70 and the MDV infection process.

Keywords: Marek's disease virus (MDV); heat shock protein 70 (HSP70); glycoprotein H; virus entry

Introduction

Herpesviruses express many glycoproteins, various types of cellular receptors and a multipartite entry-fusion system (Campadelli-Fiume *et al.*, 2007; Heldwein and Krummenacher, 2008). Recently, several studies have suggested that glycoprotein gB, expressed by herpes simplex virus 1, a member of alphaherpesviruses, interacts with the heparan sulfate proteoglycan and pair immunoglobulin-like type 2 receptor alpha to facilitate the initial attachment of the virus to the cell surface. The glycoprotein gD then binds to a specific surface receptor, such as nectin-1 or the herpesvirus entry mediator. This interaction alters the conformation of gD and enables the activation of gB and the dimer gH-gL. Finally, the gD-gB-gH-gL complex facilitates the fusion of the viral envelope with the plasma membrane (Maurer *et al.*, 2008; Satoh *et al.*, 2008). In the human cytomegalovirus of betaherpesviruses,

the gH-gL dimer associates with other glycoproteins to form either a gH-gL-gO or a gH-gL-UL128-131 complex, and virus-cell fusion is triggered by interactions between gH-gL and integrins (Parry *et al.*, 2005). In the case of the Epstein-Barr virus of gammaherpesviruses, the fusion of the virus with B lymphocytes requires gB and a 3-component complex of glycoproteins, gH-gL-gp42. Its formation is triggered by interactions between gp42 and MHC class II. However, the fusion of the virus with epithelial cells is impeded by gp42. This process is instead triggered by interactions between gH-gL and integrins alphavbeta6 and/or alphavbeta8 (Chesnokova *et al.*, 2009).

MDV, a cell-associated virus has long been of interest as a model virus, particularly with respect to the pathogenesis and immune control of virus-induced lymphoma in an easily accessible small-animal system. Owing to its biological properties, particularly its ability to induce T-cell lymphoma and its slow growth in cell culture, MDV was long thought to be closely related to Epstein-Barr virus, a member of gammaherpesviruses. Electron-microscopy studies of the MDV genome provided the first evidence that this double-stranded DNA virus possesses repeat structures that are characteristic of alphaherpesviruses, which was confirmed by detailed restriction-enzyme mapping and sequencing, first of individual genes, and, later, of the en-

E-mail: wangxj@cau.edu.cn; fax: +86-10-62732824.

Abbreviations: CEF = chicken embryo fibroblasts; gB = glycoprotein B; gD = glycoprotein D; gH = glycoprotein H; HSP70 = heat shock protein 70; HSP90 = heat shock protein 90; MDV = Marek's disease virus; p.i. = post infection

tire genome (Osterrieder *et al.*, 2006). In addition, unlike the majority of herpesviruses, MDV up-regulates MHC class II cell surface expression in infected cells both *in vitro* and *in vivo* (Nikura *et al.*, 2007). Recent advances in our knowledge of MDV genetics and functional genomics have dramatically increased our understanding of the mechanisms leading to latency and tumor formation. However, a limited amount of work has been conducted investigating the molecular mechanisms involved in MDV entry into host cell.

Glycoprotein gD of MDV lacks functions typically associated with alphaherpesvirus gD homologues (Zelník *et al.*, 1999). It has been hypothesized that the MDV gD homolog is not essential for cell-to-cell spread of MDV but is important for the generation of cell-free infectious MDV from feather follicle epithelium (Anderson *et al.*, 1998). The secreted glycoprotein gC of MDV, one of the primary antigens that triggers a substantial serological response of the immune system, is required for full virulence of MDV and was speculatively considered to be a cellular receptor binding glycoprotein (Tischer *et al.*, 2005). Some envelope and tegument proteins including tegument protein VP22 (Dorange *et al.*, 2002), envelope glycoprotein gE-gI (Schumacher *et al.*, 2001), glycoprotein gB (Schumacher *et al.*, 2000), and glycoprotein gH-gL (Wu *et al.*, 2001) are essentially required for cell-to-cell spread in cultured cells. Literature pertaining to the interactions between MDV glycoproteins and receptors is still limited. Our previous study demonstrated the presence of unidentified protein related to glycoprotein gB, with approximate molecular mass of 90 kDa. In addition, no potential receptor molecules related to gC and gE were identified. The current study focuses on recovery of potential receptor molecules corresponding to the glycoprotein gH in the early stages of MDV entry into fibroblast. The relationship between potential receptor and virus entry is further explored.

Materials and Methods

Virus and cells. Primary CEF were cultured in DMEM supplemented with 10% FCS and were allowed to attach overnight. Cells were then incubated with multi-passage CEF-associated MDV strain RB1B (kindly provided by Prof. Zhi-Zhong Cui at Shandong Agricultural University) for 2 hrs. Following incubation, the virus inoculum on the cells were replaced with DMEM supplemented with 2% FCS, and the cultures were incubated for 5 days to allow for plaque formation. Consistent and uniform plaques were observed and counted using an Olympus microscope, and images were captured using the DP Controller software. Simultaneously, indirect immunofluorescent assay was used to verify plaque formation with mouse anti-pp24 antibody diluted 1:100 (Ding *et al.*, 2008).

Preparation of cell-free MDV. CEF-associated MDV from the passages that contained 2×10^4 PFU were used in this study. Cell-free MDV was extracted from infected CEF cultures according to

the method described in a widely cited report (Lee *et al.*, 2001) and was used immediately.

Preparation of CEF proteins. Monolayers of primary CEF were pelleted at 800 x g for 5 mins and washed twice with Dulbecco's Phosphate-Buffered Saline (Invitrogen). The cells were then lysed by sonication at 4°C for 15 secs. The pellet was collected by centrifugation and resuspended in RSB-NP-40 (1.5 mmol/l MgCl₂, 10 mmol/l tris-HCl, 10 mmol/l NaCl, and 1% Nonidet P-40). Soluble membrane protein extracts were obtained by centrifugation at 12,000 x g for 15 mins at 4°C, and the amount of proteins was determined by BCA protein assay kit (Lin *et al.*, 2007).

Western blot analysis of CEF proteins for virus receptors. Briefly, cellular proteins of primary CEF were subjected to 10% SDS-PAGE and blotting. The blot was blocked overnight at 4°C using a 5% nonfat milk solution in PBS and subsequently washed twice with PBS containing 0.05% Tween 20 (PBST). The blot was then incubated with cell-free MDV freshly extracted from 2×10^4 PFU of cell-associated MDV in PBS with 5% low-fat milk for 6 hrs at 37°C (Das *et al.*, 2009). After being washed three times with PBS, the blot was incubated with polyclonal antibody against glycoprotein gH (kindly provided by Prof. Klaus Osterrieder at Free University of Berlin) for 2 hrs at 37°C. For detection, an HRP conjugated goat anti-rabbit IgG ECL antibody, and ECL substrate were used. The experiment was performed in triplicate.

Western blot analysis of CEF proteins with antibodies to potential receptors. Cellular proteins from CEF infected with 100 PFU of MDV were collected at 20, 40, and 120 mins post infection (p.i.). The blot was incubated with antibodies targeting HSP70, HSP90, CD54, and CD44 (Sigma), and subsequently incubated with a goat anti-rabbit IgG ECL antibody. All experiments were performed in triplicate.

Western blot analysis of co-immunoprecipitated receptor. Briefly, MDV-infected CEF were harvested 20 mins p.i. in PBS-EDTA and then were lysed in pre-chilled RIPA buffer (1 ml/10⁷ cells) for 1 hr at 4°C with rocking, centrifuged for 20 mins at 12,000 x g to remove cell debris and the supernatant was obtained. Protein A agarose beads with pre-clear were added into cell lysate and were incubated at 4°C rocking for 10 mins. After centrifugation at 10,000 x g, the supernatant was incubated with gH or HSP70 antibodies for 3 hrs on a rocker. The mixture was centrifuged at 10,000 x g for 15 secs, then the supernatant was carefully discarded, followed by the washing of beads twice with 1 ml RIPA buffer and then 3 times with 1 ml PBS to remove detergents. Finally, beads were resuspended in 60 µl loading buffer, boiled at 95°C for 5 mins and centrifuged at 10,000 x g for 15 secs. The blot was incubated with anti-gH antibody and subsequently incubated with a goat anti-rabbit IgG ECL.

Plaque inhibition assay. To confirm that the HSP70 molecule is involved in the entry of MDV into CEF, cells were incubated with medium containing a polyclonal antibody against HSP70 (simultaneous tests using HSP90, CD44 and CD54 antibodies were also performed) at concentrations of 50, 25, 5, 1, and 0 µg/ml in the presence of 100 PFU of cell-free MDV at 4°C for 1 hr. The infected cells were subsequently washed three times, after which

fresh medium was added, and the infection was allowed to proceed for 5 days at 37°C. After infection, cells were observed under an inverted microscope for plaque formation, as described earlier. All experiments were performed in triplicate.

HSP70 silencing assay. CEF monolayers were pre-incubated with different concentrations of quercentin (0, 75, 150, and 300 μmol/l) for 6 hrs, washed and then infected with 100 PFU of cell-free MDV for 5 days, after which the plaque inhibition rate was evaluated as described earlier. Alternatively, 200 pmoles of small interfering RNA (siRNA) targeted at HSP70 (Santa Cruz Biotechnology) with Lipofectamine-2000 (Invitrogen) complexes was added to each flask, and then mixed gently by rocking. The cells were incubated at 37°C in a CO₂ incubator for 56 hrs, and then infected with 100 PFU of MDV for 5 days.

Results and Discussion

Western blot analysis of CEF proteins for virus receptors was performed to identify cellular receptor proteins. The results demonstrated the presence of proteins corresponding to glycoprotein gH, with approximate molecular mass of 70 kDa. The result is shown in Fig. 1. Potential receptor protein with molecular weight of 70 kDa was found using cell-associated virus at same time (not shown here). Four candidate molecules, including heat shock proteins 70 and 90 (HSP70 and HSP90), intercellular adhesion molecule 1 (ICAM-1, also known as CD54) and CD44 were considered for further investigation. Heat-shock proteins HSP70 and HSP90 are highly conserved proteins that function as molecular chaperones. In virus biology, HSP70 and HSP90 have been implicated not only in the process of virus entry, but also in post-entry steps; notably, they were discovered to be a part of a receptor complex in monocytic cells involved in the entry of dengue viruses (Chavez-Salinas *et al.*, 2008). Furthermore, HSP90 is a component of the cellular receptor complex of the infectious bursal disease virus (Lin *et al.*, 2007), and HSP70 on Neuro2a cells is a putative receptor for the Japanese encephalitis virus that was targeted in vaccine designs (Ge *et al.*, 2007; Das *et al.*, 2009). Recent evidence has shown that the interaction between HSP70 and viral oncogene Meq plays a significant role in MDV oncogenesis, suggesting that HSP70 may be involved in virus pathogenicity (Zhao *et al.*, 2009). CD54 is an endothelial- and leukocyte-associated trans-membrane protein that has long been known to play a role in stabilizing cell-cell interactions and facilitating leukocyte endothelial transmigration and has been characterized as a site for the cellular entry of human rhinovirus (Bella *et al.*, 1998). The CD44 antigen is a cell-surface glycoprotein involved in cell-cell interactions, cell adhesion and cell migration (Fujisaki *et al.*, 1999).

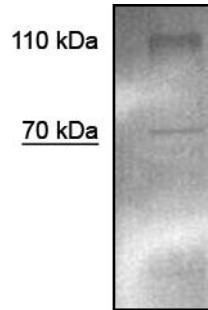


Fig. 1

Western blot analysis of cellular proteins for virus receptors

The blotted CEF proteins were incubated with the virus and the bound virus was detected with an antibody against MDV gH antibody (1: 10,000). A 70-kDa band is seen, showing the possible presence of receptors in CEF corresponding to glycoprotein gH.

To determine whether the expression of candidate molecules increases upon MDV entry, cellular proteins from CEF infected with 100 PFU of MDV were collected at 20, 40, and 120 mins p.i., and Western blot analysis was performed using antibodies targeting HSP70, HSP90, CD54, and CD44. The results observed using HSP70 antibody showed a specific band with a molecular mass of 70 kDa. This was confirmed by the expression of HSP70 in CEF, where its presence was detected at 20–40 mins p.i. Meanwhile, the band nearly disappeared at 120 mins p.i. (Fig. 2). Tests using the other antibodies described did not reveal significant bands, indicating that they are not involved in MDV entry (results not shown). Furthermore, the interaction between the MDV glycoprotein gH and HSP70 in the cell extract was confirmed through a co-immunoprecipitation assay. This experiment clearly showed detectable bands at 110 kDa when gH antibody was used in comparison with normal rabbit serum that was used as a negative control (Fig. 3). Thus, these co-immunoprecipitation experiments provided clear biochemical evidence of interaction between MDV gH and HSP70 in CEF.

To confirm that the HSP70 molecule is involved in the entry of MDV into CEF, plaque inhibition assay was performed. The percentage of plaque inhibition (i.e., the inhibition rate) was normalized to 100 PFU of cell-free MDV, which was assigned a value of 0%. The results showed potent antiviral activity; 50 μg of HSP70 antibody per ml almost completely inhibited the formation of plaques with an inhibition rate of 93 ± 5.2% (Fig. 4a, left panel). The results of the plaque inhibition assay using other antibodies described (including HSP90) up to a concentration of 50 μg/ml yielded different results (Fig. 4a, right panel), suggesting that the observations related to anti-HSP70 were specific.

To further investigate the involvement of HSP70 in the entry of the MDV into CEF, receptor reconstruction concept

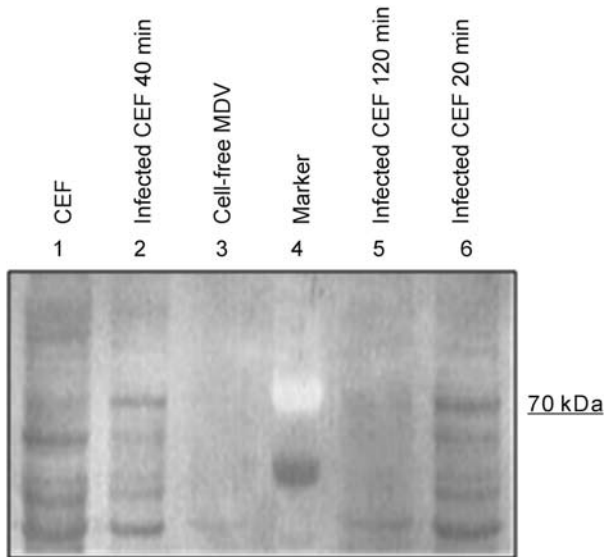


Fig. 2

Western blot analysis of CEF proteins with antibodies to potential receptors

Blotted proteins of MDV-infected CEF (20, 40, and 120 mins p.i.) were detected with an HSP70 antibody, see lanes 6, 2, and 5 in comparison to uninfected CEF (lane 1). Lane 3 shows 100 PFU of CEF-associated MDV; lane 4 is the protein marker.

was implemented by the use of the compound quercetin. Quercetin is known to deplete HSP70 from the cell surface (Das *et al.*, 2009). HSP70 knockdown and treatment with quercetin both reduced hepatitis C virus infectious particle production at nontoxic concentrations (Gonzalez *et al.*, 2009). Our results showed a significant reduction in the number of plaques, with an inhibition rate of $91 \pm 3.6\%$ at a quercetin concentration of $300 \mu\text{mol/l}$ in comparison with control cells infected with MDV but not treated with quercetin (Fig. 4b). Furthermore, HSP70 knockdown assay demonstrated that the HSP70 silencing significantly interfered with the MDV entry into CEF, with an inhibition rate of $72 \pm 2.7\%$ (Fig. 4c). These results proved that HSP70 plays a critical role in the entry of MDV. To confirm that quercetin did not exert toxic effects on CEF, monolayers were exposed to a range of concentrations ($100, 300, 500 \mu\text{mol/l}$) of the compound for 24 hrs, and the cell viability was analyzed by the lactate dehydrogenase assay according to the manufacturer's instructions using a commercial cytotoxicity detection kit (Roche). There was no statistical difference between the viability of the control (untreated) cells and the viability of cells exposed to the quercetin. Quercetin did not exhibit cytotoxic effects at the concentrations tested.

In the present paper, the results of a Western blot analysis of CEF proteins for virus receptors, Western blot analysis of CEF proteins with antibodies to potential receptors, Western blot analysis of co-immunoprecipitated receptor,

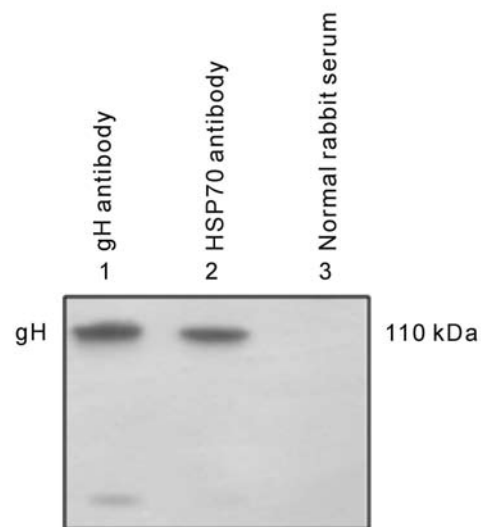


Fig. 3

Western blot analysis of co-immunoprecipitated receptor

Proteins from MDV-infected CEF were incubated with either antibodies against gH (lane 1) or HSP70 (lane 2) or normal rabbit serum (lane 3). The receptor molecules precipitated with corresponding antibodies were released and subjected to Western blot analysis for gH.

and inhibition of virus plaque formation support the conclusion that HSP70 is involved in the MDV entry into CEF. Further studies are necessary to prove the occurrence of a conformational change of HSP70 upon interaction with gH and to demonstrate the involvement of a putative ligand in the interaction of gH and HSP70. Our current research proves that CEF-associated MDV can replicate in the human tumor cell line HeLa and HeLa-associated MDV particles can re-infect CEF cells. HSP70 molecule may be involved in MDV replication in HeLa cells. A related study investigating the entry of oncogenic MDV into HeLa cells is currently in progress.

MDV is a commonly observed virus. The very virulent forms of this virus frequently cause acute explosive outbreaks in chickens, despite the availability of vaccines. Results in the present paper will facilitate the design of new antiviral agents that interfere with the viral entry into target cells once the receptor complex is defined. The work represents the first step in a series of studies of multifunctional HSP70 to enhance our understanding of the MDV infection process.

Acknowledgements. This work was supported by the Foundation for the Authors of National Excellent Doctoral Dissertations of PR China No. 2006079 and by the Chinese Universities Scientific Fund No. 2009JS10. The author thanks Prof. Klaus Osterrieder at the Free University of Berlin and Prof. Zhi-Zhong Cui at the Shandong Agricultural University for invaluable material support.

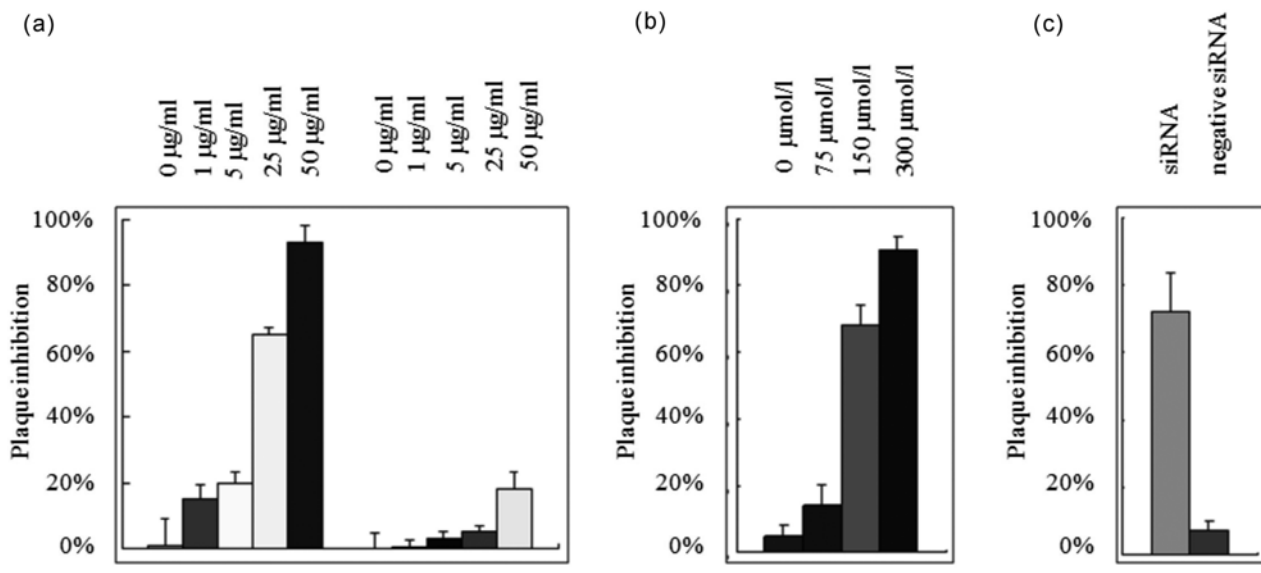


Fig. 4

Inhibition of virus plaque formation with HSP70 antibodies, quercetin and siRNA

(a) To examine the effect of HSP70 (left) and HSP90 (right) antibodies, MDV-infected CEF were incubated on day 1 p.i. with various concentrations of the two antibodies. After washing, fresh medium was added and plaques were counted on day 6 p.i. (b) To examine the effect of HSP70 depletion from the cell surface, CEF were incubated with various concentrations of quercetin for 6 hrs, washed, infected with the virus, supplied with fresh medium and 5 days later observed for plaque formation. (c) The plaque-forming inhibition assay was also used to study the effect of HSP70-siRNA or negative-siRNA treatment on plaque formation.

References

- Anderson AS, Parcells MS, Morgan RW (1998): The glycoprotein D (US6) homolog is not essential for oncogenicity or horizontal transmission of Marek's disease virus. *J. Virol.* 72, 2548–2553.
- Bella J, Kolatkar PR, Marlor CW, Greve JM, Rossmann MG (1998): The structure of the two amino-terminal domains of human ICAM-1 suggests how it functions as a rhinovirus receptor and as an LFA-1 integrin ligand. *Proc. Natl. Acad. Sci. USA* 95, 4140–4145. doi.org/10.1073/pnas.95.8.4140
- Campadelli-Fiume G, Amasio M, Avitabile E, Cerretani A, Forghieri C, Gianni T, Menotti L (2007): The multipartite system that mediates entry of herpes simplex virus into the cell. *Rev. Med. Virol.* 17, 313–326. doi.org/10.1002/rmv.546
- Chavez-Salinas S, Ceballos-Olvera I, Reyes-Del Valle J, Medina F, Del Angel RM (2008): Heat shock effect upon dengue virus replication into U937 cells. *Virus Res.* 138, 111–118. doi.org/10.1016/j.virusres.2008.08.012
- Chesnokova LS, Nishimura SL, Hutt-Fletcher LM (2009): Fusion of epithelial cells by Epstein-Barr virus proteins is triggered by binding of viral glycoproteins gHgL to integrins alphavbeta6 or alphavbeta8. *Proc. Natl. Acad. Sci. USA* 106, 20464–2069. doi.org/10.1073/pnas.0907508106
- Das S, Laxminarayna SV, Chandra N, Ravi V, Desai A (2009): Heat shock protein 70 on Neuro2a cells is a putative receptor for Japanese encephalitis virus. *Virology* 385, 47–57. doi.org/10.1016/j.virol.2008.10.025
- Ding J, Cui Z, Jiang S, Li Y (2008): Study on the structure of heteropolymer pp38/pp24 and its enhancement on the bi-directional promoter upstream of pp38 gene in Marek's disease virus. *Sci. China C Life Sci.* 51, 821–826. doi.org/10.1007/s11427-008-0099-4
- Dorange F, Tischer BK, Vautherot JF, Osterrieder N (2002): Characterization of Marek's disease virus serotype 1 (MDV-1) deletion mutants that lack UL46 to UL49 genes: MDV-1 UL49, encoding VP22, is indispensable for virus growth. *J. Virol.* 76, 1959–1970. doi.org/10.1128/JVI.76.4.1959-1970.2002
- Fujisaki T, Tanaka Y, Fujii K, Mine S, Saito K, Yamada S, Yamashita U, Irimura T, Eto S (1999): CD44 stimulation induces integrin-mediated adhesion of colon cancer cell lines to endothelial cells by up-regulation of integrins and c-Met and activation of integrins. *Cancer Res.* 59, 4427–4434.
- Ge FF, Qiu YF, Yang YW, Chen PY (2007): An hsp70 fusion protein vaccine potentiates the immune response against Japanese encephalitis virus. *Arch. Virol.* 152, 125–135. doi.org/10.1007/s00705-006-0822-z
- Gonzalez O, Fontanes V, Raychaudhuri S, Loo R, Loo J, Arumugam V, Sun R, Dasgupta A, French SW (2009): The heat shock protein inhibitor Quercetin attenuates hepatitis C virus production. *Hepatology* 50, 1756–1764. doi.org/10.1002/hep.23232
- Heldwein EE, Krümmenacher C (2008): Entry of herpesviruses into mammalian cells. *Cell Mol. Life Sci.* 65, 1653–1668. doi.org/10.1007/s00018-008-7570-z

- Lee S, Ohashi K, Sugimoto C, Onuma M (2001): Heparin inhibits plaque formation by cell-free Marek's disease viruses in vitro. *J. Vet. Med. Sci.* 63, 427–432. doi.org/10.1292/jvms.63.427
- Lin TW, Lo CW, Lai SY, Fan RJ, Lo CJ, Chou YM, Thiruvengadam R, Wang AH, Wang MY (2007): Chicken heat shock protein 90 is a component of the putative cellular receptor complex of infectious bursal disease virus. *J. Virol.* 81, 8730–8741. doi.org/10.1128/JVI.00332-07
- Maurer UE, Sodeik B, Grünwald K (2008): Native 3D intermediates of membrane fusion in herpes simplex virus 1 entry. *Proc. Natl. Acad. Sci. USA* 105, 10559–10564. doi.org/10.1073/pnas.0801674105
- Niikura M, Kim T, Hunt HD, Burnside J, Morgan RW, Dodgson JB, Cheng HH (2007): Marek's disease virus up-regulates major histocompatibility complex class II cell surface expression in infected cells. *Virology* 359, 212–219. doi.org/10.1016/j.virol.2006.09.010
- Osterrieder N, Kamil JP, Schumacher D, Tischer BK, Trapp S (2006): Marek's disease virus: from miasma to model. *Nat. Rev. Microbiol.* 4, 283–294. doi.org/10.1038/nrmicro1382
- Parry C, Bell S, Minson T, Browne H (2005): Herpes simplex virus type 1 glycoprotein H binds to alphavbeta3 integrins. *J. Gen. Virol.* 86, 7–10. doi.org/10.1099/vir.0.80567-0
- Satoh T, Arii J, Suenaga T, Wang J, Kogure A, Uehori J, Arase N, Shiratori I, Tanaka S, Kawaguchi Y, Spear PG, Lanier LL, Arase H (2008): PILRalpha is a herpes simplex virus-1 entry coreceptor that associates with glycoprotein B. *Cell* 132, 935–944. doi.org/10.1016/j.cell.2008.01.043
- Schumacher D, Tischer BK, Fuchs W, Osterrieder N (2000): Reconstitution of Marek's disease virus serotype 1 (MDV-1) from DNA cloned as a bacterial artificial chromosome and characterization of a glycoprotein B-negative MDV-1 mutant. *J. Virol.* 74, 11088–11098. doi.org/10.1128/JVI.74.23.11088-11098.2000
- Schumacher D, Tischer BK, Reddy SM, Osterrieder N (2001): Glycoproteins E and I of Marek's disease virus serotype 1 are essential for virus growth in cultured cells. *J. Virol.* 75, 11307–11318. doi.org/10.1128/JVI.75.23.11307-11318.2001
- Tischer BK, Schumacher D, Chabanne-Vautherot D, Zelník V, Vautherot JF, Osterrieder N (2005): High-level expression of Marek's disease virus glycoprotein C is detrimental to virus growth in vitro. *J. Virol.* 79, 5889–5899. doi.org/10.1128/JVI.79.10.5889-5899.2005
- Wu P, Reed WM, Lee LF (2001): Glycoproteins H and L of Marek's disease virus form a hetero-oligomer essential for translocation and cell surface expression. *Arch. Virol.* 146, 983–992. doi.org/10.1007/s007050170130
- Yoshida S, Lee LF, Yanagida N, Nazerian K (1994): Mutational analysis of the proteolytic cleavage site of glycoprotein B (gB) of Marek's disease virus. *Gene* 150, 303–306. [doi.org/10.1016/0378-1119\(94\)90442-1](https://doi.org/10.1016/0378-1119(94)90442-1)
- Zhao Y, Kurian D, Xu H, Petherbridge L, Smith LP, Hunt L, Nair V (2009): Interaction of Marek's disease virus oncoprotein Meq with heat-shock protein 70 in lymphoidtumour cells. *J. Gen. Virol.* 90, 2201–2208. doi.org/10.1099/vir.0.012062-0
- Zelník V, Majerciak V, Szabová D, Geerligs H, Kopáček J, Ross LJ, Pastorek J (1999): Glycoprotein gD of MDV lacks functions typical for alpha-herpesvirus gD homologues. *Acta Virol.* 43, 164–168.

Analysis of antigen epitopes and molecular pathogenic characteristics of the 2009 H1N1 pandemic influenza A virus in China

J.J. ZHOU^{1,2#}, J. TIAN^{1#}, D.Y. FANG^{1,2}, Y. LIANG^{1,2}, H.J. YAN^{1,2}, J.M. ZHOU^{1,2}, H.L. GAO¹, C.Y. FU¹, Y. LIU¹, H.Z. NI³, C.W. KE^{3,*}, L.F. JIANG^{1,2,*}

¹Department of Microbiology, Zhongshan School of Medicine, Sun Yat-sen University, Guangzhou, P.R.China; ²Key Laboratory of Tropical Disease Control (Ministry of Education), Sun Yat-sen University, Guangzhou, P.R. China; ³Microbiology Laboratory, Center for Disease Control and Prevention of Guangdong Province, Guangzhou, P.R. China

Received January 27, 2011; accepted June 27, 2011

Summary. – In order to further predict the epidemic trend and develop vaccines for 2009 H1N1 virus, we monitored its epitopes and molecular pathogenic characteristics during the epidemic process. We also analyzed the similarity of antigenic and genetic characteristics among the novel 2009 H1N1, representative seasonal H1N1 strains, and vaccine strains. 2009 H1N1 isolates had high similarity of hemagglutinin (HA) antigenic sites with H1N1 viruses isolated before 1940 and up to 80.0% similarity with 1918 H1N1. The elderly people born before 1940 have relatively low 2009 H1N1 infection rate, which might be responsible for their previous infection with either 1918 H1N1 virus or an early progeny. Compared to seasonal H1N1 vaccine strains from 1999 to 2010, the HA, neuraminidase (NA), and nucleoprotein (NP) proteins of the isolates had highly conserved CTL epitopes (60.5–65.8%, 69.6–82.6%, and 76.7%, respectively). The seriousness and mortality rate of 2009 H1N1 infections were similar to seasonal influenza, which may be related to the molecular characteristics of low toxicity of 2009 H1N1 and cross-T-cell immunity, due to vaccination or exposure to seasonal H1N1 virus. Some strains of 2009 H1N1 acquired mutations at antigenic and glycosylation sites. It is of particular interest that Haishu/SWL110/10 and Beijing/SE2649/09, isolated after November 2009, gained a new glycosylation site at the position 179 of HA protein, near the RBD. Thus, in the future, vaccination with glycosylated 2009 H1N1 virus may prevent the seasonal epidemic caused by strains with glycosylation site mutation near the receptor binding domain (RBD).

Keywords: antigen epitope; glycosylation site; influenza A virus; 2009 H1N1

Introduction

There have been three global influenza pandemics in the 20th century: the “Spanish flu” caused by 1918 H1N1, the “Asian flu” caused by 1957 H2N2, and the “Hong Kong flu” caused by 1968 H3N2. In 1977, the H1N1 subtype reappeared together with the H3N2 influenza virus; both strains were

relatively prevalent and, until now, had regularly resurfaced as seasonal epidemics (Palese, 2004; Neumann *et al.*, 2009).

In March 2009, a novel influenza A H1N1 virus appeared and spread rapidly to many countries and regions worldwide, developing into a global influenza pandemic (<http://www.who.int>). Studies showed that the 2009 H1N1 was a novel swine-origin recombinant virus, of which 6 genes (PB2, PB1, PA, HA, NP, and NS) were similar to triple-reassortant swine influenza viruses circulating in pigs in North America, while two genes (NA and M) were similar to the versions seen in influenza strains common to Eurasian swine (Novel Swine-Origin Influenza A (H1N1) Virus Investigation Team, 2009; Smith *et al.*, 2009; Trifonov *et al.*, 2009).

To date, this novel cross-species transmitted virus – 2009 H1N1 – has been epidemic in the population for more than

*Corresponding authors. E-mail: Jianglf@mail.sysu.edu.cn; kecw1965@yahoo.com.cn; fax: +8620-87332368. [#]These authors contributed equally to this work.

Abbreviations: CTL = cytotoxic T-lymphocyte; GD06 = Guangdong/06/09; HA = hemagglutinin; NA = neuraminidase; NP = nucleoprotein; RBD = receptor binding domain

a year. Following steps will play an important role in the prediction of its epidemic trend and in vaccine development: 1) analysis of the similarity of antigenic and genetic characteristics among the 2009 H1N1 strains, representative seasonal H1N1 strains from different periods, and vaccine strains; 2) monitoring of its antigenic and molecular pathogenic characteristics in the epidemic process; and 3) improving the understanding of its genetic and variation rules. We therefore isolated, identified and analyzed the genome sequence of the 2009 H1N1 pandemic strains in Guangdong, China. We also analyzed the epitope, genetic and evolutionary characteristics of 2009 H1N1 isolated in China, in other countries and regions, seasonal H1N1 virus strains from different periods, and vaccine strains.

Materials and Methods

Isolation and identification of the virus. Nasopharyngeal swabs of influenza-suspected patients were taken and analyzed using a novel H1N1 real-time PCR kit (Daan, China). Since this study was part of the public health program implemented by the Ministry of Health of the People's Republic of China, there was no need of ethical approval. Positive samples were inoculated into MDCK cells and maintained in Opti-MEM minimum essential medium (Invitrogen, USA) containing 0.5 mg/ml trypsin. The cells were cultured at 35°C in the presence of 5% CO₂. After significant cytopathic effect occurred, hemagglutination and hemagglutination inhibition identification tests were performed (Kendal *et al.*, 1982).

Nucleotide sequencing. The RNeasy mini kit (Qiagen, Germany) was used to extract viral RNA from cell culture supernatants. Reverse transcription of viral cDNA was performed using random primers (N6). Forty-five pairs of primers were designed to amplify the entire viral genome (Hoffmann *et al.*, 2001; Wang and Lee, 2009; Novel Swine-Origin Influenza A (H1N1) Virus Investigation Team, 2009). A gel extraction kit (Omega, USA) was used for the isolation of amplified PCR products. Sequencing was performed using an ABI sequencer (Applied Biosystems, USA).

Analyses of genetic and evolutionary characteristics. Protein sequences of 2009 H1N1 from different countries and regions obtained before August 2010 were downloaded from the influenza virus genome database; protein sequences of representative seasonal H1N1 strains from different periods, vaccine strains and swine influenza viruses were also downloaded. Clustal X and Mega 4.0 software were used to analyze variations in glycosylation sites, virulence-related sites, and antigenic sites of H1N1 viruses. 3D-JIGSAW was used for online prediction of 3D structures of viral HA and NA proteins.

Epitope prediction and analysis of conservation. The sequences of H1N1 viruses were input into the Immune Epitope Database (IEDB) and the artificial neural network (ANN) method was used for online prediction of HLA Class I epitope (CTL epitope). The unit of CTL epitope prediction measurement was IC50 (nM); lower IC50

values represented higher affinity. Typically, IC50 values of less than 50 nM represented high binding capacity, 50–500 nM represented moderate binding capacity, and higher than 500 nM represented low binding capacity (<http://tools.immuneepitope.org>).

CTL epitopes that were both nine amino acids long and had IC50 values of less than 500 were selected. The epitope conservancy analysis tool was used to analyze cross-conserved CTL epitopes among the 2009 H1N1 viruses, representative seasonal H1N1 strains and vaccine strains. Some T-cell epitopes show allele promiscuity; epitopes with up to two altered amino acids out of any 9-mer frame can still bind with the allele groove of HLA and the original T-cell receptor (Lichterfeld *et al.*, 2006). When evaluating the epitope conservation, we set the sequence similarity to ≥7/9 (77.8%).

Results

Virus isolation and sequencing

135 strains of 2009 H1N1 were isolated during the epidemic period. These isolates were named according to the isolation dates. We selected the representative epidemic strains from the different periods and sequenced the full-length genome of 2009 H1N1. The sequences have been submitted to GenBank, with accession numbers of GQ244322-GQ244325, GQ223434-GQ223447, HM780470-HM780492, and HQ011407-HQ011424.

Analysis of glycosylation sites

The HA protein of 2009 H1N1 virus had seven glycosylation sites at positions 28, 40, 104, 293, 304, 498, and 557. These glycosylation sites were located on the lateral side of HA molecule, with no glycosylation sites near the RBD. However, further analysis indicated that Haishu/SWL110/10 and Beijing/SE2649/09 from China, and Russia/178/09, Russia/180/09 and Salekhard/01/09 from other regions, isolated after November 2009, gained a novel glycosylation site at the position 179 near the RBD. Interestingly, the 1918 H1N1 virus also has no glycosylation sites near the RBD, but the seasonal H1N1 viruses gained in the epidemic process at least two glycosylation sites near the RBD of their HAs, such as at positions 144 and 179 in Marton/43, at positions 142, 172, and 177 in Denver/1/57, and at positions 142 and 177 in Guangzhou/506/06 (Fig. 1).

The NA protein of 2009 H1N1 virus had seven glycosylation sites at positions 50, 58, 63, 68, 88, 146, and 235. The strains isolated in China have no mutation at the glycosylation sites. However, Rome/623/09, Texas/45103737/09, and Texas/45071344/09 isolated in other regions after September 2009 had a new glycosylation site at the position 44. We also

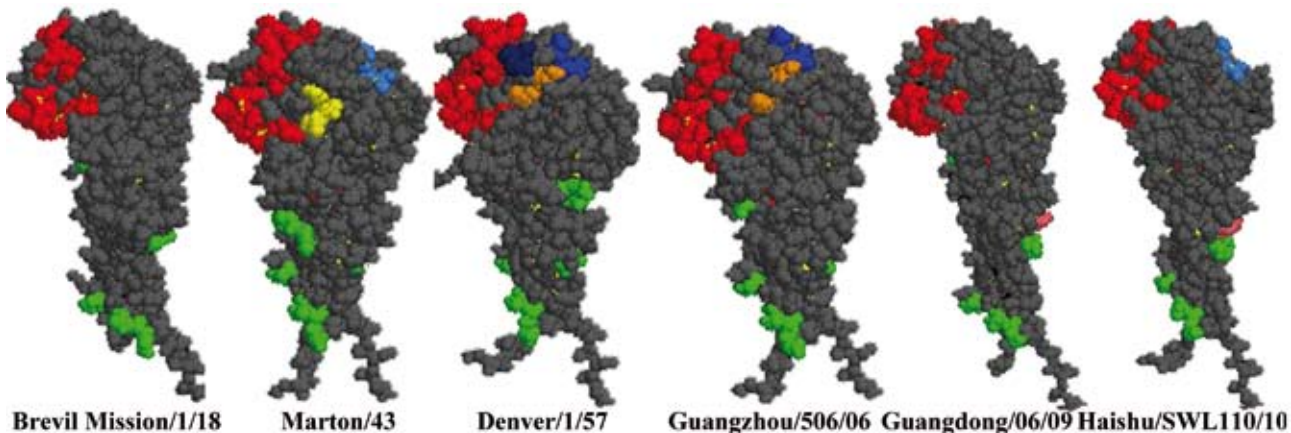


Fig. 1

Analysis of glycosylation sites of H1N1 influenza A virus HA protein

The receptor binding domains (RBD) of the HA protein are shown in red. Glycosylation sites on the side and the stem of HA protein are shown in green. Marton/43 has two new glycosylation sites at the position 144 (yellow), and the position 179 (sky blue) near the RBD of the head of HA protein. Denver/1/57 has three new glycosylation sites, at positions 142 (gold), 172 (dark blue) and 177 (blue) near the RBD. Guangzhou/506/06 had two glycosylation sites, at position 142 (gold), and at position 177 (blue) near the RBD. Apart from a novel glycosylation site at position 293 (pink), the 2009 H1N1 strains, such as Guangdong/06/09, had the same glycosylation sites as Brevil Mission/1/18, and no glycosylation sites were found near the RBD. However, several 2009 H1N1 viruses isolated after November 2009 (Haishu/SWL110/10, etc), had a new glycosylation site at position 179 (skyblue) near the RBD of the head of the HA protein.

found that 1918 H1N1 has no glycosylation site at the position 44, but seasonal H1N1 viruses isolated after 1933 gained a glycosylation site at the position 44 in the epidemic process.

Analysis of antigenic sites

X-ray crystal diffraction and monoclonal antibody analysis showed that the head of the H1N1 HA protein contained five antigenic sites: Cb (residues 78–83), Sa (residues 128–129, 156–160, and 162–167), Sb (residues 187–198), Ca1 (residues 169–173, 206–208, and 238–240), and Ca2 (residues 140–145 and 224–225) (H3 numbering) (Brownlee and Fodor, 2001). Analysis of antigenic sites showed that some 2009 H1N1 isolates had mutations at antigenic sites of the HA protein. These variations were primarily random mutations, but at two sites a variation trend was identified: at the Ca1 site, a Ser206Thr mutation was found in most epidemic strains, and at the Ca2 site, a Asp to Glu/Gly mutation of residue 225 was identified. These variations were minor and mainly restricted to changes of a single amino acid at a single antigenic site. However, there were several strains, which exhibited two or more mutated sites, such as the amino acid variations at Cb, Sa and Ca1 sites in Beijing/SE2649/09, and the amino acid variations at Cb, Ca1 and Ca2 sites in Zhejiang-Yiwu/11/09. Further, in several of these isolated strains, two amino acid mutations were found at the same antigenic site, such as the mutations of residues 78 and 81 at the Cb site in Zhejiang-Yiwu/11/09. The NA protein contains antigenic sites at residues 153, 197–199, 328–336,

339–347, 367–370, 400–403, and 431–434 (N2 numbering) (Colman *et al.*, 1983). The variation of NA antigenic sites of 2009 H1N1 strains was lower than observed in the HA protein. From 95 strains isolated from China, only 5 isolated strains, such as Guangdong/2361/09, showed mutations of one amino acid residue (Table 1).

A/Guangdong/06/09 (abbreviated as GD06), an early isolate from Guangdong, China, was used as a representative strain and compared with four seasonal H1N1 vaccine strains recommended by the WHO (BJ/262/95, NC/20/99, SI/3/06 and BS/59/07) in years 1999 to 2010. The results showed that the similarities between the antigenic sites of the HA proteins of GD06 and the four seasonal vaccine strains listed above were only 44.0%, 50.0%, 50.0%, and 50.0%, respectively. GD06 showed only 44–52% antigen similarity with representative seasonal H1N1 strains from 1940 and later. But it had a high degree of similarity of antigenic sites with Henry/36 (68.0%) and strains from before 1940, especially with antigenic sites of Brevil Mission/1/18 of the 1918 pandemic strain (80.0%). The similarity of NA antigenic sites between GD06, representative seasonal H1N1 strains, and vaccine strains resembled that observed for the HA protein (Table 2).

Prediction of CTL epitopes and analysis of conservation

CTL epitopes of H1N1 were restricted by HLA class I alleles. In this study, we used six HLA class I supertype alleles (A0101, A0201, A0301, A2402, B0702, and B4403) that are

Table 1. Analysis of the antigenic variation of HA and NA proteins of 2009 H1N1 pandemic influenza A virus in China

2009 H1N1 isolates	HA protein												NA protein				
	Cb		Sa		Sb			Ca1		Ca2		197-199		328-336	367-370	400-403	
	78	81	158	165	188	191	198	172	206	208	238	225	198	329	370	400	401
California/07/09	L	A	G	S	S	Q	A	K	S	R	E	D	D	N	S	I	N
Guangdong/06/09	-	-	-	-	-	-	-	-	T	-	-	-	-	-	-	-	-
Beijing/SE2649/09	F	S	-	N	-	-	-	-	T	-	-	-	-	-	-	-	-
Zhejiang-Yiwu/11/09	F	S	-	-	-	-	-	-	T	-	-	G	-	-	-	-	-
Jiangyin/68/09	-	T	-	-	-	-	-	-	T	-	-	-	-	-	-	-	-
Haishu/SWL110/10	-	-	-	N	-	-	-	-	T	-	-	-	-	-	-	-	-
Nanjing/1/10	-	-	E	-	-	-	-	-	T	-	-	G	-	-	-	-	-
Chengdu/18/09	-	-	-	-	-	R	-	-	T	-	-	-	-	-	-	-	-
Guangdong/1252/09	-	-	-	-	-	-	V	-	T	-	-	-	-	-	-	-	-
Nanjing/1/09	-	-	-	-	-	-	-	-	-	K	-	-	-	-	-	-	-
Guangdong/2221/09	-	-	-	-	-	-	-	-	T	-	-	E	-	-	-	-	-
Lishui/02w/09	F	S	-	-	-	-	-	-	T	-	-	-	-	-	-	-	-
Hangzhou/1/09	F	S	-	-	-	-	-	-	T	-	-	-	-	-	-	-	-
Changsha/78/09	-	-	-	-	-	-	-	-	T	-	-	E	-	-	-	-	-
Hunan-Kaifu/SWL4142/09	-	-	-	-	N	-	-	-	T	-	-	-	-	-	-	-	-
Dongcheng/SWL45/09	-	-	-	-	-	-	-	-	R	-	-	-	-	-	-	-	-
Chengdu/04/09	-	-	-	-	-	-	-	-	-	-	K	-	-	-	-	-	-
Guangdong/2361/09	-	-	-	-	-	-	-	-	T	-	-	-	-	-	L	-	-
Jiangsu/1/09	-	-	-	-	-	-	-	-	-	-	-	-	I	-	-	-	-
Guangdong/1105/09	-	-	-	-	-	-	-	-	-	-	-	-	-	-	-	H	-
Guangdong/1202/09	-	-	-	-	-	-	-	-	-	-	-	-	-	-	T	-	-
Nanjing/3/09	-	-	-	-	-	-	-	-	-	-	-	G	-	-	-	-	-

The antigenic sites of 2009 H1N1 strains isolated in China were analyzed and compared to the strain California/07/09 (2009 pandemic vaccine strain). Identical amino acid residues in the antigenic sites are indicated by “-”.

Table 2. The amino acid homology and antigenic similarity of HA and NA proteins between GD06 and H1N1 representative strains from different periods and vaccine strains

H1N1 isolates	GD06 HA amino acid homology	GD06 HA antigenic similarity						GD06 NA amino acid homology	GD06 NA Antigenic similarity						
		Cb	Sa	Sb	Ca1	Ca2	Total (%)		197	328	339	367	400	431	Total (%)
		153	199	336	347	370	403	434							
California/07/09	99.1	6	13	12	10	8	49/50(98.0)	99.8	1	3	9	9	4	4	34/34 (100)
Brevig Mission/1/18	83.7	5	12	10	9	5	40/50(80.0)	87.2	1	3	8	9	3	2	30/34(88.2)
PR/8/34	81.1	2	8	7	7	4	28/50(56.0)	83.5	1	3	7	6	3	1	24/34(70.6)
Henry/36	82.3	3	10	8	8	5	34/50(68.0)	84	1	3	7	6	3	1	25/34(73.5)
Weiss/43	80.6	2	6	5	8	5	26/50(52.0)	82.5	0	2	6	6	3	1	21/34(61.8)
FM/1/47	80.2	2	8	4	7	4	25/50(50.0)	84.0	1	2	6	6	3	1	22/34(64.7)
Denver/1/57	79.1	2	7	3	6	5	23/50(46.0)	83.4	1	2	6	4	3	1	19/34(55.9)
New Jersey/8/76	90.6	4	12	11	9	5	41/50(82.0)	82.3	1	3	5	8	4	1	25/34(73.5)
USSR/90/77	79.3	2	8	3	7	3	23/50(46.0)	83.4	1	2	6	4	3	1	19/34(55.9)
Taiwan/01/86	79.5	2	9	4	7	3	25/50(50.0)	83.4	1	2	6	5	3	1	21/34(61.8)
BJ/262/95	79.5	2	7	3	7	3	22/50(44.0)	81.4	1	3	6	4	1	1	19/34(55.9)
NC/20/99	79.4	2	8	4	7	4	25/50(50.0)	81.4	1	3	6	4	1	2	20/34(58.8)
SI/3/06	79.3	2	8	4	7	4	25/50(50.0)	80.7	1	3	6	4	1	2	20/34(58.8)
BS/59/07	78.9	2	8	4	7	4	25/50(50.0)	80.9	1	3	6	5	1	2	21/34(61.8)
swine/Iowa/15/30	85.3	4	12	11	9	5	41/50(82.0)	87.6	1	3	7	9	4	2	30/34(88.2)
swine/Indiana/P12439/00	94.9	5	12	12	10	7	46/50(92.0)	/	/	/	/	/	/	/	
swine/Belgium/1/83	81.3	4	11	10	7	1	33/50(66.0)	92.5	1	3	8	9	3	2	30/34(88.2)

The HA protein has five antigenic sites, including 50 amino acid residues. The NA protein has seven antigenic sites, including 34 amino acid residues. Numbers before “/” show the total number of identical amino acid residues between GD06 and H1N1 representative strains.

Table 3. The analysis of the conservation of HLA Class I restricted epitopes of HA, NA, and NP proteins between GD06 and H1N1 representative strains from different periods and vaccine strains

H1N1 isolates	HA										NA										NP									
	A 01	A 02	A 03	A 24	B 07	B 44	Total	Conser- vation (%)	A 01	A 02	A 03	A 24	B 07	B 44	Total	Conser- vation (%)	A 01	A 02	A 03	A 24	B 07	B 44	Total	Conser- vation (%)						
	01	01	01	02	02	03			01	01	01	02	02	03			01	01	01	02	02	03								
GD06	4	16	9	2	4	3	38		2	8	4	2	6	1	23		2	10	9	1	6	2	30							
California/ 07/09	4	16	9	2	4	3	38(38)	100	2	8	4	2	6	1	23(23)	100	2	10	9	1	6	2	30(30)	100						
Brevig Mis- sion/1/18	1	19	5	1	5	2	33(31)	81.6	2	11	5	0	5	0	23(18)	78.3	2	10	6	1	7	2	28(27)	90.0						
PR/8/34	2	15	6	1	7	2	33(24)	63.2	1	7	6	0	5	1	20(15)	65.2	2	10	7	3	7	2	31(27)	90.0						
Weiss/43	2	17	5	1	5	2	32(25)	65.8	3	9	4	0	3	2	21(13)	56.5	2	10	8	3	7	2	32(30)	100						
FM/1/47	1	16	6	1	4	3	31(26)	68.4	3	8	2	0	4	1	18(11)	47.8	2	9	7	3	6	2	29(26)	86.7						
Denver/1/57	3	15	5	1	7	3	34(23)	60.5	3	8	5	1	5	1	23(18)	78.3	3	11	8	4	6	2	34(31)	100						
New Jersey/ 8/76	2	16	6	1	5	2	32(32)	84.2	2	14	6	1	4	1	28(19)	82.6	2	10	9	2	6	2	31(31)	100						
USSR/90/77	1	17	4	1	4	3	30(26)	68.4	4	10	5	0	5	1	25(18)	78.3	3	10	6	4	6	2	31(27)	90.0						
Taiwan/01/86	2	17	3	1	4	4	31(26)	68.4	2	9	5	0	5	1	22(16)	69.6	2	9	5	4	6	2	28(24)	80.0						
BJ/262/95	3	17	3	1	4	4	32(23)	60.5	3	8	6	0	4	1	22(19)	82.6	2	9	5	3	6	2	27(23)	76.7						
NC/20/99	2	17	4	1	4	4	32(24)	63.2	3	10	6	0	4	0	23(18)	78.3	2	8	5	3	6	2	26(23)	76.7						
SI/3/06	3	17	4	1	5	5	35(25)	65.8	3	10	6	0	3	0	22(16)	69.6	/	/	/	/	/	/	/							
BS/59/07	2	17	4	1	4	5	33(24)	63.2	3	11	8	0	4	0	26(18)	78.3	/	/	/	/	/	/	/							
Taiwan/ 71720/07	2	17	4	1	4	5	33(23)	60.5	3	11	8	0	4	1	27(19)	82.6	2	8	5	3	6	2	26(23)	76.7						

Numbers in bold represent the total of CTL epitopes restricted by the selected "supertype" HLA of H1N1 isolates. Numbers in () are CTL epitopes restricted by the HLA supertype of H1N1 isolates also conserved in GD06. Conservation (%) represents the percentage of conserved CTL epitopes from the total number of CTL epitopes in GD06.

estimated to cover 99% of the population (de Groot and Berzofsky, 2004). The results showed that the number of CTL epitopes restricted by these six supertype alleles in HA, NA, and NP proteins of GD06 were 38, 23, and 30, respectively, of which the A0201 allele restricted the most. When compared to the 2009 H1N1 vaccine strain California/07/09, the GD06 epitopes showed 100% conservation.

Compared with seasonal H1N1 isolates from different periods, the conservation of GD06 NP CTL epitope was the highest (76.7–100%); the conservation of the HA CTL epitope was 60.5–84.2%; and the conservation of NA CTL epitope was comparatively low (47.8–82.6%). NP, HA, and NA CTL epitopes of GD06 shared the highest similarity with the New Jersey/08/76 of the classical swine H1N1 isolated from human, with similarities of 100%, 84.2%, and 82.6%, respectively. NP, HA, and NA CTL epitopes of GD06 were also highly similar to Brevil Mission/1/18, with similarities of 90.0%, 81.6%, and 78.3%, respectively (Table 3).

When compared to the vaccine strains (BJ/262/95, NC/20/99, SI/3/06, and BS/59/07), the conservation of CTL epitopes of the HA protein in GD06 was 60.5–65.8%, includ-

ing 23 commonly conserved epitopes. Additionally, GD06 had two conserved epitopes in the HA protein: YPKLSKSYI, which was not conserved in BJ/262/95 but was conserved in the other three strains analyzed; and FYKNLILWLV, which was only conserved in SI/3/06. The conservation of the NA CTL epitopes was 69.6–82.6%, including 16 commonly conserved epitopes. In addition, GD06 has three conserved epitopes in the NA protein: NSDTVGWSW and WPDGAELPF were not conservative in SI/3/06, but conservative in the other three strains analyzed; and AELPFTIDK, only conservative in BJ/262/95. Because the NP protein sequence of SI/3/06 and BS/59/07 was not available, we selected Taiwan/71720/07 from the same period for comparison. GD06 had 23 common epitopes with two vaccine strains and Taiwan/71720/07 with the conservation of 76.7% (Table 4).

Discussion

T-cell epitopes (HLA class I and II epitopes) play an important role in the immunological response to the in-

Table 4. The HLA Class I epitope peptides of GD06 also conserved in the seasonal H1N1 vaccine strains (BJ/262/95, NC/20/99, SI/3/06, and BS/59/07)

HLA Class Allele	HA conserved epitopes	NA conserved epitopes	NP conserved epitopes
A0101	WTGMVDGKY ***	VSFNQNLEY ** NSDTVGWSW *	CTELKLSDY ** HSNLNDATY **
A0201	TVLEKNVTV *** VLWGIHHPS * RMNYYWTLV * FQNIHPITI * AIDEITNKV * KMNTQFTAV *** FLDIWTYNA *** WTYNAELLV *** TLDYHDSNV ** YQILAIYST *** QILAIYSTV *** ILAIYSTVA *** TVASSLVLV ** SLGAISFWM ***	LQIGNIISI *** ITYENNTWV ** NTWVNQTYV * AIYSKDNSV * LMSCPIGEV * CVNGSCFTV ** FSFKYGNVG **	KLSDYDGRL * RLIQNSITI ** GMDPRMCSL *** FLARSALIL *** CLPACVYGL ** IMDSNTLEL * FQGRGVFEL *** KLLQNSQVV *
A0301	KLRLATGLR * RIYQILAIY *	VSGWAIYSK * KIFRIEKKGK **	LMQGSTLPR *** AMELIRMIK * RMCNILKGK *** ILRGSVAAHK *** SLVGIDDPFK **
A2402	FYKNLIWLV * IYSTVASSL***	IWISHSIQL * VWIGRTKSI**	IFLARSALI **
B0702	YPKLSKSYI * LPFQNIHPI * VPSIQSRGL **	EPFISCPL ** SPLCERTFF ** VPSPYNSRF * GPDNGAVAV *** WPDGAELPF ***	DPKKTGGPI *** LPFERATVM * LPRRSGAAG *** NPAHKSQLV *** NPIVPSFDM ***
B4403	KEVLVLWGI ** QEGRMNYYW *** LENERTLDY **	AELPFTIDK ***	EEIRRVWRQ ** AEIEDLIFL **

YPKLSKSYI was not conservative in the HA of BJ/262/95 but conservative in the HAs of other three strains; FYKNLIWLV was only conservative in the HA of SI/3/06. NSDTVGWSW and WPDGAELPF were not conservative in the NA of SI/3/06 but conservative in the NAs of other three strains; AELPFTIDK was only conservative in the NA of BJ/262/95. *** showed 100% (9/9) conservation, ** 88.9% (8/9) conservation, * 77.8% (7/9) conservation.

fluenza virus. In particular, the HLA class I epitope (CTL epitope) can activate CD8⁺ T-cells and is involved in both virus clearance and disease recovery (Boon *et al.*, 2004; Kreijtz *et al.*, 2007). When compared to seasonal H1N1 vaccine strains from 1999 to 2010, the GD06 antigenic sites of HA and NA proteins showed 44.0–50.0% and 55.9–61.8% similarity, respectively. However, CTL epitopes of HA and NA proteins were highly conserved (60.5–65.8% and 69.6–82.6%, respectively) when compared to vaccine strains. The CTL epitopes of the NP protein were 76.7% conserved. Thus the cross-T-cell immunity, acquired due to the vaccination or exposure to seasonal H1N1 virus, may alleviate the disease progress of 2009 H1N1. The severity and mortality of 2009 H1N1

infections were similar to seasonal influenza (Uyeki, 2009; Cowling *et al.*, 2010). This epidemic feature was related to the low-pathogenic molecular characteristics of the 2009 H1N1 virus, and might also be associated with conserved T-cell epitope-induced cross-cell immunity after the infection with seasonal H1N1 viruses or vaccination.

Antibodies against the HA protein of the influenza virus can neutralize infectivity of the virus and, therefore, play an important role in the protection against viral infections (Skehel and Wiley, 2000). The antigenic sites of the HA protein of 2009 H1N1 viruses were highly similar to H1N1 viruses isolated before 1940, in particular to the 1918 H1N1 virus (up to 80.0% similarity). Apart from the HA antigenic similarity, the glycosylation sites of the 2009 pandemic H1N1 virus were

very similar to the 1918 H1N1 virus, with no glycosylation sites near the RBD of the HA protein. Antibodies against the 1918 H1N1 virus showed good cross-neutralization of the 2009 H1N1 (Krause *et al.*, 2010; Manicassamy *et al.*, 2010). The high titer of cross-protective antibodies in people born before 1940, who are likely to have been previously infected with either 1918 H1N1 virus or an early progeny, might be responsible for their relatively low 2009 H1N1 infection rate.

Pandemic strain of influenza virus can evade the host immune response through the mutation of antigenic sites, enabling them to develop into seasonal epidemics. However, viral protein glycosylation, particularly the glycosylation near the RBD, can lead to an antigenic drift and escape from neutralizing antibodies against the virus by shielding antigenic sites. Thus, evasion of antibodies by glycosylation represents another mechanism for the development of seasonal flu from pandemic infections (Wang *et al.*, 2009; Cohen, 2010; Xu *et al.*, 2010). During the epidemic process of 2009 H1N1, some strains acquired mutations at antigenic sites; however, the variation of these sites was small, typically caused by the mutation of single amino acid at a single antigenic site. But it should be noted that several 2009 H1N1 strains had obvious variation at the glycosylation sites. Rome/623/09, Texas/45071344/09, and Texas/45103737/09, isolated after September 2009, gained new glycosylation site at the position 44 of the NA protein, the same as seasonal H1N1 viruses. It is of particular interest that Haishu/SWL110/10, Beijing/SE2649/09, Russia/178/09, Russia/180/09, and Salekhard/01/09, isolated after November 2009, gained a new glycosylation site at the position 179 of the HA protein near the RBD. Critically, the anti-serum against 2009 H1N1 California/04/09 cannot neutralize the infectivity of mutated strains with glycosylation at the position 179 of HA (Settembre *et al.*, 2010; Wei *et al.*, 2010). This trend of resistance through glycosylation should be monitored closely to avoid a seasonal epidemic of 2009 H1N1. Studies have shown that antibody prepared by immunization of mice using HA proteins glycosylated near the RBD of 2009 H1N1 can bind to the HA protein with or without glycosylation (Wei *et al.*, 2010). Thus, in the future strategy of vaccine development, vaccination with glycosylated 2009 H1N1 virus may prevent the seasonal epidemic caused by mutated strains with glycosylation near the RBD.

Acknowledgments. This study was supported by the Science and Technology Project of Guangdong province (Grant No. 2009B020600001), the Natural Science Foundation of Guangdong province (Grant No. 8451008901000445), the National Natural Science Foundation of China (Grant No. 81071367), and the special fund of Sun Yat-sen University (Grant No. 09ykpy82).

References

- Boon ACM, de Mutsert G, van Baarle D, Smith DJ, Lapedes AS, Fouchier RAM, Sint Nicolaas K, Osterhaus ADME, Rimmelzwaan GF (2004): Recognition of Homo- and Hetero-subtypic Variants of Influenza A Viruses by Human CD8+ T Lymphocytes. *J. Immunol.* 172, 2453–2460.
- Brownlee GG, Fodor E (2001): The predicted antigenicity of the haemagglutinin of the 1918 Spanish influenza pandemic suggests an avian origin. *Phil. Trans. R. Soc. Lond. B.* 356, 1871–1876. doi.org/10.1098/rstb.2001.1001
- Cohen J (2010): Swine flu pandemic. What's old is new: 1918 virus matches 2009 H1N1 strain. *Science* 327, 1563–1564. doi.org/10.1126/science.327.5973.1563
- Colman PM, Varghese JN, Laver WG (1983): Structure of the catalytic and antigenic sites in influenza virus neuraminidase. *Nature* 303, 41–44. doi.org/10.1038/303041a0
- Cowling BJ, Chan KH, Fang VJ, Lau LLH, So HC, Fung ROP, Ma ESK, Kwong ASK, Chan CW, Tsui WWS (2010): Comparative epidemiology of pandemic and seasonal influenza A in households. *N. Engl. J. Med.* 362, 2175–2184. doi.org/10.1056/NEJMoa0911530
- de Groot AS, Berzofsky JA (2004): From genome to vaccine – new immunoinformatics tools for vaccine design. *Methods* 34, 425–428. doi.org/10.1016/j.ymeth.2004.06.004
- Hoffmann E, Stech J, Guan Y, Webster RG, Perez DR (2001): Universal primer set for the full-length amplification of all influenza A viruses. *Arch. Virol.* 146, 2275–2289. doi.org/10.1007/s007050170002
- Kendal AP, Pereira MS, Skehel J (1982): Concepts and procedures for laboratory-based influenza surveillance. Geneva: World Health Organization.
- Krause JC, Tumpey TM, Huffman CJ, McGraw PA, Pearce MB, Tsibane T, Hai R, Basler CF, Crowe JE, Jr. (2010): Naturally occurring human monoclonal antibodies neutralize both 1918 and 2009 pandemic influenza A (H1N1) viruses. *J. Virol.* 84, 3127–3130. doi.org/10.1128/JVI.02184-09
- Kreijtz JH, Bodewes R, van Amerongen G, Kuiken T, Fouchier RA, Osterhaus AD, Rimmelzwaan GF (2007): Primary influenza A virus infection induces cross-protective immunity against a lethal infection with a heterosubtypic virus strain in mice. *Vaccine* 25, 612–620. doi.org/10.1016/j.vaccine.2006.08.036
- Lichterfeld M, Williams KL, Mui SK, Shah SS, Mothe BR, Sette A, Kim A, Johnston MN, Burgett N, Frahm N (2006): T cell receptor cross-recognition of an HIV-1 CD8+ T cell epitope presented by closely related alleles from the HLA-A3 superfamily. *Int. Immunol.* 18, 1179–1188. doi.org/10.1093/intimm/dxl052
- Manicassamy B, Medina RA, Hai R, Tsibane T, Stertz S, Nistal-Villán E, Palese P, Basler CF, García-Sastre A (2010): Protection of mice against lethal challenge with 2009 H1N1 influenza A virus by 1918-like and classical swine H1N1 based vaccines. *PloS Pathog.* 6, 1–14. doi.org/10.1371/journal.ppat.1000745
- Neumann G, Noda T, Kawaoka Y (2009): Emergence and pandemic potential of swine-origin H1N1 influenza virus. *Nature* 459, 931–939. doi.org/10.1038/nature08157

- Novel Swine-Origin Influenza A (H1N1) Virus Investigation Team (2009): Emergence of a novel swine-origin influenza A (H1N1) virus in humans. *N. Engl. J. Med.* 360, 2605–2615. doi.org/10.1056/NEJMoa0903810
- Palese P (2004): Influenza: old and new threats. *Nat. Med.* 10 (Suppl. 1), S82–S87. doi.org/10.1038/nm1141
- Settembre EC, Dormitzer PR, Rappuoli R (2010): H1N1: can a pandemic cycle be broken? *Sci. Transl. Med.* 2, 24ps14.
- Skehel JJ, Wiley DC (2000): Receptor binding and membrane fusion in virus entry: The influenza hemagglutinin. *Annu. Rev. Biochem.* 69, 531–569. doi.org/10.1146/annurev.biochem.69.1.531
- Smith GJD, Vijaykrishna D, Bahl J, Lycett SJ, Worobey M, Pybus OG, Ma SK, Cheung CL, Raghwanji J, Bhatt S (2009): Origins and evolutionary genomics of the 2009 swine-origin H1N1 influenza A epidemic. *Nature* 459, 1122–1125. doi.org/10.1038/nature08182
- Trifonov V, Khiabanian H, Rabadian R (2009): Geographic dependence, surveillance, and origins of the 2009 influenza A (H1N1) virus. *N. Engl. J. Med.* 361, 115–119. doi.org/10.1056/NEJMmp0904572
- Uyeki TM (2010): 2009 H1N1 virus transmission and outbreaks. *N. Engl. J. Med.* 362, 2221–2223. doi.org/10.1056/NEJMMe1004468
- Wang CC, Chen JR, Tseng YC, Hsu CH, Hung YF, Chen SW, Chen CM, Khoo KH, Cheng TJ, Cheng YSE (2009): Glycans on influenza hemagglutinin affect receptor binding and immune response. *Proc. Natl. Acad. Sci.* 106, 18137–18142. doi.org/10.1073/pnas.0909696106
- Wang L, Lee CW (2009): Sequencing and mutational analysis of the non-coding regions of influenza A virus. *Vet. Microbiol.* 135, 239–247. doi.org/10.1016/j.vetmic.2008.09.067
- Wei CJ, Boyington JC, Dai K, Houser KV, Pearce MB, Kong WP, Yang ZY, Tumpey TM, Nabel GJ (2010): Cross-neutralization of 1918 and 2009 influenza viruses: Role of glycans in viral evolution and vaccine design. *Sci. Transl. Med.* 2, 24ra21.
- Xu R, Ekiert DC, Krause JC, Hai R, Crowe JE, Jr., Wilson IA (2010): Structural basis of preexisting immunity to the 2009 H1N1 pandemic influenza virus. *Science* 328, 357–360. doi.org/10.1126/science.1186430

Horizontal gene transfer in herpesviruses identified by using support vector machine

M. FU¹, R. DENG², J. WANG², X. WANG^{2*}

¹Bioengineering and food science department, Guangdong University of Technology, Guangzhou, P.R. China; ²State Key Laboratory of Biocontrol, School of Life Science, Sun Yat-Sen (Zhongshan) University, Guangzhou, P.R. China

Received December 21, 2010; accepted July 22, 2011

Summary. – Horizontal gene transfer (HGT) is the probable origin of new genes. Identification of HGT-introduced genes would be helpful to the understanding of the genome evolution and the function prediction of new genes. In this study, a method using support vector machine (SVM) was used to distinguish horizontally transferred genes and non-horizontally transferred genes of mammalian herpesviruses based on the atypical composition identification, with accuracy higher than 95% within a reasonable length of time by using just a common PC. This identified 302 putative horizontally transferred genes, 171 genes being identified for the first time. Although most putative transferred genes are of unknown function, many genes have been discovered or predicted to encode glycoproteins or membrane proteins.

Keywords: horizontal gene transfer; identification; herpesvirus

Introduction

HGT is one of the main mechanisms contributing to microbial genome evolution (Ochman *et al.*, 2000; Shackelton and Holmes, 2004), allowing rapid diversification and adaptation. It is also an important resource of new genes. Many “captured” new genes are biased to antibiotic resistance and pathogenicity-related function (Nakamura *et al.*, 2004; Willms *et al.*, 2006). Identification of genes introduced by HGT is important for the study of the genome evolution and the function prediction of new genes. In Lawrence and Ochman’s studies (Lawrence and Ochman, 1997, 1998), three parameters, χ^2 of codon usage, the codon adaptation index CAI, and various indices of GC content, were used to evaluate HGT in *Escherichia coli*. In our previous paper, a novel method based on the frequencies of oligonucleotides was

used to discover horizontally transferred genes in herpesvirus (Fu *et al.*, 2008). Here we present another novel method that exploits genomic composition to discover putative horizontally transferred genes in herpesviruses.

The herpesviruses are a group of large DNA viruses, which infect members of all groups of vertebrates, as well as some invertebrates. Herpesviruses have been typically classified into three subfamilies based upon biological and molecular characteristics. To date, eight discrete human herpesviruses have been described, each causing a characteristic disease. Herpesviruses have large genomes. One of them, cyprinid herpesvirus 3, has the largest genome, with approximately 300 kb of DNA encoding about one hundred and sixty genes. Among the proteins they encode, many have been distinguished to have essential viral functions, such as in genome replication and capsid assembly, or are being involved in direct interaction with the host, effecting immune evasion, cell proliferation, and apoptosis control. Many of these proteins are likely to have been acquired from the host to mimic or block normal cellular functions (Moore *et al.*, 1996; Alcami and Koszinowski, 2000; McFadden and Murphy, 2000). Identification and analysis of such “acquired” viral genes may lead to better understanding of the origin and evolution of these transferred genes and to

*Corresponding author. E-mail: wxz@mail.sysu.edu.cn; fax: +8620-84113964.

Abbreviations: COGs = cluster of orthologous groups; GCR = G protein-coupled receptor; HGT = horizontal gene transfer; SVM = support vector machine

the development of therapeutic strategies to combat persistent viral infections.

Materials and Methods

General description. Each genome has a characteristic “signature”, such as codon biases, short oligonucleotide composition and others, which is relatively constant throughout the genome (Mrazek and Karlin, 1999; Garcia-Vallvé *et al.*, 2000, 2003). Genes transferred from foreign organisms would retain the characteristic signature of its origin for a relatively long time (Lawrence and Ochman, 1997; Nakamura *et al.*, 2004). Hence, transferred genes can be detected on the basis of the signature difference between donor and receptor. This paper describes a distinct method that uses SVM to distinguish between transferred

and non-transferred genes. SVM was trained using the signature of conserved mammalian herpesvirus genes as the features of the receptor, and that of conserved mammalian genes as the features of the donor. The method includes following steps: (1) collecting datasets, (2) generalizing the compositional features, and (3) training the SVM program and detecting the horizontally transferred genes.

Collection of datasets. Gene sequences of 33 mammalian herpesvirus genomes (Table 1) and the full-length gene sequences of four mammals (human, bovine, mouse and rat) were downloaded from Genbank. The conserved proteins were determined using the Tatusov method that was used to identify clusters of orthologous groups (COGs) in NCBI (Tatusov *et al.*, 1997, 2003). COGs of proteins were recognized by an all-against-all BLASP similarity search (Altschul *et al.*, 1997) among the 33 complete genomes. Herpesvirus genes were classified into COGs based on the protein sequence

Table 1. List of mammalian herpesvirus genomic sequences

Subfamily	Genus	Virus name	Acc. No.	ORFs	Abbre-viation	Length (kb)
<i>Alpha-herpesvirinae</i>	<i>Simplexvirus</i>	Cercopithecine herpesvirus 1	NC_004812	75	CeHV-1	157
		Cercopithecine herpesvirus 2	NC_006560	75	CeHV-2	151
		Human herpesvirus 1	NC_001806	77	HHV-1	152
		Human herpesvirus 2	NC_001798	77	HHV-2	155
	<i>Varcellovirus</i>	Bovine herpesvirus 1	NC_001847	73	BoHV-1	135
		Bovine herpesvirus 5	NC_005261	73	BoHV-5	138
		Cercopithecine herpesvirus 9	NC_002686	72	CeHV-9	124
		Equid herpesvirus 1	NC_001491	80	EHV-1	150
		Equid herpesvirus 4	NC_001844	79	EHV-4	146
		Human herpesvirus 3 (strain Dumas)	NC_001348	73	HHV-3	125
		Suid herpesvirus 1	NC_006151	77	SuHV-1	143
<i>Beta-herpesvirinae</i>	<i>Cytomegalovirus</i>	Cercopithecine herpesvirus 8	NC_006150	223	CeHV-8	221
		Human cytomegalovirus	NC_001347	151	HCMV	230
		Human herpesvirus 5 strain Merlin	NC_006273	165	HHV-5	236
		Pongine herpesvirus 4	NC_003521	165	PoHV-4	241
	<i>Muromegalovirus</i>	Murid herpesvirus 1	NC_004065	161	MuHV-1	230
		Murid herpesvirus 2	NC_002512	167	MuHV-2	230
	<i>Roseolovirus</i>	Human herpesvirus 6	NC_001664	123	HHV-6	159
		Human herpesvirus 6B	NC_000898	104	HHV-6B	162
		Human herpesvirus 7	NC_001716	86	HHV-7	153
	Unclassified	Tupaiid herpesvirus 1	NC_002794	158	TuHV-1	196
<i>Gamma-herpesvirinae</i>	<i>Lymphocryptovirus</i>	Callitrichine herpesvirus 3	NC_004367	72	CalHV-3	150
		Cercopithecine herpesvirus 15	NC_006146	80	CeHV-15	171
		Human herpesvirus 4	NC_001345	94	HHV-4	172
		Alcelaphine herpesvirus 1	NC_002531	71	AlHV-1	131
		Bovine herpesvirus 4	NC_002665	79	BoHV-4	109
	<i>Rhadinovirus</i>	Cercopithecine herpesvirus 17	NC_003401	89	CeHV-17	134
		Equid herpesvirus 2	NC_001650	79	EHV-2	184
		Human herpesvirus 8	NC_003409	82	HHV-8	138
		Murid herpesvirus 4	NC_001826	81	MuHV-4	119
		Saimiriine herpesvirus 2	NC_001350	76	SaHV-2	113
Unclassified		Ateline herpesvirus 3	NC_001987	73	AtHV-3	108
		Macaca fuscata rhadinovirus	NC_007016	171	MFRV	131

similarity. Homology was determined by the significance of the BLAST hit and by the length of the maximal scoring pair alignment in the BLASTP search. Two proteins were deemed homologous if bidirectional BLASTP hits (score ≥ 50) produced alignments that covered at least 50% of the query sequence with e-value $\leq 10^{-4}$. Given pairwise hits among herpesvirus proteins, COGs were defined by single-linkage clustering. 20 groups of proteins (660 genes, listed in Table 2) that were conserved in 33 herpesviruses were used as the dataset of non-transferred genes. The same number of mammalian conserved genes identified with the same method was used as the dataset of transferred genes for module training. All genes, excluding the 660 conserved genes in herpesviruses, were used as the test dataset, and the same number of genes from the four mammals (other than the 660 conserved genes) were selected and used as the negative control dataset.

Generalization of compositional features. The compositional feature vector for any given DNA sequence over a set of templates $\pi = \{\pi_1, \pi_2, \dots, \pi_q\}$ is denoted as $\Phi(s) = (p_1, p_2, \dots, p_q)$; here π_i is k-mer oligonucleotide template $\alpha_1\alpha_2\dots\alpha_k$, p_i is the frequency of template π_i in sequence. Instead of using the absolute template frequencies, we normalize these frequencies over the expected template frequencies, which can be derived from the single nucleotide composition:

$$P = \frac{p(\alpha_1\alpha_2\dots\alpha_k)}{\prod_{j=1}^k p(\alpha_j)}$$

where $p(\alpha_1\alpha_2\dots\alpha_k)$ is the frequency of template $\alpha_1\alpha_2\dots\alpha_k$, $p(\alpha_j)$ is the frequency of the j^{th} nucleotide of the template $\alpha_1\alpha_2\dots\alpha_k$. So every gene is depicted by a 4^k dimension vector.

Training of the svm_learn.exe in the SVMlight and discrimination of the transferred genes by svm_classify.exe in SVMlight. SVMlight (Joachims, 1998), including svm_learn.exe and svm_classify.exe, is an implementation of SVMs in C. SVM is a new pattern-recognition method based on recent advances in statistical learning theory. Given two sets of training data points in a high-dimensional input space, the objective of the SVM method is to learn a function that will take the value of +1 in the region, where the positive data points are concentrated, and the value of -1, where the negative points are concentrated. The function to be learned is modeled as a hyperplane in a transformed space (=feature space), and hyperplane parameters are estimated so that its margin with respect to the training data is maximized.

The compositional features calculated from the training datasets were used to train the learning module svm_learn.exe with the linear kernel function and cost factor 1. The ideal output of positive data and negative data were set to +1 and -1, respectively. The training result was used as a classifier input file for the classify module svm_classify.exe to discriminate between transferred and non-transferred genes in the test dataset. The negative control dataset was used to test the accuracy of discrimination.

Table 2. List of herpesvirus conserved gene families

Acc. No. (HHV-1)	Gene name (HHV-1)	Function ^a	Functional class ^b
GI:9629382	UL2	uracil-DNA glycosylase	Nuc
GI:9629385	UL5	component of DNA helicase-primase complex	Rep
GI:9629386	UL6	minor capsid protein	Str
GI:9629387	UL7	unknown	Unk
GI:9629390	UL10	virion glycoprotein M	Gly
GI:9629392	UL12	deoxyribonuclease	Nuc
GI:9629393	UL13	protein kinase	Oth
GI:9629398	UL18	capsid protein	Str
GI:9629402	UL22	virion glycoprotein H	Gly
GI:9629404	UL24	unknown	Unk
GI:9629405	UL25	capsid associated tegument protein	Str
GI:9629406	UL26	protease	Str
GI:9629408	UL27	virion glycoprotein B	Gly
GI:9629409	UL28	DNA packaging	Str
GI:9629412	UL31	unknown	Unk
GI:9629413	UL32	virion protein	Str
GI:9629420	UL39	ribonucleotide reductase large subunit	Nuc
GI:9629432	UL50	deoxyuridine triphosphatase	Rep
GI:9629434	UL52	component of DNA helicase-primase complex	Rep
GI:9629436	UL54	immediate early protein	Trf

^aFunction as derived from GenBank annotations. ^bFunctional classes: Rep (replication), Nuc (nucleotide metabolism and DNA repair), Str (structural), Trf (transcription), Gly (glycoprotein), Oth (other), Unk (unknown).

Table 3. The accuracy (%) of discrimination based on SVM

	k=2		k=3		k=4	
	T ^a	F ^b	T ^a	F ^b	T ^a	F ^b
human	96.7	3.3	94.4	5.6	94.0	6.0
mouse	95.8	4.2	94.6	5.4	95.2	4.8
rat	96.1	3.9	95.8	4.2	95.1	4.9
bovine	94.6	5.4	94.8	5.2	94.1	5.9
average	95.8		94.9		94.6	

^aT: correct discrimination; ^bF: incorrect discrimination.

Results

Datasets and their composition features

The k-mer oligonucleotide frequencies of the 660 conserved genes in herpesviruses and the 660 conserved genes in the four mammals were used as the positive dataset and the negative dataset (non-transferred genes and transferred genes), respectively. The frequencies of 2721 genes other than the conserved genes in herpesviruses were taken as the test dataset, and those of 1143 genes other than the conserved genes for every mammal were taken as the negative control dataset (the maximum number of the bovine full length genes other than the conserved genes in the database was 1143, so the same number of other mammalian genes was used). The number of data for every gene was dependent on the number of the nucleotides in the template, which was 4^k in k-mer oligonucleotide frequency.

Training of the learning module and discrimination for the transferred genes

The output of each training procedure was a classifier file, which was then used for the classify module to discriminate the test data. Using this new method, altogether 302 genes in herpesviruses (length ≥ 500 bp) were detected as putative transferred genes (Table 4), among which 266 were from Gammaherpesviruses, 32 from Betaherpesviruses, and 4 from Alphaherpesviruses, implying that gene acquisition in Gammaherpesvirus was more active than in the other two groups, which agreed with Holzerlandt's results (Holzerlandt *et al.*, 2002) and our previous conclusion (Fu *et al.*, 2008). Although most putative transferred genes are of unknown function, many genes have been discovered or predicted as encoding glycoproteins or membrane proteins.

Discrimination accuracy

The result of transferred gene discrimination (shown in Table 3) indicated that discrimination accuracy reached more than 90% when normalized frequencies of k-mer oligonucleotide ($k = 2, 3$, or 4) were taken as the compositional feature vectors to quantify the genes. Comparative evaluation of different methods for quantifying genes demonstrated that using dinucleotides as a template already has yielded the best discrimination result, which only required to process 4^2 data for every gene, computer resource affordable using even a general private computer.

Table 4. Horizontally transferred genes predicted by the method based on SVM

Abbreviation	Gene name	Description ^a	Acc. No. (Gi)	Length (bp)
CeHV-8	rh31 rh31*	similar to human cytomegalovirus UL13	GI:51556491	1307
CeHV-8	rh167*		GI:51556622	503
CeHV-8	rh224		GI:51556677	617
HCMV	UL122	IE2; immediate-early transcriptional regulator;	GI:28373220	3401
HCMV	UL123	IE1; immediate-early transcriptional regulator;	GI:9625811	1759
HHV-5	UL122*	IE2; immediate-early transcriptional regulator;	GI:52139286	3401
HHV-5	UL123*	IE1; immediate-early transcriptional regulator;	GI:52139287	1761
PoHV-4	tegument protein UL71	similar to HSV-1 UL51	GI:20026662	1121
PoHV-4	immediate-early transcriptional regulator UL122	IE2	GI:20026703	3521
PoHV-4	immediate-early transcriptional regulator UL123	IE1	GI:20026704	1806
PoHV-4	glycoprotein US6*	inhibits TAP-mediated peptide translocation; US6 family	GI:20026737	578
PoHV-4	US19	contains multiple hydrophobic regions; US12 family	GI:20026750	818
PoHV-4	US34*		GI:20026763	509
CalHV-3	ORF6*	similar to EBV BILF1; glycoprotein gp64; GCR (Paulsen <i>et al.</i> , 2005)	GI:24943096	917
CalHV-3	ORF19	similar to EBV BDLF2	GI:24943110	1175

Table 4 continued

CalHV-3	ORF21	similar to EBV BDLF4	GI:24943112	635
CalHV-3	ORF32*	similar to EBV BBLF3; helicase-primase complex	GI:24943123	602
CalHV-3	ORF41	similar to EBV BRRF1	GI:24943132	911
CalHV-3	C3		GI:24943136	2569
CalHV-3	C4*		GI:24943157	764
CeHV-15	BCRF1*	similar to Epstein-Barr virus BCRF1; viral interleukin-10 (Rivailler et al., 2002)	GI:51518017	533
CeHV-15	EBNA-LP	similar to Epstein-Barr virus EBNA-LP	GI:51518018	18102
CeHV-15	BHRF1*	similar to Epstein-Barr virus BHRF1; bcl-2 homologue (Rivailler et al., 2002)	GI:51518020	575
CeHV-15	BFRF1	similar to Epstein-Barr virus BFRF1; tegument (Rivailler et al., 2002)	GI:51518023	989
CeHV-15	BFRF2	similar to Epstein-Barr virus BFRF2	GI:51518024	1811
CeHV-15	BFRF3	similar to Epstein-Barr virus BFRF3; capsid protein (Rivailler et al., 2002)	GI:51518094	512
CeHV-15	BaRF1*	similar to Epstein-Barr virus BaRF1; Ribonucleotide reductase (Rivailler et al., 2002)	GI:51518029	908
CeHV-15	BMRF1*	similar to Epstein-Barr virus BMRF1; dsDNA binding protein	GI:51518030	1214
CeHV-15	BMRF2	similar to Epstein-Barr virus BMRF2; Membrane protein (Rivailler et al., 2002)	GI:51518031	1073
CeHV-15	BSRF1*	similar to Epstein-Barr virus BSRF1; tegument	GI:51518034	665
CeHV-15	EBNA-3A*	similar to Epstein-Barr virus EBNA-3A; latent infection nuclear proteins important for Epstein-Barr virus (EBV)-induced B-cell immortalization and the immune response to EBV infection. (Jiang et al., 2000)	GI:51518092	2912
CeHV-15	EBNA-3B*	similar to Epstein-Barr virus EBNA-3B; latent infection nuclear proteins important for Epstein-Barr virus (EBV)-induced B-cell immortalization and the immune response to EBV infection. (Jiang et al., 2000)	GI:51518091	2867
CeHV-15	BZLF2	similar to Epstein-Barr virus BZLF2; Glycoprotein, gp42	GI:51518040	665
CeHV-15	BZLF1*	similar to Epstein-Barr virus BZLF1; Transactivator (Rivailler et al., 2002)	GI:51518041	1096
CeHV-15	BRLF1*	similar to Epstein-Barr virus BRLF1; Transactivator (Rivailler et al., 2002)	GI:51518042	1808
CeHV-15	BRRF1*	similar to Epstein-Barr virus BRRF1	GI:51518043	929
CeHV-15	BRRF2	similar to Epstein-Barr virus BRRF2	GI:51518044	1505
CeHV-15	EBNA-1*	similar to Epstein-Barr virus EBNA-1; sequence-specific DNA-binding proteins (Johannsen et al., 2004)	GI:51518045	1535
CeHV-15	BKRF4*	similar to Epstein-Barr virus BKRF4; tegument protein (Johannsen et al. 2004)	GI:51518048	719
CeHV-15	BDRF1	similar to Epstein-Barr virus BDRF1; Packaging protein (Rivailler et al., 2002)	GI:51518058	5824
CeHV-15	BDLF4	similar to Epstein-Barr virus BDLF4	GI:51518062	716
CeHV-15	BDLF3*	similar to Epstein-Barr virus BDLF3; envelope glycoprotein (Johannsen et al., 2004)	GI:51518063	779
CeHV-15	BcLF1*	similar to Epstein-Barr virus BcLF1; capsid protein (Johannsen et al., 2004)	GI:51518066	4142
CeHV-15	BcRF1	similar to Epstein-Barr virus BcRF1	GI:51518067	1733
CeHV-15	BTRF1*	similar to Epstein-Barr virus BTRF1	GI:51518068	1211
CeHV-15	BXLF1*	similar to Epstein-Barr virus BXLF1; thymidine kinase (Johannsen et al., 2004)	GI:51518070	1823
CeHV-15	LF3	similar to Epstein-Barr virus LF3	GI:51518075	2672
CeHV-15	BILF1*	similar to Epstein-Barr virus BILF1; GCR (Paulsen et al., 2005)	GI:51518078	938
CeHV-15	BALF5*	similar to Epstein-Barr virus BALF5; DNA polymerase (Rivailler et al., 2002)	GI:51518080	3047
CeHV-15	ECRF4	similar to Epstein-Barr virus ECRF4	GI:51518079	1136
CeHV-15	BARF1*	similar to Epstein-Barr virus BARF1; CSF-1R (Rivailler et al., 2002)	GI:51518086	662
CeHV-15	LMP1*	similar to Epstein-Barr virus LMP1	GI:51518089	1939
HHV-4	unnamed protein product*	BNRF1 reading frame; major tegument protein; vFGAM	GI: 9625579	3956

Table 4 continued

HHV-4	unnamed protein product*	BCRF1 reading frame; vIL-10	GI: 9625580	512
HHV-4	unnamed protein product	BCRF2 reading frame 1	GI: 9625581	1151
HHV-4	unnamed protein product	BWRF1 reading frame 2	GI: 9625582	1151
HHV-4	unnamed protein product	BWRF1 reading frame 3	GI: 9625583	1151
HHV-4	unnamed protein product	BWRF1 reading frame 4	GI: 9625584	1151
HHV-4	unnamed protein product	BWRF1 reading frame 5	GI: 9625585	1151
HHV-4	unnamed protein product	BWRF1 reading frame 6	GI: 9625586	1151
HHV-4	unnamed protein product	BWRF1 reading frame 7	GI: 9625587	1151
HHV-4	unnamed protein product	BWRF1 reading frame 8	GI: 9625588	1151
HHV-4	unnamed protein product	BWRF1 reading frame 9	GI: 9625589	1151
HHV-4	unnamed protein product	BWRF1 reading frame 10	GI: 9625590	1151
HHV-4	unnamed protein product	BWRF1 reading frame 11	GI: 9625591	1151
HHV-4	unnamed protein product	BWRF1 reading frame 12	GI: 9625592	1151
HHV-4	unnamed protein product	BFRF2 early reading frame, homologous to HFLF5 in CMV	GI: 9625597	1775
HHV-4	unnamed protein*	BPLF1 reading frame; Tegument protein	GI: 9625599	9449
HHV-4	unnamed protein product*	BaRF1 early reading frame, Ribonucleotide reductase, small subunit	GI: 9625603	908
HHV-4	unnamed protein product*	BMRF1 early reading frame. Early antigen protein recognised by R3 monoclonal	GI: 9625604	1214
HHV-4	unnamed protein product	BMRF2 early reading frame. Membrane protein (Rivailler <i>et al.</i> , 2002)	GI: 9625605	1073
HHV-4	unnamed protein product	BSRF1 reading frame	GI: 9625609	656
HHV-4	unnamed protein product*	EBNA3B (EBNA4A); latent infection nuclear proteins important for <i>Epstein-Barr virus</i> (EBV)-induced B-cell immortalization and the immune response to EBV infection. (Jiang <i>et al.</i> , 2000)	GI: 9625617	2894
HHV-4	unnamed protein product	EBNA3C (EBNA 4B) latent protein (Jiang <i>et al.</i> , 2000)	GI: 9625618	3052
HHV-4	unnamed protein product	BZLF1 reading frame; Transactivator	GI: 9625620	945
HHV-4	unnamed protein product*	BRLF1 reading frame, (immediate?) early gene, acts as transcription activator	GI: 9625622	1817
HHV-4	unnamed protein product	BRRF1 early reading frame	GI: 9625621	932
HHV-4	unnamed protein product	BRRF2 reading frame	GI: 9625623	1613
HHV-4	unnamed protein product*	BKRF1 encodes EBNA-1 protein, latent cycle gene	GI: 9625624	1925
HHV-4	unnamed protein product*	BKRF4 reading frame, contains complex repetitive sequence	GI: 9625627	653
HHV-4	unnamed protein product	BBLF3 early reading frame, spliced to BBLF2. BBLF3 contains a consensus nucleotide binding site; Helicase-primase complex (Rivailler <i>et al.</i> , 2002)	GI: 9625631	602
HHV-4	unnamed protein product	BGLF3 reading frame	GI: 9625638	998

Table 4 continued

HHV-4	unnamed protein product	probable DNA packaging protein; BDRF1 reading frame	GI:9625642	5413
HHV-4	unnamed protein product	BGRF1 reading frame, Packaging protein (Rivailler et al, 2002)	GI:9625637	977
HHV-4	unnamed protein product	BGLF1 late reading frame	GI:9625640	1523
HHV-4	unnamed protein product	BDLF4 early reading frame	GI:9625641	677
HHV-4	unnamed protein product*	BDLF2 late reading frame; tegument	GI: 9625644	1262
HHV-4	unnamed protein product	BcRF1 reading frame		1727
HHV-4	unnamed protein product	BTRF1 reading frame. Northern blots detect 0.95 late and 3.8kb early RNA		1274
HHV-4	unnamed protein product*	BXLF1 early reading frame, thymidine kinase.	GI: 9625651	1823
HHV-4	unnamed protein product*	BILF1 reading frame, membrane protein, 3xNXS /T; GCR (Paulsen et al., 2005)	GI: 9625656	938
HHV-4	unnamed protein product*	BALF5 DNA polymerase (early), homologous to many DNA polymerases, CMV HFLF2 and RF 28 VZV. 4.5kb early RNA apparently encodes BALF5, RNA ends unknown	GI:9625657	3047
HHV-4	unnamed protein product*	BARF1 reading frame a secretory protein with transforming and mitogenic activities (Wang et al., 2006); CSF-1R (Rivailler et al., 2002)	GI: 9625661	665
MHV-2	pR122-EX5		GI:9845417	1517
MHV-2	pR123-EX3		GI:9845419	2611
MHV-2	pR123-EX4		GI:9845418	1295
MHV-2	pr128	US22 family homolog;	GI:9845425	1226
AlHV-1	A3	semaphorin homolog; AHV-sema, similar to Vaccinia A39	GI:10140929	1961
AlHV-1	ORF03*	tegument protein; similar to H. saimiri and EHV2 ORF3, similar to ORF75; Virion protein, FGARAT (Ensser et al., 1997)	GI:10140931	4109
AlHV-1	Putative BALF1 homolog*	Putative antagonist of herpesvirus BCL-2;	GI:19343407	695
AlHV-1	ORF06	major ss DNA binding protein	GI:10140932	3383
AlHV-1	ORF09*	DNA Polymerase; similar to EBV BALF5, CMV UL54, HSV UL30	GI:10140935	3080
AlHV-1	A5*	similar to EBV BILF1; possible seven transmembrane protein with similarity to G-protein coupled receptors	GI:10140936	908
AlHV-1	ORF10*	similar to H. saimiri, EHV2, KSHV ORF10, EBV Raji LF1	GI:10140937	1214
AlHV-1	ORF18	similar to CMV UL 79	GI:10140940	827
AlHV-1	ORF 23	similar to EBV BTRF1	GI:10140945	1205
AlHV-1	ORF25	major capsid protein; ORF25; similar to EBV BCLF1, CMV UL75, HSV UL22	GI:10140947	4112
AlHV-1	ORF33	similar to EBV BGLF2, CMV UL94, HSV UL16	GI:10140954	1007
AlHV-1	ORF34	similar to EBV BGLF3, CMV UL95, HSV UL14	GI:10140955	1031
AlHV-1	ORF45	similar to EBV BKRF4	GI:10140966	707
AlHV-1	ORF47	similar to CMV UL115 gL, HSV UL1 and EBV BKRF2; weak positional homologue	GI:10140968	506
AlHV-1	ORF48	similar to EBV BRRF2	GI:10140969	1259
AlHV-1	ORF50*	R-transactivator; similar to EBV BRLF1; splicing predicted by splice site analysis	GI:10140970	2078
AlHV-1	A6*	position similar to EBV BZLF1; Transactivator (Rivailler et al., 2002)	GI:10140971	632
AlHV-1	ORF55	similar to EBV BSRF1, CMV UL71, HSV UL51	GI:10140977	662
AlHV-1	ORF58	similar to EBV BMRF2 and HSV UL43	GI:10140980	1055
AlHV-1	ORF59*	processivity factor; DNA replication; subunit of DNA-polymerase; similar to EBV BMRF1 (EA-D), CMV UL44, HSV UL42	GI:10140981	1235
AlHV-1	ORf60*	ribonucleotide-reductase, small subunit; RRsmall; similar to EBV BARF1, HSV UL40	GI:10140982	917
AlHV-1	ORF63	tegument protein; similar to EBV BOLF1, CMV UL47, HSV UL37	GI:10140985	2858
AlHV-1	ORF64	large tegument protein; similar to EBV BPLF1, CMV UL48, HSV UL36	GI:10140986	7820

Table 4 continued

AlHV-1	ORF65	capsid protein; positional similar to EBV BFRF3 and HSV UL35	GI:10140987	758
AlHV-1	ORF66	similar to EBV BFRF2, CMV UL39	GI:10140988	1313
AlHV-1	ORF67	tegument protein; virion tegument protein; similar to EBV BFRF1, CMV UL50, HSV UL34	GI:10140989	791
AlHV-1	ORF73*	putative immediate early protein; similar to H. saimiri and KSHV ORF73	GI:10140993	3902
AlHV-1	ORF75*	similar to ORF3 of EHV2 and AHV-1, and ORF75 of all rhadinoviruses, and EBV BNRF1; also similar to formylglycineamide-synthase	GI:10140994	3947
AlHV-1	A9*	similar to Bcl-family of proteins; contains only conserved BH1 domain; functional similarity may exist to ORF16 of H. saimiri, KSHV, BHV4 and EBV BHRF1	GI:10140995	506
AlHV-1	A10	putative glycoprotein	GI:10140996	1418
BoHV-4	ORF3 BORFA1*	v-FGAM-synthase; tegument protein;	GI:13095580	3866
BoHV-4	ORF 6*	single-stranded DNA-binding protein MDBP	GI:13095583	3404
BoHV-4	ORF 9*	DNA polymerase;	GI:13095586	3017
BoHV-4	ORF 10	BORFB1; conserved in other gamma-herpesviruses	GI:13095587	1280
BoHV-4	pBo5	hypothetical protein; long ORF of immediate early transcript 1 RNA, exons I-IV	GI:13095589	1139
BoHV-4	ORF 16*	BORFB2; v-Bcl-2 protein	GI:13095593	680
BoHV-4	ORF 21*	thymidine kinase	GI:13095598	1337
BoHV-4	ORF 23	conserved in other gamma-herpesviruses	GI:13095600	1202
BoHV-4	ORF 24	conserved in other herpesviruses	GI:13095601	2258
BoHV-4	ORF 25	major capsid protein	GI:13095602	4121
BoHV-4	ORF 27	conserved in other gamma-herpesviruses	GI:13095604	638
BoHV-4	ORF 29	cleavage/packaging protein; exons I and II	GI:13095610	5174
BoHV-4	ORF 31	conserved in other gamma-herpesviruses	GI:13095607	641
BoHV-4	ORF 32	viral DNA cleavage/packaging protein	GI:13095608	1370
BoHV-4	ORF 33	conserved in other herpesviruses	GI:13095609	998
BoHV-4	ORF 34	conserved in other herpesviruses	GI:13095611	986
BoHV-4	ORF 40	helicase-primase complex component	GI:13095617	1373
BoHV-4	ORF 41	helicase-primase complex component	GI:13095618	521
BoHV-4	ORF 45*	unknown	GI:13095622	725
BoHV-4	ORF 48	conserved in other gamma-herpesviruses	GI:13095625	1544
BoHV-4	ORF 50	R transactivator protein; exons I and II; encoded by immediate early transcript 2 RNA	GI:13095626	2593
BoHV-4	ORF 49*	unknown	GI:13095627	899
BoHV-4	ORF 55*	unknown	GI:13095632	602
BoHV-4	ORF 58	conserved in other gamma-herpesviruses	GI:13095635	1052
BoHV-4	ORF 59	DNA replication protein	GI:13095636	1175
BoHV-4	ORF 60*	ribonucleotide reductase small subunit	GI:13095637	917
BoHV-4	ORF 62	assembly/DNA maturation protein	GI:13095639	1019
BoHV-4	ORF 63	tegument protein	GI:13095640	2819
BoHV-4	ORF 64	tegument protein	GI:13095641	7709
BoHV-4	ORF 66	conserved in other herpesviruses	GI:13095643	1274
BoHV-4	ORF 67	tegument protein	GI:13095644	770
BoHV-4	ORF 71	v-FLIP; BORFE2	GI:13095651	548
BoHV-4	ORF 75*	tegument protein/v-FGAM-synthetase	GI:13095653	3917
BoHV-4	ORF Bo14*	BORFF1; hypothetical protein pBo14; proline rich (Zimmermann et al., 2001)	GI:13095654	512
BoHV-4	ORF Bo17*	BORFF3-4; v-beta-1,6GnT	GI:13095657	1322
EHV-2	ORF E4*		GI:9628007	551
EHV-2	ORF E6*	putative GCR	GI:9628013	977
EHV-2	ORF 17.5	capsid scaffold protein	GI:9628018	1010
EHV-2	ORF 21*	thymidine kinase	GI:9628023	1841
EHV-2	ORF 33		GI:9628035	1025
EHV-2	ORF 45		GI:9628048	965
EHV-2	ORF 48	glycoprotein L	GI:9628051	1832

Table 4 continued

EHV-2	ORF 50	transcriptional control	GI:9628053	1892
EHV-2	ORF 55*		GI:9628058	674
EHV-2	ORF 59*	DNA polymerase processivity subunit	GI:9628062	1244
EHV-2	ORF 62	capsid protein; intercapsomeric triplex	GI:9628065	1016
EHV-2	ORF 63	tegument protein	GI:9628066	2897
EHV-2	ORF 64	tegument protein	GI:9628067	10310
EHV-2	ORF 65	capsid protein; external to capsomers	GI:9628068	539
EHV-2	ORF 66		GI:9628069	1370
EHV-2	ORF 67	tegument protein	GI:9628070	863
EHV-2	ORF E7*	interleukin 10-like protein, similar to protein encoded by GenBank Accession Number S59624	GI:9628072	539
EHV-2	ORF 70*	thymidylate synthase	GI:9628075	869
EHV-2	ORF 74*	GCR	GI:9628076	992
EHV-2	ORF E8*		GI:9628077	515
EHV-2	ORF 75	tegument protein	GI:9628078	4037
EHV-2	ORF E10		GI:9628080	632
MFRV	JM145		GI:66476694	869
MHV-4	M1	serpin	GI:9629554	1262
MHV-4	M2*		GI:9629599	599
MHV-4	M3*		GI:9629600	1220
MHV-4	M4*	GCR homologue	GI:9629555	1379
MHV-4	ORF4	complement regulatory protein	GI:9629556	1166
MHV-4	ORF6*	ssDNA binding protein	GI:9629557	3311
MHV-4	ORF9*	DNA polymerase	GI:9629560	3083
MHV-4	ORF10		GI:9629561	1256
MHV-4	ORF11*		GI:9629562	1166
MHV-4	K3	BHV4-IE1 homolog	GI:9629601	605
MHV-4	M6		GI:9629564	1757
MHV-4	ORF18b		GI:9629565	854
MHV-4	ORF21*	thymidine kinase	GI:9629566	1934
MHV-4	ORF23*		GI:9629605	1145
MHV-4	ORF24		GI:9629606	2153
MHV-4	ORF25	major capsid protein	GI:9629568	4121
MHV-4	ORF27*		GI:9629570	764
MHV-4	ORF29b	packaging protein	GI:9629607	1046
MHV-4	ORF31		GI:9629572	602
MHV-4	ORF32*		GI:9629573	1334
MHV-4	ORF33*		GI:9629574	983
MHV-4	ORF29a	packaging protein	GI:9629608	920
MHV-4	ORF34		GI:9629575	998
MHV-4	ORF40*	helicase-primase	GI:9629580	1832
MHV-4	ORF45*		GI:9629612	620
MHV-4	ORF47*	glycoprotein L	GI:9629614	521
MHV-4	ORF48*		GI:9629615	1001
MHV-4	ORF49		GI:9629616	905
MHV-4	ORF50	transcriptional activator	GI:9629582	1469
MHV-4	M7*	glycoprotein 150	GI:9629583	1451
MHV-4	ORF55*		GI:9629619	572
MHV-4	ORF58		GI:9629620	1043
MHV-4	ORF59*	DNA replication protein	GI:9629621	1184
MHV-4	ORF60*	ribonucleotide reductase small subunit	GI:9629622	917
MHV-4	ORF62	assembly/DNA maturation	GI:9629624	1142
MHV-4	ORF63	tegument protein	GI:9629588	2816
MHV-4	ORF64	tegument protein	GI:9629589	7373
MHV-4	M9*		GI:9629625	560
MHV-4	ORF66		GI:9629626	1229
MHV-4	ORF67	tegument protein	GI:9629627	680

Table 4 continued

MHV-4	M10a		GI:9629592	2324
MHV-4	M10b		GI:9629593	2120
MHV-4	ORF72*	cyclin D homolog	GI:9629628	758
MHV-4	M11*	bcl-2 homolog	GI:9629595	515
MHV-4	ORF73	immediate-early protein	GI:9629629	944
MHV-4	ORF74*	GCR (IL8 receptor homolog?)	GI:9629596	1013
MHV-4	ORF75C*	tegument protein G75C	GI:9629630	3932
MHV-4	ORF75B*	tegument protein G75B	GI:9629631	3827
MHV-4	ORF75A*	tegument protein G75A	GI:9629632	3875
MHV-4	M12		GI:9629597	692
MHV-4	M13		GI:9629598	638
SaHV-2	ORF 02*	dihydrofolate reductase	GI:9625957	563
SaHV-2	ORF 03*	similarity to ORF 75 and EBV BNRF1	GI:9625958	3740
SaHV-2	Orf 09 KCRF2*	DNA polymerase	GI:9625965	3029
SaHV-2	ORF 10 KCRF3		GI:9625966	1223
SaHV-2	ORF 12 KCLF1		GI:9625968	509
SaHV-2	ORF 23	similar to EBV BTRF1	GI:9625979	761
SaHV-2	ORF 25	major capsid protein	GI:9625981	4115
SaHV-2	ORF 33	similar to other herpesviruses	GI:9625988	992
SaHV-2	ORF 34	similar to other herpesviruses	GI:9625989	950
SaHV-2	ORF 40	similar to EBV BBLF2	GI:9625996	1352
SaHV-2	ORF 45*	similar to EBV BKRF4	GI:9626001	773
SaHV-2	ORF 48	EDLF5 similar to EBV BRRF2	GI:9626004	2393
SaHV-2	ORF 49 EDLF4*	similar to EBV BRRF1	GI:9626006	911
SaHV-2	ORF 50 EDRF1	Herpesvirus S.R transactivator; sim. to EBV BRLF1, putative 3'-ORF, 5'-exon unknown"	GI:9626005	1607
SaHV-2	ORF 55 EDLF1*	similar to EBV BSRF1	GI:9626012	602
SaHV-2	ORF 59 EELF4	similar to EBV BMRF1	GI:9626015	1106
SaHV-2	ORF 60 EELF3*	ribonucleotide reductase, small subunit	GI:9626016	917
SaHV-2	ORF 62	EELF1 similar to other herpesviruses	GI:9626018	992
SaHV-2	ORF 64	EERF2 similar to other herpesviruses	GI:9626020	7409
SaHV-2	ORF 70 ECLF4*	thymidylate synthase	GI:9626026	884
SaHV-2	ORF 71 ECLF3		GI:9626027	503
SaHV-2	ORF 72 ECLF2*	cyclin homologue	GI:9626028	764
SaHV-2	ORF 73 ECLF1*		GI:9626029	1223
SaHV-2	ORF 75*	EILF1 similar to ORF 03 and EBV BNRF1	GI:9626031	3899
HHV-6	U86, IE2	Transactivation; old name BCLF1; homologue HCMV UL122, IE2; region IE-A, immediate early gene	GI:9628388	2147
HHV-6	U87	possible glycoprotein; region IE-B, highly charged, pro repeats; presenting U86 /U87 as one ORF, BCLF0	GI:9628389	2492
HHV-6	U89*	Transactivation, IE1	GI:9628391	2519
HHV-6B	U44	major immediate-early protein; IE-A	GI:9633155	4562
HHV-6B	U45*	IE-A transactivator	GI:9633156	3433
HHV-7	U7*	betaherpesvirus US22 gene family; exons 1 and 2 are similar to HHV-5 UL28/UL29; exon 3 related to HHV-7 U4 and similar to HHV-5 UL27	GI:89112557	3855
HHV-7	U25	betaherpesvirus US22 gene family; similar to HHV-5 UL43	GI:51874247	962
HHV-7	U30	tegument protein; herpesvirus core gene UL37 family; similar to HHV-5 UL47	GI:51874252	2816
HHV-7	U45	herpesvirus core gene UL50 family; herpesvirus DURP gene family; similar to HHV-5 UL72; related to dUTPase but probably not enzymatically active	GI:51874267	1139
HHV-7	U52*	similar to HHV-5 UL79	GI:51874274	764
HHV-7	U53.5*	major capsid scaffold protein; herpesvirus core gene UL26.5 family; similar to HHV-5 UL80.5	GI:51874276	692
HHV-7	U86	IE-A protein; similar to HHV-5 UL122	GI:51874305	3617
HHV-7	U90*	IE-A transactivator; similar to HHV-5 UL123	GI:51874306	3760

Table 4 continued

HHV-7	U95	betaherpesvirus US22 gene family; possible HHV-5 TRS1	GI:51874308	2822
CeHV-2	immediate early protein ICP0	multifunctional regulatory protein	GI:56694722	2491
CeHV-2	immediate early protein ICP0	multifunctional regulatory protein	GI:56694781	2491
EHV-1	ORF 64	transcriptional activator	GI:50313305	4463
EHV-1	ORF 64	transcriptional activator	GI:50313321	4463
AtHV-3	orf 06	major ssDNA binding protein	GI:9631197	3386
AtHV-3	orf 10	similar to Raji LF1	GI:9631200	1220
AtHV-3	orf 11	similar to Raji LF2	GI:9631201	1217
AtHV-3	orf 14*	Mitogen	GI:9631202	821
AtHV-3	orf 18		GI:9631208	770
AtHV-3	orf 21*	thymidine kinase	GI:9631211	1583
AtHV-3	orf 23	similar to BTRF1	GI:9631213	767
AtHV-3	orf 33		GI:9631225	992
AtHV-3	orf 34		GI:9631226	950
AtHV-3	orf 45*		GI:9631236	782
AtHV-3	orf 48*		GI:9631239	2378
AtHV-3	orf 49*		GI:9631240	914
AtHV-3		Probable transcription activator EDRF1	GI:19343431	1343
AtHV-3	orf 55*		GI:9631246	602
AtHV-3	orf 59*		GI:9631249	1100
AtHV-3	orf 60*	small subunit of ribonucleotide reductase	GI:9631250	917
AtHV-3	orf 62		GI:9631252	992
AtHV-3	orf 64	large tegument protein	GI:9631254	7415
AtHV-3	orf 66		GI:9631256	1334
AtHV-3	orf 70*	thymidylate synthase	GI:9631261	872
AtHV-3	orf 72*	v-cyclin	GI:9631263	788
AtHV-3	orf 75		GI:9631266	3899
TuHV-1	t123*	hypothetical protein	GI:14251117	1103
HHV-8	ORF 73*	extensive acidic domains, potential leucine zipper; immediate early protein homolog	GI:18846043	3488

^aDescription as derived from GenBank annotations and other papers. *reported in previous papers or found in previous papers to have cellular homologues and suggested to be acquired from other organisms.

Discussion

In this paper, we introduced a composition-based framework for the detection of horizontal gene transfers by using SVM. This method reached a higher accuracy (over 95%) in detecting horizontally transferred genes compared to the Tsirigos and Rigoutsos's paper (2005a, b) (less than 70%) and our previous method (less than 95%) (Fu *et al.*, 2008). Using this method, 302 transferred genes were identified in 33 mammalian herpesviruses. However, in our previous paper, only 141 transferred genes were predicted (Fu *et al.*, 2008).

This paper used the SVM instead of the Mahalanobis distance, the posterior probability, or stepwise and Fischer linear discriminant analysis used in previous reports (Nakamura and Itoh, 2004; Tsirigos and Rigoutsos, 2005a; Fu *et al.*, 2008) to classify the two opposite groups. SVM is a new pattern recognition method based on statistical learning theory and has been used on a large variety of problems, including text classification (Joachims, 1998, 1999), image

recognition tasks, bioinformatics and medical applications. It showed many advantages in the classification of small samples, nonlinear and multidimensional data. The algorithm has scalable memory requirements and can handle problems with many thousands of support vectors efficiently.

Although SVM has been used to detect the HGT of the herpesviruses in Tsirigos and Rigoutsos's paper (2005b), they used this algorithm to analyze only one herpesvirus – HHV-5, and reached the accuracy of less than 70%. In their analysis, the general signatures of most genes in the genome were used for discrimination: a gene with a signature outside of the general signatures of most genes in this genome would be considered as transferred gene. However, by training the learning module of *SVMlight* for subsequent horizontally transferred gene detection with the conserved genes of viruses as the dataset of non-transferred genes and the conserved genes of mammals as the dataset of transferred genes, our method avoids artificial setting of a threshold for discrimination, as the previous method does, which calcu-

lates the distance between the gene and the genome. In our method, all mammalian herpesviruses were considered as a cluster to be analyzed because they have similar genome composition. This increased the amount of the analyzed data, but it also enlarged the distribution scope of the points of gene compositional signature, and probably decreased the exactness of the analysis. Fortunately, the opposite data are the host genomes, which have very different gene compositional signature, so that using all mammalian herpesviruses would not influence the exactness of the result. For the same reason, using the dinucleotides as the template to generalize the compositional signatures of genes have yielded the best discrimination results, and this procedure required to process only 4^2 data for every gene, comparing to 4^8 data for every gene in previous reports, which used 8-ker oligonucleotide template (Tsirigos and Rigoutsos, 2005a,b) and 4^3 in our previous paper, which used trinucleotide template. The result indicated that our method is perfect for the detection of herpesvirus transferred genes that could be recently acquired from the mammalian hosts (some genes transferred anciently were not detectable, the reason see below). This method can be expanded to the detection of transferred genes from hosts other than mammals just by training learning module of SVMlight with the conserved genes from those hosts as the dataset of transferred genes.

Short sequences (<500 bp) often appear atypical for stochastic reasons and might be misidentified as having been transferred (Lawrence and Ochman, 2002). In order to overcome this problem, we avoided using short conserved genes (for example UL49A in HHV-1) as the non-transferred genes and deleted all short sequences (<500 bp) in our sequence datasets.

Although the function of most of the transferred genes detected with this method is unknown, many had been determined or predicted to be glycoproteins, membrane proteins or involved in the interaction with host, for example, dealing with the immune response, such as IL-10, cell apoptosis such as Bcl-2, and cell proliferation control, such as cyclin and mitogen, which was well consistent with other investigators' conclusion (Raftery *et al.*, 2000; Holzerlandt *et al.*, 2002; Fu *et al.*, 2008).

131 transferred genes detected by our method had been reported to be transferred genes in previous studies or to have cellular homologues and had been suggested that they might have been pilfered from their host (marked with * in Table 4). For example, the beta-1,6-N-acetyl-glucosaminyltransferase was suggested to have been acquired from an ancestor of the buffalo after the origin of the *Bovinae* (Markine-Goriaynoff *et al.*, 2003). UL122 and UL123 in HHV-5 had been predicted by Tsirigos and Rigoutsos (Tsirigos and Rigoutsos, 2005b). IL-10 in HHV-4 and CeHV-15 was believed to have a eukaryotic origin in many previous papers (Raftery *et al.*, 2000; Holzerlandt *et al.*, 2002; Hughes, 2002; Fu *et al.*,

2008). Herpesvirus homologues of cellular genes include G protein-coupled receptor (GCR) or its homologues in EHV-2, CalHV-3, CeHV-15, MuHV-4, AlHV-1 and HHV-4, Bcl-2 or its homologues in MuHV-4, CeHV-15, AlHV-1 and BoHV-4, DNA polymerase or its homologues in CeHV-15, HHV-4, AlHV-1, BoHV-4, MuHV-4 and SaHV-2, dihydrofolate reductase in SaHV-2, small subunit of ribonucleotide reductase in AlHV-1, BoHV-4, MuHV-4, SaHV-2, AtHV-3, CeHV-15 and HHV-4, thymidylate synthase in CeHV-15, BoHV-4, EHV-2, MuHV-4, SaHV-2 and AtHV-3, v-FGAM-synthetase or its homologues in HHV-4, AlHV-1, BoHV-4, MuHV-4 and SaHV-2, cyclin or its homologues in MuHV-4, SaHV-2 and AtHV-3 (Raftery *et al.*, 2000; Holzerlandt *et al.*, 2002). Apart from these predicted genes, other transferred genes detected in this study were identified as horizontally transferred genes for the first time.

As for these firstly identified transferred genes, some of them are homologues of transferred genes, which had been predicted previously. For example, the ORF19 in CalHV-3 is homologous to the BDLF2 in HHV-4, and BFRF2 in CeHV-15 is similar to that in HHV-4. The latters were predicted as transferred genes in our previous paper. The formers were identified in this research. This may be due to the high sensitivity of SVM method over others. The high sensitivity could also mark some non-transferred genes as transferred genes because of their only a little atypical composition, which may result from factors other than transfer. So we had to combine different methods to analyze the transferred genes.

Many of the transferred genes predicted in this paper were linked with some of the transferred genes identified previously. For example, BCRF2 and BWRF1 in HHV-4 are linked with BCRF1 (IL-10). BMRF1 and BMRF2 in HHV-4 are linked with BaRF1 (ribonucleotide reductase, small subunit). ORF58 in AlHV-1 is linked with ORF59 (DNA polymerase). ORF73 and A10 in AlHV-1 are linked with ORF75 (formylglycineamide-synthetase) and A9 (Bcl-family of proteins). ORF10 in BoHV-4 is linked with ORF9 (DNA polymerase). ORF58 and ORF59 in BoHV-4 are linked with ORF60 (ribonucleotide reductase, small subunit). ORFE8 and ORF75 in EHV-2 are linked with ORF74 (GCR). ORF4 and ORF6 in MuHV-4 are linked with M4 (GCR homologue). M6 and ORF16b in MuHV-4 are linked with ORF21 (thymidine kinase). ORF10 in SaHV-2 is linked with ORF9 (DNA polymerase). ORF71 in SaHV-2 is linked with ORF72 (cycline homologue). ORF10 and ORF11 in AtHV-3 are linked with ORF14. HGT always occurred in cluster, so these newly identified genes may have been horizontally transferred together with their linked genes.

Some transferred genes, which might have been transferred very early and have undergone long time of "amelioration", might already have the features of the recipient genomes (Lawrence and Ochman, 1997) and already lost their atypical

characteristics. Genes like these were not detectable by this method and were considered as non-transferred genes. For example, the UL2 and UL50, which have been reported to be transferred from their host very early (Baldo and McClure, 1999; Holzerlandt *et al.*, 2002; Davison and Stow, 2005), were considered as non-transferred genes in our study.

Unusual nucleotide composition was what this method was based on. Some conserved genes were identified as transferred genes in this paper due to their atypical composition such as BcLF1 in CeHV-15 and ORF25 in AlHV-1, BoHV-4, MuHV-4 and SaHV-2, which encode the major capsid protein, UL71 in PoHV-4 and ORF55 in AlHV-1, which encode tegument protein, U53.5 in HHV-7 and ORF 17.5 in EHV-2, which encode the capsid scaffold protein. Although unusual nucleotide composition mainly resulted from the transfer events, other reasons may also cause unusual nucleotide composition. For example, BZLF and RTA transactivators as well as EBNA-1 and IE1, IE2 proteins contain anomalous clusters of charged amino acid residues (Karlin *et al.*, 1989), which would result in unusual nucleotide composition and would bias the results towards identifying these genes as transferred genes. In this case, the unusual nucleotide composition is the result of the function of the gene itself rather than recent HGT. Transfer events may sometimes not lead to an unusual composition because of the "amelioration" or the similar composition of the donor. These factors limit the development of detection methods based on composition to some extent. Our method is based on the result of unusual composition from the transfer events. Its accuracy reached the value of over 95%, though the sensitivity of detection for every herpesvirus may be different because of their different evolution rates.

When the result of this paper was compared with that of our previous paper, which used the discrimination package of SPSS to identify HGTs, it was found that there were 93 genes identified by both composition-based methods. Other genes identified by only one composition-based method may be the result of different accuracy or transferring at different time. We also compared our composition-based method with the method based on the similarity search, the earliest and the most intuitive way of identifying horizontally acquired genes. In the similarity method, gene transfers are recognized by an unusually high level of similarity among genes found in otherwise unrelated organisms. Using this method, altogether 23 groups of proteins were identified to be horizontally transferred genes (Table 5). Among them, 14 groups (marked * in Table 5) were detected by the composition-based method, other 9 groups were identified only by the similarity method. So the results of these two prediction methods overlap to some extent. This occurs because each of the methods used to detect HGT recognized different features in their target genes and are thus testing different types of hypotheses. The impact of HGT on the entire evolution of a lineage must be inferred from present-day sequences,

and the different approaches used to recognize HGT must rely on specific models of sequence evolution. The different methods are based on different assumptions. The similarity-search method identifies genes, whose closest homologues are found in taxa not otherwise related to the query genome, and thus it uncovers a set of genes biased towards those that have been transferred across large phylogenetic distance, regardless of their time of arrival into a genome. On the other hand, the composition-based method examines sequence features and preferentially identifies genes that have been recently introduced into a genome from an organism having different mutational biases, regardless of phylogenetic distance. Assuming that the frequency of transfer between lineages is inversely related to their phylogenetic distance, these two methods would identify quite different sets of genes (Lawrence and Ochman, 2002). This phenomenon has been observed by Ragan (Ragan, 2001), who used the different methods to recognize significantly different subsets of genes as being subject to horizontal transfer.

Every method has its own advantage and disadvantage in identification of HGT. The composition-based method can

Table 5. Horizontally transferred genes identified by the similarity method

Virus taxon	Virus/Eukaryote function
Alpha, Beta, Gamma	Uracil DNA glycosylase
Alpha	Large tegument protein
Alpha, Gamma	Ribonucleotide reductase large subunit
Alpha, Gamma	*Ribonucleotide reductase small subunit
Alpha	Ser/Thr protein kinase
Alpha	Transactivating tegument protein
Alpha, Gamma	*DNA polymerase
Alpha, Gamma	*Thymidylate synthase
Beta	rh10 (CeHV-8); Prostaglandin synthase, cyclooxygenase-2 (other organisms)
Gamma	*FGAM
Gamma	*IL-10
Gamma	*Semaphorin 7A
Gamma	* β -1,6-acetylglucosaminyltransferase
Gamma	*Complement binding protein
Gamma	*Cyclin D homologue
Gamma	CD200antigen, OX-2
Gamma	*GCR (IL-8)
Gamma, Beta	GCR (CC chemokine receptor)
Gamma	*DHFR
Gamma	*Complementary control protein
Gamma	IL-17
Gamma	*collagen
Gamma	*Latent nuclear antigen

*Identified by the SVM-based method.

escape from the complicated phylogenetic analysis, it requires a completed genome and can employ many mathematic models to design the arithmetic. But it has its limitation as illuminated above. Transferred gene is not the only reason of atypical composition. Evolution selection, mutation preference and the different orientation of transcription can influence the composition. The genes transferred from a donor having similar composition and the ameliorated genes transferred anciently can not be detected. The similarity-search method is simple and intuitive, but it also has its limitation: first, horizontally transferred gene is not the only mechanism that produces conflicts between phylogenies. Some genes might be coincidentally deleted from multiple lineages, leading to unusual distributions among extant organisms, or similarity can result from convergent evolution. Moreover, the proliferation of gene families can make the identification of orthologous sequences difficult, and rapid sequence evolution makes alignment of homologous sites equivocal. Second, the result of the similarity-search method is limited by the capacity of the search database. Third, the level of similarity is a man-made factor, if it is set too high, the sensitivity will be very low, if it is set too low, the accuracy will be also very low. In our analysis, the similarity score is 100 and this is relatively high. So using this method still led to the loss of many horizontally transferred genes, but this can be compensated by the atypical composition identification. Fourth, the similarity-search method can not decide the direction of transfer. Horizontally transferred gene may be transferred from the virus to the host, but also from the host to the virus. Fifth, the similarity usually combines the phylogenetic analysis to predict the HGT, but this deduction could be incorrect due to the low number of sequences used for analysis or the incredible phylogenetic relationship. For example, most phylogenetic trees showed that the rates of evolution of viral genes were faster than the evolution rates in the genes of other organism. This may lead to the most frequent problem, the long branch attraction. To solve this problem, more and nearer sequences should be analyzed and a more excellent method for reconstruction of phylogenetic trees should be used. So whenever possible, application of a variety of methods provides the best information about the scope of gene transfer across broad timescales.

Acknowledgments. This work was funded by the National Science Foundation of Guangdong Province under Grant number 04009785, and a grant from 211 Project of Guangdong University of Technology.

References

- Alcami A, Koszinowski UH (2000): Viral mechanisms of immune evasion. *Trends Microbiol.* 8, 410–418. [doi.org/10.1016/S0966-842X\(00\)01830-8](https://doi.org/10.1016/S0966-842X(00)01830-8)
- Altschul SF, Madden TL, Schaffer AJ, Zhang J, Zhang Z, Miller W, Lipman DJ (1997): Gapped BLAST and PSI-BLAST: A new generation of protein database search programs. *Nucleic Acids Res.* 25, 3389–2402. doi.org/10.1093/nar/25.17.3389
- Baldo AM, McClure MA (1999): Evolution and horizontal transfer of dUTPase-encoding genes in viruses and their hosts. *J. Virol.* 73, 7710–7721.
- Davison AJ, Stow ND (2005): New genes from old: redeployment of dUTPase by herpesviruses. *J. Virol.* 79, 12880–12892. doi.org/10.1128/JVI.79.20.12880-12892.2005
- Ensser A, Pflanz R, Fleckenstein B (1997): Primary structure of the alcelaphine herpesvirus 1 genome. *J. Virol.* 71, 6517–6525.
- Fu MH, Deng RQ, Wang JW, Wang XZ (2008): Detection and analysis of horizontal gene transfer in Herpesvirus. *Virus Res.* 131, 65–76. doi.org/10.1016/j.virusres.2007.08.009
- Garcia-Vallvé S, Romeu A, Palau J (2000): Horizontal gene transfer in bacterial and archaeal complete genomes. *Genome Res.* 10, 1719–1725.
- Garcia-Vallvé S, Guzman E, Montero MA, Romeu A (2003): HGTD-DB: a database of putative horizontally transferred genes in prokaryotic complete genomes. *Nucleic Acids Res.* 31, 187–189.
- Holzerlandt R, Orengo C, Kellam P, Alba MM (2002): Identification of new herpesvirus gene homologs in the human genome. *Genome Res.* 12, 1739–1748. doi.org/10.1101/gr.334302
- Hughes AL (2002): Origin and evolution of viral interleukin-10 and other DNA virus genes with vertebrate homologues. *J. Mol. Evol.* 54, 90–101. doi.org/10.1007/s00239-001-0021-1
- Jiang H, Cho YG, Wang F (2000): Structural, functional, and genetic comparisons of Epstein-Barr virus nuclear antigen 3A, 3B, and 3C homologues encoded by the rhesus lymphocryptovirus. *J. Virol.* 74, 5921–5932.
- Joachims T (1998): Text Categorization with Support Vector Machines: Learning with Many Relevant Features. *Proceedings of the European Conference on Machine Learning.* Dortmund, pp. 137–142.
- Joachims T (1999): Transductive Inference for Text Classification using Support Vector Machines. *International Conference on Machine Learning (ICML).* Bled, pp. 200–209.
- Johannsen E, Luftig M, Chase MR, Weicksel S, Cahir-McFarland E, Illanes D, Sarracino D, Kieff E (2004): Proteins of purified Epstein-Barr virus. *Proc. Natl. Acad. Sci. USA* 101, 16286–16289. doi.org/10.1073/pnas.0407320101
- Karlin S, Blaisdell BE, Mocarski ES, Brendel V (1989): A method to identify distinctive charge configurations in protein sequences, with application to human herpesvirus polypeptides. *J. Mol. Biol.* 205, 165–177. [doi.org/10.1016/0022-2836\(89\)90373-2](https://doi.org/10.1016/0022-2836(89)90373-2)
- Lawrence JG, Ochman H (1997): Amelioration of bacterial genomes: rates of change and exchange. *J. Mol. Evol.* 44, 383–397. doi.org/10.1007/PL00006158
- Lawrence JG, Ochman H (1998): Molecular archaeology of the Escherichia coli genome. *Proc. Natl. Acad. Sci. USA* 95, 9413–9417. doi.org/10.1073/pnas.95.16.9413
- Lawrence JG, Ochman H (2002): Reconciling the many faces of lateral gene transfer. *Trends Microbiol.* 10, 1–4. [doi.org/10.1016/S0966-842X\(01\)02282-X](https://doi.org/10.1016/S0966-842X(01)02282-X)

- Markine-Goriaynoff N, Georin JP, Golta M, Zimmermann W, Broll H, Wamwayi HM, Pastoret PP, Sharp PM, Vanderplasschen A (2003): The core 2 β -1,6-N-acetylglucosaminyltransferase-mucin encoded by bovine herpesvirus 4 was acquired from an ancestor of the African Buffalo. *J. Virol.* 77, 1784–1792. doi.org/10.1128/JVI.77.3.1784-1792.2003
- McFadden G, Murphy PM (2000): Host-related immunomodulators encoded by poxviruses and herpesviruses. *Curr. Opin. Microbiol.* 3, 371–378. [doi.org/10.1016/S1369-5274\(00\)00107-7](https://doi.org/10.1016/S1369-5274(00)00107-7)
- Moore PS, Bossoff C, Weiss RA, Chang Y (1996): Molecular mimicry of human cytokine and cytokine response pathway genes by KSHV. *Science* 274, 1739–1744. doi.org/10.1126/science.274.5293.1739
- Mrazek J, Karlin S (1999): Detecting alien genes in bacterial genomes. *Ann. NY. Acad. Sci.* 870, 314–329. doi.org/10.1111/j.1749-6632.1999.tb08893.x
- Nakamura Y, Itoh T, Matsuda H (2004): Gojobori T. Biased biological functions of horizontally transferred genes in prokaryotic genomes. *Nature Genetcs* 36, 760–766. doi.org/10.1038/ng1381
- Ochman H, Lawence JG, Groisman EA (2000): Lateral gene transfer and the nature of bacterial innovation. *Nature* 405, 299–304. doi.org/10.1038/35012500
- Paulsen SJ, Rosenkilde MM, Eugen-Olsen J, Kledal TN (2005): Epstein-Barr virus-encoded BILF1 is a constitutively active G protein-coupled receptor. *J. Virol.* 79, 536–546. doi.org/10.1128/JVI.79.1.536-546.2005
- Raftery M, Muller A, Schonrich G (2000): Herpesvirus homologues of cellular genes. *Virus Genes* 21, 65–75. doi.org/10.1023/A:1008184330127
- Ragan MA (2001): On surrogate methods for detecting lateral gene transfer. *FEMS Microbiol. Lett.* 210, 187–191. doi.org/10.1111/j.1574-6968.2001.tb10755.x
- Rivailler P, Jiang H, Cho Y, Quink C, Wang F (2002): Complete nucleotide sequence of the rhesus lymphocryptovirus: genetic validation for an Epstein-Barr virus animal mode. *J. Virol.* 76, 421–426. doi.org/10.1128/JVI.76.1.421-426.2002
- Shackelton LA, Holmes EC (2004): The evolution of large DNA viruses: combining genomic information of viruses and their hosts. *Trends Microbiol.* 12, 458–465. doi.org/10.1016/j.tim.2004.08.005
- Tatusov RL, Fedorova ND, Jackson JD, Jacobs AR, Kiryutin B, Koonin EV, Krylov DM, Mazumder R, Mekhedov SL, Nikolskaya AN, Rao BS, Smirnov S, Sverdlov AV, Vasudevan S, Wolf YI, Yin JJ, Natale DA (2003): The COG database: an updated version includes eukaryotes. *BMC Bioinformatics* 4, 41–44. doi.org/10.1186/1471-2105-4-41
- Tatusov RL, Koonin EV, Lipman DJ (1997): A genomic perspective on protein families. *Science* 278, 631–637. doi.org/10.1126/science.278.5338.631
- Tsirigos A, Rigoutsos I (2005a): A new computational method for the detection of horizontal gene transfer events. *Nucleic Acids Res.* 33, 922–933. doi.org/10.1093/nar/gki187
- Tsirigos A, Rigoutsos I (2005b): A sensitive, support-vector-machine method for the detection of horizontal gene transfers in viral, archaeal and bacterial genomes. *Nucleic Acids Res.* 33, 3699–3707. doi.org/10.1093/nar/gki660
- Willms AR, Rouqhan PD, HeineMann JA (2006): Static recipient cells as reservoirs of antibiotic resistance during antibiotic therapy. *Theor. Popul. Biol.* 70, 436–451. doi.org/10.1016/j.tpb.2006.04.001

Molecular characterization and pathogenicity of swine influenza H9N2 subtype virus A/swine/HeBei/012/2008/(H9N2)

ZHANG RUI-HUA¹, CUI HONG-YU¹, XU MING-JU¹, LI KAI¹, CHEN HUA-LAN², WANG CUN-LIAN¹, WEI DONG¹, LI CUN-XIN, XU TONG^{1*}

¹Department of Veterinary Medicine, College of Animal Science, HeBei North University, Zhangjiakou, 075131, Hebei, P.R. China;

²China Animal Influenza Laboratory of Ministry of Agriculture, National Key Laboratory of Veterinary Biotechnology, Harbin Veterinary Research Institute of CAAS, Harbin 150001, P.R. China

Received November 15, 2010; accepted August 4, 2011

Summary. – The H9N2 subtype influenza virus (IV) is a remarkable member of the influenza A viruses because it can infect not only chickens, ducks and pigs, but also humans. Pigs are susceptible to both human and avian influenza viruses and have been proposed to be intermediate hosts for the generation of pandemic influenza viruses through reassortment or adaptation to the mammalian host. To further understand the genetic characteristics and evolution, we investigated the source and molecular characteristics of the H9N2 subtype swine influenza virus (SIV), and observed its pathogenicity in BALB/c mice. The BALB/c mice were inoculated intranasally with 100 median mouse infectious dose of A/swine/HeBei/012/2008/(H9N2) viruses to observe the pathogenicity. The HA, NP, NA and M gene were cloned, sequenced and phylogenetically analyzed with related sequences available in GenBank. The infected mice presented with inactivity, weight loss and laboured respiration, while the pathological changes were characterized by diffuse alveolar damage in the lung. The nucleotide and deduced amino acid sequence of HA, NP, NA and M gene was similar with that of A/chicken/Hebei/4/2008(H9N2). The HA protein contained 6 glycosylation sites and the motif of HA cleavage site was PARSSR GLF, which is characteristic of low pathogenic IV. In the HA, NP, M and NA gene phylogenetic trees, the isolate clustered with A/chicken/Hebei/4/2008(H9N2). The isolate possibly came from A/chicken/Hebei/4/2008(H9N2) and was partially varied during its cross-species spread.

Keywords: swine influenza virus; H9N2 subtype; sequence analysis; pathogenicity

Introduction

The RNA genome of SIV is divided into eight segments numbered one to eight. Segments number 4, 5, 6, and 7 encode HA, NP, NA, and M, respectively. The other segments and genes are important for other parts of the virion structure or function (Yin and Liu, 1997; Brown, 2000). Since each segment functions as individual gene coding

for one of the viral proteins, it enables a mutation to easily jump to another subtype. Among all eight genes, the HA and NA genes of influenza A virus mutate at highest frequencies (Fitch *et al.*, 1997, 2000). It has been generally believed that influenza adaptation to a new host requires a long evolutionary process (Webster *et al.*, 1992; Katz, 2003; Peiris *et al.*, 2007), but the IV spread from poultry and human to swine has occurred under the natural conditions (Peiris *et al.*, 2001; Xu *et al.*, 2004). Therefore, IV might spread among different species, even resulting in death of the infected host (Kendal *et al.*, 1977; Wentworth *et al.*, 1994, 1997). It was reported that the SIV virus spread to humans and led to illness and death in 1976 (Top and Russell, 1977), this strain of the IV has been spreading among humans, swine and poultry. The swine is considered as the

*Corresponding author. E-mail: xutong1969@sohu.com; fax: +86-313-4029336.

Abbreviations: EID₅₀ = median egg infectious dose; IV = influenza virus; SIV = swine influenza virus; SIV H9N2 = swine influenza H9N2 subtype virus; p.i. = post inoculation

mixer for producing new virus by gene rearrangement of human, poultry and swine influenza (Scholtissek, 1990). In recent years, the increasing number of infection and death cases caused by H5N1, H9N2, and H7N7 virus in humans has brought public interest to the IV genetics and variation in different host species.

The frequent occurrence of influenza outbreaks among humans, swine, and birds has not only caused a huge economic loss but also posed a severe threat to human health. Due to low pathogenicity of H9N2, the studies of influenza currently focus mostly on the highly pathogenic influenza viruses, such as H5N1. However, the novel H1N1 IV, which HA cleavage site appears as low virulence, emerged in humans in Mexico in early 2009 (Brown *et al.*, 1998). As of June 18, 2010, the World Health Organization (WHO) had announced that the H1N1 influenza cases have been found in 214 countries and regions worldwide, and more than 18,336 patients died from influenza A/H1N1 (WHO, 2009). The epidemic of H1N1 influenza has alarmed the world: SIV with low virulence may infect humans and cause serious public health problems. Therefore, it is urgent to further supervise the epidemic and molecular evolution of SIV. H9N2 SIV was isolated from the Hebei province of China in 2008. The genes were cloned, sequenced, phylogenetically analyzed and compared with other sequences available in GenBank. In addition, the pathogenicity in mice was investigated, with the objectives to understand the molecular evolution characteristics and pathogenic condition of mammals, and to facilitate studies of the pathogenesis of H9N2 swine influenza disease in animals and humans.

Materials and Methods

Bacterial strains and experimental animals *Escherichia coli* DH5a were conserved by Microbiology Lab of Hebei North University; SPF female BALB/c mice (6–8-week-old) and SPF chicken embryos come from Beijing Laboratory Animal Research Center, Beijing, P.R. China.

Virus isolation and identification Total 20 nasal swabs and 12 materials of lung and trachea were obtained from pigs suspected to die of swine influenza in 2008. The samples processed by conventional method were inoculated into 10-day-old chicken embryos (0.1 ml/embryo). Inoculated embryos were incubated at 37°C for 96 hrs. The allantoic fluid was then harvested and tested for hemagglutination activity. If the allantoic fluid showed hemagglutination activity, the influenza virus subtype was identified by China Animal Influenza Laboratory of Ministry of Agriculture (Harbin, P.R. China) by means of hemagglutination inhibition and neuraminidase inhibition tests.

The pathogenicity of H9N2 isolate in BALB/c mice Six- to eight-week-old female specific pathogen-free BALB/c mice

were divided into 3 groups of 16 mice each. During the experiment, animals had access to food and water ad libitum. Sixteen mice in the first group were all inoculated with A/swine/HeBei/012/2008/(H9N2) virus, which had been diluted 1:10 by sterile saline, by the natural routes of infection (50 µl, intraocular and intranasal). Eight mice in the second group were inoculated in the same way as the first group. The remaining 8 mice were not infected, but lived together with the H9N2-infected mice, in order to investigate whether the virus was transmitted from the inoculated mice to the neighbors by direct contact. The mice of the third group received diluted noninfectious allantoic fluid in place of the virus and served as mock-infected controls. All manipulations were performed under bio-safety level 3+ laboratory conditions. The study was approved by the Animal Care Committee of Hebei North University (Zhangjiakou, Hebei Province, P.R. China).

The clinical signs in infected mice were observed daily. Eight mice in the first and third group were monitored daily for morbidity, as measured by weight loss, and mortality for 14 days post inoculation (p.i.). The infected mice were necropsied timely and gross pathologic changes were observed when they died. Two of the remaining mice in the first group and living together with infected mice in second group were sacrificed on days 2, 6, and 14 p.i. The main organs were collected for virus isolation, histopathological observation, and demonstration of SIV by immunohistochemical methods.

Virus titration Virus titration was performed as previously described (Lu *et al.*, 1999). The lungs, brains, spleens, kidneys, livers, and hearts were collected, weighed, and homogenized by using a mortar and pestle in cold PBS plus antibiotics on days 2, 6, and 14 p.i. Clarified homogenates were titrated for viral infectivity in embryonated chicken eggs from initial dilutions of 1:10 (lung) or 1:2 (other organs). Viral titers were expressed as mean \log_{10} EID₅₀/gram.

Histopathologic and immunohistochemical analysis Tissues were fixed in 10% neutral buffered formalin solution, sectioned, and stained with hematoxylin-and-eosin. Duplicate sections were processed for immunohistochemistry by using biotin-streptavidin method essentially as described previously (Zaki *et al.*, 1995). A monoclonal antibody to influenza A nucleoprotein was used as the primary antibody.

RT-PCR Viral RNA was extracted from the infected allantoic fluid of SPF embryos using the RNA-SOLV® reagent RNA isolation solvent (Omega Bio-teck, Lilburn, GA) according to the manufacturer's instructions. The HA, NA, NP, and M genes were RT-PCR amplified with specific primers for IV of H9 subtype. The primers were as follows:

HA F: 5'-AGT AGT ATC ACT AAT AAC TAT AAT AC-3' and
HA R: 5'-AGG CGA CAG TCG AAT AAA TGG TGA GG-3';

NA F: 5'-GCA GGA GTG AAC ATG AAT CCA AAT C-3' and
NA R: 5'-ATT GCG AGA GCT TAT ATA GGC ATG AAG-3';

NP F: 5'-CCG AGT GAC ATC AAC ATC ATG ACG TCT C-3' and
NP R: 5'-TCT CTA ATT GTC ATA CTC CTC TGC ATT G-3';

M F: 5'-TTA TTA CTC CAG CTC TAT CTT GAC-3' and M R: 5'-GAA AGA TGA GCG TTC TAA CCG AGG-3'

The RT-PCR amplification was performed with the Onestep RNA PCR Kit (AMV) (TaKaRa, Dalian, P.R. China).

RT-PCR product cloning, identification and sequencing The RT-PCR products were separated in a 0.8% agarose gel by electrophoresis, and amplicons of the appropriate sizes were purified using an Agarose Gel DNA extraction kit (Shanghai Sheng Gong Bioengineering Co., Ltd., Shanghai, P.R. China). The RT-PCR products were cloned into the pMD-18T carrier (Takara, Dalian, P.R. China) and transformed into *E. coli* DH5α. Positive plasmid were sequenced on a ABI Prism® 377XL DNA sequencer.

Sequence analysis and phylogenetic analysis Besides the isolated viruses described above, we also utilized the sequences of other H9N2 viruses that were deposited in GenBank. The homology analyses of nucleotide and deduced amino acid sequence for HA, NA, NP, M gene were performed using DNAMAN Sequence Analysis Software package (Lynnon Biosoft, Quebec, Canada). The phylogenetic trees based on the nucleotide sequences were generated using the Software package described above.

Results

Virus isolation and identification

The total of 32 samples included nasal swabs and tissue materials. These were inoculated into SPF chicken embryos as well as consecutively blind passaged for 3 generations, and the allantoic fluid was collected for hemagglutination test. The allantoic fluids with the hemagglutination titers between 2⁶ and 2⁹ were selected, and the subtype was identified by China Animal Influenza Laboratory of Ministry of Agriculture. The isolate was then identified as swine influenza A H9N2 virus by means of hemagglutination inhibition and neuraminidase inhibition tests, and was designated as A/swine/HeBei/012/2008/ (H9N2).

The pathogenicity of the H9N2 isolate in BALB/c mice

All 8 observed mice in the first group presented inactivity, lethargy, ruffled fur, inappetence and weight loss. The weight of the infected mice decreased obviously, and was only 2/3 of the weight compared to that of the mock-infected mice (15.8 ± 1.5 vs. 21.3 ± 0.4 g) on day 6 p.i. with the A/swine/HeBei/012/2008/(H9N2) virus ($p < 0.01$). Three mice died between days 3 and 6 p.i. The H9N2-infected mice in the second group showed similar clinical signs as those in the first group from days 2 p.i. but the remaining 8 non-infected mice, living together with infected-mice, did not present abnormal signs; no mice in the control group showed abnormal symptoms.

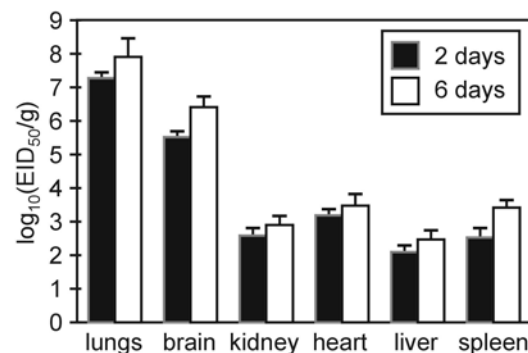


Fig. 1

Replication of influenza A (H9N2) virus in the tissues of mice infected with H9N2 virus

Mice were infected with A/swine/HeBei/012/2008/(H9N2) virus, tissues were collected on days 2 and 4 (b) p.i. and the virus was titrated in embryonated eggs. Viral titers are expressed as \log_{10} EID₅₀/g. The limit of virus detection was ≤ 101.1 EID₅₀/g for all other tissues.

Replication of the H9N2 Virus in mouse tissues

We examined the kinetics of virus replication on days 2, 6, and 14 p.i. in brain, lung, kidney, spleen, heart, and liver tissue following infection with the H9N2 isolate. As shown in Fig. 1, the H9N2 viral infection resulted in detectable virus in all the organs above on day 2 p.i. However, none of the H9N2 viruses could be detected in these tissues on day 14. Moreover, viral infection resulted in higher titers of the virus in the lungs than other organs on days 2 and 6 p.i. The peak viral titer appeared on day 6 p.i., reaching $7.2 \log_{10}$ EID₅₀/g in the lungs. However, the virus had not been isolated from any organs of the mice in co-habitation infection group and the control group.

Gross and histopathological lesions in H9N2-infected mice

Gross observation of the infected mice demonstrated lungs to be highly edematous, with profuse areas of hemorrhage and congestion, and a lot of bloody foam-like liquid flowing out of the bronchus. The lung wet-weight of infected mice increased significantly ($p < 0.01$) and was 3–5 times that of normal lung wet-weight (0.1–0.2g/0.3–0.67g, normal/infected). Liver can be seen to have a slight congestion; heart, spleen, brain and kidney did not show apparent changes. The organs of the non-inoculated mice in co-habitation infection group were normal as well as those of the control group.

Histopathological lesions mainly occurred in the lungs. It was characterized by diffuse alveolar damage in lung. In Fig. 2a: (1) there were a large number of red blood cells, inflammatory cells and edema fluid in the alveoli; Moreover, alveolar wall thickening and alveolar interstitial edema were

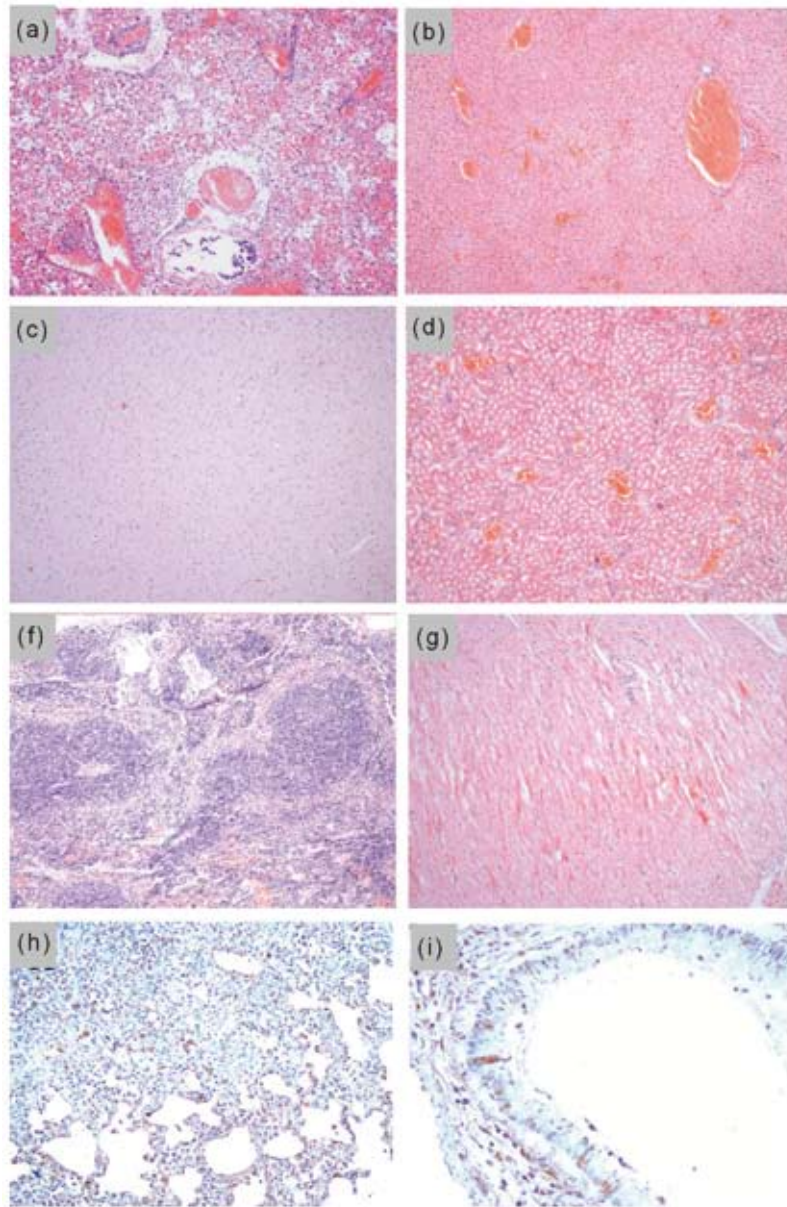


Fig. 2

Histopathologic changes and immunostaining in tissues of mice infected with H9N2 virus

Tissues were processed for H&E (a, b, c, d, e, and g) or lung sections were stained by IHC methods to demonstrate SIV (h and i). (a) H&E staining of the lungs of H9N2-infected mice showing red blood cells, inflammatory cells and edema fluid in the alveoli; Edema and thickening of alveolar walls; Edema of alveolar wall interstitium; Blood vessels and trachea surrounded by inflammatory cells; (b) H&E staining of the liver tissues of H9N2-infected mice showing congestion, red blood cell deposited in the lobular central vein (*solid arrow*) and hepatic cord; (c) H&E staining of the brain tissues of H9N2-infected mice showing congestion (*solid arrow*); (d) H&E staining of the kidney tissues of H9N2-infected mice showing congestion (*solid arrow*), tubular epithelial cell swelling, lumen narrowing, tubular epithelium stretched in the lumen to form the apophysis; (f) H&E staining of the splenic tissues of H9N2-infected mice showing normal histology; (g) H&E staining of the heart of H9N2-infected mice showing Congestion and hemorrhage in myocardial fibers (*solid arrow*). (h) SIV antigen in the nuclei and cytoplasm of type II pneumocytes (*arrow*) and (i) bronchial epithelium (*solid arrow*). Magnifications: x100 (a), x100 (b), x100 (c), x100 (d), x100 (f), x100 (g), x100 (h), x200 (i).

present; (2) there was interstitial edema around small blood vessels, surrounded with a large number of inflammatory cells (open arrow); (3) small bronchial mucous epithelium

dropout (*solid arrow*), and a large number of inflammatory cells were observed in the bronchial lumen. Immunohistochemical analysis demonstrated the presence of viral antigen

in nuclei and cytoplasm of type II pneumocytes and bronchial epithelium (Fig. 2h and i). The pathological changes in the liver showed different degrees of congestion. A number of red blood cells were found in the lobular central vein (solid arrow) and hepatic cord (Fig. 2b); The brain tissue presented mild congestion (Fig. 2c); Kidney showed congestion (solid arrow), tubular epithelial cell swelling, lumen narrowing (Fig. 2d); Splenic white pulp and red pulp were normal (Fig. 2f); Mild congestion and hemorrhage could be seen in myocardial fibers (Fig. 2g).

Cloned and sequenced HA, NA, NP, and M gene

HA, NA, NP, and M genes were amplified from A/swine/HeBei/012/2008/(H9N2) SIV, cloned into pMD-18 T vector, and sequenced. The nucleotide sequence data from this study were deposited in the GenBank (the accession numbers are CY063662, CY063664, CY063663, and CY063665).

The sequence analysis of HA, NA, NP, and M gene HA

The proteolytic cleavage site was RSSR \downarrow GLF, representing low pathogenicity, and differed from the sequence RERRRK \downarrow GLF characteristic for the high pathogenicity. Analysis of the potential glycosylation sites in the HA of the H9N2 virus isolates revealed six sites. Glycosylation sites 1 (aa 27 to 29), 2 (aa 80 to 82), 3 (aa 139 to 141), 4 (aa 296 to 298), 5 (aa 303 to 305), 6 (aa 490 to 492) were: NST, NPS, NVS, NTT, NVS, and NGT, respectively. The nucleotide sequence and deduced amino acid sequence of the HA gene was compared for sequence identity with the HA gene sequences of representative H9N2 strains from GenBank. The nucleotide sequence of HA gene from this strain shared 99% sequence identity with the HA gene from A/chicken/Hebei/4/2008(H9N2), and 83% sequence identity with the HA gene from A/mallard/Switzerland/WV3080036/2008(H9N2). The deduced amino acid sequence of the HA gene from this strain shared 99% sequence identity with the HA gene from A/chicken/Hebei/4/2008(H9N2), and 90% sequence identity with the HA gene from A/mallard/Switzerland/WV3080036/2008(H9N2). The HA phylogenetic tree is shown in the figure (Fig. 3 HA) and shows that the HA gene of this H9N2 virus shared the same clade with A/chicken/Hebei/4/2008(H9N2).

NA

ORF including the start codon and stop codon of NA was determined to encode 467 amino acids. Analysis of the potential glycosylation sites in the NA of the H9N2 virus isolates revealed five sites. Glycosylation sites 1 (aa 44 to 46), 2 (aa 66 to 68), 3 (aa 83 to 85), 4 (aa 143 to 145), 5 (aa 231 to 235) were: NPS, NST, NWS, NGT, and NGT, respectively.

The homologies of the nucleotide sequence and deduced amino acid sequence of the NA gene from this H9N2 virus and the NA gene from A/chicken/Hebei/4/2008(H9N2) and A/chicken/korea/38349-p96323/96(H9N2) were 86%–99% and 98%–100%, respectively. The NA phylogenetic tree is shown in the figure (Fig. 3 NA). The NA gene of this H9N2 virus was closely related to the A/chicken/Hebei/4/2008(H9N2), and unrelated to the A/chicken/korea/38349-p96323/96.

NP

ORF of the NP was determined to encode 498 amino acids. The nucleotide sequence and deduced amino acid sequence of NP gene from this strain both shared 99% sequence identity with the NP gene from A/chicken/Hebei/4/2008(H9N2), and 95% and 98%, sequence identity with the NP gene from A/swine/Guangxi/S11/2005(H9N2), respectively. The NP phylogenetic tree is shown in the figure (Fig. 3 NP). The NP gene of this H9N2 virus shared the same clade with the A/chicken/Hebei/4/2008(H9N2).

M

The matrix protein (M) gene encodes two viral proteins, M1 and M2. M1 coding region was 6–764 bp and was determined to encode 252 amino acids. M2 coding region containing 2 parts: region 6–31 bp and region 730–987 bp was determined to encode 97 amino acids following RNA splicing. M2 protein has amino acids (Thr11, Gly14, Glu16 Ser20, Tyr57) (Zhou *et al.*, 1999), which have poultry IV character. The nucleotide sequence and deduced amino acid sequence of M gene from this strain both shared 99% sequence identity with the M gene from A/chicken/Hebei/4/2008(H9N2), and 93% and 94% sequence identity with the M gene from A/swine/Guangxi/S11/2005(H9N2), respectively. The phylogenetic tree of the M protein is shown in the figure 3 (Fig. 3 M). The M gene of this H9N2 virus was closely related to that of A/chicken/Hebei/4/2008(H9N2).

Discussion

The investigation of IV demonstrates that the HA homology in the same subtype is about 80%–100%, and the inter-subtype homology is below 68.5% (Nobusawa *et al.*, 1991). The HA gene from A/swine/HeBei/012/2008/(H9N2) in this study shared 99% sequence identity with the HA gene from A/chicken/Hebei/4/2008(H9N2), which suggested that they were closely related to each other and may be derived from the same strain progenitors. But the HA gene from the strain in this study also shared 83% sequence identity with the HA gene from A/mallard/Switzerland/

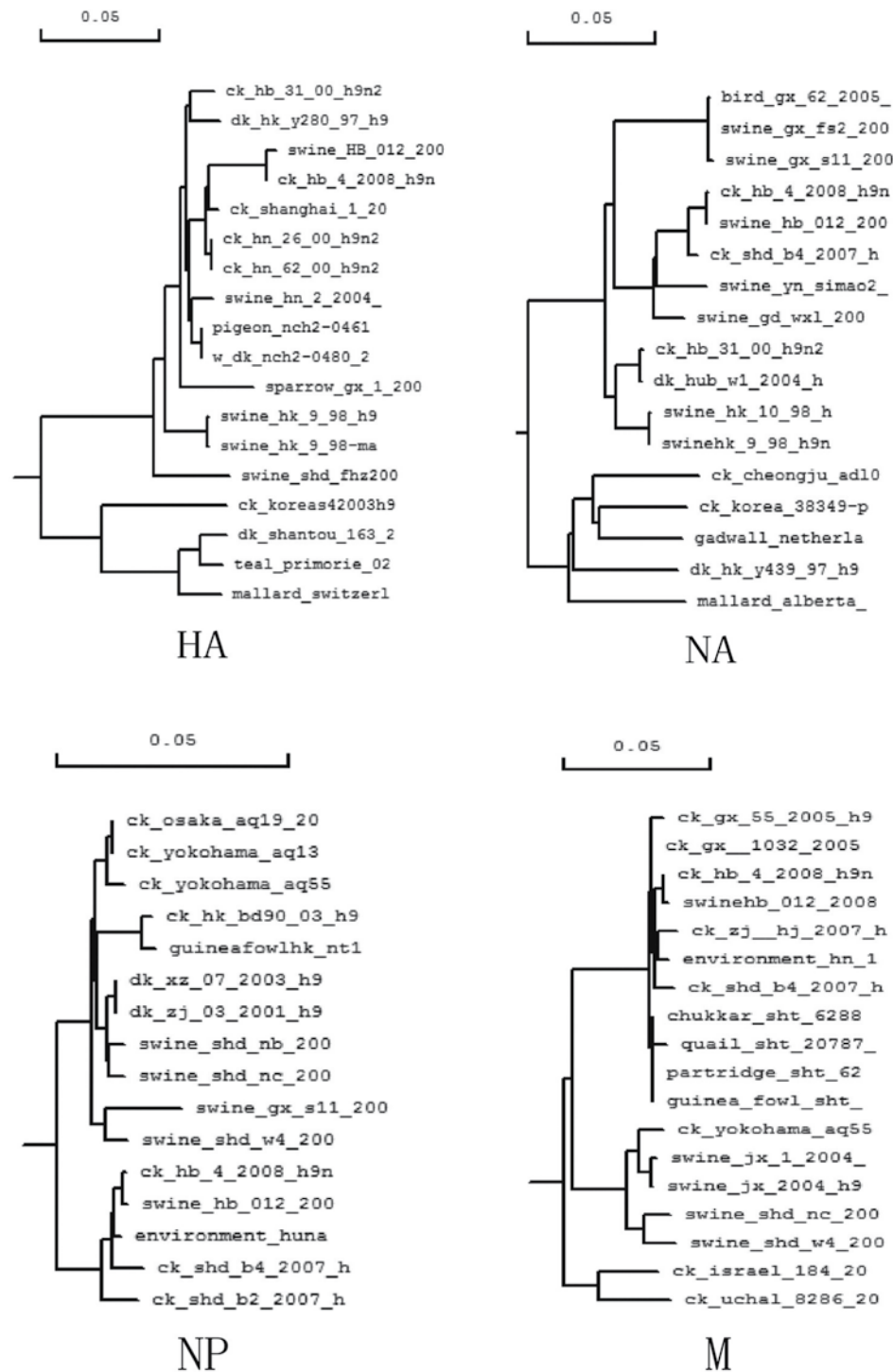


Fig. 3

Phylogenetic tree of the HA, NA, NP, and M gene of A/HeBei/012/2008/(H9N2)

Phylogenetic analysis of HA, NA, NP, and M gene of A/HeBei/012/2008/(H9N2) virus circulating in China. Reference strains were obtained from the GenBank. CK = chicken; DK = duck.

WV3080036/2008(H9N2). The representative sequences of H9N2 virus isolated from different hosts were downloaded from GenBank in order to investigate the origin and distribution of A/swine/HeBei/012/2008/(H9N2). The results of sequence analysis and phylogenetic trees show that the investigated H9N2 SIV was separated in different time and place then A/chicken/Hebei/4/2008(H9N2), A/duck/hongkong/y280/97(H9N2), A/pigeon/nangchang/2-04612000(H9N2) and A/sparrow/guangxi/1/2005 (H9N2). As the A/swine/HeBei/012/2008/(H9N2) virus is closely related to these isolates, it can be concluded that the H9N2 influenza viruses from different hosts may have the same origin and have no obvious regional characters. This also proves the notion that IV can spread across species. It also suggests that the virus isolated far away from the prevailing area may have the same origin. However, the variation may occur during its spread, because the virus always tends to avoid the hosts' immune system (Brown, 2000). Therefore, the cross-species spread increases the possibility of variation and improves the variation capability of the virus antigen, which makes it more difficult to prevent and control the influenza.

The motif of the HA cleavage site is PARSSR GLF, which is characteristic of low pathogenic IV. Our data indicates that A/swine/HeBei/012/2008/(H9N2) virus HA has a substitution G226Q. This altered HA doesn't exhibit the characteristics of avian IV HAs (Vines *et al.*, 1998). This mutation may occur during the virus transmission from birds to swine and the adaptation to the new host. However, the amino acid residues (Thr11, Gly14, Glu16, Ser20, Tyr57) related to host specificity of matrix protein 2 were all avian-specific, suggesting the mutation did not occur in related regions. It also indicates that the mutation rate of the external protein HA is higher than that of the internal protein M. It is consistent with the results of the nucleotide homology analysis. HA protein is an important external glycoprotein of influenza virus, which plays an important role in its virulence, host specificity and immune response. The increasing or decreasing number of glycosylation sites can affect the characteristics of virus antigen, receptor binding site and biology (Meng *et al.*, 2009). The analysis of the deduced glycosylation sequence indicated that some glycosylation sites were lost in HA of A/swine/HeBei/012/2008/(H9N2). The lost glycosylation sites might have influence on the biological character of the virus, which needs to be further investigated in the future.

BALB/c mice have been successfully used for evaluation of pathogenesis, immunization and antiviral drugs to the H5N1 IV, indicating that BALB/c mice are a suitable animal model to study the highly pathogenic H5 virus (Xu *et al.*, 2006, 2009). Because of its low pathogenicity, there are few studies on pathogenicity of H9N2 IV in the BALB/c mouse model. Therefore, the pathogenicity of H9N2 SIV in mice was also investigated in this study. The results showed that A/swine/HeBei/012/2008/(H9N2) virus not only could in-

fect BALB/c mice but also was highly pathogenic to them. However, this result is in contrast with the theory of low pathogenicity due to a specific HA protein cleavage site. The difference may be due to the molecular pathogenesis of IV in poultry and mammals. Moreover, the novel H1N1 flu, that first emerged in Mexico early in 2009, and quickly spread throughout nearly the whole the world, was also confirmed to be a low pathogenic virus by the analysis of the HA cleavage site motif. However, the strain caused fatal infections in some individuals, and resulted in death of thousands of patients. In this study we found that the pathogenicity of A/swine/HeBei/012/2008/(H9N2) virus in mice is in a way similar to the novel H1N1 virus. Because of the fatal H9N2-SIV infections in mice, it may potentially become a virus causing human infection. Therefore, further investigation of the isolate's pathogenesis in mammals has to be conducted in the future. Combined with the sequencing results of A/swine/HeBei/012/2008/(H9N2) HA, NA, NP and M and the phylogenetic tree, it can be found that the virus strain used in this study is closely related to the A/chicken/Hebei/4/2008(H9N2) virus and may be derived from the same strain progenitor. Therefore, it can be concluded that A/swine/HeBei/012/2008/(H9N2) may come from H9N2 avian IV and was partially varied during cross-species spread.

Acknowledgements. This study was supported by the Natural Science Foundation of HeBei province of China (Grant No. C2009001028).

References

- Brown IH (2000): The epidemiology and evolution of influenza viruses in pigs. *Vet. Microbiol.* 4, 29–46. [doi.org/10.1016/S0378-1135\(00\)00164-4](https://doi.org/10.1016/S0378-1135(00)00164-4)
- Brown IH, Harris PA, McCauley JW, Alexander DJ (1998): Multiple genetic reassortment of avian and human influenza A viruses European pigs, resulting in the emergence of an H1N2 virus of novel genotype. *J. Gen. Virol.* 79, 2947–2955
- Fitch WM, Bush RM, Bender CA, Cox NJ (1997): Long term trends in the evolution of H (3) HA1 human influenza type A. *Proc. Natl. Acad. Sci. USA* 94, 7712–7718. doi.org/10.1073/pnas.94.15.7712
- Fitch WM, Bush RM, Bender CA, Subbarao K, Cox NJ (2000): Predicting the evolution of human influenza A. *J. Hered.* 91, 183–185. doi.org/10.1093/jhered/91.3.183
- Katz JM (2003): The impact of avian influenza viruses on public health. *Avian Dis.* 47 (Suppl.) 914–920. doi.org/10.1637/0005-2086-47.s3.914
- Kendal AP, Goldfield M, Noble GR, Dowdle WR (1977): Identification and preliminary antigenic analysis of swine influenza-like viruses isolated during an influenza outbreak at Fort Dix, New Jersey. *J. Infect. Dis.* 136 (Suppl.),

- S381–385. doi.org/10.1093/infdis/136.Supplement_3.S381
- Lu X, Tumpey TM, Morken T, Zaki SR, Cox NJ, Katz JM (1999): A mouse model for the evaluation of pathogenesis and immunity to influenza A (H5N1) viruses isolated from humans. *J. Virol.* 73, 5903–5911
- Meng XQ, Chen YX, Liu Q, Zheng M, Shi KC, Hu J (2009): Cloning and Sequence Analysis of the HA, NP, NA, M and NS Genes of H1N2 Swine Influenza Viruses. *Acta Veterinaria et Zootechnica Sinica* 40, 221–227 (in Chinese).
- Nobusawa E, Aoyama T, Kato H, Suzuki Y, Tateno Y, Nakajima K (1991): Comparison of complete amino acid sequence and receptor-binding properties among 13 serotypes of hemagglutinin of influenza A virus. *Virology* 182, 475–485. [doi.org/10.1016/0042-6822\(91\)90588-3](https://doi.org/10.1016/0042-6822(91)90588-3)
- Peiris JS, Guan Y, Markwell D, Ghose P, Webster RG, Shortridge KF (2001): Cocirculation of avian H9N2 and contemporary "human" H3N2 influenza A viruses in pigs in southeastern China: potential for genetic reassortment? *J. Virol.* 75, 9679–9686. doi.org/10.1128/JVI.75.20.9679-9686.2001
- Peiris JS, de Jong MD, Guan Y (2007): Avian influenza virus (H5N1): a threat to human health. *Clin. Microbiol. Rev.* 20, 243–267. doi.org/10.1128/CMR.00037-06
- Scholtissek C (1990): Pig as the "mixing vessel" for the creation of new pandemic influenza A viruses. *Med. Princ. Pract.* 2, 65–271.
- Top FH Jr, Russell PK (1977): Swine influenza A at Fort Dix, New Jersey (January–February 1976). IV summary and speculation. *J. Infect. Dis.* 136 (Suppl.), S376–380. doi.org/10.1093/infdis/136.Supplement_3.S376
- Vines A, Wells K, Matrosovich M, Castrucci MR, Ito T, Kawaoka Y (1998): The role of influenza A virus hemagglutinin residues 226 and 228 in receptor specificity and host range restriction. *J. Virol.* 72, 7626–7631.
- Webster RG, Bean WJ, Gorman OT, Chambers TM, Kawaoka Y (1992): Evolution and Ecology of Influenza A Viruses. *Microbiol. Rev.* 56, 152–179.
- Wentworth DE, Thompson BL, Xu X, Regnery HL, Cooley AJ, McGregor MW, Cox NJ, Hinshaw VS (1994): An influenza A(H1N1) virus, closely related to swine influenza virus, responsible for a fatal case of human influenza. *J. Virol.* 68, 2051–2058.
- Wentworth DE, McGregor MW, Macklin MD, Neumann V, Hinshaw VS (1997): Transmission of swine influenza virus to humans after exposure to experimentally infected pigs. *J. Infect. Dis.* 175, 7–15. doi.org/10.1093/infdis/175.1.7
- World Health Organization. Pandemic (H1N1) 2009 – update 110 Available from: http://www.who.int/csr/don/2010_07_23a/en/index.html (accessed July 2010).
- Xu T, Qiao J, Zhao L, He G, Li K, Wang J, Tian Y, Wang H (2009): Effect of dexamethasone on acute respiratory distress syndrome induced by the H5N1 virus in mice. *Eur. Respir. J.* 33, 852–860. doi.org/10.1183/09031936.00130507
- Xu T, Qiao J, Zhao LH, Wang GR, He GM, Li K, Tian Y, Gao M, Wang JL, Wang HY, Dong CG (2006): Acute respiratory distress syndrome induced by avian influenza A (H5N1) virus in mice. *Am. J. Respir. Crit. Care Med.* 174, 1011–1017. doi.org/10.1164/rccm.200511-1751OC
- Xu C, Fan W, Wei R, Zhao H (2004): Isolation and identification of swine influenza recombinant A/Swine/Shangdong/1/2003 (H9N2) virus. *Microbes Infect.* 6, 919–925. doi.org/10.1016/j.micinf.2004.04.015
- Yin Z, Liu JH (1997): Animal Virology. 2nd ed. Beijing : Science Press, pp. 708–709 (in Chinese).
- Zaki SR, Greer PW, Coffield LM, Goldsmith CS, Nolte KB, Foucar K, Feddersen RM, Zumwalt RE, Miller GL, Khan AS, Rollin PE, Ksiazek TG, Nichols ST, Mahy BW, Peters CJ (1995): Hantavirus pulmonary syndrome: pathogenesis of an emerging infectious disease. *Am. J. Pathol.* 146, 552–579.
- Zhou NN, Senne DA, Landgraf JS, Swenson SL, Erickson G, Rossow K, Liu L, Yoon K, Krauss S, Webster RG (1999): Genetic reassortment of avian, swine, and human influenza A viruses in American pigs. *J. Virol.* 73, 8851–8856.

Immunogenicity of a truncated enterovirus 71 VP1 protein fused to a Newcastle disease virus nucleocapsid protein fragment in mice

W.C. CH'NG, W.T. SAW, K. YUSOFF, N. SHAFEE*

Department of Microbiology, Faculty of Biotechnology and Biomolecular Sciences, Universiti Putra Malaysia,
43400 UPM Serdang, Malaysia

Received February 7, 2011; accepted August 25, 2011

Summary. – Enterovirus 71 (EV71) is one of the viruses that cause hand, foot and mouth disease. Its viral capsid protein 1 (VP1), which contains many neutralization epitopes, is an ideal target for vaccine development. Recently, we reported the induction of a strong immune response in rabbits to a truncated VP1 fragment (Nt-VP1t) displayed on a recombinant Newcastle disease virus (NDV) capsid protein. Protective efficacy of this vaccine, however, can only be tested in mice, since all EV71 animal models thus far were developed in mouse systems. In this study, we evaluated the type of immune responses against the protein developed by adult BALB/c mice. Nt-VP1t protein induced high levels of VP1 IgG antibody production in mice. Purified VP1 antigen stimulated activation, proliferation and differentiation of splenocytes harvested from these mice. They also produced significant levels of IFN- γ , a Th1-related cytokine. Taken together, Nt-VP1t protein is a potent immunogen in adult mice and our findings provide the data needed for testing of its protective efficacy in mouse models of EV71 infections.

Keywords: enterovirus 71; recombinant VP1 protein; immunogenicity

Introduction

EV71 is a small, non-enveloped virus with an icosahedral shape (Chang *et al.*, 2007), which was first isolated and identified from a fecal specimen in 1969, during an outbreak in California, USA (Schmidt *et al.*, 1974). The virus has been classified into the family of *Picornaviridae*, the genus *Enterovirus* and the species *Human enterovirus A* (King *et al.*, 2000). It is normally associated with uncomplicated diseases such as hand, foot and mouth disease (Melnick, 1996), herpangina and pharyngitis. However, neurological complications such as aseptic meningitis, acute flaccid paralysis and encephalitis may arise (Huang *et al.*, 1999; Chang, 2008).

The risk of symptomatic EV71 infection is inversely proportional to the age of patients (Abzug, 2009). During an outbreak in Taiwan in 1998, most of the victims with fatal cases were children younger than 5 years of age (Ho *et al.*, 1999). Recently, a similar outbreak in China has resulted in more than ten thousand cases, including 50 fatal cases in children (Ding *et al.*, 2009). To prevent further emergence and spread of EV71, good personal hygiene practice, quarantine, and clinical surveillance activities are commonly used (McMinn, 2002; Chang, 2008).

EV71 VP1 protein is one of the structural proteins responsible for EV71 antigenic diversity (Rotbart *et al.*, 1998). It contains many neutralization epitopes (Rueckert, 1990; Oberste *et al.*, 1999), which are crucial for virus identification and evolution studies (Chang *et al.*, 2007). Hence, VP1 has become an ideal target for immunogenicity studies and vaccine development (Wu *et al.*, 2001; Foo *et al.*, 2007b). Recently, we showed that immunization with the first 100 amino acids of VP1 (VP1t) fused to a truncated nucleocapsid protein (Nt) of NDV, which served as a carrier molecule (Kho *et al.*, 2001; Yusoff and Tan, 2001; Rabu

*Corresponding author. Email: nshafee@biotech.upm.edu.my; fax: +603-8943-0913.

Abbreviations: EV71 = enterovirus 71; IFN- γ = interferon gamma; IL-2 = interleukin 2; N = full length nucleocapsid protein; NDV = Newcastle disease virus; Nt = truncated nucleocapsid protein; VP1 = full length viral protein 1; VP1t = truncated viral protein 1

et al., 2002), induced strong antibody responses in rabbits (Sivasamugham *et al.*, 2006). This study showed that this recombinant protein, labeled as Nt-VP1t, may represent a useful candidate for EV71 vaccine development. However, its protective effects need to be studied in appropriate animal models of EV71 infection. Thus far mouse models have been found to be the most informative (Wu *et al.*, 2001; Chen *et al.*, 2006; Foo *et al.*, 2007a; Tung *et al.*, 2007). Therefore, prior to an investigation into the protective efficacy of the Nt-VP1t in a mouse model of EV71 infection, it is necessary to investigate the types of mouse immune responses that are mounted against this protein. Hence, in the present study we explored the potential immunogenic characteristics of the purified Nt-VP1t protein in adult female BALB/c mice. Our results indicate that Nt-VP1t is a potent immunogen, which is capable of inducing both humoral and cell-mediated immunity in mice.

Materials and Methods

Production and purification of recombinant proteins. Nt-VP1t and the control full length nucleocapsid protein of NDV (N) proteins were produced and purified as described previously (Sivasamugham *et al.*, 2006). The proteins were quantitated by the Bradford assay, electrophoresed in a 12% SDS-PAGE gel and blotted onto a nitrocellulose membrane. Immunodetection using primary antibodies against the VP1 protein (1:2000 dilution) and rabbit NDV antiserum (1:9000 dilution), was used to confirm the presence of each protein.

Immunization of mice. All animal experiments were approved by The Animal Care and Use Committee, Universiti Putra Malaysia (AUP No: 10R84). All animals used in this research were cared for in accordance with The Code to Care and Use of Animals in Research. Eight adult female BALB/c mice, ages six to eight weeks, were inoculated intraperitoneally with 10 µg of purified Nt-VP1t protein. Seven mice served as a control group and were inoculated intraperitoneally with 10 µg of purified N protein. The protein samples (200 µl) were emulsified with 50% Freund's complete adjuvant (Sigma, USA) for primary injection or 50% Freund's incomplete adjuvant (Sigma, USA) for booster injections. Two booster injections were given at 2 and 4 weeks after primary immunization (2-week intervals). The mice were pre-bled prior to each injection. Blood samples were collected at weeks 0, 2, 4, 6, 8, 9, and 10 after immunization. The collected sera were stored at -20°C until used.

ELISA of antibodies. The presence of VP1- and NP-IgG antibodies in sera was determined by ELISA, using purified VP1 and N proteins as the coating antigens. Purified VP1 protein was kindly provided by Prof. Mary Jane Cardosa of the Institute of Health and Community Medicine, Universiti Malaysia Sarawak. Briefly, 1.5 µg/ml of purified VP1 and N proteins were coated onto wells of 96-well ELISA plates. Following blocking and washings, 100 µl of the collected and positive control sera

(1:50 dilution) were added in duplicate into individual wells and incubated for 1 hr at room temperature. Reactions were detected using HRP-conjugated goat anti-mouse IgG antibody and the *o*-phenylenediamine dihydrochloride substrate (Sigma Aldrich, USA). Reaction intensities were measured at A490 using an ELISA microplate reader (Model 550, BioRAD, USA). The positive cut off absorbance value was defined as 3 times the absorbance of the pre-immune mice sera.

Western blot analysis. Purified VP1 and N proteins were used to examine the immunoreactivity of sera collected from immunized mice. Briefly, each viral protein was separated by SDS-PAGE and blotted onto nitrocellulose membranes. Individual lanes of the membranes were cut into strips followed by incubation with either sera from the immunized mice or the positive control VP1-antiserum and NDV-antiserum.

Splenocyte proliferation assay. Five mice from both the Nt-VP1t-immunized and control groups were sacrificed at week 9 post-immunization. Spleens from the mice were harvested and dissociated splenocytes were subjected to a Proliferation ELISA Assay (Calbiochem, Germany), according to the manufacturer's protocol. Briefly, the splenocytes were cultured in 96-well tissue culture plates at a concentration of 2×10^5 cells per well. Proliferation was induced with either 3 µg of VP1 protein or phytohemagglutinin (PHA; Sigma Aldrich, USA) at 37°C in a humidified atmosphere with 5% CO₂ for 72 hrs. Spontaneous proliferation of splenocytes in a complete medium served as a background control.

ELISA of cytokines. Culture supernatants of VP1 antigen-induced splenocytes were harvested and assayed for IL-2, IL-4, IL-10, IFN-γ production, using the Mouse Th1/Th2 ReadySETGo! ELISA Set (eBioscience, USA) as suggested by the manufacturer.

Statistical analysis. The Student *t*-test was used to analyze the experimental data in this study. Results were expressed as mean ± standard error (SE). Differences with *p* < 0.05 were considered significant. All of the tests were performed using GraphPad Prism 5 and Windows Microsoft Excel 2007.

Results

Production and purification of recombinant proteins

Nt-VP1t or the control N proteins were purified as previously described (Sivasamugham *et al.*, 2006). Each fractionated protein was analyzed by Western blot analysis and pooled selected fractions were confirmed by SDS-PAGE. N protein fractions showed a band with the expected size of approximately 55 kDa when probed with NDV antibodies (Fig. 1a, arrowhead), while Nt-VP1t fractions showed a band of approximately 60 kDa (Fig. 1b, arrow). A similar 60 kDa band was also observed when the Nt-VP1t fractions were re-probed with VP1 antibodies (Fig. 1c, arrow). Pooled and concentrated N and Nt-VP1t proteins appeared as single bands when separated by SDS-PAGE (Fig. 1d).

Induction of specific antibodies in mice

To determine the immunogenicity of the Nt-VP1t protein, immunization of adult BALB/c mice was performed. Results of an indirect ELISA on the collected sera, using VP1 as a coating antigen, showed that Nt-VP1t protein elicited high titers of VP1 IgG antibody (Fig. 2a, shaded bars). The antibody titers significantly increased ($p < 0.05$) after the primary immunization and were further enhanced following subsequent booster injections (Fig. 2a, arrows and shaded bars). The highest titers were reached after the last booster injection and the level was maintained until week 9 post-immunization. No significant VP1 IgG antibody level was detected in sera of mice immunized with the control N protein (Fig. 2a, white bars). When purified N protein was used as the capturing antigen, titers of N IgG antibodies were also found to be high in sera of both the Nt-VP1t-immunized (Fig. 2b, shaded bar) as well as in the control N-immunized sera (Fig. 2b, white bar).

In addition to the analysis by ELISA, the collected sera were also assayed against purified VP1 (Fig. 2c, upper panel) and N (Fig. 2c, lower panel) proteins by Western blot to confirm the presence of VP1- and N-antibodies, respectively. Pooled sera from Nt-VP1t-immunized mice gave a band of ~40 kDa when probed against separated VP1 protein (Fig. 2c, arrow) and a band of ~55 kDa when probed against separated N protein (Fig. 2c, arrowhead). As expected, pre-immune sera showed no reactivity with both proteins.

Stimulation of splenocytes in immunized mice

Cell-mediated immunity is important for viral clearance. In the present study, a splenocyte proliferation assay was used to monitor and investigate T-cell responses after the Nt-VP1t immunization. PHA was used as a positive stimulator to give a non-specific T-cell stimulation. When the splenocytes were activated either by PHA or VP1 proteins, the cells formed clusters (Fig. 3a, arrows). Upon PHA stimulation (Fig. 3b, white bar), there was no difference in splenocyte proliferation ($p > 0.05$) between the control and the Nt-VP1t-immunized groups. The Nt-VP1t-immunized group, on the other hand, showed significantly increased level of T-cell proliferative responses ($p < 0.05$) to VP1 protein when compared to the control group (Fig. 3b, shaded bar). The stimulation index (S.I.) for this group ($S.I. = 1.267 \pm 0.104$) was approximately 1.7 fold greater than the S.I. value for the control group.

Production of cytokines in stimulated splenocytes

To determine the secreted cytokine levels in culture supernatants of the splenocytes, a Mouse Th1/Th2 ReadySETGo! ELISA Set (eBioscience, USA) was employed. The VP1 antigen-induced splenocytes secreted a number of Th1/Th2

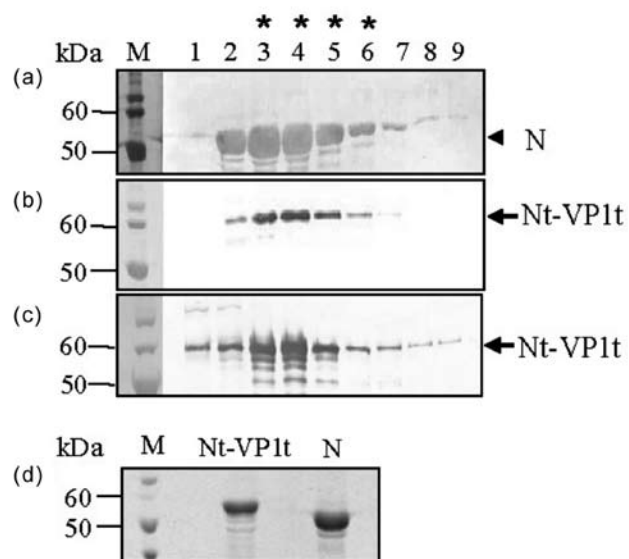


Fig. 1

Purification and concentration of N and Nt-VP1t recombinant proteins

(a-c) Western blot analysis of fractions collected after sucrose gradient centrifugation. The blots were probed using either a NDV-antisera (a, b), or a VP1-antisera (c). Asterisks indicate the fractions that were pooled and used for the SDS-PAGE in d. (d) SDS-PAGE of the pooled and concentrated Nt-VP1t and N proteins. M, Marker.

cytokines such as IL-2, IL-4, IL-10, and IFN- γ (Fig. 4) into the culture supernatant. Both of the groups produced high levels of cytokines but IL-2, IL-4, and IL-10 showed no significant differences ($p > 0.05$) between the control (Fig. 4, white bar) and the Nt-VP1t-immunized groups (Fig. 4, shaded bar). In contrast, IFN- γ , a Th1-related cytokine, was produced at significantly higher levels ($p < 0.05$) by splenocytes from Nt-VP1t-immunized mice compared to those from the control group. This result strongly suggests that the Nt-VP1t protein induced a Th1 cellular response.

Discussion

Further purification and concentration of the N and Nt-VP1t proteins yielded highly purified recombinant proteins. However, minor impurities were noted when the proteins were separated on a SDS-PAGE. Similar observations were also reported by others (Kho *et al.*, 2001; Sivasamugham *et al.*, 2006), suggesting that there was a slight degradation of the proteins following concentration and purification. Other studies also suggested that the N recombinant proteins may generate small molecular mass proteins as a result of proteolytic degradation (Mountcastle *et al.*, 1970; Makkay *et al.*, 1999).

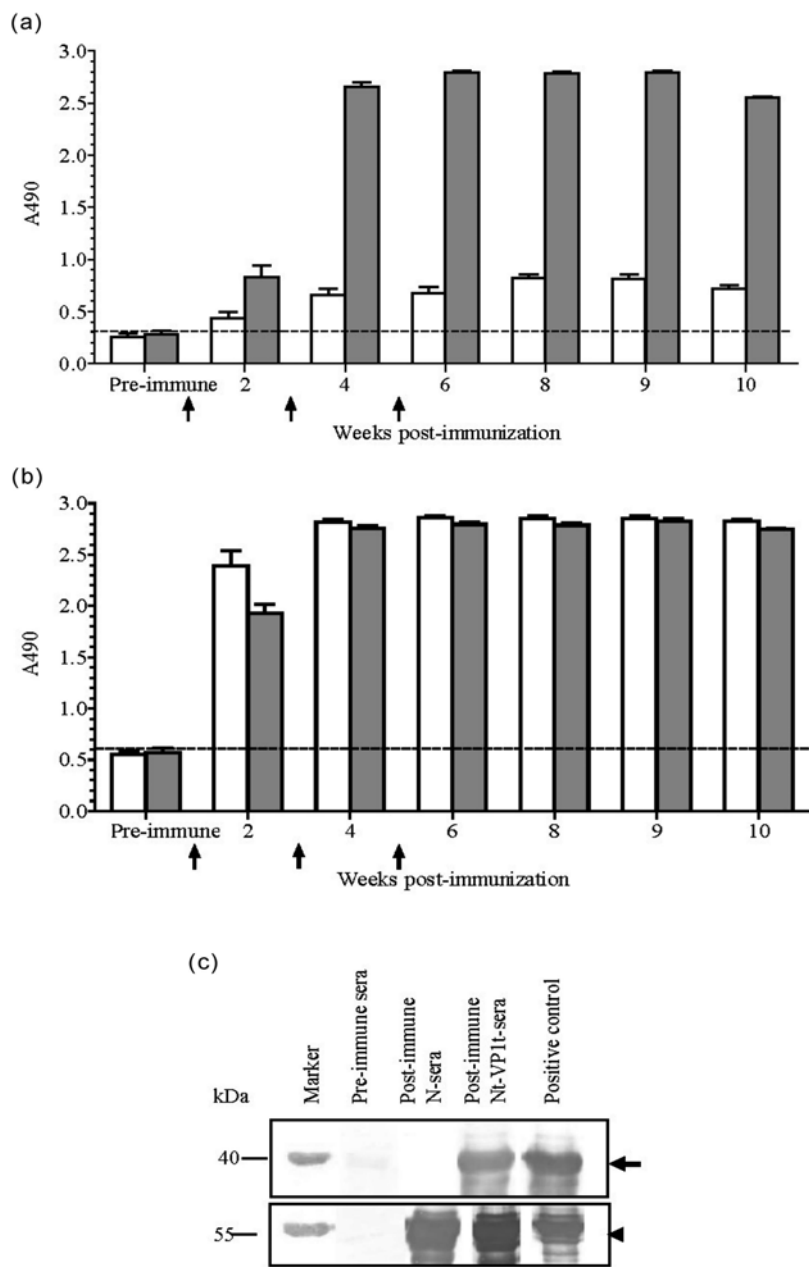


Fig. 2

IgG antibodies to N and Nt-VP1t recombinant proteins

(a, b) ELISA of VP1- (a) and N- (b) antibodies at different times post immunization with N (white bars) and Nt-VP1t (shaded bars) proteins. Broken lines indicate the cut-off values. Arrows indicate immunization time points. (c) Western blot analysis of purified VP1 (upper panel) and N (lower panel) probed with pooled sera from the immunization experiment shown in Fig. 2 a and b. VP1, EV71 viral capsid protein 1; N, full length nucleocapsid protein of NDV.

IgG is the most abundant form of immunoglobulin in serum, playing important roles in complement activation and opsonization (Wood, 2006). In most cases, high levels of IgG are formed after a secondary immunization (Wood, 2006). In the present study, purified N protein of NDV, and

VP1 protein of EV71 were used to determine murine IgG responses, as measured by ELISA and Western blot analyses. The potential of the individual N (Makkay *et al.*, 1999) and VP1 proteins (Shih *et al.*, 2000) as diagnostic agents has been evaluated. In our study, a recombinant N-VP1 fusion protein,

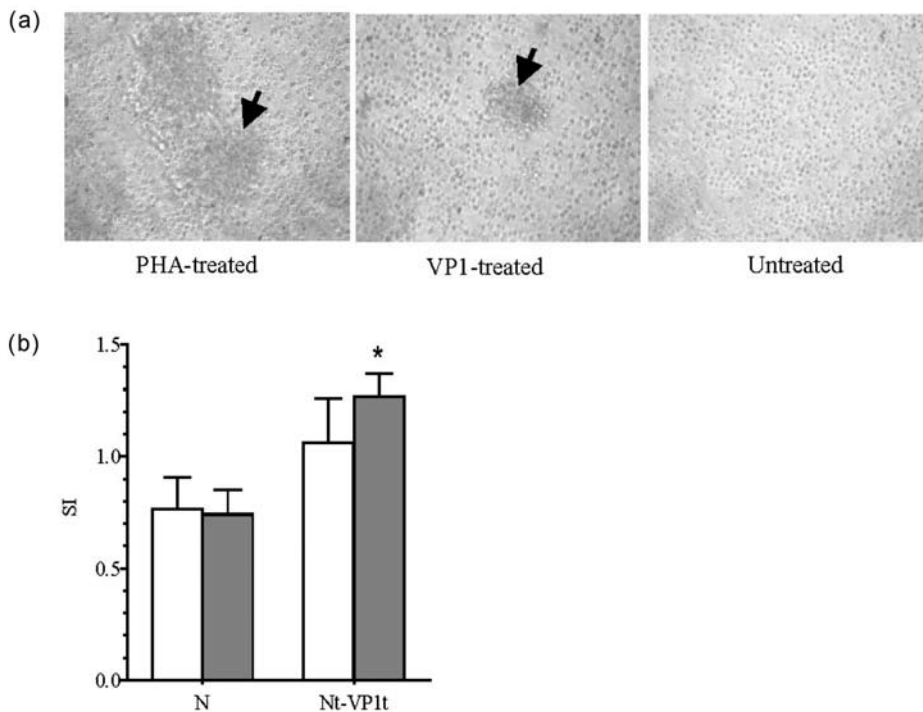


Fig. 3

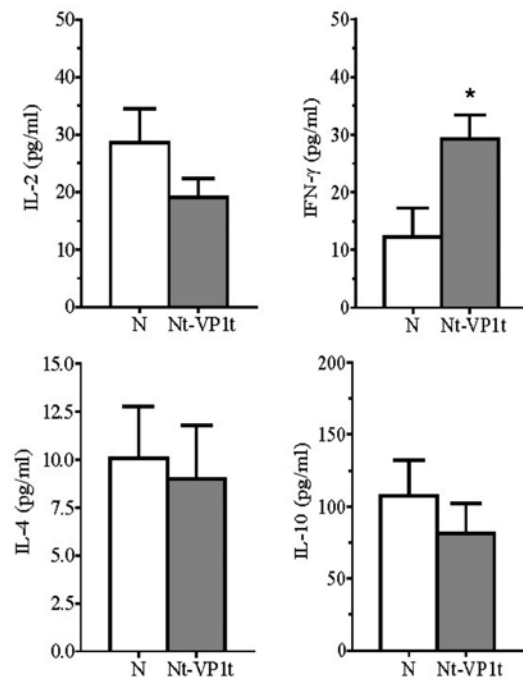
Activation of proliferation of splenocytes from the mice immunized with recombinant proteins

(a) Clumping of splenocytes stimulated with VP1 or PHA (arrows). Magnification 200x. (b) Splenocyte proliferation assay, using splenocytes harvested from mice immunized with either N and Nt-VP1t proteins, and stimulated with VP1 (shaded column) or PHA (white column). * $p < 0.05$ for the Nt-VP1t- versus the N-vaccinated mice.

namely Nt-VP1t was used. Since the N protein was used as a carrier for the VP1 protein, it was also used as an antigen for the control group. It was also chosen because it has a molecular mass similar to that of the Nt-VP1t protein.

ELISA analyses showed that mice that received Nt-VP1t protein generated statistically significant high levels of VP1 IgG antibodies when compared to the control group. This suggests that the Nt-VP1t protein acted as a strong immunogen for the humoral response. It is well known that when naïve B-cells encounter specific antigen(s), they will divide rapidly and differentiate into immunoglobulin-producing plasma cells (Goldsby *et al.*, 2003). In the present study, two booster injections of the Nt-VP1t probably led to memory B-cell activation at weeks 2 and 4 post-immunization. Consequently, greater magnitudes of antibody response were generated.

To study the pattern of cell-mediated immune responses in these mice, their spleens were harvested and further processed. In the present study, increased levels of splenocyte proliferation in the vaccinated group were observed. This suggested that this group was able to generate better immune responses, especially cell-mediated immunity, when compared to the control group. Feng *et al.* (2009) suggested that splenocyte proliferation reaction is directly proportional



Cytokines produced by VP1-stimulated splenocytes harvested from mice immunized with N and Nt-VP1t recombinant proteins

Levels of IL-2, IL-4, IL-10 and IFN- γ were detected with ELISA. * $p < 0.05$. White bars – control, shaded bars – Nt-VP1t.

to the cellular immune response that is important for viral killing. In another study, mice which received inactivated EV71 virus showed greater splenocyte proliferation than mice that received subunit vaccines (Wu *et al.*, 2001). At a high EV71 virus challenge dose, these mice also showed 80% survival after viral challenge, while the subunit vaccine failed to give protection (Wu *et al.*, 2001).

According to Wu *et al.* (2001), immunization of mice using the full-length VP1 recombinant protein resulted in a mixed Th1 and Th2 response. Th1 and Th2 subsets of helper T-cells express distinct cytokine patterns, reflecting the different immune response pathways (Del Prete and Romagnani, 1994). Th1-cells are known to be involved in cell-mediated immunity, while Th2-cells function as helper T-cells in humoral immunity (Goldsby *et al.*, 2003). In the present study, significantly higher levels of IFN- γ in culture supernatants of splenocytes from the Nt-VP1t-vaccinated group suggest that this protein promoted the Th1 immune response. This type of immune response is observed in responses to viruses and other intracellular pathogens (Bergmann *et al.*, 2001). Human patients infected with EV71 and suffering from pulmonary edema showed weaker cellular IFN- γ responses (Chang *et al.*, 2006). Since the Nt-VP1t immunization produced high levels of IFN- γ response, this subunit vaccine may hold promise as an effective EV71 vaccine and improve the outcome of EV71 infections. This notion is further supported by Cafruny and colleagues (1997), who demonstrated that mice that received IFN- γ treatment were protected from paralytic disease in cases of poliomyelitis (Cafruny *et al.*, 1997).

Altogether, our findings suggested that the Nt-VP1t protein is an ideal candidate vaccine, since it is capable of inducing humoral immunity as well as cell-mediated immunity in adult mice. However, strong antibody responses generated after immunization can only indicate good immunogenicity of the protein. Additional studies such as viral challenge should be performed in suitable animal models to evaluate the protective efficacy of Nt-VP1t against EV71 infection.

Acknowledgments. This work was partially supported by grants 04-01-09-0802RU, 07-05-IFN-MEB006 and 07-05-MGI-GMB009 from the Malaysian Ministry of Science, Technology and Innovation. The authors would like to thank Professor Eric J. Stanbridge for his editorial assistance in the preparation of this manuscript, and J. Y. Lim for his technical assistance.

References

- Abzug MJ (2009): Enterovirus 71: emergence of the new poliomyelitis. *South Afr. J. Epidemiol. Infect.* 24, 5–8 Bergmann C, Van Hemmen JL, Segel LA (2001): Th1 or Th2: how an appropriate T helper response can be made. *Bull. Math. Biol.* 63, 405–430. doi.org/10.1006/bulm.2000.0215
- Cafruny WA, Haven TR, Lawson SR, Wong GH, Rowland RR (1997): Inhibition of virus-induced age-dependent poliomyelitis by interferon-gamma. *Antiviral Res.* 36, 1–9. [doi.org/10.1016/S0166-3542\(97\)00031-4](https://doi.org/10.1016/S0166-3542(97)00031-4)
- Chang LY (2008): Enterovirus 71 in Taiwan. *Pediatr. Neonatol.* 49, 103–112. [doi.org/10.1016/S1875-9572\(08\)60023-6](https://doi.org/10.1016/S1875-9572(08)60023-6)
- Chang LY, Hsiung CA, Lu CY, Lin TY, Huang FY, Lai YH, Chiang YP, Chiang BL, Lee CY, Huang LM (2006): Status of cellular rather than humoral immunity is correlated with clinical outcome of enterovirus 71. *Pediatr. Res.* 60, 466–471. doi.org/10.1203/01.pdr.0000238247.86041.19
- Chang LY, Shih SR, Huang LM, Lin TY (2007): Enterovirus 71 encephalitis. In Fong, IW, Alibeck K (Eds): *New and Evolving Infections of the 21st Century*. Springer, New York, pp. 295–325. doi.org/10.1007/978-0-387-32830-0_8
- Chen HF, Chang MH, Chiang BL, Jeng ST (2006): Oral immunization of mice using transgenic tomato fruit expressing VP1 protein from enterovirus 71. *Vaccine* 24, 2944–2951. doi.org/10.1016/j.vaccine.2005.12.047
- Del Prete G, and Romagnani S (1994): The role of TH1 and TH2 subsets in human infectious diseases. *Trends Microbiol.* 2, 4–6. [doi.org/10.1016/0966-842X\(94\)90336-0](https://doi.org/10.1016/0966-842X(94)90336-0)
- Ding NZ, Wang XM, Sun SW, Song Q, Li SN, He CQ (2009): Appearance of mosaic enterovirus 71 in the 2008 outbreak of China. *Virus Res.* 145, 157–161. doi.org/10.1016/j.virusres.2009.06.006
- Feng CY, Li QT, Zhang XY, Dong K, Hu BY, Guo XK (2009): Immune strategies using single-component LipL32 and multi-component recombinant LipL32-41-OmpL1 vaccines against leptospira. *Braz. J. Med. Biol. Res.* 42, 796–803. doi.org/10.1590/S0100-879X2009005000013
- Foo DG, Alonso S, Chow VT, Poh CL (2007a): Passive protection against lethal enterovirus 71 infection in newborn mice by neutralizing antibodies elicited by a synthetic peptide. *Microbes Infect.* 9, 1299–1306. doi.org/10.1016/j.micinf.2007.06.002
- Foo DG, Alonso S, Phoon MC, Ramachandran NP, Chow VT, Poh CL (2007b): Identification of neutralizing linear epitopes from the VP1 capsid protein of Enterovirus 71 using synthetic peptides. *Virus Res.* 125, 61–68. doi.org/10.1016/j.virusres.2006.12.005
- Goldsby RA, Kindt TJ, Osborne BA, Kuby J (2003): Immunology. W.H. Freeman and Company, New York Ho M, Chen ER, Hsu KH, Twu SJ, Chen KT, Tsai SF, Wang JR, Shih SR (1999): An epidemic of enterovirus 71 infection in Taiwan. Taiwan Enterovirus Epidemic Working Group. *N. Engl. J. Med.* 341, 929–935. doi.org/10.1056/NEJM199909233411301
- Huang CC, Liu CC, Chang YC, Chen CY, Wang ST, Yeh TF (1999): Neurologic complications in children with enterovirus 71 infection. *N. Engl. J. Med.* 341, 936–942. doi.org/10.1056/NEJM199909233411302
- Kho CL, Tan WS, Yusoff K (2001): Production of the nucleocapsid protein of Newcastle disease virus in Escherichia coli and its assembly into ring-and nucleocapsid-like particles. *J. Microbiol.* 39, 293–299.
- King AMQ, Brown F, Christian P, Hovi T, Hyypia T, Knowles NJ, Lemon SM, Minor PD, Palmenberg AC, Skern T,

- Stanway G (2000): Picornaviridae. In MHV Van Regenmortel, CM Fauquet, DHL Bishop, CH Calisher, EB Carsten, MK Estes, SM Lemon, J Maniloff, MA Mayo, DJ McGeoch, CR Pringle, RB Wickner (Eds): Virus Taxonomy: the Classification and Nomenclature of Viruses. The Seventh Report of the International Committee for the Taxonomy of Viruses. Academic Press, New York, pp. 657–673.
- Makkay AM, Krell PJ, Nagy E (1999): Antibody detection-based differential ELISA for NDV-infected or vaccinated chickens versus NDV HN-subunit vaccinated chickens. *Vet. Microbiol.* 66, 209–222. [doi.org/10.1016/S0378-1135\(99\)00016-4](https://doi.org/10.1016/S0378-1135(99)00016-4)
- McMinn PC (2002): An overview of the evolution of enterovirus 71 and its clinical and public health significance. *FEMS Microbiol. Rev.* 26, 91–107. doi.org/10.1111/j.1574-6976.2002.tb00601.x
- Melnick JL (1996): Enteroviruses: polioviruses, coxsackieviruses, echoviruses, and newer enteroviruses. In BN Fields, DM Knipe, PM Howley, RM Chanlock, JL Melnick, TP Monath, B Roizman, E Straus (Eds): *Fields Virology*. Lippincott-Raven Publishers, Philadelphia, pp. 655–712.
- Mountcastle WE, Compans RW, Caliguiria LA, Choppin PW (1970): Nucleocapsid protein subunits of simian virus 5, Newcastle disease virus, and Sendai virus. *J. Virol.* 6, 677–684.
- Oberste MS, Maher K, Kilpatrick DR, Pallansch MA (1999): Molecular evolution of the human enteroviruses: correlation of serotype with VP1 sequence and application to picornavirus classification. *J. Virol.* 73, 1941–1948.
- Rabu A, Tan WS, Kho CL, Omar AR, Yusoff K (2002): Chimeric Newcastle disease virus nucleocapsid with parts of viral hemagglutinin-neuraminidase and fusion proteins. *Acta Virol.* 46, 211–217.
- Rotbart HA, O'Connell JF, McKinlay MA (1998): Treatment of human enterovirus infections. *Antiviral Res.* 38, 1–14. [doi.org/10.1016/S0166-3542\(97\)00068-5](https://doi.org/10.1016/S0166-3542(97)00068-5)
- Rueckert RR (1990): Picornaviruses and their replication. In BN Fields, and DM Knipe (Eds): *Virology*. Raven Press, New York, pp. 507–548.
- Schmidt NJ, Lennette EH, Ho HH (1974): An apparently new enterovirus isolated from patients with disease of the central nervous system. *J. Infect. Dis.* 129, 304–349. doi.org/10.1093/infdis/129.3.304
- Shih SR, Li YS, Chiou CC, Suen PC, Lin TY, Chang LY, Huang YC, Tsao KC, Ning HC, Wu TZ, Chan EC (2000): Expression of capsid protein VP1 for use as antigen for the diagnosis of enterovirus 71 infection. *J. Med. Virol.* 61, 228–234. [doi.org/10.1002/\(SICI\)1096-9071\(200006\)61:2<228::AID-JMV9>3.0.CO;2-R](https://doi.org/10.1002/(SICI)1096-9071(200006)61:2<228::AID-JMV9>3.0.CO;2-R)
- Sivasamugham LA, Cardosa MJ, Tan WS, Yusoff K (2006): Recombinant Newcastle Disease virus capsids displaying enterovirus 71 VP1 fragment induce a strong immune response in rabbits. *J. Med. Virol.* 78, 1096–1104. doi.org/10.1002/jmv.20668
- Tung WS, Bakar SA, Sekawi Z, Rosli R (2007): DNA vaccine constructs against enterovirus 71 elicit immune response in mice. *Genet. Vaccines Ther.* 5, 6. doi.org/10.1186/1479-0556-5-6
- Wood P (2006): *Understanding Immunology*. Benjamin Cummings, New York.
- Wu CN, Lin YC, Fann C, Liao NS, Shih SR, Ho MS (2001): Protection against lethal enterovirus 71 infection in newborn mice by passive immunization with subunit VP1 vaccines and inactivated virus. *Vaccine* 20, 895–904. [doi.org/10.1016/S0264-410X\(01\)00385-1](https://doi.org/10.1016/S0264-410X(01)00385-1)
- Yusoff K, Tan WS (2001): Newcastle disease virus: macromolecules and opportunities. *Avian Pathol.* 30, 439–455. doi.org/10.1080/03079450120078626

Studies on interaction of cucurbit aphid-borne yellow virus proteins using yeast two-hybrid system and bimolecular fluorescence complementation

X.H. CHEN¹, H.Y. XIANG², Z. WANG³, Y.J. ZHANG⁴, C.G. HAN^{2,4}, D.W. LI⁴, J.L. YU⁴, Y.Q. CHENG^{1*}

¹Pomology/Laboratory of Stress Physiology and Molecular Biology for Tree Fruits, Key Laboratory of Beijing Municipality, College of Agronomy and Biotechnology, China Agricultural University, Beijing 100193, P.R. China; ²Department of Plant Pathology, College of Agronomy and Biotechnology, China Agricultural University, Beijing 100193, P.R. China; ³Beijing Agricultural Products Quality Service Station, Beijing 100101, P.R. China; ⁴State Key Laboratory for Agrobiotechnology, College of Biological Sciences, China Agricultural University, Beijing 100193, P.R. China

Received January 21, 2011; accepted August 22, 2011

Summary. – In this article, yeast two-hybrid system (YTHS) and bimolecular fluorescence complementation (BiFC) were used to analyze the interactions of cucurbit aphid-borne yellows virus (CABYV)-encoded proteins. P0, P1, P1-2, P3, P4, and P5 were tested by YTHS in all possible pairwise combinations, and only P3/P3 interaction was detected. Results obtained by BiFC further confirmed the self-interaction of P3, and the subcellular localization of reconstituted YFP fluorescence was observed mainly in nuclei of *Nicotiana benthamiana* leaf epidermal cells. Domains involved in P3/P3 self-interaction were analyzed by YTHS and BiFC using deletion mutants. The results showed that R domain (residues 1–61) in the N-terminus could self-interact, and it also interacted with the S domain (residues 62–199) in the C-terminus of P3. The present work would serve as a molecular basis for further characterization of CABYV proteins, and the regions involved in P3/P3 self-interaction could provide the clue for understanding the capsid assembly pathway of CABYV.

Keywords: Polerovirus; protein-protein interaction; subcellular localization; interaction domain

Introduction

CABYV is a member of the genus *Polerovirus* in the family *Luteoviridae*. Its icosahedral virion is approximately 25 nm in diameter, containing a single-stranded RNA of 5.6 Kb in length (Guilley *et al.*, 1994). The virus was first reported to infect cultivated cucurbits in France, causing a severe disease (Lecoq *et al.*, 1992). CABYV now infects cucurbits (almost all *Cucurbitaceae*) widely throughout the world with economic importance. In China, our previous works showed that CABYV occurred widely in Mainland (Xiang *et al.*, 2008; Shang *et al.*,

2009) and the complete RNA genome of the CABYV Chinese isolate (CABYV-CHN) was determined (Xiang *et al.*, 2008).

CABYV genome comprises six major open reading frames (ORFs 0–5) encoding proteins P0, P1, P1-2, P3, P4, and P5 (Guilley *et al.*, 1994; Xiang *et al.*, 2008). In the genus *Polerovirus*, P0 encoded by the first open reading frame (ORF0) is a potent suppressor of gene silencing (Pazhouhandeh *et al.*, 2006), and it is indispensable for virus accumulation (Sadovy *et al.*, 2001). P1 and P1-2 (expressed as an ORF1-ORF2 fusion protein by translational frameshift) are necessary for virus replication (Nickel *et al.*, 2008). P3 (the major capsid protein), encoded by the ORF3, controls the virion formation, and it is essential in the aphid transmission process (Brault *et al.*, 2003). P4 is thought to be the movement protein based on its biochemical properties and subcellular localization (Tacke *et al.*, 1993; Schmitz *et al.*, 1997), but the requirement of the putative movement protein might be host dependent (Lee *et al.*, 2002). P5, known as readthrough protein, is a minor coat protein required for aphid transmission (Brault *et al.*, 1995) and is also involved in

*Corresponding author. E-mail: chengyuqin@cau.edu.cn; fax: +86-10-62732771.

Abbreviations: BiFC = bimolecular fluorescence complementation; CABYV = cucurbit aphid-borne yellows virus; CP = coat protein; DAPI = 4', 6-diamidino-2-phenylindole; YTHS = yeast two-hybrid system

virus movement and accumulation in plants (Mutterer *et al.*, 1999; Peter *et al.*, 2008).

Poletroviruses are strictly phloem-limited and dependent on aphids for transmission. Infectious cDNA clones served to investigate biological roles of viral proteins (Prüfer *et al.*, 1995; Lee *et al.*, 2002; Brault *et al.*, 2003; Peter *et al.*, 2008), however, the functions of poletroviral proteins remain largely unclear. The assessment of protein interactions is an important way to better understand functions of viral proteins and the interplay between virus and host. Many examples of viral protein interactions have been reported (Guo *et al.*, 2001; Lin *et al.*, 2009; Stewart *et al.*, 2009; Shen *et al.*, 2010), however, very limited information is available for the family *Luteoviridae*, except that potato leafroll virus P4 could form homodimers (Tacke *et al.*, 1993).

In this article, we now report the protein interaction properties of CABYV using YTHS and BiFC. Our results could provide novel information about functions of proteins and capsid assembly pathway of CABYV.

Materials and methods

Plant materials and growth conditions. *N. benthamiana* plants were grown in 10 cm pots filled with a mixture of 60% vermiculite and 40% meadow soil and cultured in growth chambers (16 hrs light/8 hrs dark at 25–26°C).

Construction of plasmids. Full-length cDNA of CABYV-CHN (GenBank accession no. EU000535) was kept in our laboratory. The plasmids used in BiFC assay, pSPYNE-35S and pSPYCE-35S (for split YFP N-terminal/C-terminal fragment expression), were kind gifts from Dr Jörg Kudla (Walter *et al.*, 2004). To construct plasmids for YTHS, the coding sequences of P0, P1, P1-2, P3, P4, P5, and N-terminal (amino acid residues 1–61) and C-terminal (residues 62–199) fragments of CABYV P3 were amplified separately using LaTaq polymerase (Takara) with primer pairs F1(5'-CGCGAATTCTGAAATTGAGTCTG-3')/R1(5'-ACTGGATCCTCAGCGTTGTAAGATCTTC-3'), F2(5'-CGACATATGATGGAAGCGAACACTTTTC-3')/R2(5'-TCACATATGTCAGTTCAAGCTCCGC-3'), F2/R3(5'-GACCATATGTTATCTTTGTGGCTGC-3'), F3(5'-ACTGAATTCTGAAATACGCCGTGGCTAG-3')/R4(5'-CTAGGATCCCTATTCGGGTTTGGAC-3'), F4(5'-AATGAATTCTGCAAGGGAGGCGGAGG-3')/R5(5'-GATGGATCCCTACCTATTCGGGTTTGG-3'), F5(5'-GCACATATGATGAAATACGCCGTGGCTAG-3')/R6(5'-GCAGGATTCTTATGAGGTTTATCAGCTAG-3'), F3/R7(5'-TATGGATCCGCTGGACTCCTCC-3'), and F6(5'-CCGAAATTGAAACATTCGTATTTC-3')/R4, respectively. The PCR fragments were digested with EcoRI/BamHI (for P0, P4, P3, and P3 deletion mutants), NdeI (for P1 and P1-2), or NdeI/BamHI (for P5), and then cloned into vectors pGBKT7 and pGADT7 (Clontech laboratories, inc.), to generate the recombinant

plasmids pGBK-P0, pGAD-P0, pGBK-P1, pGAD-P1, pGBK-P1-2, pGAD-P1-2, pGBK-P3, pGAD-P3, pGBK-P4, pGAD-P4, pGBK-P5, pGAD-P5, pGBK-P3(1–61), pGAD-P3(1–61), pGBK-P3(62–199) and pGAD-P3(62–199), respectively.

For BiFC, the full-length coding sequences of P0, P4, P3, N- and C-terminal fragments of P3 were amplified separately with the primer pairs F7(5'-CGAGGATCCATGCAAATTGAGTCTGTTTC-3')/R8(5'-AGTCTCGAGGCCGTTGTAAGATCTCTG-3'), F8(5'-TATGGATCCATGCAGGGAGGCGGAGG-3')/R9(5'-CAGCTCGAGCCTATTCGGGTTTGG-3'), F9(5'-TATGGATCCATGAATAACGCCGTGGC-3')/R10(5'-ACGCTCGAGTTTCGGGTTTGGACC-3'), F9/R11(5'-GATCTCGAGGCCTGGCTCCTCCTC-3'), and F10(5'-CGCGGATCCATGAAACATTGATTTTC-3')/R10, respectively. The PCR fragments were digested with BamHI/XbaI and cloned into the vectors pSPYCE-35S and pSPYNE-35S to produce recombinant plasmids pP0-YFP^C, pP0-YFP^N, pP4-YFP^C, pP4-YFP^N, pP3-YFP^C, pP3-YFP^N, pP3(1–61)-YFP^C, pP3(1–61)-YFP^N, pP3(62–199)-YFP^C, and pP3(62–199)-YFP^N, respectively.

YTHS. YTHS tests were performed using the BD Matchmaker Library Construction and Screening kits (Clontech). Small-scale lithium acetate-mediated transformation method was used to transform pairs of constructs simultaneously into *Saccharomyces cerevisiae* strain AH109 according to the manufacturer's protocols. Transformed yeast cells were plated on synthetic dropout (SD) medium lacking leucine, tryptophan, adenine and histidine (SD/-Leu/-Trp/-Ade/-His) (high-stringency selection medium). Protein interaction was determined by colony growth on the SD/-Leu/-Trp/-Ade/-His medium. Plasmid combination of pGBKT7-53/pGADT7-RecT supplied with the kits served as a positive control. All experiments were repeated at least three times, and identical results were obtained.

BiFC assay and confocal laser scanning microscopy. *N. benthamiana* leaves were used for agroinfiltration. Agrobacterium tumefaciens strain EHA105 carrying pP0-YFP^C, pP4-YFP^C, pP3-YFP^C, pP3(1–61)-YFP^C, pP3(62–199)-YFP^C, pP0-YFP^N, pP4-YFP^N, pP3-YFP^N, pP3(1–61)-YFP^N, or pP3(62–199)-YFP^N was separately cultured in a shaker overnight at 28°C in LB medium containing streptomycin (100 mg/ml) and kanamycin (50 mg/ml), and the cells were resuspended to an OD₆₀₀ of 0.6 with MMA buffer (10 mmol/l MES/NaOH, pH 5.6, 10 mmol/l MgCl₂, 200 mmol/l acetosyringone). For coinfiltration, equal volumes of combinations were mixed prior to infiltration. *yb* protein encoded by barley stripe mosaic virus could self-interact (Bragg and Jackson, 2004). Therefore the combination of pyb-YFP^C/pyb-YFP^N (Kept in State Key Laboratory for Agrobiotechnology, China Agricultural University) was used as a positive control, and the pair of pSPYNE-35S/pSPYCE-35S served as the negative control. Observation of leaf epidermal cells for fluorescence was performed at 48–72 hrs after infiltration. To locate nuclei, the leaf tissues were infiltrated with PBS containing 10 µg/ml 4',6-diamidino-2-phenylindole (DAPI) for about 5 mins prior to observation.

Confocal microscopy was performed on a confocal laser scanning microscope (Nikon C1). A 488 nm argon laser with an emission band of 550–590 nm and a 408 nm argon laser with an emission band of 515–530 nm were used for YFP and DAPI staining detections, respectively.

Results and Discussion

P3/P3 self-interaction in yeast cells

CABYV-encoded proteins, P0, P1, P1-2, P3, P4, and P5 were assessed in all possible pairwise combinations

(6 activation domain fusions \times 6 binding domain fusions = 36 pairwise combinations) for interactions in a YTHS. It was concluded that six CABYV proteins could not interact with each other, because transformants of protein pairs (P0/P1, P0/P1-2, P0/P3, P0/P4, P0/P5, P1/P1-2, P1/P3, P1/P4, P1/P5, P1-2/P3, P1-2/P4, P1-2/P5, P3/P4, P3/P5, and P4/P5) could not grow on agar plates of SD/-Leu/-Trp/-Ade/-His media. Limitations of YTHS may account for the failure to detect some interactions, but it is possible that proteins of CABYV might not interact directly, or host factors are necessary to detect interactions. Further studies on protein-protein interaction in CABYV-infected plants are needed to test these possibilities.

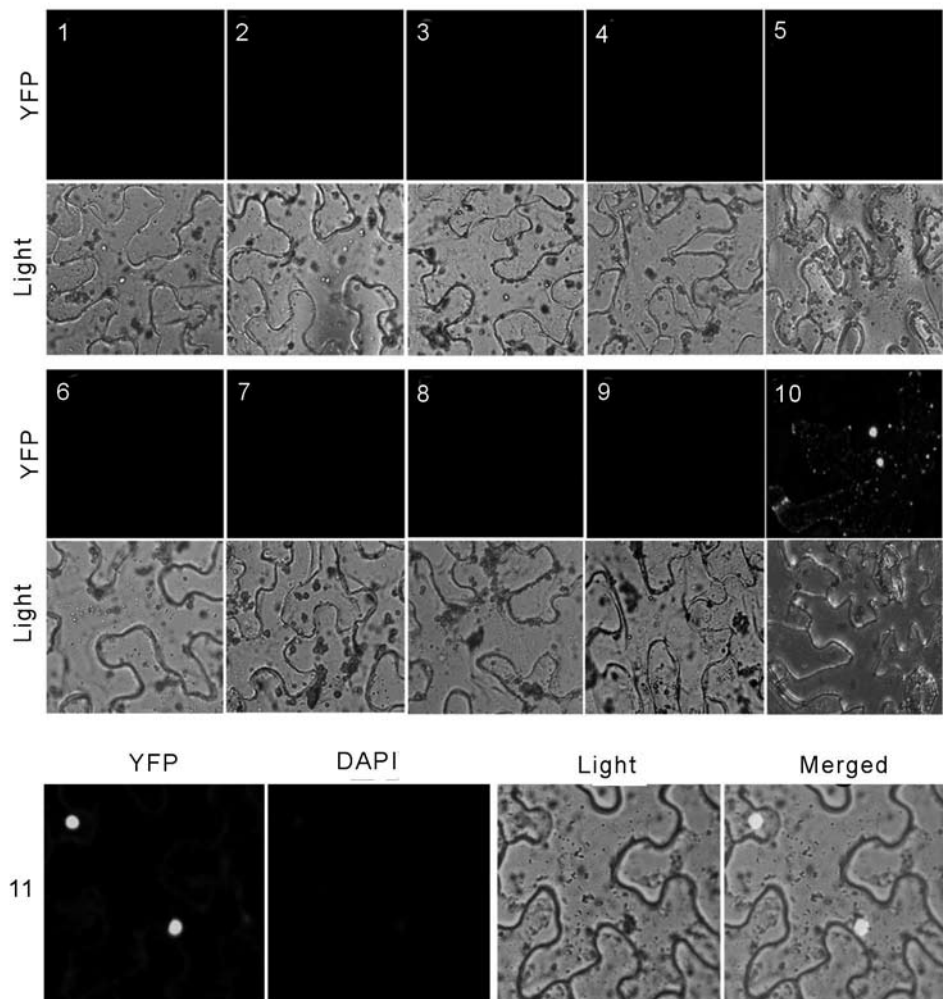


Fig. 1

Analysis of interactions of P0, P3, and P4 of CABYV by BiFC

Panels 1–11, images of *N. benthamiana* leaf epidermis transformed with constructs pP0-YFP^N/pP0-YFP^C, pP0-YFP^N/pP3-YFP^C, pP0-YFP^N/pP4-YFP^C, pP0-YFP^C/pP3-YFP^N, pP0-YFP^C/pP4-YFP^N, pP3-YFP^N/pP4-YFP^C, pP3-YFP^C/pP4-YFP^N, pP4-YFP^N/pP4-YFP^C, pSPYNE-35S/pSPYCE-35S (negative control), pyb-YFP^C/pyb-YFP^N (positive control), and pP3-YFP^N/pP3-YFP^C, respectively. YFP: YFP fluorescence image (green); Light: bright-field image; DAPI: DNA-selective dye DAPI image indicating the positions of nuclei in cells; Merged:YFP, DAPI, and bright-field overlay.

We also tested for self-interaction properties of P0, P1, P1-2, P3, P4, and P5, and only transformants of pGBK-P3/pGAD-P3 could grow on the high-stringency selection medium, which suggested P3 could self-interact. Virus capsid assembly requires repeated interaction of CP (coat protein) subunits. Self-interaction of CABYV P3 in yeast is consistent with observations in other viruses (Guo *et al.*, 2001; Hallan and Gafni, 2001; Lin *et al.*, 2009).

Confirmation of P3/P3 interaction in living plant cells by BiFC

Based on the results obtained by YTHS, we further analyzed interaction properties of P3 by BiFC, and also chose P0 and P4 for further demonstration. No or negligible fluorescence was displayed in leaves that were co-infiltrated with combinations of pP0-YFP^N/pP0-YFP^C, pP0-YFP^N/pP3-YFP^C, pP0-YFP^N/pP4-YFP^C, pP0-YFP^C/pP3-YFP^N, pP0-YFP^C/pP4-YFP^N, pP3-YFP^N/pP4-YFP^C, pP3-YFP^C/pP4-YFP^N, or pP4-YFP^N/pP4-YFP^C (Fig. 1, panels 1–8), indicating that P0, P3, and P4 could not interact with each other, and P0, P4 were not able to self-interact in plant cells. However, the reconstitution of YFP fluorescence was observed in *N. benthamiana* leaf epidermis coinfiltrated with the pair of pP3-YFP^N/pP3-YFP^C (Fig. 1, panel 11), which confirmed the P3 self-interaction.

We did not observe the P4/P4 interaction neither by YTHS nor by BiFC. Each member in the same genus may have unique protein-protein interaction patterns (Urcuqui-Inchima *et al.*, 1999), and as for P4, sequence identity between potato leafroll virus and CABYV is relatively low (about 40%), so homotypic interaction of P4 may not be a general phenomenon for all *Polerovirus* members. Another possibility is that the limitations of YTHS and BiFC, such as nuclear entry of fusion proteins in YTHS and insufficient flexibility to allow reconstitution of the split YFP fragments in BiFC assay, might account for the failure to detect the interaction.

Self-interaction of intact CABYV P3 protein was observed mainly in nucleus, and weak fluorescence was detected in the cytoplasm (Fig. 2, panel 11). Predicted nuclear localization signals (NLSs) in arginine-rich region of CABYV P3 analyzed with PSORT II prediction (<http://psort.hgc.jp/form2.html>) (data not shown here) might account for the nuclear targeting. We currently do not know why CABYV CP enters the nucleus, however, our results are quite similar to those reported for other *Luteoviridae* members (Nass *et al.*, 1995; Haupt *et al.*, 2005).

R domain interacted with itself and with S domain in P3

Polerovirus capsids are thought to be assembled from approximately 180 CP subunits according to $T = 3$ symme-

try (Lee *et al.*, 2005). The CP of icosahedral viruses generally contains two domains, the N-terminal arginine-rich domain(R) and the shell domain (S) (Terradot *et al.*, 2001), and both domains are critical for viral capsid formation (Lokesh *et al.*, 2002; Brault *et al.*, 2003; Kaplan *et al.*, 2007). Therefore, two deletion mutants for each YTHS and BiFC assay were created to define regions required for the P3 self-interaction. R domain (residues 1–61) in the N-terminus of P3 could self-interact, for positive and reproducible interaction was detected when yeast cells were co-transformed with combination of pGBK-p3(1–61)/pGAD-p3(1–61) (Fig. 2a). R domain also interacted with S domain (residues 62–199) in the C-terminus of P3, but it showed directionality, because interaction was observed only when the pair of pGBK-p3(62–199)/ pGAD-p3(1–61) was co-transformed (Fig. 2a).

Fluorescent signal observed in *N. benthamiana* leaf epidermis coinfiltrated with pP3(1–61)-YFP^N/pP3(1–61)-YFP^C pair further confirmed the R / R self-interaction (Fig. 2b, panel 5). The interaction between R and S domains was also detected in plant cells and also showed directionality, because reconstituted YFP fluorescence was only observed in leaves coinfiltrated with the pair of pP3(1–61)-YFP^N/pP3(62–199)-YFP^C (Fig. 2b, panel 6). The interaction between the N-terminus of one CP and the C-terminus of the other has been reported to be needed for dimer formation in $T = 1$ icosahedral particles (Choi and Loesch-Fries, 1999; Hallan and Gafni, 2001). Based on our results we suggest that R/R and R/S interactions are probably required to assemble three CABYV capsid subunits to form a trimer.

We observed that both R/R and R/S interactions were exclusively presented in nuclei (Fig. 2b, panel 5 and 6), suggesting the capability for directing nuclear transport might be enhanced when R domain was expressed alone.

The phenomenon of directional interaction between R and S domains in yeast may be due to the fact that protein fusions in one direction might have a more favorable protein folding or exposure of binding site than those in the other direction (Guo *et al.*, 2001). On the other hand, in BiFC assay, the phenomenon may be caused by the orientation of the interacting protein pair relative to the split YFP domain that results in the insufficient flexibility to allow reconstitution of the split YFP fragments (Bracha-Drori *et al.*, 2004).

Taken together, it was demonstrated that CABYV P3 protein could interact with itself in yeast and plant cells. Our results also showed that the R domain interacting with itself and with S domain in P3 was responsible for self-interaction of P3. There is no crystallographic data available for *Luteovirid* coat protein, thus the domains involved in self-interaction of P3 might provide the clue to the understanding of polerovirus capsid assembly.

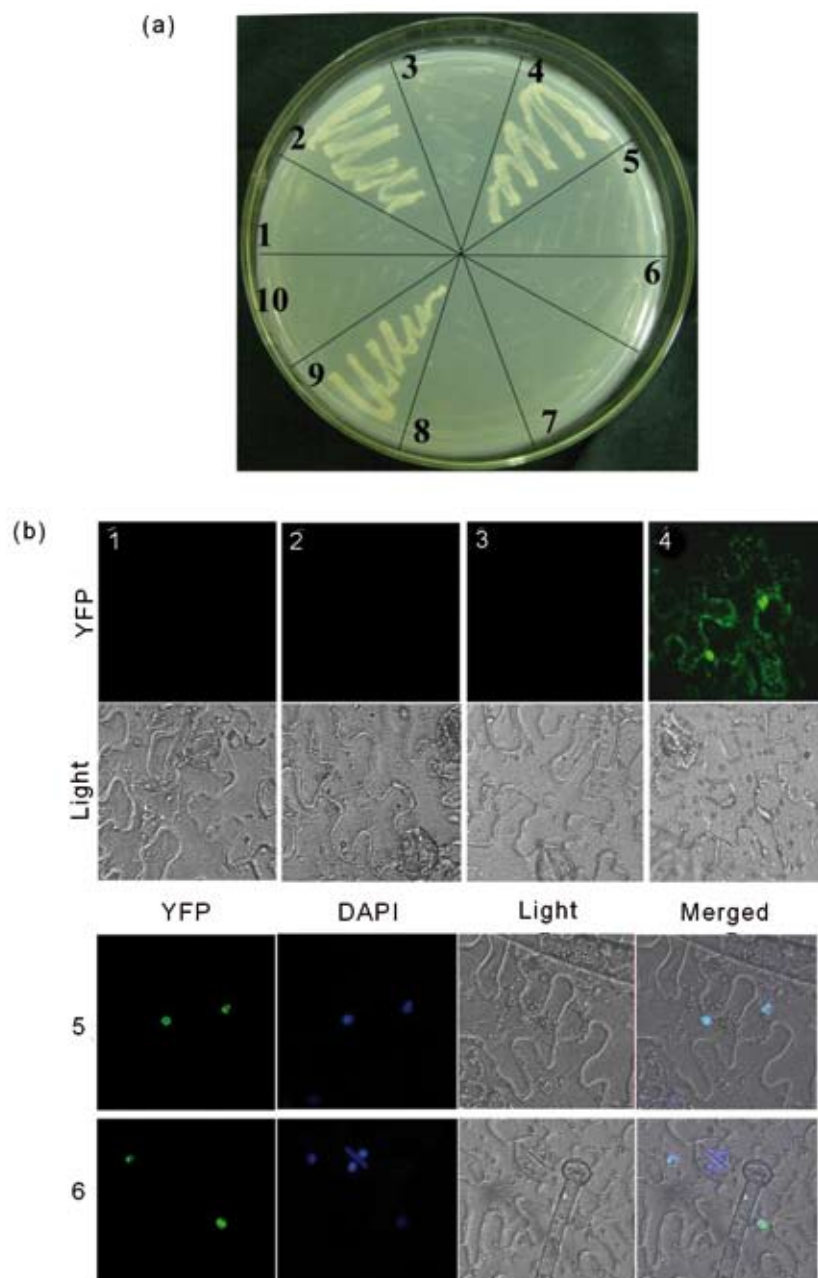


Fig.2

Domains involved in P3/P3 self-interaction

(a) Detection of domains required for P3/P3 interaction by YTHS. 1, pGBK7/pGADT7 (negative control); 2, pGBK7-53/pGADT7-RecT (positive control); 3, pGBK-P3(1-61)/pGADT7 (negative control); 4, pGBK-P3(1-61)/pGAD-P3(1-61); 5, pGBK7/pGAD-P3(1-61) (negative control); 6, pGBK-P3(62-199)/pGAD-P3(62-199); 7, pGBK-P3(62-199)/pGADT7 (negative control); 8, pGBK7/pGAD-P3(62-199) (negative control); 9, pGBK-p3(62-199)/pGAD-p3(1-61); 10, pGBK-P3(1-61)/pGAD-P3(62-199). (b) Detection of domains involved in self-interaction of P3 by BiFC. Panels 1-6, images of *N. benthamiana* leaf epidermis transformed with constructs of pP3(62-199)-YFP^N/pP3(62-199)-YFP^C, pP3(1-61)-YFP^N/pP3(62-199)-YFP^C, pSPYNE-35S/pSPYCE-35S (negative control), p β b-YFP^C/p β b-YFP^N (positive control), pP3(1-61)-YFP^N/pP3(1-61)-YFP^C, and pP3(1-61)-YFP^N/pP3(62-199)-YFP^C. YFP: YFP fluorescence image (green); Light: bright-field image; DAPI: DAPI image; Merged: YFP, DAPI, and bright-field overlay.

Acknowledgements. This work was partially supported by the National Natural Science Foundation of China (31071663, 30971896), and the Natural Science Foundation of Beijing, P.R. China (6082006).

References

- Bracha-Drori K, Shichrur K, Katz A, Oliva M, Angelovici R, Yalovsky S, Ohad N (2004): Detection of protein-protein interactions in plants using bimolecular fluorescence complementation. *Plant J.* 40, 419–427. doi.org/10.1111/j.1365-313X.2004.02206.x
- Bragg JN, Jackson AO (2004): The C-terminal region of the Barley stripe mosaic virus yb protein participates in homologous interactions and is required for suppression of RNA silencing. *Mol. Plant Pathol.* 5, 465–481. doi.org/10.1111/j.1364-3703.2004.00246.x
- Brault V, van den Heuvel JF, Verbeek M, Ziegler-Graff V, Reutenauer A, Herrbach E, Garaud JC, Guille H, Richards K, Jonard G (1995): Aphid transmission of beet western yellows luteovirus requires the minor capsid read-through protein P74. *EMBO J.* 14, 650–659.
- Brault V, Bergdoll M, Mutterer J, Prasad V, Pfeffer S, Erdinger M, Richards KE, Ziegler-Graff V (2003): Effects of point mutations in the major capsid protein of beet western yellows virus on capsid formation, virus accumulation, and aphid transmission. *J. Virol.* 77, 3247–3256. doi.org/10.1128/JVI.77.5.3247-3256.2003
- Choi J, Loesch-Fries LS (1999): Effect of C-terminal mutations of alfalfa mosaic virus coat protein on dimer formation and assembly in vitro. *Virology* 260, 182–189. doi.org/10.1099/vir.0.81696-0
- Guille H, Wipf-Scheibel C, Richards K, Lecoq H, Jonard G (1994): Nucleotide sequence of cucurbit aphid-borne yellows luteovirus. *Virology* 202, 1012–1017. doi.org/10.1006/viro.1994.1429
- Guo D, Rajamäki ML, Saarma M, Valkonen JP (2001): Towards a protein interaction map of potyviruses: protein interaction matrixes of two potyviruses based on the yeast two-hybrid system. *J. Gen. Virol.* 82, 935–939.
- Hallan V, Gafni Y (2001): Tomato yellow leaf curl virus (TYLCV) capsid protein (CP) subunit interactions: implications for viral assembly. *Arch. Virol.* 146, 1765–1773. doi.org/10.1007/s007050170062
- Haupt S, Stroganova T, Ryabov E, Kim S H, Fraser G, Duncan G, Mayo MA, Barker H, Taliansky M (2005): Nucleolar localization of potato leafroll virus capsid proteins. *J. Gen. Virol.* 86, 2891–2896. doi.org/10.1099/vir.0.81101-0
- Kaplan IB, Lee L, Ripoll DR, Palukaitis P, Gildow F, Gray SM (2007): Point mutations in the potato leafroll virus major capsid protein alter virion stability and aphid transmission. *J. Gen. Virol.* 88, 1821–1830. doi.org/10.1099/vir.0.82837-0
- Lecoq H, Bourdin D, Wipf-Scheibel C, Bon M, Lot H, Lemaire O, Herrbach E (1992): A new yellowing disease of cucurbits caused by a luteovirus, cucurbit aphid-borne yellows virus. *Plant Pathol.* 41, 749–761. doi.org/10.1111/j.1365-3059.1992.tb02559.x
- Lee L, Palukaitis P, Gray SM (2002): Host-dependent requirement for the Potato leafroll virus 17-kDa protein in virus movement. *Mol. Plant Microbe Interact.* 15, 1086–1094. doi.org/10.1094/MPMI.2002.15.10.1086
- Lee L, Kaplan I B, Ripoll DR, Liang D, Palukaitis P, Gray SM (2005): A surface loop of the potato leafroll virus coat protein is involved in virion assembly, systemic movement, and aphid transmission. *J. Virol.* 79, 1207–1214. doi.org/10.1128/JVI.79.2.1207-1214.2005
- Lin L, Shi Y, Luo Z, Lu Y, Zheng H, Yan F, Chen J, Chen J P, Adams MJ, Wu Y (2009): Protein-protein interactions in two potyviruses using the yeast two-hybrid system. *Virus Res.* 142, 36–40. doi.org/10.1016/j.virusres.2009.01.006
- Lokesh GL, Gowri TD, Satheshkumar PS, Murthy MR, Savithri HS (2002): A molecular switch in the capsid protein controls the particle polymorphism in an icosahedral virus. *Virology* 292, 211–212. [doi: 10.1006/viro.2001.1242](https://doi.org/10.1006/viro.2001.1242)
- Mutterer JD, Stussi-Garaud C, Michler P, Richards KE, Jonard G, Ziegler-Graff V (1999): Role of the beet western yellows virus readthrough protein in virus movement in Nicotiana clevelandii. *J. Gen. Virol.* 80, 2771–2778.
- Nass P H, Jakastys BP, D'Arcy CJ (1995): In situ localization of Barley yellow dwarf virus coat protein in oats. *Phytopathology* 85, 556–560. doi.org/10.1094/PHYTO.1998.88.10.1031
- Nickel H, Kawchuk L, Twyman RM, Zimmermann S, Junghans H, Winter S, Fischer R, Prüfer D (2008): Plantibody-mediated inhibition of the Potato leafroll virus P1 protein reduces virus accumulation. *Virus Res.* 136, 140–145. doi.org/10.1016/j.virusres.2008.05.001
- Pazhouhandeh M, Dieterle M, Marrocco K, Lechner E, Berry B, Brault V, Hemmer O, Kretsch T, Richards KE, Genschik P, Ziegler-Graff V (2006): F-box-like domain in the polerovirus protein P0 is required for silencing suppressor function. *Proc. Natl. Acad. Sci. USA* 103, 1994–1999. doi.org/10.1073/pnas.0510784103
- Peter KA, Liang D, Palukaitis P, Gray SM (2008): Small deletions in the potato leafroll virus readthrough protein affect particle morphology, aphid transmission, virus movement and accumulation. *J. Gen. Virol.* 89, 2037–2045. doi.org/10.1099/vir.0.83625-0
- Prüfer D, Wipf-Scheibel C, Richards K, Guille H, Lecoq H, Jonard G (1995): Synthesis of a full-length infectious cDNA clone of cucurbit aphid-borne yellows virus and its use in gene exchange experiments with structural proteins from other luteoviruses. *Virology* 214, 150–158. [doi: 10.1006/viro.1995.9945](https://doi.org/10.1006/viro.1995.9945)
- Sadowsy E, Maasen A, Juszczuk M, David C, Zagórski-Ostoja W, Gronenborn B, Hulanicka MD (2001): The ORFO product of potato leafroll virus is indispensable for virus accumulation. *J. Gen. Virol.* 82, 1529–1532.
- Schmitz J, Stussi-Garaud C, Tacke E, Prüfer D, Rohde W, Rohfritsch O (1997): In situ localization of the putative movement protein (pr17) from potato leafroll luteovirus (PLRV) in infected and transgenic potato plants. *Virology* 235, 311–322. doi.org/10.1006/viro.1997.8679

- Shang QX, Xiang HY, Han CG, Li DW, Yu JL(2009): Distribution and molecular diversity of three cucurbit-infecting poleroviruses in China. *Virus Res.* 145, 341–346. doi.org/10.1016/j.virusres.2009.07.017
- Shen WT, Wang MQ, Yan P, Gao L, Zhou P (2010): Protein interaction matrix of Papaya ringspot virus type P based on a yeast two-hybrid system. *Acta Virol.* 54, 49–54. doi.org/10.4149/av-2010-01-49
- Stewart LR, Hwang MS, Falk BW (2009): Two Crinivirus-specific proteins of Lettuce infectious yellows virus (LIYV), P26 and P9, are self-interacting. *Virus Res.* 145, 293–299. doi.org/10.1016/j.virusres.2009.07.021
- Tacke E, Schmitz J, Prüfer D, Rohde W (1993): Mutational analysis of the nucleic acid-binding 17kDa phosphoprotein of potato leafroll luteovirus identifies an amphipathic α -helix as the domain for protein-protein interactions. *Virology* 197, 274–282. doi.org/10.1006/viro.1993.1588
- Terradot L, Souchet M, Tran V, Giblot Ducray-Bourdin D (2001): Analysis of a three-dimensional structure of Potato leaf-roll virus coat protein obtained by homology modeling. *Virology* 286, 72–82. doi.org/10.1006/viro.2001.0900
- Urcuqui-Inchima S, Walter J, Drugeon G, German-Retana S, Haenni AL, Candresse T, Bernardi F, Le Gall O (1999): Potyvirus helper component-protease self-interaction in the yeast two-hybrid system and delineation of the interaction domain involved. *Virology* 258, 95–99. doi.org/10.1006/viro.1999.9725
- Walter M, Chaban C, Schütze K, Batistic O, Weckermann K, Näke C, Blazevic D, Grefen C, Schumacher K, Oecking C, Harter K, Kudla J (2004): Visualization of protein interactions in living plant cells using bimolecular fluorescence complementation. *Plant J.* 40, 428–438. doi.org/10.1111/j.1365-313X.2004.02219.x
- Xiang HY, Shang QX, Han CG, Li DW, Yu JL (2008): Complete sequence analysis reveals two distinct poleroviruses infecting cucurbits in China. *Arch. Virol.* 153, 1155–1160. doi.org/10.1007/s00705-008-0083-0

Blockade of Lyn kinase upregulates both canonical and non-canonical TLR-3 pathways in THP-1 monocytes exposed to human cytomegalovirus

K.-H. YEW^{1,2}, C. J. HARRISON^{1,2}

¹Pediatric Infectious Disease, Children's Mercy Hospitals, Kansas City, Missouri, USA; ²Department of Pediatrics, University of Missouri School of Medicine, Kansas City, Missouri, USA

Received November 12, 2010; accepted August 25, 2011

Summary. – Regulation of monocyte response to human cytomegalovirus (HCMV) occurs via activation of receptors that elicit innate antiviral effects and later T-cell responses. Our previous data (Yew *et al.*, 2010) demonstrated that human monocyte scavenger receptor A type 1 (SR-A1) are required for sensing of HCMV by endosomal toll-like receptors (TLRs)-3 and -9, which in turn induce critical pro-inflammatory cytokines. However, it remains unclear which subcellular molecules associated with SR-A1 lead to downstream activation of TLR-3 and/or TLR-9 signaling pathways. Herein we report that Lyn kinase, associated physically and functionally with SR-A for low density lipoprotein (LDL) recognition, acts as a key SR-A1-induced kinase that plays a critical role in TLR-3/9 signal transduction upon HCMV exposure to THP-1 monocytes. We found that disruption of the SR-A1 signal transduction through molecular inhibition by Lyn kinase oligonucleotides not only blocks the activation of downstream TLR-9 pathway but also alters the downstream TLR-3 pathway. In particular, Lyn kinase oligonucleotides resulted in decreased expression of TLR-9-induced tumor necrosis factor alpha (TNF- α) but strongly upregulated canonical TLR-3-induced interferon beta (IFN- β) and non-canonical TLR-3-induced NF- κ B-dependent p35 (35 kDa) subunit of interleukin 12 (IL-12p35) gene transcription. Thus, the observed shift away from TNF- α to robust IFN- β and IL-12p35 induction may offer opportunities for therapeutic interventions.

Keywords: HCMV; THP-1 monocytes; TLR-3/-9; Lyn kinase; TNF- α ; IFN- β ; IL-12p35

Introduction

HCMV (the subfamily *Betaherpesvirinae*, the family *Herpesviridae*) is a ubiquitous opportunistic pathogen capable of causing both congenital and acquired infections. HCMV infection is widespread in the general population, but it is usually asymptomatic. However, when primary infection occurs early in pregnancy, HCMV can cause human congenital infection, which affects the developing neurological

system *in utero*, thereby leading to sensorineural hearing loss and other neurological sequelae after birth (Landolfo *et al.*, 2003; Abate *et al.*, 2004; Scanga *et al.*, 2006). Human congenital HCMV infection occurs in ~1% of all births but is symptomatic in 10% to 20% of affected infants (Scanga *et al.*, 2006). Moreover, HCMV is a common cause of morbidity and mortality in immunocompromised individuals, including AIDS patients and recipients of bone marrow allografts or of solid organ transplants, but rarely causes disease in immunocompetent people (Bentz *et al.*, 2006). The mechanism of HCMV dissemination remains poorly resolved; however, cells of the innate immune system, which act as the first line of defense, specifically monocytes, are thought to play several key roles in this process (Bentz *et al.*, 2006). Results from *in vitro* and *in vivo* studies suggest that the infectious cycle of HCMV starts with virus binding to the monocyte cell surface receptors and is followed by fusion of the envelope with the plasma membrane with the release of viral structural components into the cell (Abate *et al.*, 2004). Binding and

E-mail: hyew@kumc.edu; fax: +816-983-6515.

Abbreviations: HCMV = human cytomegalovirus; IFN- β = interferon beta; IL-12p35 = p35 (35 kDa) subunit of interleukin 12; IRF3 = interferon regulatory factor 3; LDL = low-density lipoproteins; MYD88 = myeloid differentiation primary response gene (88); NF- κ B = nuclear factor kappa-light-chain-enhancer of activated B cells; SR-A1 = scavenger receptor A type 1; TLRs = toll-like receptors; TNF- α = tumor necrosis factor alpha; TRIF = TIR-domain-containing adapter-inducing IFN- β

penetration of virus or viral envelope glycoprotein B (gB) or gH triggers a receptor-mediated signal transduction leading to pro-inflammatory cytokine responses in host macrophages, the differentiated counterparts of monocytes (Bentz *et al.*, 2006). Recent evidence from our laboratory further indicates that monocytes upon HCMV exposure undergo cellular activation and the induction of pro-inflammatory cytokines, i.e. TNF- α , IFN- β , and IL-12p35, through SR-A1 and TLRs 3 and 9 (Yew *et al.*, 2010).

TLRs serve as sensors against pathogens that invade the host by recognizing pathogen-associated molecular patterns (Matsushima *et al.*, 2004). Each TLR has been identified to recognize a distinct ligand, supported and confirmed by previous observation of TLR-knockout mice and specific gene modifications. For example, TLR-3 and TLR-9 recognize viral dsRNA and unmethylated consensus DNA sequences, including the CpG motif in bacteria and viruses, respectively (Matsushima *et al.*, 2004). All TLRs mediate signaling through their cytoplasmic TIR domains linked to adaptor proteins, such as MYD-88 and TRIF, which induce the activation of NF- κ B and IRF3, respectively. Subsequently, these complexes translocate into the nucleus where they regulate transcription of target genes. For instance, TLR-3 signaling activates TRIF and IRF3, which then mediate IFN- β promoter activation as an innate response to infectious agents (Jiang *et al.*, 2004). Alternatively, TLR-3-mediated TRIF can also signal through TRAF6 and recruit NF- κ B p65 to induce cytokine expression (Jiang *et al.*, 2004). In contrast, TLR-9 engagement triggers MYD-88 and NF- κ B p65 activation, which regulates gene expression of multiple cytokines, e.g. TNF- α (Tran *et al.*, 2007) and IL-12 (Jiang *et al.*, 2009).

SR-A1, often referred to as CD204, is expressed primarily on the innate immune cells, such as monocytes/macrophages and dendritic cells and functions as a pattern recognition receptor (PRR) (Peiser *et al.*, 2002; Wang *et al.*, 2007). While SR-A1 was initially described to be able to uptake modified LDL through endocytosis, it is also thought to be mainly a trafficking receptor for a wide range of endogenous and microbial ligands, including lipopolysaccharide (LPS) on Gram-negative bacteria (Ishiguro *et al.*, 2001), lipoteichoic acid (LTA) on Gram-positive bacteria (Thomas *et al.*, 2000), apoptotic cells, as well as viral DNA and RNA (Amiel *et al.*, 2008). Subsequent work has demonstrated that the binding of LPS to SR-A on macrophages induces the production of cytokines and nitric oxide (NO), indicating that SR-A might play a pivotal role in host defense mechanism of macrophages (Hampton *et al.*, 1991; Miki *et al.*, 1996).

There is increasing evidence that SR-A1 can function as a carrier or "shuttle" molecule, bringing ligands to endosomal receptors to modulate intracellular signaling pathways. Multiple published reports from a number of

groups have speculated that SR-A1 appears to have an essential function in viral dsRNA uptake into the cell via endocytosis, in which SR-A1 may be delivering extracellular viral dsRNA to endosomes to be recognized by TLR-3 (Limmon *et al.*, 2008; DeWitte-Orr *et al.*, 2010). Alternately, MARCO (a member of SR-As) might participate in CpG-ODN delivery to endosomal sites of interaction with TLR9 (Józefowski *et al.*, 2006). Later findings further supported the idea that SR-A1 is required for sensing of HCMV by endosomal TLR-3 and -9, which in turn induce critical pro-inflammatory cytokines (Yew *et al.*, 2010). Thus, the question arises as to whether a subcellular molecule associated with SR-A1 could play a critical role in leading to downstream activation of TLR-3 and/or TLR-9 signaling pathways.

Given the fact that Lyn kinase, one of the members of the Src tyrosine kinase, has been reported to be functionally associated with SR-A1 in monocytes (Miki *et al.*, 1996) and involved in many cellular processes including gene differentiation and transcription (Corey *et al.*, 1999), we hypothesized that SR-A1-mediated Lyn kinase recruitment / activation is key to regulating endosomal TLR-3 and TLR-9 signaling mechanisms and subsequent cytokine gene transcription in HCMV-exposed THP-1 monocytes. To test this hypothesis, we evaluated the regulatory role of Lyn kinase and the effect of blocking Lyn kinase signaling by antisense oligonucleotides in THP-1 monocytes upon HCMV exposure. We first observed that mRNA levels of Lyn kinase are significantly increased in THP-1 monocytes within 10 mins after exposure to HCMV assessed by RT-PCR. Furthermore, immunocytochemistry for Lyn kinase revealed that many Lyn-positive cells were seen within 10 mins after HCMV exposure of THP-1 monocytes compared to the control. Importantly, inhibition of Lyn's function by the antisense oligonucleotides prevented the normal rise in TLR-9-induced TNF- α mRNA that occurs in response to HCMV, suggesting that the TLR-9-induced TNF- α is critically regulated by Lyn kinase. The most striking observation was that the transcription of canonical TLR-3-induced IFN- β as well as "non-canonical" TLR-3-induced NF- κ B-dependent IL-12p35 were elevated as a result of Lyn kinase inhibition. In retrospect, due to the inhibitory effect of Lyn kinase oligonucleotides, a shift toward an enhanced IFN- β and IL-12p35 induction associated with a decline in TNF- α expression might be caused by an as yet unidentified SR-A1-mediated protein kinase, possibly via the alternative TLR-3 signaling mechanism, upon HCMV exposure to THP-1 monocytes. This report describes a new role of SR-A1-mediated Lyn kinase in HCMV-exposed monocytes and raises a number of interesting opportunities for clinical intervention that might enhance innate antiviral defense and HCMV-specific T-cell responses.

Materials and Methods

Reagents and kits. DMEM, FBS, SYBR Green, Reference Dye for Quantitative PCR, and Protease Inhibitor Cocktail were obtained from Sigma-Aldrich (St. Louis, MO). RPMI 1640 was obtained from Gibco/Invitrogen. RNeasy Mini Kit, Sensiscript Reverse Transcriptase Kit, QIAamp DNA Micro Kit, and QIAquick Gel Extraction Kit were all purchased from Qiagen (Valencia, CA). AmpliTaq Gold with GeneAmp 10X PCR Buffer and MgCl₂ solution were from Applied Biosystems (Foster City, CA).

Antibodies. Normal donkey serum and FITC-conjugated AfiniPure donkey anti-mouse IgG antibodies were from Jackson ImmunoResearch Laboratories (West Grove, PA). Mouse monoclonal antibody [ab6276] to human β-actin and mouse monoclonal antibody [ab1890] to human Lyn kinase were all purchased from ABCAM (Cambridge, MA).

Endo-Porter delivery of antisense oligonucleotides assay. Oligonucleotides complementary to Lyn kinase gene (5'-TT TATACATCCCATTTCCTCGCTC-3'), and missense control oligonucleotides (5'-CCTCTTACCTCAgTTACAATTATA-3') were designed and synthesized by Gene Tools (Philomath, OR). Delivery of antisense oligonucleotides with Endo-Porter transfection method was performed according to the manufacturer's protocol. All oligonucleotides were complexed with Endo-Porter delivery reagent and confirmation of delivery was measured by the Western blot analysis. Note that all Endo-Porter transfection experiments were carried out in triplicate and repeated three times.

Cell culture and treatment. Human THP-1 monocytes and human foreskin fibroblasts, purchased from ATCC (Manassas, VA), were grown in RPMI 1640 and DMEM, respectively, with 2 mmol/l L-glutamine, 250 µg/ml amphotericin, 100 U/ml penicillin, 100 µg/ml streptomycin and 10% fetal bovine serum at 37°C under a humidified condition of 95% air and 5% CO₂. Upon 90% confluence, THP-1 monocytes at passage 10 to 15 were plated at a density of ~10⁵ cells/well in 12-well plates with serum-free RPMI 1640 overnight. On the following day, cells were either treated with serum-free medium alone or exposed to HCMV (Toledo) at a multiplicity of infection of 10 throughout the culture period. Antisense oligonucleotide or missense control was added separately to culture media at 5 µmol/l.

RT-PCR (non-quantitative). Total RNA was extracted from cells and treated with DNase. RNA was subjected to reverse transcription. cDNA was then amplified by PCR for 40 cycles (Table 1). All PCR products were separated by electrophoresis in 2% agarose gel. PCR cycles were as follows: initial denaturation at 95°C for 10 mins, followed by 40 cycles of 94°C for 30 secs, 60°C for 30 secs, 72°C for 30 secs and final extension at 72°C for 10 mins.

SYBR Green real-time quantitative PCR. PCR amplifications were performed using an Applied Biosystems 7500 (Carlsbad, CA) sequence detection system. Unless otherwise specified, each reaction mixture contained 10X Gold Buffer, 25 mmol/l

Table 1. PCR Primers

Gene	Accession #	Primers (5'-3')	Product (bp)
β-actin	NM_001101	FP: AGAAAATCT- GGCACACACC RP: GGGGTGTTGAAG- GTCTCAA	142
HCMV-gB	X04606	FP: TGGTCTACAACGCG- CAACATC RP: GCCACGTATTCCG- TATTGCT	130
SR-A1	NM_138715	FP: GACAT- GGAAGCCAACCTCAT RP: CCCTGGACTGAG- GAAAACAA	116
Lyn Kinase	M16038	FP: GCAGAGGGAAT- GGCATACAT RP: CTAGCAAG- GCCAAATCTGC	116
TLR-3	NM_003265	FP: CCGCCAACCT- TCACAAGGTAT RP: AGCTCATTGTGCT- GGAGGTT	130
TLR-9	NM_017442	FP: AATTCCCATTCTCTC- CCTGCT RP: TCCTTCACCCCT- TCCTCTTT	135
TRIF	AB093555	FP: ACGCCACTC- CAACTTCTGT RP: TCAGGTGAGCT- GAACAAAGGA	136
IRF3	NM_001571	FP: GATGCACAGCAG- GAGGATT RP: TCTGCTAACAGC- CAACCCTTC	149
MYD88	NM_002468	FP: TGCAGAGCAAG- GAATGTGAC RP: AGGATGCT- GGGAACTCTTT	121
NF-κB p65	M55643	FP: TGGAGTCT- GGGAAGGAGTTG RP: CGAAGCT- GGACAAACACAGA	129
IFN-β	M28622	FP: CATTACCTGAAG- GCCAGGA RP: AGCAATTGTC- CAGTCCCAGA	150
TNF-α	M10988	FP: GCCCAATCCCTT- TATTACC RP: CACATTCTGAATC- CCAGGT	145
IL-12p35	AF101062	FP: GAGGCCTGTTAC- CATTGGA RP: GCACAGGGCCAT- CATAAAAG	123

FP = forward primer; RP = reverse primer

MgCl₂, 2.5 mmol/l dNTPs, 10X SYBR Green, AmpliTaq Gold polymerase, Reference Dye, dH₂O, DNA template and 10 µmol of each primer. Amplification was performed by initial polymerase

activation for 10 mins at 95°C, and 40 cycles of denaturation at 95°C for 15 secs, annealing at 60°C for 20 secs and elongation for 30 secs at 72°C. The fluorescence threshold value was calculated using the iCycle system software. The calculation of relative change in mRNA was performed using the delta-delta method (Pfaffl *et al.*, 2001), with normalization for the house-keeping gene β -actin.

Quantitative PCR for HCMV. Viral concentrations in the supernatant of human fibroblast cultures infected with HCMV at 5–7 days post infection were collected using the Millipore® Steriflip® disposable vacuum filtration system (Billerica, MA) with PVDF membrane to remove cellular debris produced during infection of fibroblasts and later using QIAamp DNA Micro Kit for the extraction of total viral DNA, following the manufacturer's recommendation. HCMV DNA copy number was then determined and detected by the same protocol used in the SYBR Green real-time quantitative PCR, except for the addition of HCMV primers and the HCMV DNA sample. All virus stocks were aliquotted and stored at -80°C until used as viral inocula.

Immunocytochemistry. Upon 10 mins and 1 hr exposure of HCMV to THP-1 monocytes at a multiplicity of infection of 10, cytopsin preparations were performed on untreated and treated THP-1 monocytes at a density of $\sim 10^5$ cells/ml by centrifugation for 5 mins. Cells were fixed with 4% phosphate-buffered paraformaldehyde for 15 mins at RT. After fixation, the cells were permeabilized with 0.2% Triton X-100 (Sigma, St. Louis, MO) for 5 mins at RT, blocked with normal donkey serum for 30 mins and then incubated with primary mouse anti-human Lyn kinase antibody at a dilution of 1/100 in a moist chamber for 2 hrs at RT. The cells were rinsed with PBS and incubated with secondary fluorescein (FITC)-conjugated donkey anti-mouse IgG for 2 hrs at RT in a dark cabinet. After several washes, coverslips containing cells were mounted onto slides in aqueous mounting medium with anti-fading agents (Biomedica corp., Foster City, CA). Fluorescence digital images were captured using an Olympus BX60 (Melville, NY) microscope attached with Olympus U-PMTVC camera adaptor. Optronics DEI-750 (Goleta, CA) software was used to acquire and analyze images. Each slide was evaluated independently and immuno-positive cells were counted from representative areas of the sections. Results were expressed as the number of positive cells per low power field or the percentage of the total number of cells that were positive for antibody staining.

SDS-PAGE and Western blot analysis. Proteins were separated on a 10% Tris-HCl Ready Gel (Bio-Rad, Hercules, CA), transferred onto nitrocellulose membranes, and incubated with β -actin antibody at a dilution of 1/5000 or Lyn antibody at a dilution of 1/1000 overnight at 4°C. After incubation, the blots were washed 3x for 15 mins in washing buffer (PBS-0.05% Tween20) and incubated with a secondary anti-mouse β -actin or a secondary anti-mouse Lyn antibody coupled to horseradish peroxidase (Vector Labs, Burlingame, CA) for 1 hr at room temperature. Then, the blots were washed 3x for 15 mins in washing buffer, and immunoreactivity was normalized by chemiluminescence (Amersham, ECL+Plus

Kit) according to the manufacturer's instructions. The blots were exposed to Kodak scientific imaging films (Rochester, NY) within 1 min for detection.

Statistical analysis. Data were analyzed using the Microsoft Office Excel 2003 and expressed as means \pm S.D. where appropriate. Two group comparisons were evaluated using the unpaired Student's *t*-test. Differences were found significant by the Student's *t*-test in case $p < 0.05$.

Results

A novel role for Lyn kinase in HCMV exposed THP-1 monocytes

In a previous study (Yew *et al.*, 2010), our group indicated that Lyn kinase is involved in signaling cascades leading to cytokine production in THP-1 monocytes upon exposure of HCMV. To expand on our previous observations that the mRNA levels of Lyn kinase were upregulated in THP-1 monocytes within 1–10 mins but gradually decreased within 1–6 hrs after HCMV exposure as assessed by real time quantitative PCR analysis, we next performed a narrow exposure time-response of HCMV to THP-1 monocytes and found that Lyn kinase mRNA levels exhibit a strong expression at 10 mins compared to 1 hr, as determined by a simple RT-PCR (reverse transcription-polymerase chain reaction) screen (Fig. 1a). Further, immunocytochemistry for Lyn kinase revealed that many Lyn-positive cells were seen at 10 mins post HCMV exposure, whereas only a modest number of THP-1 monocytes were Lyn positive at 1 hr post HCMV exposure (Fig. 1b,c). These results obtained by different techniques convincingly confirm and extend our previous observation that Lyn kinase plays a functional role in HCMV-mediated THP-1 monocytes.

Lyn kinase blockade up-regulates canonical TLR-3-induced cytokines

In accordance with previous studies (Yew *et al.*, 2010), we found that SR-A1 and Lyn kinase are activated simultaneously upon exposure of THP-1 monocytes to HCMV at 10 mins. Furthermore, THP-1 monocytes pretreated with the SR-A1/MSR antibody exhibited markedly decreased mRNA levels of Lyn kinase and TLR-3 and TLR-9 as well as their downstream signaling factors at 1 hr. This suggests that SR-A1 engagement is functionally associated with Lyn kinase, which is important for activation of TLR-3 and TLR-9 (Yew *et al.*, 2010). In an effort to better delineate the role of Lyn kinase and further validate SR-A1-mediated Lyn kinase signaling mechanisms, we utilized antisense oligonucleotides to block, in a sequence-specific manner, the translation of Lyn kinase mRNA in THP-1 monocytes prior to and during HCMV exposure. Here, there

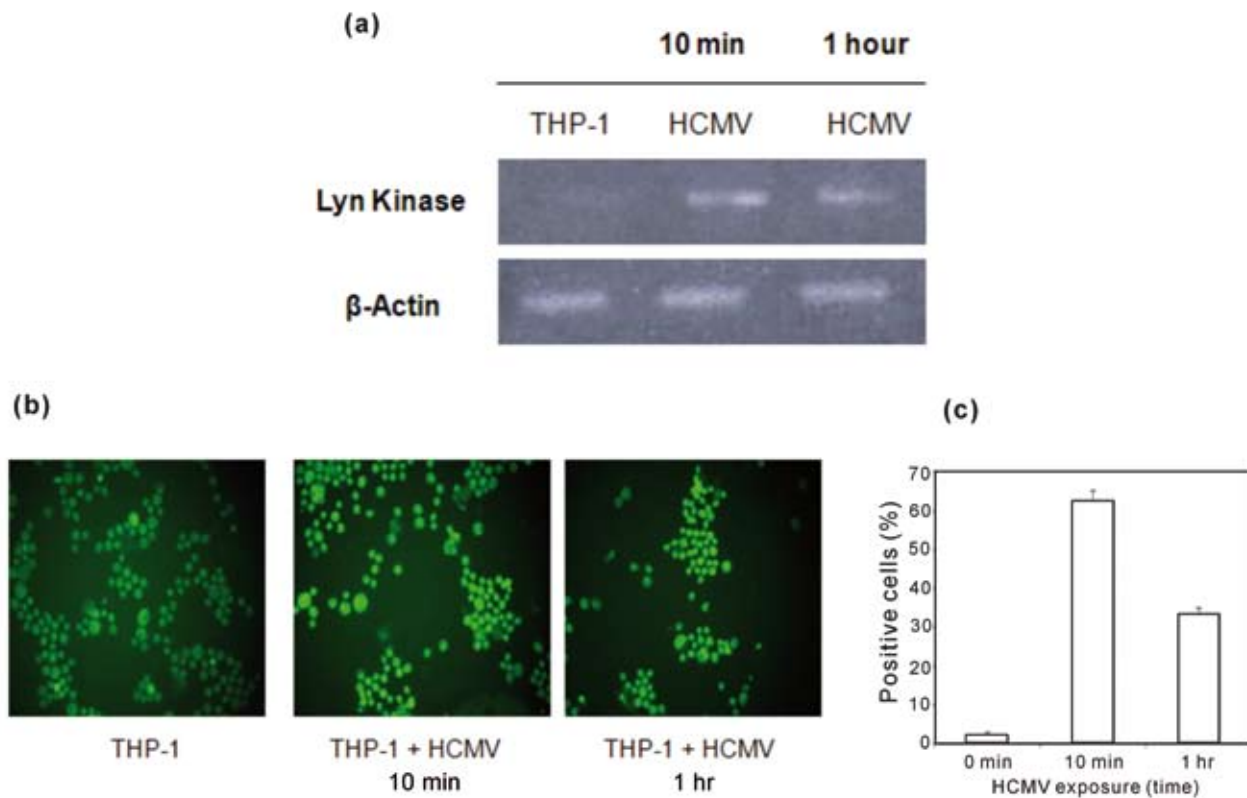


Fig. 1

Induction of Lyn kinase and immunofluorescence detection of Lyn kinase in THP-1 monocytes upon exposition to HCMV

RT-PCR screening for mRNA levels of Lyn kinase expression in THP-1 monocytes upon HCMV exposure. RNA was extracted from THP-1 monocytes upon HCMV exposure within a 10 mins–1 hr time span. All mRNAs were analyzed from the same preparation. Reaction mixtures without reverse transcriptase served as controls for genomic DNA contamination in all cases (data not shown). (a) The gene expression of Lyn kinase mRNAs was weakly present in the baseline THP-1 monocytes but was strongly present in HCMV-exposed THP-1 monocytes at 10 mins and became markedly decreased at 1 hr. β -actin expression is shown for normalization purposes. (b) Similar to the mRNA levels, immunostaining of HCMV-exposed THP-1 monocytes at 10 mins shows marked upregulation of Lyn kinase staining. (c) Quantification of the immunocytochemistry in (b) reflects an increased number of positive cells and an increased percentage of positive cells.

was a dramatic increase in TLR-3 mRNA levels at 1 hr (Fig. 2b). Like TLR-3, its downstream signaling effectors such as TRIF and interferon regulatory factor 3 (IRF3) were found to have the highest expression at 1 hr (Fig. 2c,d). Similarly, IFN- β mRNA (Fig. 2e) also was maximal at the same incubation time. The changes in the levels of these TLR-3 signaling factors may be a key point of “alternative” regulation modulated by an unidentified SR-A1-mediated protein kinase to replace Lyn kinase. No apparent effect on the inhibition of SR-A1 was seen (Fig. 2a); suggesting that SR-A1 is working upstream of Lyn kinase, which is critically regulated by SR-A1.

Lyn kinase blockade down-regulates TLR-9-induced cytokines but up-regulates non-canonical TLR-3-induced cytokines

Our data in Figure 2 shows that the deficiency of Lyn kinase plays an unprecedented role in cytokine expression

induced by the TLR-3 signaling pathway upon HCMV exposure of THP-1 monocytes. However, inhibitory effects of Lyn kinase in HCMV-exposed THP-1 monocytes have a direct impact on the TLR-9 signaling pathway. The Lyn kinase oligonucleotides specifically blocked the upregulation of both TLR-9 (Fig. 3a) and TNF- α (Fig. 3d) at 1 hr, suggesting that Lyn kinase is essential for inducing TLR-9 and TNF- α transcription. MYD88 (Fig. 3B), a TLR adapter common to TLR-9 but not TLR-3, was not found to be greatly altered, indicating that it might serve as a rate-limiting factor. Strikingly, NF- κ B (Fig. 3c) and IL-12p35 (Fig. 3e) mRNA levels were elevated as a result of Lyn kinase inhibition. Similar to IFN- β mRNA (Fig. 2e), we postulated that the elevated levels of NF- κ B and IL-12p35 might be triggered by an unknown SR-A1-mediated enzyme due to the deficiency of Lyn kinase and could represent the abrupt shift of pathway, possibly via the non-canonical TLR-3 signaling mechanism. To confirm the inhibiting effects of the Lyn kinase

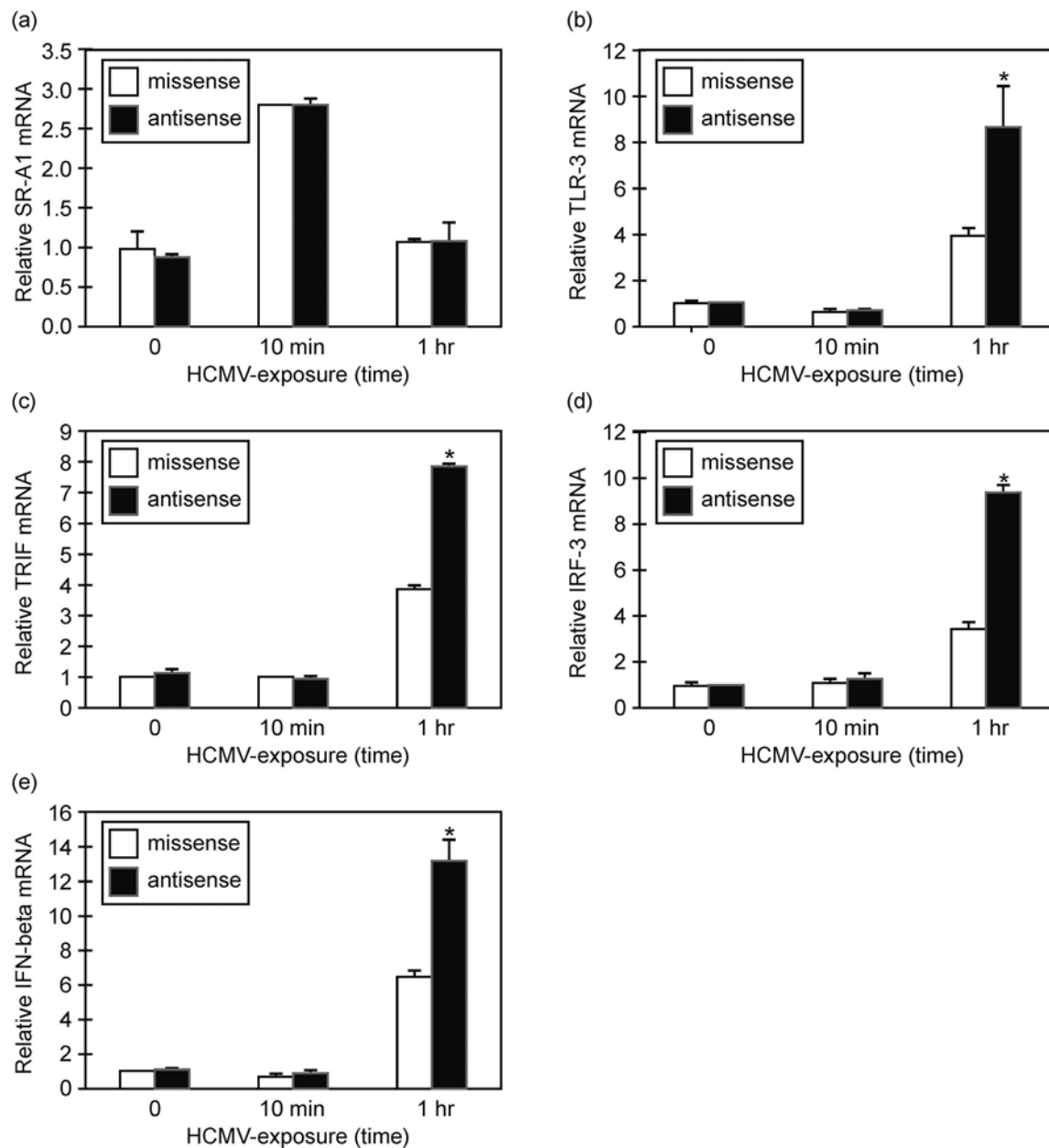


Fig. 2

Effect of blockade of Lyn kinase with antisense oligonucleotide on TLR-3 signaling pathway in THP-1 monocytes

(a) Lyn kinase missense oligonucleotides had no apparent effect on SR-A1, suggesting that SR-A1 is working upstream of Lyn kinase effects. Conversely, TLR-3 (b) and its downstream factors, such as TRIF (c), IRF3 (d), and IFN- β (e) showed marked elevation of mRNA levels in response to Lyn kinase missense oligonucleotides, particularly at 1 hr (means \pm SD, n = 4). *p < 0.05 compared with control at 1 hr; empty columns = missense; full columns = Lyn kinase oligonucleotides.

oligonucleotides, Western blot analysis was performed in antisense oligonucleotide-treated and sense-treated controls, confirming sequence-specific decreases in target Lyn kinases by antisense oligonucleotides (Fig. 4).

Taken together with our previous findings (Yew *et al.*, 2010), a model for the proposed integrated role of SR-A1-

mediated Lyn kinase, which might function as an intracellular signaling messenger to induce activation of endosomal TLR-3 and TLR-9 signaling pathways, thereby leading to transcription of cytokine genes, is depicted in Fig. 5. The diagram illustrates a sequence of events whereby HCMV is initially recognized by SR-A1. The interaction between

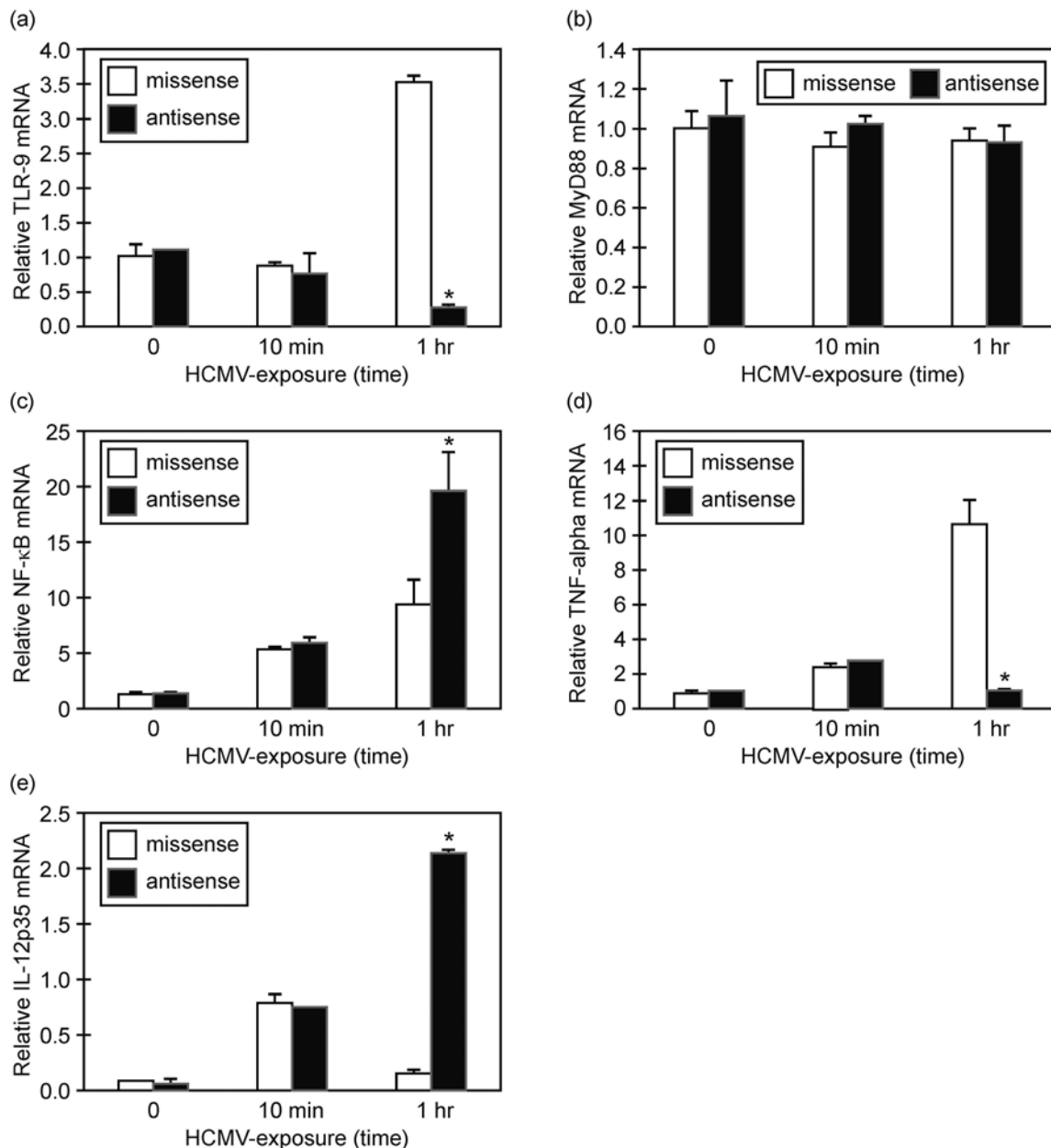


Fig. 3

Effect of blockade of Lyn kinase with antisense oligonucleotide on TLR-9 signaling pathway in THP-1 monocytes

(a) The increase in TLR-9 mRNA levels of THP-1 monocytes at 1 hr in response to HCMV is completely ablated by the missense Lyn kinase oligonucleotides. (b) MYD88, which serves as a universal adapter protein for all TLRs, but TLR-3, to activate transcription factor NF-κB, was not found to be significantly altered by the missense Lyn kinase oligonucleotides. (c-e) Interestingly, missense Lyn kinase oligonucleotides treatment dramatically enhances levels of NF-κB p65 (c) and IL-12p35 (e) at 1 hr. Unlike upregulations of NF-κB p65 and IL-12p35 mRNA, TNF-α mRNA level (d) was downregulated back to baseline (means ± SD, n = 4). *p < 0.05 compared with control at 1 hr; empty columns = missense; full columns = Lyn kinase oligonucleotides.

HCMV and SR-A1 triggers activation of Lyn kinase, which in turn serves as an intracellular signaling effector to regulate the activation of the endosomal TLR-9 pathway. The normal activation of NF-κB p65 through MYD-88 by TLR-9, which later induces enhanced TNF-α expression in HCMV-exposed THP-1 monocytes, was not seen. Conversely, when Lyn

kinase is blocked, TRIF-mediated IRF3 leading to IFN-β activation triggered by TLR-3 was found to be strongly upregulated upon THP-1 monocyte exposure to HCMV. Thus, we hypothesized that an unidentified SR-A1-mediated kinase exists, comes into play when there is a defect in Lyn kinase activity, and triggers an alternative TLR-3-mediated

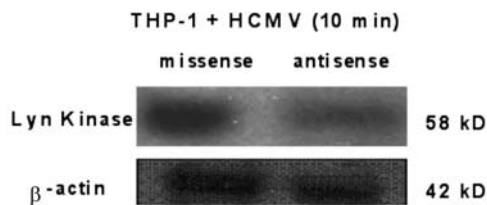


Fig. 4

Western blot analysis for Lyn kinase in HCMV-exposed THP-1 monocytes with Lyn kinase antisense oligonucleotides and missense control
SDS-PAGE and Western blot analysis confirms the inhibitory effects of the antisense oligonucleotide on Lyn kinase levels ($n = 3$). β -actin served as control for equal loading.

NF- κ B p65 induction of IL-12p35. Hence, the observed shift away from TNF- α to a robust effect of IFN- β and IL-12p35 in HCMV-exposed monocytes by Lyn blockade may provide new immunotherapeutic intervention for HCMV congenital infection.

Discussion

Despite a better understanding of the HCMV infection in congenitally infected infants due to recent advances in antenatal and perinatal screening and neuroimaging, late-onset deafness and mental retardation are still unpredictable. During HCMV infection, monocytes and their derivative cells, which represent the first line of defense, are thought to participate in innate immune response by restricting viral dissemination. Experimental studies indicate that recognition or binding of HCMV particles, which can take place either on the cell surface (Hampton *et al.*, 1991; Peiser *et al.*, 2002; Abate *et al.*, 2004; De Witte-Orr *et al.*, 2010) or within intracellular endosome (Jiang *et al.*, 2004; Matsushima *et al.*, 2004; Jiang *et al.*, 2009), is an early and potent regulatory signal for the activation of pro-inflammatory cytokines. Monocyte-derived cytokines are essential in triggering T-cell response.

The exact mechanism of action, by which HCMV-encoded proteins interact with immune cells and induce

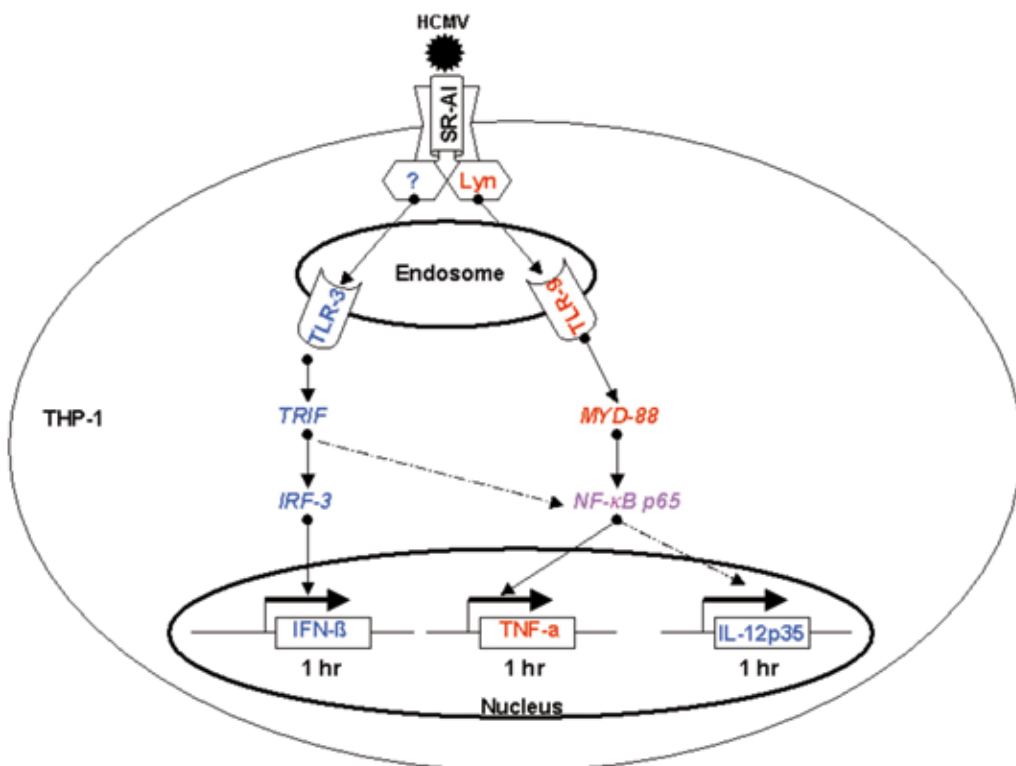


Fig. 5

Schematic diagram of hypothesized interrelationship of SR-A1 and TLR-3/-9 in HCMV-exposed THP-1 monocytes

Together, the diagram illustrates a sequence event whereby HCMV is recognized by SR-A1 and triggers activation of Lyn kinase, which serves as a shuttle molecule for the endosomal TLR-9 pathway. The TLR-9-induced TNF- α is critically regulated by Lyn kinase. However, the transcriptions of canonical TLR-3-induced IFN- β as well as "non-canonical" TLR-3-induced NF- κ B-dependent IL-12p35 may possibly be regulated by an unknown SR-A1-mediated protein kinase upon HCMV exposure to THP-1 monocytes.

innate immune response, has not been fully elucidated, but several receptors and protein kinases have been reported to be essential in the early HCMV-induced pro-inflammatory cytokine production leading to a very robust T-cell response. These receptors and kinases include SR-A1 (Limmon *et al.*, 2008; DeWitte-Orr *et al.*, 2010), TLR-3 (Tabeta *et al.*, 2004), TLR-9 (Tabeta *et al.*, 2004; Iversen *et al.*, 2009), Src kinases (Baron *et al.*, 2008), and RIP1-interacting protein (Mack *et al.*, 2008). Overwhelming evidence has accumulated that ligand binding to SR-As triggers activation of intracellular signaling through phosphorylation of phospholipase C (PLC)- γ 1, phosphoinositide 3 (PI3)-kinase, and protein kinase C (PKC), which lead to cytokine induction and production (Limmon *et al.*, 2008).

Given the supportive role of Lyn kinase associated with SR-A1 in monocytes (Miki *et al.*, 1996) in many cellular processes including gene differentiation and transcription (Corey *et al.*, 1999), and that SR-A1 has been shown to deliver extracellular viral dsRNA to endosomes (DeWitte-Orr *et al.*, 2010), we sought to determine whether Lyn kinase may mediate a similar effect in HCMV-exposed THP-1 monocytes. Earlier, our group suggested an involvement of SR-A-mediated Lyn kinase in cytokine induction by HCMV-exposed THP-1 monocytes (Yew *et al.*, 2010) as assessed by real time quantitative PCR analysis. Here, we have shown by several different techniques that there is a dramatic increase in Lyn kinase mRNA levels, suggesting that Lyn kinase is an enzyme with a potentially novel function that we observed in the THP-1 monocytes HCMV exposed to HCMV. These results are in agreement with a previous study conducted by Cheung and co-workers (Cheung *et al.*, 2008), who have demonstrated that concomitant activation of Lyn kinase is required for HIV-1 envelope glycoprotein gp120-induced cytokine production in primary human monocyte-derived macrophages.

We previously reported that SR-A1 along with the expression of Lyn kinase is required for sensing HCMV by endosomal TLR-3 and TLR-9, which in turn induce critical pro-inflammatory cytokines (Yew *et al.*, 2010). We found that SR-A1-mediated Lyn kinase blocked by antisense oligonucleotides resulted in greatly decreased mRNA levels of both TLR-9 and TNF- α . The necessity of Lyn kinase for TLR-9 is consistent with recent reports from the Sanjuan group (Sanjuan *et al.*, 2006) that knockdown of Lyn kinase expression or the use of specific kinase inhibitors blocked TLR-9-dependent signaling and cytokine secretion, providing evidence that Lyn tyrosine phosphorylation is an upstream requirement for the activation of TLR-9. Therefore, it seems plausible that the SR-A1-induced Lyn kinase may be a key mediator in regulating the activation of endosomal TLR-9 pathway. In addition, the Sanjuan group also found that knockdown of Lyn kinase resulted in a significant decrease in cellular spreading, adhesion, and motility.

However, the inhibitory effects of Lyn kinase in HCMV-exposed THP-1 monocytes point to an unexpected but unprecedented role for the TLR-3 signaling pathway. We found that the transcriptions of canonical TLR-3-induced IFN- β as well as non-canonical TLR-3-induced NF- κ B-dependent IL-12p35 were elevated as a result of Lyn kinase inhibition. The elevated levels of TLR-3-induced IFN- β and IL-12p35 might be triggered by an unidentified SR-A1-mediated enzyme, which replaces the Lyn kinase and could represent the abrupt shift of pathway, possibly via the non-canonical TLR-3 signaling pathway. In agreement with these *in vitro* experiments, Keck and Freudenberg recently reported that Lyn-deficient mice produced higher amounts of pro-inflammatory cytokines than did wild-type mice after injection of LPS (Keck *et al.*, 2010). Other evidence also indicates that Lyn ablation in B-cells induced an enhanced MAP kinase activation (Chan *et al.*, 1997), which may serve as a potential target kinase for future exploration. This possibility is supported by the fact that the regulation of protein phosphorylation requires a balance in the activity of protein kinases and protein phosphatases.

Taken collectively with our previous observations (Yew *et al.*, 2010), the current findings establish a novel paradigm of interaction between SR-A1-mediated Lyn kinase and two endosomal pattern-recognition receptors, TLR-3 and TLR-9, resulting in an inflammatory response. Fig. 5 depicts a hypothetical model of association of SR-A1-mediated Lyn kinase with TLR-9 that accommodates our data. In this study, we provide the first evidence that Lyn kinase is an upstream mediator of the TLR-9 signaling pathway and a key determinant for the regulation of TLR-9 and TNF- α expression in THP-1 monocytes upon HCMV exposure. The model indicates that when Lyn kinase activity is reduced, induction of an unknown SR-A1-mediated enzyme leads to the activation of TRIF and NF- κ B to regulate a robust IFN- β and IL-12p35 cytokine response, respectively. The substantial induction of NF- κ B-dependent IL-12p35 in response to Lyn kinase inhibition appears to signal via a non-canonical TLR-3 signaling mechanism. Future studies investigating the mechanisms, by which the unidentified SR-A1-mediated kinase interacts directly with TLR-3 or indirectly, through an intermediate adapter, should prove informative and indicate promising areas for further investigation. Ultimately, greater understanding of the mechanisms behind the potential importance of Lyn kinase in TLR-3/-9 signaling will hopefully lead to the development of novel therapeutic regimes targeting HCMV-specific T-cell responses against HCMV disease.

Acknowledgements. This work was supported by the Marion Merrell Dow Foundation Clinical Scholar Grant 01.4915. The authors would like to thank Dr. D.I. Bernstein from the University of Cincinnati Children's Hospital Research Foundation for kindly providing the Toledo strain of human cytomegalovirus and Roberta Morgan for her technical assistance.

References

- Abate DA, Watanabe S, Mocarski ES (2004): Major human cytomegalovirus structural protein pp65 (ppUL83) prevents interferon response factor 3 activation in the interferon response. *J. Virol.* 78, 10995–1006. doi.org/10.1128/JVI.78.20.10995-11006.2004
- Amiel E, Alonso A, Uematsu S, Akira S, Poynter ME, Berwin B (2008): Pivotal Advance: Toll-like receptor regulation of scavenger receptor-A-mediated phagocytosis. *J. Leukoc. Biol.* 85, 595–605. doi.org/10.1189/jlb.1008631
- Baron M, Davignon JL (2008): Inhibition of IFN-gamma-induced STAT1 tyrosine phosphorylation by human CMV is mediated by SHP2. *J. Immunol.* 181, 5530–5536.
- Bentz GL, Jarquin-Pardo M, Chan G, Smith MS, Sinzger C, Yurochko AD (2006): Human cytomegalovirus (HCMV) infection of endothelial cells promotes naive monocyte extravasation and transfer of productive virus to enhance hematogenous dissemination of HCMV. *J. Virol.* 80, 11539–1155. doi.org/10.1128/JVI.01016-06
- Chan VW, Meng F, Soriano P, DeFranco AL, Lowell CA (1997): Characterization of the B lymphocyte populations in Lyn-deficient mice and the role of Lyn in signal initiation and down-regulation. *Immunity* 7, 69–81. [doi.org/10.1016/S1074-7613\(00\)80511-7](https://doi.org/10.1016/S1074-7613(00)80511-7)
- Cheung R, Ravyn V, Wang L, Ptaszniak A, Collman RG (2008): Signaling mechanism of HIV-1 gp120 and virion-induced IL-1beta release in primary human macrophages. *J. Immunol.* 180, 6675–6684.
- Corey SJ, Anderson SM (1999): Src-related protein tyrosine kinases in hematopoiesis. *Blood* 93, 1–14.
- DeWitte-Orr SJ, Collins SE, Bauer CM, Bowdish DM, Mossman KL (2010): An accessory to the Trinity: SR-As are essential pathogen sensors of extracellular dsRNA, mediating entry and leading to subsequent type I IFN responses. *PLoS Pathog.* 6, e1000829. doi.org/10.1371/journal.ppat.1000829
- Hampton RY, Golenbock DT, Penman M, Krieger M, Raetz CR (1991): Recognition and plasma clearance of endotoxin by scavenger receptors. *Nature* 352, 342–344. doi.org/10.1038/352342a0
- Ishiguro T, Naito M, Yamamoto T, Hasegawa G, Gejyo F, Mitsuyama M, Suzuki H, Kodama T (2001): Role of macrophage scavenger receptors in response to *Listeria monocytogenes* infection in mice. *Am. J. Pathol.* 158, 179–188. [doi.org/10.1016/S0002-9440\(10\)63956-9](https://doi.org/10.1016/S0002-9440(10)63956-9)
- Iversen AC, Steinkjer B, Nilsen N, Bohnhorst J, Moen SH, Vik R, Stephens P, Thomas DW, Benedict CA, Espenvik T (2009): A proviral role for CpG in cytomegalovirus infection. *J. Immunol.* 182, 5672–5681. doi.org/10.4049/jimmunol.0801268
- Jiang W, Sun R, Zhou R, Wei H, Tian Z (2009): TLR-9 activation aggravates concanavalin A-induced hepatitis via promoting accumulation and activation of liver CD4+ NKT cells. *J. Immunol.* 182, 3768–3774. doi.org/10.4049/jimmunol.0800973
- Jiang Z, Mak TW, Sen G, Li X (2004): Toll-like receptor 3-mediated activation of NF-kappaB and IRF3 diverges at Toll-IL-1 receptor domain-containing adapter inducing IFN-beta. *Proc. Natl. Acad. Sci. USA* 101, 3533–3538. doi.org/10.1073/pnas.0308496101
- Józefowski S, Sulahian TH, Arredouani M, Kobzik L (2006): Role of scavenger receptor MARCO in macrophage responses to CpG oligodeoxynucleotides. *J. Leukoc. Biol.* 80, 870–879.
- Keck S, Freudenberg M, Huber M (2010): Activation of murine macrophages via TLR2 and TLR4 is negatively regulated by a Lyn/PI3K module and promoted by SHIP1. *J. Immunol.* 184, 5809–5818. doi.org/10.4049/jimmunol.0901423
- Landolfo S, Gariglio M, Gribaudo G, Lembo D (2003): The human cytomegalovirus. *Pharmacol. Ther.* 98, 269–297. [doi.org/10.1016/S0163-7258\(03\)00034-2](https://doi.org/10.1016/S0163-7258(03)00034-2)
- Limmon GV, Arredouani M, McCann KL, Corn Minor RA, Kobzik L, Imani F (2008): Scavenger receptor class-A is a novel cell surface receptor for double-stranded RNA. *FASEB J.* 22, 159–167. doi.org/10.1096/fj.07-8348com
- Mack C, Sickmann A, Lembo D, Brune W (2008): Inhibition of proinflammatory and innate immune signaling pathways by a cytomegalovirus RIP1-interacting protein. *Proc. Natl. Acad. Sci. USA* 105, 3094–3099. doi.org/10.1073/pnas.0800168105
- Matsushima H, Yamada N, Matsue H, Shimada S (2004): TLR3-, TLR7-, and TLR9-mediated production of proinflammatory cytokines and chemokines from murine connective tissue type skin-derived mast cells but not from bone marrow-derived mast cells. *J. Immunol.* 173, 531–541.
- Miki S, Tsukada S, Nakamura Y, Aimoto S, Hojo H, Sato B, Yamamoto M, Miki Y (1996): Functional and possible physical association of scavenger receptor with cytoplasmic tyrosine kinase Lyn in monocytic THP-1-derived macrophages. *FEBS Lett.* 399, 241–244. [doi.org/10.1016/S0014-5793\(96\)01332-4](https://doi.org/10.1016/S0014-5793(96)01332-4)
- Peiser L, Mukhopadhyay S, Gordon S (2002): Scavenger receptors in innate immunity. *Curr. Opin. Immunol.* 14, 23–128. [doi.org/10.1016/S0952-7915\(01\)00307-7](https://doi.org/10.1016/S0952-7915(01)00307-7)
- Pfaffl MW (2001): A new mathematical model for relative quantification in real-time RT-PCR. *Nucleic Acids Res.* 29, e45. doi.org/10.1093/nar/29.9.e45
- Sanjuan MA, Rao N, Lai KT, Gu Y, Sun S, Fuchs A, Fung-Leung WP, Colonna M, Karlsson L (2006): CpG-induced tyrosine phosphorylation occurs via a TLR9-independent mechanism and is required for cytokine secretion. *J. Cell Biol.* 172, 1057–1068. doi.org/10.1083/jcb.200508058
- Scanga L, Chaing S, Powell C, Aylsworth AS, Harrell LJ, Henshaw NG, Civalier CJ, Thorne LB, Weck K, Booker J, Gulley ML (2006): Diagnosis of human congenital cytomegalovirus infection by amplification of viral DNA from dried blood spots on perinatal cards. *J. Mol. Diagn.* 8, 240–245. doi.org/10.2353/jmoldx.2006.050075
- Tabeta K, Georgel P, Janssen E, Du X, Hoebe K, Crozat K, Mudd S, Shamel L, Sovath S, Goode J, Alexopoulou L, Flavell RA, Beutler B (2004): Toll-like receptors 9 and 3 as essential components of innate immune defense against mouse cytomegalovirus infection. *Proc. Natl. Acad. Sci. USA* 101, 3516–3521. doi.org/10.1073/pnas.0400525101

- Thomas CA, Li Y, Kodama T, Suzuki H, Silverstein SC, El Khoury J (2000): Protection from lethal gram-positive infection by macrophage scavenger receptor-dependent phagocytosis. *J. Exp. Med.* 191, 147–156. doi.org/10.1084/jem.191.1.147
- Tran N, Koch A, Berkels R, Boehm O, Zacharowski PA, Baumgarten G, Knuefermann P, Schott M, Kanczkowski W, Bornstein SR, Lightman SL, Zacharowski K (2007): Toll-like receptor 9 expression in murine and human adrenal glands and possible implications during inflammation. *J. Clin. Endocrinol. Metab.* 92, 2773–2783. doi.org/10.1210/jc.2006-2697
- Wang XY, Facciponte J, Chen X, Subjeck JR, Repasky EA (2007): Scavenger receptor-A negatively regulates antitumor immunity. *Cancer Res.* 67, 4996–5002. doi.org/10.1158/0008-5472.CAN-06-3138
- Yew KH, Carsten B, Harrison C (2010): Scavenger receptor A1 is required for sensing HCMV by endosomal TLR-3/-9 in monocytic THP-1 cells. *Mol. Immunol.* 47, 883–893. doi.org/10.1016/j.molimm.2009.10.009

Antiviral properties of polysaccharides from *Agaricus brasiliensis* in the replication of bovine herpesvirus 1

M.C. MINARI¹, V.P. RINCÃO¹, S.A. SOARES², N.M.P.S. RICARDO², C. NOZAWA¹, R.E.C. LINHARES^{1,*}

¹Laboratório de Virologia, Departamento de Microbiologia, CCB, Universidade Estadual de Londrina (UEL), Londrina, 86051-970, PR, Brazil; ²Laboratório de Polímeros, Departamento de Química Orgânica e Inorgânica, Universidade Federal do Ceará (LP/DQOI/UFC), Fortaleza, 60455-760, CE, Brazil

Received March 18, 2011, accepted July 22, 2011

Summary. – Natural products are an inexhaustible source of compounds with promising pharmacological activities, including antiviral action. In the present study, the antiviral potential of polysaccharide-peptide (PLS) and an extracted β -glucan from *Agaricus brasiliensis* were investigated in the replication of bovine herpesvirus 1 (BoHV-1) in HEp-2 cell cultures. The cytotoxicity (CC_{50}) was assayed by the MTT method and the antiviral activity (IC_{50}) was estimated by the plaque reduction assay. To study the possible mode of action of PLS and β -glucan, the following protocols were performed: the virucidal assay, adsorption assay and the time-of-addition assay. The PLS presented a selectivity index (SI) higher than 12.50 and β -glucan 9.19. The antiviral inhibition (67.9%) in cells treated with PLS during virus infection was higher than that in cells treated prior to or post infection. The β -glucan presented high inhibition of virus replication by plaque assay (83.2%) and by immunofluorescence assay (63.8%). Although the mechanism has yet to be defined, we suggest that PLS and β -glucan inhibited BoHV-1 replication by interfering with the early events of viral penetration. Additional studies are required for a better understanding of the mechanism of action of PLS and β -glucan.

Keywords: bovine herpesvirus 1; *Agaricus brasiliensis*; antiviral activity

Introduction

The lack of effective therapies and/or vaccines for several viral infections and the emergence of drug-resistant strains have stimulated the research of new antiviral drugs. Natural products have proven to be an important source of both new pharmaceuticals and compounds that can be modified for improved efficacy (Ghosh *et al.*, 2009).

Among the fungi, molds have been a significant source of antimicrobial and immunomodulatory compounds. Higher fungi have been tested for antibacterial activity, but only

recently has it been demonstrated that some mushrooms also possess antiviral activity. For example, a proteoglycan from the basidiomycete *Ganoderma lucidum* has antiviral activity against herpes simplex viruses (Li *et al.*, 2005). An extract of the edible Japanese mushroom *Lentinus edodes* has been found to inhibit the replication of herpes simplex virus (HSV), western equine encephalitis virus, poliovirus, measles virus, mumps virus, vesicular stomatitis virus and human immunodeficiency virus (Tochikura *et al.*, 1988; Sorimachi *et al.*, 1990; Suzuki *et al.*, 1990; Sarkar *et al.*, 1993; Sasaki *et al.*, 2001). Thus, the screening of other mushroom species may lead to the identification of additional antiviral drugs.

Agaricus brasiliensis (formerly *Agaricus blazei*), a native species from Brazil, popularly known as Sun Mushroom and *Himematsutake* in Japan, is thought to possess medicinal values in folk medicine. Infusion of the dried fruiting bodies of this mushroom has been popularly consumed both as a stimulant and as an auxiliary treatment for various diseases, including cancer (Pinto *et al.*, 2009). Studies

*Corresponding author. E-mail address: relin@uel.br; fax: +55-43 33715828.

Abbreviations: BoHV-1 = bovine herpesvirus 1; CC_{50} = 50% cytotoxic concentration; HSV-1 = herpes simplex virus 1; IC_{50} = 50% inhibitory concentration; IFA = immunofluorescence assay; PLS = polysaccharide-peptide; SI = selectivity index

showed that ethanol fractions obtained from an aqueous extract of *A. brasiliensis* mycelium completely inhibited the cytopathic effect of the western equine encephalomyelitis virus (Sorimachi *et al.*, 2001).

The extracts of *A. brasiliensis* contain a high amount of β -glucans, the class of polysaccharides that consist of a central chain of (β 1 \rightarrow 6)-D-glucose with branches made of (β 1 \rightarrow 3)-D-glucose. It has been shown that these compounds have antitumor and immunomodulatory properties (Kawagishi *et al.*, 1989; Dong *et al.*, 2002).

BoHV-1 belongs to the subfamily *Alphaherpesvirinae* and shares a number of biological properties with HSV-1 and HSV-2. The virus causes conjunctivitis, upper respiratory infection, pneumonia, genital disorders and abortions (Tikoo *et al.*, 1995). This disease represents annually a significant cost to the cattle industry. Although vaccines are available, they can cause abortions and disease in young calves (Jones, 2003).

As few reports exist investigating the antiviral activity of *A. brasiliensis*, the aim of the present study is to evaluate the antiviral potential of PLS and an extracted β -glucan from *A. brasiliensis* against BoHV-1.

Materials and Methods

Polysaccharides. *A. brasiliensis*-derived PLS obtained at LP/DQOI/UFC (Gonzaga *et al.*, 2005) was dissolved in Dulbecco's Modified Eagle Medium (DMEM), filter-sterilized and kept at 4°C for a maximum of 72 hrs. The β -glucan was isolated from the polysaccharide-peptide assemblage extracted from *A. brasiliensis* (Angeli *et al.*, 2006) and supplied by Laboratório de Polímeros, Departamento de Química Orgânica e Inorgânica, UFC, Brazil. The compounds were dissolved in DMEM, submitted to sterilization by ultra-filtration in 0.2 μ m pore size membrane, and stored at -20°C.

Cells and virus. HEp-2 cells (human larynx carcinoma, ATCC, CCL- 23) were grown at 37°C in DMEM supplemented with 10% fetal bovine serum (Gibco BRL, USA), 2 mmol/l glutamine*, 100 IU/ml penicillin*, 100 μ g/ml streptomycin* (*Sigma, Chem. Co., USA) and 2.5 μ g/ml amphotericin B (Bristol Myers-Squibb, Brazil). BoHV-1 was supplied by DMVP-UEL, Brazil. The virus was propagated in HEp-2 cells and stored at -80°C, and titers were determined by a plaque assay.

Cytotoxicity assay. For the cytotoxicity assay, HEp-2 cells were seeded in 96-well plates at a density of 10⁵ cells/ml. After 24 hrs, cultures were incubated with various concentrations (15–2,000 μ g/ml) of PLS and β -glucan for 48 hrs. Cell viability was determined by MTT kit (methyl-thiazolyl-diphenyl-tetrazolium bromide) (Sigma Chem. Co., USA) according to manufacturer's instructions. The 50% cytotoxic concentration (CC₅₀) corresponding to the concentration of substances that reduces cell viability by 50% was calculated by linear regression analysis.

Antiviral assay. The inhibitory effect of PLS and β -glucan on BoHV multiplication was investigated by plaque reduction assay and immunofluorescence assay (IFA). HEp-2 cells seeded onto 24-well culture plates or glass coverslips were infected and treated with β -glucan (100 to 250 μ g/ml) or PLS (50 to 400 μ g/ml) and submitted to plaque reduction assay and Immunofluorescence assay as described below. The 50% inhibitory concentration (IC₅₀), defined as the concentration of substances required to reduce virus titer by 50%, was calculated by linear regression analysis. The SI was calculated by the ratio CC₅₀/IC₅₀. Interferon (human alpha-2 B, Meizler Com. Intern. SA, Brazil) at a concentration of 1000 U/ml was used as a positive control for inhibition of BoHV-1 replication.

Plaque reduction assay. Semi-confluent HEp-2 cell monolayers grown in 24-well plates were treated with PLS or β -glucan and after infection overlaid with nutrient agarose. Cultures were incubated for 48 hrs, fixed with 10% formalin and stained with 0.5% crystal violet. The antiviral activity was calculated as the percentage of plaque reduction as follows: % Plaque reduction = [1 – (Number of plaques in test/Number of plaques in control) x 100].

IFA to detect BoHV proteins was performed at time 0 hr of infection. HEp-2 cells grown on glass coverslips were infected with BoHV-1 at a MOI of 1. PLS (50 to 400 μ g/ml) or β -glucan (100 to 250 μ g/ml) were added at 0 hr, and the cells were incubated for 24 hrs. The cells were fixed with cold acetone (-20°C) for 20 mins followed by immunofluorescence staining using polyclonal bovine anti-BoHV-1 antibodies (DMVP/UEL) and rabbit anti-bovine IgG FITC conjugate (Sigma Chem. Co., USA). The cells were examined under UV light (Leica DM 4500 B, Germany) and 100 cells/coverslip were scored.

Time-of-addition assay of PLS. The time-of-addition of the PLS in viral replication was done as previously described (Yang *et al.*, 2005). Semi-confluent HEp-2 cell cultures were incubated with PLS at concentrations of 50, 100, 200 or 400 μ g/ml before (-1 hr and -2 hrs), during (0 hr) and after (1 hr and 2 hrs) infection, at 37°C under 5% CO₂. Cultures were infected with 50–100 PFU/ml of BoHV-1. The viral inhibition was monitored by plaque reduction assay 48 hrs after the infection.

Virucidal assay. BoHV-1 at 10⁶ PFU/ml was diluted with equal volumes of DMEM containing respectively 50, 100, 200, and 400 μ g/ml of PLS, or 100, 200, and 250 μ g/ml of β -glucan, followed by incubation for 1 hr at 37°C. Monolayers were incubated for 1 hr with virus plus substances, followed by washing and incubation, and plaque counting was performed after 48 hrs.

Virus adsorption assay. The virus adsorption assay was performed according to Zhu *et al.* (2004), with modifications. Cell monolayers were infected with BoHV-1 in the presence or absence of PLS or β -glucan at the concentrations previously mentioned. After a viral adsorption period of 1 hr at 4°C, the cells were washed with PBS to remove non-adsorbed virus, and after 48 hrs of incubation, plaques were counted.

Statistics. The statistical significance of the difference between mean values was determined by Student's t-test at a significance level of P ≤ 0.05. The experiments were carried out in triplicate.

Results

Cytotoxicity of polysaccharides

The viability of HEp-2 cells was not affected by PLS even at the highest concentration used, i.e., 2,000 µg/ml. However, CC₅₀ of the β-glucan in HEp-2 cells reached the value of 1,250 µg/ml.

Influence of time of addition of PLS on BoHV replication

HEp-2 cell monolayers were treated with PLS before, during or after virus infection, and the results demonstrated a concentration-dependent virus inhibition with the highest inhibitory effect in cell cultures treated at time 0 hr. Fig. 1 shows that PLS was more effective when present during the infection. When PLS was added at the concentration of 400 µg/ml, two hours or one hour prior to infection (-2 hrs and -1 hr), the highest inhibition of viral replication was 9.4% and 3.4%, respectively. At the same concentration, PLS added at time zero (0 hr) caused 67.9% inhibition. However, when PLS was added at 1hr or 2hrs post infection, inhibition was 42.9% and 28.6%, respectively. With PLS added at time zero at concentrations of 200 µg/ml, 100 µg/ml, and 50 µg/ml, inhibition were 58.5, 36.5, and 30.1%, respectively. When PLS was added before or after infection, the antiviral effect was lower (Fig. 1).

Effect of PLS and β-glucan on BoHV replication

The effect of PLS and β-glucan on BoHV-1 protein synthesis assayed by IFA is shown in Table 1. PLS concentrations of 400 µg/ml, 200 µg/ml, 100 µg/ml, and 50 µg/ml reduced the number of fluorescent cells (FC) by 61, 54, 38.8, and 29%, respectively. The IFA results demonstrated a concentration-dependent antiviral effect similar to that found for the plaque assay.

The antiviral activity of β-glucan on BoHV-1 replication monitored by plaque assay, at concentration of 250 µg/ml, 200 µg/ml, and 100 µg/ml, resulted in inhibition of 83.2, 72.4, and 37.8% (Fig. 2). When monitored at the same concentrations by IFA, the inhibition was 63.8, 56.5, and 39.1% (Table 1). The SI, determined as CC₅₀/IC₅₀, at time 0 hr and at the highest concentrations of PLS (400 µg/ml) and β-glucan (250 µg/ml) are shown in Table 2. The SI of PLS was higher than that of β-glucan, but both exhibited a good antiviral activity, with SI values higher than 12.50 and 9.19, respectively. The IC₅₀ was calculated by regression analysis of the dose-response curve.

PLS and beta-glucan neither acted directly on virus particles (virucide protocol) nor affected virus attachment step. In both protocols there was no significant reduction

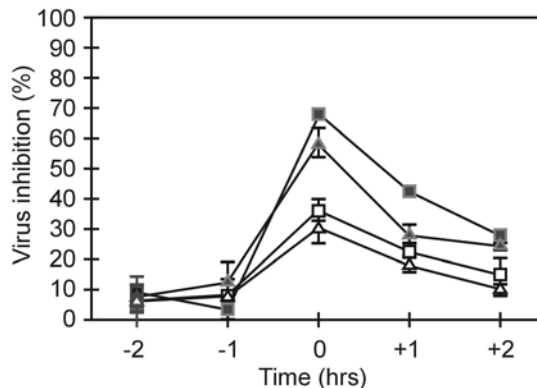


Fig. 1

The effect of the polysaccharide from Agaricus brasiliensis on BoHV-1 replication monitored by plaque assay in HEp-2 cell cultures

The drug was used at concentrations of 50 µg/ml (△), 100 µg/ml (□), 200 µg/ml (▲), and 400 µg/ml (■), where it was added before (-2 hrs and -1 hr), during (0 hr) or after (1 hr and 2 hrs) infection. Percent inhibition of virus plaque formation is indicated with the respective standard deviation.

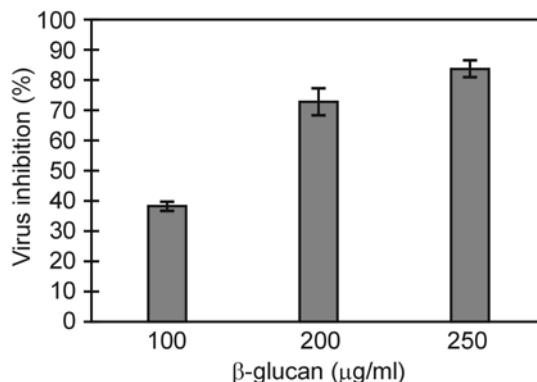


Fig. 2

The antiviral activity of β-glucan on BoHV-1 replication monitored by plaque assay

The drug was used at concentrations of 100, 200, and 250 µg/ml, and was added at time 0 hr of infection. The values represent the percentage of inhibition of plaque formation with the respective standard deviation, in comparison to untreated infected cultures (control).

in virus yield. Interferon used as control inhibited BoHV-1 replication by 100%.

Discussion

Current chemotherapeutic antiviral drugs have been characterized as having in many cases limited clinical efficacy, resistance and toxic side effects (Strasfeld and Chou, 2010). Therefore, it is necessary to identify and develop

Table 1. The effect of PLS and β -glucan from *Agaricus brasiliensis* on BoHV-1-infected HEp-2 cells monitored by IFA

Concentra-tions ($\mu\text{g/ml}$)	PLS		β -glucan	
	FC	% FCI	FC	% FCI
0	59 \pm 2	----	69 \pm 3	----
50	42 \pm 4	29.1 \pm 3.1	----	----
100	36 \pm 3	38.8 \pm 5.8	42 \pm 2	39.1 \pm 3.1
200	27 \pm 3	54.0 \pm 5.2	30 \pm 3	56.5 \pm 4.5
250	----	----	25 \pm 2	63.8 \pm 2.8
400	23 \pm 1	61.0 \pm 2.5	----	----

The values represent the number of fluorescent cells with the respective standard deviation and corresponding percentage of inhibition. FC = number of fluorescent cells; % FCI = percentage of inhibition of fluorescent cells.

Table 2. The antiviral activity, expressed as SI, of PLS and β -glucan isolated from *Agaricus brasiliensis* on BoHV-1 in plaque reduction assay

Substance	CC ₅₀ ^a ($\mu\text{g/ml}$)	IC ₅₀ ^b ($\mu\text{g/ml}$)	SI ^c (CC ₅₀ /IC ₅₀)
β -glucan	1250	140	9.19
PLS	>2000	160	>12.50

^aFifty percent cytotoxic concentration. ^bFifty percent inhibitory concentration. ^cSelectivity index.

new antiviral agents with new targets different from those in conventional therapy.

A number of polysaccharides with antiviral activity have been described. Polysaccharides isolated from *Antrodia camphorata* have anti-hepatitis B virus activity (Lee *et al.*, 1999). A protein-bound polysaccharide isolated from the mushroom *Ganoderma lucidum* was found to decrease significantly the viral titer of both HSV-1 and HSV-2 and the authors suggest that this polysaccharide impedes the complex interactions of viruses with cell, thus inhibiting the early stages of viral infection (Eo *et al.*, 2000).

Antiviral activity of polysaccharides is linked to the anionic features of the molecules, resulting in inhibition of the early stages of viral infection such as attachment and penetration (Marchetti *et al.*, 1995). Several sulfated polysaccharides, such as heparin, dextran sulfate, pentosan polysulfate, mannan sulfate, sulfated cyclodextrins, carrageenans, xylofuranan sulfate, and ribofuranan sulfate have been shown to inhibit the replication of various enveloped viruses, including HSV, human cytomegalovirus and human immunodeficiency virus (Damonte *et al.*, 1994; Witvrouw *et al.*, 1994; Zhu *et al.*, 2006).

The results reported here are in agreement with the previous studies on the antiviral

activity of polysaccharides, such as carrageenan. This polysaccharide inhibited a step in the HSV cycle following viral internalization, but preceding the onset of late viral protein synthesis (Gonzalez *et al.*, 1987). Some anionic sulfate

polysaccharides isolated from algae, such as rhamnan sulfate from *Monostroma latissimum* and fucose sulfate from *Sargassum horneri*, were found to inhibit the HSV-1 replication even when added at 2 hrs post infection, after some virus-specific proteins had already been synthesized (Hoshino *et al.*, 1998; Lee *et al.*, 1999). Aqueous and ethanol extracts and an isolated polysaccharide from the fruiting body of *A. brasiliensis*, also demonstrated higher antiviral activity against poliovirus type 1 in HEp-2 cells, when added just after virus inoculation, at time 0 hr (Faccin *et al.*, 2007).

β -glucan demonstrated concentration-dependent antiviral against BoHV-1 at the time 0 hr of infection. This substance was isolated from a polysaccharide fraction derived from the fruiting body of *A. brasiliensis*, whose antiviral activity against poliovirus - 1 was previously described by Faccin *et al.* (2007). The authors demonstrated that the polysaccharide was more effective when added at time 0 hr of infection in agreement, therefore with the results obtained in our study. Zhang *et al.* (2004) evaluated the β -glucans extracted from the fungus *Pleurotus tuber-regium* and found antiviral activity against HSV-1 and -2, where the inhibition was observed at time 0 hr of infection, similarly.

In conclusion, we demonstrated that PLS and the extracted β -glucan from *A. brasiliensis* possess antiviral activity against BoHV-1. The effective antiviral concentrations of PLS are far from the cytotoxicity threshold, and, consequently, this natural product shows a considerable selectivity index. Therefore, PLS as well as β -glucan can be used for the development of antiviral agents. The antiviral activity of PLS may be due to the effect at the stage of BoHV-1 penetration into host cell, as described for other polysaccharides, but the exact steps affected remain to be elucidated.

Acknowledgements. This work was supported by CNPq, CAPES, Fundação Araucária, Proppg/UEL, and is part of MC Minari M.Sc. manuscript.

References

- Angeli JPF, Ribeiro LR, Gonzaga MLC, Soares SdeA, Ricardo MPSN, Tsuboy MS, Stidl R, Knasmueller S, Linhares RE, Mantovani MS (2006): Protective effects of β -glucan extracted from *Agaricus brasiliensis* against chemically induced DNA damage in human lymphocytes. Cell Biol. Toxicol. 22, 285–291. doi.org/10.1007/s10565-006-0087-z
- Damonte E, Neyts J, Pujol CA, Snoeck R, Andrei G, Ikeda S, Wittenbrouw M, Reymen D, Haines H, Matulewicz MC, Cerezo A, Coto CE, De Clercq E (1994): Antiviral activity of a sulphated polysaccharide from the red seaweed *Nothogenia fastigita*. Biochem. Pharmacol. 47, 2187–2192. [doi.org/10.1016/0006-2952\(94\)90254-2](https://doi.org/10.1016/0006-2952(94)90254-2)
- Dong Q, Yao J, Yang X, Fang J (2002): Structural characterization of water-soluble β -D-glucan from fruiting bodies of

- Agaricus blazei Murr. Carbohydr. Res. 337, 1417–1421. [doi.org/10.1016/S0008-6215\(02\)00166-0](https://doi.org/10.1016/S0008-6215(02)00166-0)
- Eo SK, Kim Y, Lee CK, Han SS (2000): Possible mode of antiviral activity of acidic protein bound polysaccharide isolated from *Ganoderma lucidum* on herpes simplex viruses. J. Ethnopharmacol. 72, 475–481. [doi.org/10.1016/S0378-8741\(00\)00266-X](https://doi.org/10.1016/S0378-8741(00)00266-X)
- Faccin LC, Benati F, Rincão VP, Mantovani MS, Soares SA, Gonzaga ML, Nozawa C, Linhares REC (2007): Antiviral activity of aqueous and ethanol extracts and of an isolated polysaccharide from *Agaricus brasiliensis* against poliovirus type 1. Lett. Appl. Microbiol. 45, 24–28. doi.org/10.1111/j.1472-765X.2007.02153.x
- Ghosh T, Chattopadhyay K, Marschall M, Karmakar P, Mandal P, Ray B (2009): Focus on antivirally active sulfated polysaccharides: From structure-activity analysis to clinical evaluation. Glycobiology 19, 2–15. doi.org/10.1093/glycob/cwn092
- Gonzaga MLC, Ricardo NMPS, Heatley F, Soares SA (2005): Isolation and characterization of polysaccharides from *Agaricus blazei* Murill. Carbohydr. Polym. 60, 43–49. doi.org/10.1016/j.carbpol.2004.11.022
- Gonzalez ME, Alarcon B, Carraasco L (1987): Polysaccharides as antiviral agents: antiviral activity of carrageenan. Antimicrob. Agents Chemother. 31, 1388–1393
- Hoshino T, Hayashi T, Hayashi K, Hamada J, Lee JB, Sankawa U (1998): An antivirally active sulphated polysaccharide from *Sargassum horneri*. Biol. Pharm. Bull. 21, 730–734. doi.org/10.1248/bpb.21.730
- Jones C (2003): Herpes Simplex Virus Type 1 and Bovine Herpesvirus 1 Latency. Clin. Microbiol. Rev. 16, 79–95. doi.org/10.1128/CMR.16.1.79-95.2003
- Kawagishi H, Inagaki R, Kanao T, Mizuno T, Shimura K, Ito H, Hagiwara T, Nakamura T (1989): Fractionation and anti-tumor activity of the water-insoluble residue of *Agaricus blazei* fruiting bodies. Carbohydr. Res. 186, 267–274. [doi.org/10.1016/0008-6215\(89\)84040-6](https://doi.org/10.1016/0008-6215(89)84040-6)
- Lee JB, Hayashi K, Hayashi T, Sankawa U, Maeda M (1999): Antiviral activities against HSV-1, HCMV and HIV-1 of Rhamnan sulfate from *Monostroma latissimum*. Planta Med. 65, 439–41. doi.org/10.1055/s-2006-960804
- Li Z, Liu J, Zhao Y (2005): Possible mechanism underlying the anti-herpetic activity of a proteoglycan isolated from the Mycelia of *Ganoderma lucidum* in Vitro. J. Biochem. Mol. Biol. 38, 34–40. doi.org/10.5483/BMBRep.2005.38.1.034
- Marchetti M, Pisani S, Pietropaolo V, Seganti L, Nicoletti R, Orsi N (1995): Inhibition of herpes simplex virus infection by negatively charged and neutral carbohydrate polymers. J. Chemother. 7, 90–96.
- Pinto AV, Martins PR, Romagnoli GG, Campanelli AP, Terezan AP, Filho ER, Ferreira da Eira A, Kaneno R (2009): Polysaccharide fraction of *Agaricus brasiliensis* avoids tumor-induced IL-10 production and changes the microenvironment of subcutaneous Ehrlich adenocarcinoma. Cell Immunol. 256, 27–38. doi.org/10.1016/j.cellimm.2009.01.002
- Sarkar S, Koga J, Whitley R.J, Chatterjee S (1993): Antiviral effect of the extract of culture medium of *Lentinus edodes* mycelia on the replication of herpes simplex virus type 1. Antiviral Res. 20, 293–303. ISSN 0166–3542.
- Sasaki SH, Linhares REC, Nozawa CM, Montalván R, Paccola-Meirelles LD (2001): Strains of *Lentinula edodes* suppress growth of phytopathogenic fungi and inhibit Alagoas serotype of vesicular stomatitis virus. Braz. J. Microbiol. 32, 52–55. doi.org/10.1590/S1517-83822001000100012
- Sorimachi K, Ikebara Y, Maezato G, Okubo A, Yamazaki S, Akitomo K, Niwa A (2001): Inhibition by *Agaricus blazei* Murrill fractions of cytopathic effect induced by western equine encephalitis (WEE) virus on Vero cells in vitro. Biosci. Biotech. Bioch. 65, 1645–1647. doi.org/10.1271/bbb.65.1645
- Sorimachi K, Niwa A, Yamazaki S, Toda S, Yasumura Y (1990): Antiviral activity of water-solubilized lignin derivatives in vitro. Agric. Biol. Chem. 54, 1337–1339. doi.org/10.1271/bbb1961.54.1337
- Strasfeld L, Chou S (2010): Antiviral drug resistance: mechanisms and clinical implications. Infect. Dis. Clin. N. Am. 24, 413–437. doi.org/10.1016/j.idc.2010.01.001
- Suzuki H, Iiyama K, Yoshida O, Yamazaki S, Yamamoto N, Toda S (1990): Structural characterization of the immunoactive and antiviral water-solubilized lignin in an extract of the culture medium of *Lentinus edodes* mycelia (LEM). Agric. Biol. Chem. 54, 479–487. doi.org/10.1271/bbb1961.54.479
- Tikoo SK, Campos M, Babiuk ALA (1995): Bovine herpesvirus 1 (BHV-1): biology, pathogenesis, and control. Adv. Virus Res. 45, 191–223. [doi.org/10.1016/S0065-3527\(08\)60061-5](https://doi.org/10.1016/S0065-3527(08)60061-5)
- Tochikura TS, Nakashima H, Ohashi Y, Yamamoto N (1988): Inhibition (in vitro) of replication and of the cytopathic effect of human immunodeficiency virus by an extract of the culture medium of *Lentinus edodes* mycelia. Med. Microbiol. Immunol. 177, 235–244. doi.org/10.1007/BF00189409
- Witvrouw M, Desmyter J, De Clercq E (1994): Polysulfates as inhibitors of HIV and other enveloped viruses. Antivir. Chem. Chemoth. 5, 345–359.
- Yang CM, Cheng HY, Lin TC, Chiang LC, Lin CC (2005): Acetone, ethanol and methanol extracts of *Phyllanthus urinaria* inhibit HSV-2 infection in vitro. Antiviral Res. 67, 24–30. doi.org/10.1016/j.antiviral.2005.02.008
- Zhang M, Cheung PC, Ooi VE, Zhang L (2004): Evaluation of sulfated fungal β-glucans from the sclerotium of *Pleurotus tuber-regium* as a potential water-soluble anti-viral agent. Carbohydr. Res. 339, 2297–2301. doi.org/10.1016/j.carres.2004.07.003
- Zhu W, Chiu LC, Ooi VE, Chan PK, Ang PO Jr (2006): Antiviral property and mechanisms of a sulphated polysaccharide from the brown alga *Sargassum patens* against Herpes simplex virus type 1. Phytomedicine 13, 695–701. doi.org/10.1016/j.phymed.2005.11.003
- Zhu W, Chiu LC, Ooi VE, Chan PK, Ang PO Jr (2004): Antiviral property and mode of action of a sulphated polysaccharide from *Sargassum patens* against herpes simplex virus type 2. Int. J. Antimicrob. Agents 24, 81–85. doi.org/10.1016/j.ijantimicag.2004.02.022

Evaluation of anti-influenza efficiency of polyclonal IgG antibodies specific to the ectodomain of M2 protein of influenza A virus by passive immunization of mice

J. KIRÁLY, E. VAREČKOVÁ, V. MUCHA, F. KOSTOLANSKÝ*

Department of Orthomyxoviruses, Institute of Virology, Slovak Academy of Sciences, Dúbravská cesta 9, 845 05 Bratislava,
Slovak Republic

Received May 24, 2011; accepted June 27, 2011

Summary. – We attempted to quantify the protective potential of polyclonal IgG antibodies specific to the ectodomain of M2 protein (eM2) of influenza A virus (IAV) against lethal influenza infection of mice. For this purpose, eM2 conjugated with keyhole limpet hemocyanin (KLH) or KLH alone were administered with Freund's adjuvant intraperitoneally (i.p.) to BALB/c mice. IgG antibodies specific to the KLH-eM2 conjugate (anti-KLH-eM2 IgGs) and KLH (anti-KLH IgGs), respectively, were purified from ascitic fluids. Analysis of the preparation of anti-KLH-eM2 IgGs by ELISA revealed that it contained about 25% of anti-eM2 IgGs and 75% of anti-KLH IgGs. Taking into account this finding mice were passively immunized by intravenous route with 320, 160, 80, and 40 µg of anti-eM2 IgGs per mouse, respectively, while 320 µg of anti-KLH IgGs were used in control. Following subsequent infection with 3 LD₅₀ IAV the survival of mice was determined. An absolute protection (100% survival) was obtained with 320 µg of anti-eM2 IgGs, and a relatively strong significant protection (~80% survival, p = 0.024) with 160 µg. The amount 160 µg of IgGs represents approx. 100 µg IgGs per 1 ml of blood.

Keywords: influenza; M2 protein; eM2-specific IgG concentration; protection

Introduction

There are current efforts to avoid every year vaccination against influenza with a vaccine containing seasonally actualized hemagglutinin (HA) and neuraminidase (NA) antigens by use of a vaccine based on a conserved antigen(s). Such a vaccine should evoke a long-lasting immune response efficiently suppressing the infection with various antigenic variants or even subtypes. The main candidate molecule is the M2 protein of IAV, particularly its 23 aa-long ectodomain

(eM2) that is characteristic by an outstanding antigenic conservativity and is abundantly expressed in the membrane of infected cells (Neirynck *et al.*, 1999; Palese and Garcia-Sastre, 2002; Lamb, 1985; Zebedee and Lamb, 1988). Nevertheless, its immunogenicity during the natural influenza infection is very weak and short-term (Feng *et al.*, 2006). These inconvenient properties of eM2 represent the main issues to be solved. A number of various approaches for preparation of eM2-based vaccine focused on increasing its immunogenicity have been published (Slepuskin *et al.*, 1995; Neirynck *et al.*, 1999; Wynne *et al.*, 1999; Okuda *et al.*, 2001; Liu *et al.*, 2004; Ben-Yedidia and Arnon, 2005; Huleatt *et al.*, 2008; DeFilette *et al.*, 2008). The mechanism of the eM2-associated biological action was described as the antibody-dependent cell-mediated cytotoxicity (ADCC), in which NK cells with their low-affinity Fc gamma receptors bind IgG antibodies already bound to the M2 protein expressed on the surface of infected cells and mediate their lysis (Jagerlehner *et al.*, 2004). This hypothesis explains why anti-eM2 IgGs, when present in sufficiently high

*Corresponding author. E-mail: virufkos@savba.sk; fax: +421-2-54114284.

Abbreviations: IAV = influenza A virus; eM2 = ectodomain of M2 protein; HA = hemagglutinin; anti-KLH-eM2 IgGs = IgG antibodies to KLH-eM2; anti-KLH IgGs = IgG antibodies to KLH; i.n. = intranasally; i.p. = intraperitoneally; i.v. = intravenously; KLH = keyhole limpet hemocyanin; MAbs = monoclonal antibody(ies); NA = neuraminidase

concentration, only attenuate the infection while neutralizing antibodies to HA that directly inhibit the binding of virus to the cell receptor provide a very effective instant protection.

Despite the lower efficiency of eM2-specific antibodies, the idea of utilization of eM2 in future influenza vaccine remains actual and promising as this molecule has a potential to elicit a broad cross-protective response (Sui *et al.*, 2010; Staneková *et al.*, 2011). In addition to the eM2 immunogenicity, the concentration of eM2-specific antibodies remains an important characteristic to be followed that can also serve as an indicator of effectiveness of particular eM2-based vaccine preparation.

In this study, we attempted to quantify the protective potential of polyclonal IgG antibodies specific to eM2 IAV against lethal influenza infection of mice by determining the dependence of survival of infected mice on actual concentration of these antibodies in their blood following passive immunization.

Materials and Methods

Virus. A/Mississippi/1/85 (H3N2) was propagated in allantoic fluid of 10-day chicken embryos and stored at -70°C.

Mice. Six-week-old female BALB/c mice purchased from the Faculty of Medicine, Masaryk University, Brno, Czech Republic, were used. The animals were treated according to the European Union standards and fundamental ethical principles including animal welfare requirements.

eM2 peptide and KLH-eM2 conjugate. A 23-aa-long synthetic eM2 peptide of IAV (H3 subtype) of the sequence SLLTEVET-PIRNEWGSRSNDSSD, M_r of 2,592.74 and 93.94% purity was purchased from ProImmune (USA). The peptide contained substitutions C17S and C19S to avoid formation of disulphide bonds in

the peptide. The conjugation of eM2 with KLH (Sigma) was done using glutaraldehyde as described by Staneková *et al.* (2011).

Immunization of mice. BALB/c mice were immunized i.p. with three doses of KLH-eM2 (30 µg of eM2 per mouse) or KLH (30 µg pre mouse), respectively, supplemented with Freund's adjuvant, in 14 day intervals Staneková *et al.* (2011).

Polyclonal antibodies were purified from ascitic fluids by affinity chromatography on Protein A-Sepharose columns (Ey *et al.*, 1978).

Passive immunization of mice. BALB/c mice – 5 animals per group – were administered i.v. anti-eM2 IgGs in 200 µl doses of 320, 160, 80, and 40 µg per mouse, respectively, while control mice obtained 320 µg of anti-KLH IgGs and 200 µl of PBS, respectively.

Infection of mice. Two hrs after passive immunization the mice were intranasally (i.n.) inoculated with 3 LD₅₀ of A/Mississippi/1/85 (H3N2) in 40 µl. Survival of mice was recorded daily for 14 days. Statistical significance of survival was evaluated by Fisher exact test.

ELISA. eM2- or KLH-specific antibodies were assayed by a binding test according to Varečková *et al.* (2003a). Wells of 96-well plates were coated overnight with 100 ng of eM2 or KLH as antigens in 100 µl at 4°C. The antibody titer was calculated as the reciprocal of sample dilution at the point where the regression line drawn through the titration curve crossed the cut-off line. The latter value was the mean from 5 negative control samples plus 3 SD.

Results and Discussion

Antibody response in mice to immunization with eM2

In this work, we used a simple model of the eM2-KLH conjugate as immunogen supplemented with the Fre-

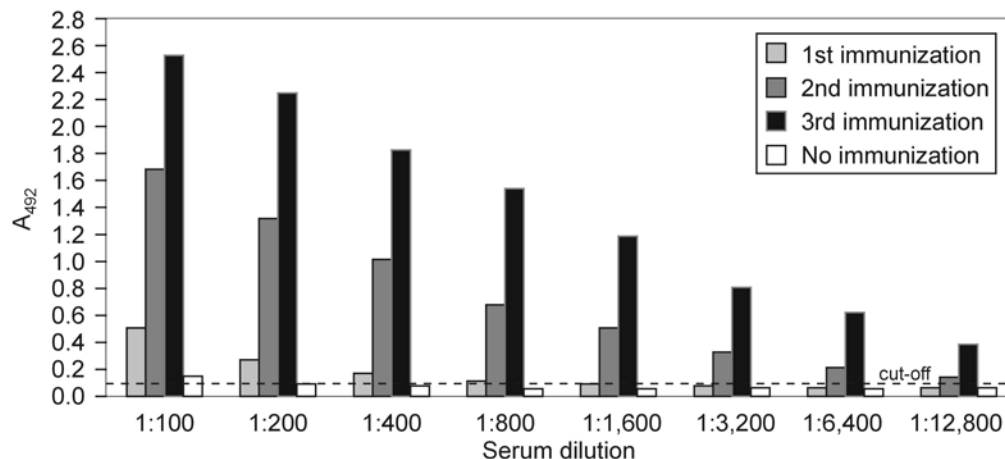


Fig. 1

Antibody response in mice to immunization with KLH-eM2

Mice were i.p. immunized with 3 doses of KLH-eM2 and their sera were assayed for eM2-specific IgG antibodies by ELISA.

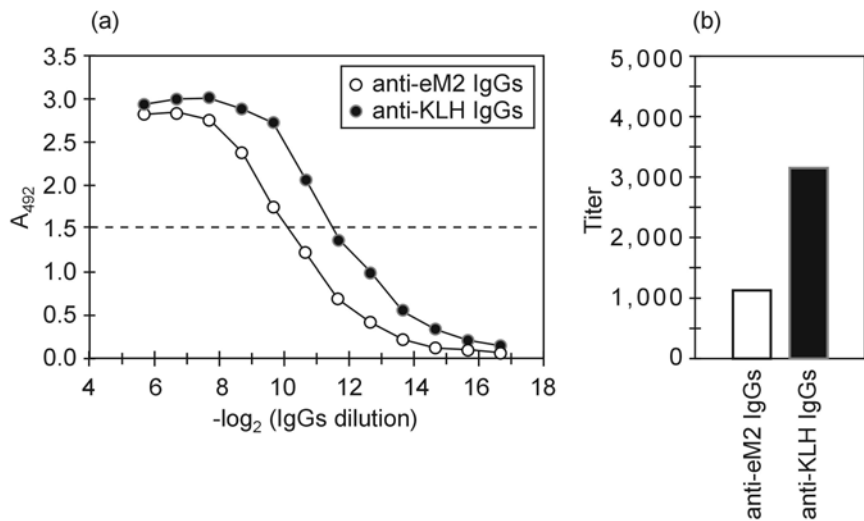


Fig. 2

Proportions of eM2- and KLH-specific antibodies in IgGs purified from ascitic fluid of mice immunized with KLH-eM2
Titration curves of anti-eM2 and anti-KLH IgGs (a) and titers of anti-eM2 and anti-KLH IgGs at A_{492} of 1.5 (b) in ELISA.

und's adjuvant to induce an antibody response in mice. Control mice were given KLH alone. Following three immunizations the majority of mice developed ascites due to administration of the adjuvant. The antibody response to eM2 gradually increased, corresponding to serum titers of 528, 10,800, and 28,800, respectively (Fig. 1). Ascitic fluids obtained after the last immunization served for purification of polyclonal IgG antibodies.

Proportions of eM2- and KLH-specific antibodies in IgGs purified from ascitic fluid from mice immunized with KLH-eM2

Proportions of IgG antibodies specific to eM2 and KLH, present in IgGs purified from mice immunized with KLH-eM2, were assayed by ELISA (Fig. 2). The distance of titration curves at A_{492} of 1.5 was estimated at 1.49 log₂ units and corresponding titers of anti-eM2 and anti-KLH IgGs were 1120 and 3149, respectively. This means that provided equal numbers of accessible eM2 epitopes specific to anti-eM2 IgGs and KLH epitopes specific to anti-KLH IgGs adsorbed onto respective wells, the ratio of anti-eM2 and anti-KLH IgGs was approximately 1:3.

Effective anti-eM2 IgG concentration required for the protection to influenza infection

Taking into account the anti-eM2 IgGs content of the anti-KLH-eM2 IgGs purificate, groups of mice were given i.v. 320, 160, 80, and 40 µg of anti-eM2 IgGs per animal. Control mice were administered 320 µg of anti-KLH IgGs

and 200 µl of PBS, respectively. Two hrs later the mice were infected with 3 LD₅₀ IAV and observed for survival. An absolute protection (100% survival) was obtained with 320 µg, a relatively strong significant protection (~80% survival) with 160 µg ($p = 0.024$), and a weak protection (~20% survival) with 80 and 40 µg of anti-eM2 IgGs (Fig. 3). Control mice scored a 100% mortality.

Estimating total blood volume in mouse at 1.5 ml, the applied doses 320 µg and 160 µg of anti-eM2 IgGs resulting in significant protection corresponded to the concentrations of 213 and 107 µg/ml anti-eM2 IgGs, respectively, in the blood.

These results roughly agree with those of Fu *et al.* (2009), who also evaluated the anti-eM2 protective response, however, by use of MAbs. They found that two of four tested MAbs at doses of 0.2–2.0 mg per mouse ensured a high survival, while 20 µg resulted in a low survival. Another group of authors (Beerli *et al.*, 2009) found that a most effective anti-eM2 MAb exhibited a fair protection against infection with 4 LD₅₀ of virus at a dose of 20 µg per mouse, but only a weak one at a dose of 6 µg. Such a high efficiency of this MAb as compared with our observations as well as those of Fu *et al.* (2009) can be most probably ascribed to a high affinity ($K_d = 4 \text{ nmol/l}$) of that particular MAb.

In conclusion, we assume that results of this study contribute to a recently accepted presumption that the eM2 molecule can be an effective and cross-protective immunogen. Its immunogenicity can be enhanced by applying it in appropriate form and/or with an optimally selected adjuvant. Its cross-reactivity can be ensured mainly by polyclonal character of the resulting antibody response. Moreover, the

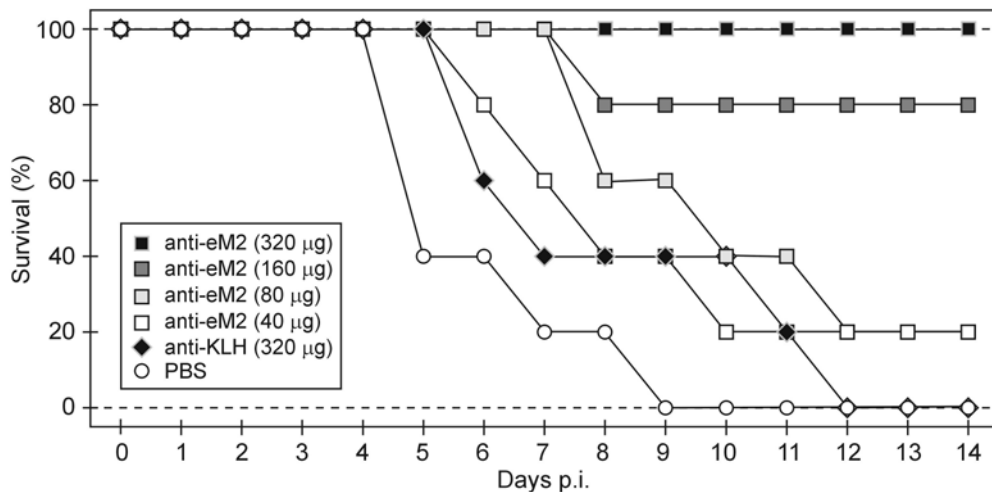


Fig. 3

Survival of mice passively immunized with purified anti-KLH-eM2 IgGs and infected with IAV

In immunization, the purified anti-KLH-eM2 IgGs were applied in amounts corresponding to 320, 160, 80, and 40 µg of anti-eM2 IgGs. Control mice obtained 320 µg of purified anti-KLH IgGs and PBS, respectively.

latter may contribute to the prevention of the appearance of antibody-escape mutants during natural infection (Zharikova *et al.*, 2005).

Acknowledgements. The authors thank Mmes M. Némethová and M. Mišovičová for excellent technical assistance. This work was supported by the VEGA grants Nos. 2/0101/10 and 2/0154/09 from the Scientific Grant Agency of Ministry of Education of Slovak Republic and Slovak Academy of Sciences and the Slovak Research and Development Agency under the contract No. APVV-0250-10.

References

- Beerli RR, Bauer M, Schmitz N, Buser RB, Gwerder M, Muntwiler S, Renner WA, Saadan P, Bachmann MF (2009): Prophylactic and therapeutic activity of fully human monoclonal antibodies directed against influenza A M2 protein. *Virology* J. 6, 224. doi.org/10.1186/1743-422X-6-224
- Ben-Yedid T, Arnon R (2006): Flagella as a Platform for Epitope-Based Vaccines. *Isr. Med. Assoc. J.* 8, 316–318 8
- De Filette M, Martens W, Roose K, Deroo T, Vervalle F, Bentahir M, Vandekerckhove J, Fiers W, Saelens X (2008): An influenza A vaccine based on tetrameric ectodomain of matrix protein 2. *J. Biol. Chem.* 283, 11382–11387. doi.org/10.1074/jbc.M800650200
- Ey PL, Prowse SJ, Jenkin CR (1978): Isolation of pure IgG1, IgG2a and IgG2b immunoglobulins from mouse serum using Protein A-Sepharose. *Immunochemistry* 15, 429–436. [doi.org/10.1016/0161-5890\(78\)90070-6](https://doi.org/10.1016/0161-5890(78)90070-6)
- Feng J, Zhang M, Mozdzanowska K, Zharikova D, Hoff H, Wunner W, Couch RB, Gerhard W (2006): Influenza A virus infection engenders a poor antibody response against the ectodomain of matrix protein 2. *Virology* J. 3, 102. doi.org/10.1186/1743-422X-3-102
- Fu TM, Freed DC, Horton MS, Fan J, Citron MP, Joyce JG, Garsky VM, Casimiro DR, Zhao Q, Shiver JW, Liang X (2009): Characterizations of four monoclonal antibodies against M2 protein ectodomain of influenza A virus. *Virology* 385, 218–226. doi.org/10.1016/j.virol.2008.11.035
- Huleatt JW, Nakar V, Desai P, Huang Y, Hewitt D, Jacobs A, Tang J, McDonald W, Song L, Evans RK, Umlauf S, Tussey L, Powell TJ (2008): Potent immunogenicity and efficacy of a universal influenza vaccine candidate comprising a recombinant fusion protein linking influenza M2e to the TLR5 ligand flagellin. *Vaccine* 26, 201–214. doi.org/10.1016/j.vaccine.2007.10.062
- Jegerlehner A, Schmitz N, Storni T, Bachmann MF (2004): Influenza A vaccine based on the extracellular domain of M2e: weak protection mediated via antibody-dependent NK cell activity. *J. Immunol.* 172, 5598–5605.
- Lamb RA, Zebedee SL, Richardson CD (1985): Influenza virus M2 protein is an integral membrane protein expressed on the infected-cell surface. *Cell* 40, 627–633. [doi.org/10.1016/0092-8674\(85\)90211-9](https://doi.org/10.1016/0092-8674(85)90211-9)
- Liu W, Peng Z, Liu Z, Lu Y, Ding J, Chen YH (2004): High epitope density in a single recombinant protein molecule of the extracellular domain of influenza A virus M2 protein significantly enhances protective immunity. *Vaccine* 23, 366–371. doi.org/10.1016/j.vaccine.2004.05.028
- Neirynck S, Deroo T, Saelens X, Vanlandschoot P, Jou WM, Fiers W (1999): A universal influenza A vaccine based on the extracellular domain of the M2 protein. *Nat. Med.* 5, 1157–1163. doi.org/10.1038/13484
- Okuda K, Ihata A, Watabe S, Okada E, Yamakawa T, Hamajima K, Yang J, Ishii N, Nakazawa M, Okuda K, Ohnari K, Nakajima K, Xin KQ (2001): Protective immunity against influ-

- enza A virus induced by immunization with DNA plasmid containing influenza M gene. *Vaccine* 19, 3681–3691. [doi.org/10.1016/S0264-410X\(01\)00078-0](https://doi.org/10.1016/S0264-410X(01)00078-0)
- Palese P, Garcia-Sastre A (2002): Influenza vaccines: present and future. *J. Clin. Invest.* 110, 9–13.
- Slepushkin VA, Katz JM, Black RA, Gamble WC, Rota PA, Cox NJ (1995): Protection of mice against influenza A virus challenge by vaccination with baculovirusexpressed M2 protein. *Vaccine* 13, 1399–1402. [doi.org/10.1016/0264-410X\(95\)92777-Y](https://doi.org/10.1016/0264-410X(95)92777-Y)
- Staneková Z, Király J, Stropkovská A, Mikušková T, Mucha V, Kostolanský F, Varečková E (2011): Heterosubtypic protective immunity against influenza A virus induced by fusion peptide of the hemagglutinin in comparison to ectodomain of M2 protein. *Acta Virol.* 55, 61–67. doi.org/10.4149/av-2011-01-61
- Sui Z, Chen Q, Wu R, Zhang H, Zheng M, Wang H, Chen Z (2010): Cross-protection against influenza virus infection by intranasal administration of M2-based vaccine with chitosan as an adjuvant. *Arch. Virol.* 155, 535–544. doi.org/10.1007/s00705-010-0621-4
- Varečková E, Mucha V, Wharton SA, Kostolanský F (2003a): Inhibition of fusion activity of influenza A hemagglutinin mediated by HA2-specific monoclonal antibodies. *Arch. Virol.* 148, 469–486. doi.org/10.1007/s00705-002-0932-1
- Wynne SA, Crowther RA, Leslie AG (1999): The crystal structure of the human hepatitis B virus capsid. *Mol. Cell.* 3, 771–780. [doi.org/10.1016/S1097-2765\(01\)80009-5](https://doi.org/10.1016/S1097-2765(01)80009-5)
- Zebedee SL, Lamb RA (1988): Influenza A virus M2 protein: monoclonal antibody restriction of virus growth and detection of M2 in virions. *J. Virol.* 62, 2762–2772.
- Zharikova D, Mozdzanowska K, Feng J, Zhang M, Gerhard W (2005): Influenza type A virus escape mutants emerge in vivo in the presence of antibodies to the ectodomain of matrix protein 2. *J. Virol.* 79, 6644–6654.

Prevalence of porcine circovirus 2 infection in pig population in Slovakia

T. CSANK¹, J. PISTL¹, J. POLLÁKOVÁ¹, E. HOLODA¹, M. HARVAN²

¹Department of Microbiology and Immunology, University of Veterinary Medicine and Pharmacy in Košice, 041 81 Košice, Slovak Republic; ²Böehringer Ingelheim, Bratislava, Slovak Republic

Received April 11, 2011; accepted July 22, 2011

Summary. – The prevalence of porcine circovirus 2 (PCV-2) infection in the pig population in Slovakia was investigated. Sera from pigs suspected for post-weaning multisystemic wasting syndrome (PMWS) as well as clinically healthy pigs were tested for viral DNA and specific IgM and IgG antibodies. Pigs (n = 198) were categorized to weaning, grower and fattening ones and sows. The results showed that PCV-2 antibodies were present in 53.4% of PMWS-suspects, in 50.0% of healthy pigs and in 69.0% of sows. In PMWS-suspect grower pigs, 40.7% were positive for IgM+IgG antibodies and 22.2% for viral DNA. In PMWS-suspect fattening pigs, 50.0% were positive for IgM+IgG antibodies and 25.0% for viral DNA. In healthy fattening pigs, almost 90.0% were positive for IgG antibodies and 38.5% for viral DNA. The highest proportion of PMWS-suspects was in grower pigs and specific antibodies were increasing with the age of pigs. A combination of positivities for IgG+IgM antibodies and viral DNA was a highly significant marker of PMWS. Viral DNA was detected in seropositive as well as seronegative PMWS-suspects. Overall, in all categories of pigs tested, specific antibodies and viral DNA were detected in 54.0% and 35.5%, respectively.

Keywords: porcine circovirus 2; pigs; prevalence; Slovakia

Introduction

PCV-2 is a non-enveloped, single-stranded circular DNA virus and belongs to the family *Circoviridae* and the genus *Circovirus* (Fenaux *et al.*, 2000; Mankertz *et al.*, 2000). There are two phenotypically different and genetically related species namely PCV-1 and PCV-2. PCV-1 is generally considered as non-pathogenic, whereas PCV-2 is associated with PMWS (Harding and Clark, 1997; Allan *et al.*, 1998; Allan and Ellis, 2000). PMWS is clinically characterized by progressive weight loss, dyspnea, pallor, diarrhea and jaundice from suckling to the growing stages of pigs, typically affecting animals between 7 and 15 weeks of age (Harding, 2004). However, PCV-2 is ubiquitous and

can be isolated from both diseased and healthy pigs (Allan and Ellis, 2000). It is the cause of major economical losses in pig industry.

Segalés (2007) in his review classified Slovakia as a country with unknown PMWS status. Two years later the first official data on detection of PCV-2 in PMWS-affected pigs at antigenic and genetic level was described in Slovakia (Pistl *et al.*, 2009). In the last decade, several studies were published, which document PCV-2 infection and the occurrence of PMWS in domestic or feral pigs in Poland (Stadejek *et al.*, 2006), Hungary (Kiss *et al.*, 2000; Tibor, 2004), Romania (Cadar *et al.*, 2007), Slovenia (Toplak *et al.*, 2004), Croatia (Lipej *et al.*, 2005), Greece (Sofia *et al.*, 2008), Czech Republic (Celer and Carasova, 2002; Sedlak *et al.*, 2008) and Austria (Schmoll *et al.*, 2002, 2003).

Till to date, no data is available that presents the prevalence of PCV-2 infection in the pig population in Slovakia. Therefore, the aim of this study was to determine the prevalence of PCV-2 infection in PMWS-suspect as well as clinically healthy pigs of different age categories. For this purpose, serum samples from total of 198 pigs were collected and subjected to ELISA for specific IgM and IgG antibodies and PCR for viral DNA.

E-mail: csank@uvm.sk; fax: +42155-6711674.

Abbreviations: MAb(s) = monoclonal antibody(ies); OR = odds ratio; PCV-2 = porcine circovirus 2; PMWS = post-weaning multisystemic wasting syndrome

Table 1. Prevalence of PCV-2 antibodies in different age categories of PMWS-suspect and healthy pigs in Slovakia

Pig category	No. of sera		No. (%) of antibody-positive sera						No. (%) of antibody negative sera	
			IgM+IgG		IgM		IgG			
	PMWS	H	PMWS	H	PMWS	H	PMWS	H	PMWS	H
Weaning	22	32	0	0	2 (9.1)	0	4 (18.2)	2 (6.3) ^a	16 (72.7)	30 (93.8)
Growers	27	25	11 (40.7)	6 (24.0)	1 (3.7)	0	0	3 (12.0) ^b	15 (55.6)	16 (64.0)
Fattening	24	39	12 (50.0)*	2 (5.1)	1 (4.2)	0	8 (33.3)	35 (89.7) ^{a,b}	3 (12.5)	2 (5.1)

PMWS = PMWS-suspects; H = healthy pigs; ^aP < 0.001; ^bP < 0.001; *P < 0.05 (OR = 12.67).

Materials and Methods

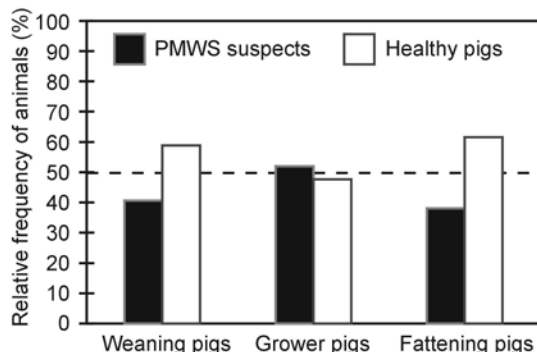
Serum samples. Total 198 serum samples from 16 farms located in different regions of Slovakia were collected during years 2009–2010. Sera were obtained from PMWS-suspect (n = 73) as well as healthy (n = 96) pigs. As PMWS clinical signs like wasting, enlarged inguinal lymph nodes and dyspnea are restricted to the nursery and early grower stages (Harding, 2004), sera from sows (n = 29) were excluded from categorization based on clinical picture. Animals were further categorized into weaning (3–6-week-old; n = 54), grower (7–12-week-old; n = 52); fattening (>13-week-old; n = 63) pigs and sows. None of the tested animals was vaccinated against PCV-2.

ELISA. Specific PCV-2 IgM and IgG antibodies were determined by commercially available capture ELISA (INGENZIM Circovirus IgG/IgM, Ingenasa, Spain) according to manufacturer's instructions. The ELISA kit contained two different plates with fixed pig-specific IgM and IgG monoclonal antibodies (MAbs). When a pig serum is added on each plate, the IgM and IgG antibodies present in the sample are captured by MAb adsorbed on the plate. After washing, the added PCV-2 antigen (recombinant empty capsid) is captured by the IgM and/or IgG in the serum sample. In the next step, HRP-conjugated PCV-2 MAb was used. The colorimetric reaction was measured after addition of TMB substrate by LEDETECT

96 Microplate Reader. Samples with A_{450} lower than cut off levels of positive controls were considered as negative for PCV-2 IgM and/or IgG antibodies.

PCR. Total DNA was isolated from 200 µl of serum. Briefly, after overnight digestion at 50°C in SDS/Proteinase K solution (SDS 0.1 g/ml, Proteinase K 0.5 mg/ml) the DNA was extracted with phenol-chloroform and ethanol-precipitated. PCR mixture (25 µl) contained 0.5 µl of extracted DNA, 1 × PCR reaction buffer, 3 mmol/l MgCl₂, 0.1 mmol/l of each dNTP, 0.3 µmol/l of each primer (ORF2.PCV2.S4 and ORF2.PCV2.AS4; (Ouardani *et al.*, 1999) and 0.5 U of Taq DNA Polymerase (Invitrogen, Brazil). Amplification was performed with an initial denaturation at 94°C for 5 mins, followed by 35 cycles of amplification (94°C for 1 min, 60°C for 1 min, 72°C for 1 min), with a final extension at 72°C for 7 mins. PCR products of 494 bp size were separated on 1.5% agarose gel at 80 V, stained with ethidium bromide and visualised using an ultraviolet transiluminator.

Statistical analyses. Association between the presence of both PCV-2 antibodies and viral DNA in PMWS-suspect pigs was calculated by odds ratio (OR) supported by chi-square test with Fisher's exact test. The association was significant if OR > 1 and P < 0.05 and not significant when OR ≤ 1 and P > 0.05. To assess the differences in positivity for PCV-2 antibodies and viral DNA, and distribution of PMWS-suspects in different age groups, chi-square test and Fisher's exact test was used.

**Fig. 1**

Age distribution of PMWS-suspect and healthy pigs
PMWS-suspect pigs (full columns); healthy pigs (empty columns).

Results

Age distribution of PMWS-suspect and healthy pigs

Based on clinical picture, the distribution of PMWS-suspects in different age categories was determined (Fig. 1). There was no significant difference between the prevalence of PMWS-suspect pigs in age groups.

Prevalence of specific IgM and IgG antibodies and viral DNA in PMWS-suspect and healthy pigs

Altogether 53.4% serum samples of PMWS-suspect pigs and 50.0% of healthy pigs were seropositive for PCV-2 antibodies. Most of the PMWS-suspect and healthy pigs

Table 2. Prevalence of PCV-2 antibodies and PCV-2 DNA in different age categories of PMWS-suspects and healthy pigs in Slovakia

Pig category	No. of sera		No. (%) of antibody-positive and viral DNA-positive sera						No. (%) of antibody-negative and viral DNA-positive sera	
			IgM+IgG		IgM		IgG			
	PMWS	H	PMWS	H	PMWS	H	PMWS	H	PMWS	H
Weaning	22	32	0	0	2 (9.1)	0	0	0 ^a	0	0
Growers	27	25	6 (22.2)	2 (8.0)	1 (3.7)	0	0	2 (8.0) ^b	5 (18.5)	0
Fattening	24	39	6 (25.0) ^c	1 (2.6)	0	0	1 (4.2)	15 (38.5) ^{a,b,c}	1 (4.1)	0

PMWS = PMWS-suspects; H = healthy pigs; ^aP < 0.001; ^bP < 0.01; ^cP < 0.01 between sows (Table 3); ^cP < 0.05 (OR = 12.67).

Table 3. Prevalence of PCV-2 antibodies and PCV-2 DNA in different age categories of pigs in Slovakia

Pig category (No. of sera)	PMWS and healthy pigs		PMWS pigs
	No. (%) of positive sera		
	Specific antibodies	Specific antibodies + viral DNA	
Weaning (54)	8	2	2
Growers (52)	21	11	7
Fattening (63)	58	23	7
Sows (29)	20	2 ^c	—
Total (198)	107 (54.0)	38 (35.5)	16 (42.1)

PMWS = PMWS-suspects; ^cP < 0.01 between fattening pigs (Table 2).

in weaning groups were seronegative; however, in growers showing PMWS symptoms we observed increase of PCV-2 IgM+IgG- and PCV-2 DNA-positive serum samples (Table 1). In the fattening pigs, significant association ($P < 0.05$, OR = 12.67) was observed between PMWS clinical signs and the presence of PCV-2 IgM+IgG antibodies as well as viral DNA (Tables 1 and 2). The highest number of PCV-2 antibody- and viral DNA-positive serum samples was detected in the fattening pigs (Table 3). Almost 90.0% of serum samples of healthy fattening pigs were PCV-2 IgG positive, which differs significantly from healthy weaner and grower pigs ($P < 0.0001$; Table 1). In addition, the presence of PCV-2 DNA in the same age group was also significantly higher in comparison to all age categories of pigs (Tables 2 and 3).

Prevalence of PCV-2 antibodies was 54.0% of total number of pigs from different regions of Slovakia (Table 3). PCV-2 DNA was detected in 35.5% of the seropositive samples but 6 seronegative PMWS-suspect sera showed presence of viral DNA (Table 2). None of seronegative sample from the clinically healthy group was positive for PCV-2 DNA (Table 2).

Discussion

The highest number of PMWS-suspects was observed in weaning and growing pigs. These results are in parallel with the findings reported by Segalés and Cortey (2010), where more than 80.0% of PMWS-affected pigs fall between two and

four months of age. Low number of PCV-2 IgG-positive pigs in the weaning group implies that these animals had low, if at all, colostral antibodies against PCV-2. This fact is also supported by 31.0% seronegativity in the sows. Pigs have epitheliochorial placenta impermeable to immunoglobulins and are therefore hypo- or agammaglobulinemic at birth (Kim, 1975). Thus, the survival of neonatal piglets depends upon their ingestion of colostrum during the first hours of life (Salmon *et al.*, 2009). The amount and persistence of colostral PCV-2 IgG in the serum of piglets depends on their level in the blood of sows. The mean PCV-2 antibody half-life was estimated to be 19 days, and the level of passively acquired antibodies decay below ELISA cut off levels approximately at five weeks of age in weanlings derived from sows with low PCV-2 IgG (Opriessnig *et al.*, 2004).

Most of the PCV-2 IgM- and IgG-positive pigs were detected among grower and fatterer pigs regardless of the clinical status. High prevalence of IgM+IgG-positive animals in our study confirms that pigs get infected after the weaning period (Harding, 2004). Detection of both PCV-2 antibodies and viral DNA in PMWS-suspects suggest acute infection at the time of sampling. A combination of the presence of both IgM and IgG antibodies, and viral DNA can be a significant marker for detection of PMWS-suspect fattening pigs.

Viral DNA in combination with PCV-2 antibodies had the highest prevalence within the group of fattening pigs. Surprisingly, despite of a repeated PCR, we noted low number of PCV-2 DNA-positive samples in all age categories. This event can be explained with low amount of virus in the blood at time of sampling, which cannot be detected by conventional PCR. The same pattern was observed in a study by McIntosh *et al.* (2006),

where higher detection rate was reached by nested-PCR. PCV-2 is present in PMWS-free as well as affected farms (Larochelle *et al.*, 2003; Sibila *et al.*, 2004; Meerts *et al.*, 2006), what supports our results, since approximately 50.0% of healthy and PMWS-suspect pigs were seropositive and a high number of healthy ones was PCV-2 DNA-positive too.

Overall, among all four age categories, specific PCV-2 antibodies were detected in 54.0% of samples, which is lower in comparison with data from other European countries with intensive pig industry, like Spain with 72.7% seroprevalence (Rodriguez-Arrioja *et al.*, 2003), France with 80.0% (Blanchard *et al.*, 2003), Belgium with 100.0% (Lefebvre, 2008), Austria with 60.0% (Schmoll *et al.*, 2008), but also Canada with 82.4% (Liu *et al.*, 2002) and USA with 80.0% seroprevalence (Nawagitgul *et al.*, 2002).

From the results we conclude: i) the development of PCV-2 antibodies was age dependent, ii) the prevalence of PCV-2 antibodies was almost the same in PMWS-suspect and healthy pigs, iii) PMWS-suspect pigs were mostly PCV-2 IgM+IgG-positive, while in healthy pigs, IgG were prevalent, which shows a different trend in the distribution of PCV-2 antibodies between PMWS-suspects and healthy animals, iv) simultaneous detection of IgM+IgG antibodies and viral DNA can be a significant marker for PMWS-suspect pigs, and v) the prevalence of antibodies against PCV-2 in the Slovak pig population was 54.0%, which is lower in comparison with countries with enzootic PCV-2 infection.

Acknowledgements. This work was supported by the following grants: INFEKTZOOON – Centrum of excellence for infections of animals and zoonoses, ITMS code 26220120002, supported by operational program Research and Development financed by European Fund of Regional Development and by the Slovak Research and Development Agency under the contract No. APVV-20-019605. We thank MVDr. Mangesh Bhide, PhD. for revision of the scientific English of the manuscript.

References

- Allan GM, Ellis JA (2000): Porcine circoviruses: a review. *J. Vet. Diagn. Invest.* 12, 3–14. doi.org/10.1177/104063870001200102
- Allan GM, McNeilly F, Kennedy S, Daft B, Clarke EG, Ellis JA, Haines DM, Meehan BM, Adair BM (1998): Isolation of porcine circovirus-like viruses from pigs with a wasting disease in the USA and Europe. *J. Vet. Diagn. Invest.* 10, 3–10. doi.org/10.1177/104063879801000102
- Blanchard P, Mahe D, Cariolet R, Truong C, Le Dimna M, Arnauld C, Rose N, Eveno E, Albina E, Madec F, Jestin A (2003): An ORF2 protein-based ELISA for porcine circovirus type 2 antibodies in post-weaning multisystemic wasting syndrome. *Vet. Microbiol.* 94, 183–194. [doi.org/10.1016/S0378-1135\(03\)00131-7](https://doi.org/10.1016/S0378-1135(03)00131-7)
- Cadar D, Csagola A, Dan A, Deim Z, Spinu M, Miclaus V, Kobolkuti L, Czirjak G, Tuboly T (2007): Porcine circovirus type 2 and associated diseases in Romania. *Acta Vet. Hungarica* 55, 151–156. doi.org/10.1556/AVet.55.2007.1.14
- Celer V, Carasova P (2002): First evidence of porcine circovirus type 2 (PCV-2) infection of pigs in the Czech Republic by semi-nested PCR. *J. Vet. Med. Ser. B Infect. Dis. Vet. Public Health* 49, 155–159.
- Fenaux M, Halbur PG, Gill M, Toth TE, Meng XJ (2000): Genetic characterization of type 2 porcine circovirus (PCV-2) from pigs with postweaning multisystemic wasting syndrome in different geographic regions of North America and development of a differential PCR-restriction fragment length polymorphism assay to detect and differentiate between infections with PCV-1 and PCV-2. *J. Clin. Microbiol.* 38, 2494–2503.
- Harding J, Clark E (1997): Recognizing and diagnosing postweaning multisystemic wasting syndrome (PMWS). *J. Swine Health Prod.* 5, 201–203.
- Harding JCS (2004): The clinical expression and emergence of porcine circovirus 2. *Vet. Microbiol.* 98, 131–135. doi.org/10.1016/j.vetmic.2003.10.013
- Harding JCS, Clark EG, Strokappe JH, Willson PI, Ellis JA (1998): Postweaning multisystemic wasting syndrome: Epidemiology and clinical presentation. *Swine Health Prod.* 6, 249–254.
- Kim YB (1975): Developmental immunity in the piglet. *Birth Defects Orig. Artic. Ser.* 11, 549–557.
- Kiss I, Kecskemeti S, Tuboly T, Bajmocy E, Tanyi J (2000): New pig disease in Hungary: postweaning multisystemic wasting syndrome caused by circovirus (short communication). *Acta Vet. Hungarica* 48, 469–475.
- Larochelle R, Magar R, D'Allaire S (2003): Comparative serologic and virologic study of commercial swine herds with and without postweaning multisystemic wasting syndrome. *Can. J. Vet. Res. Revue Canadienne De Recherche Veterinaire* 67, 114–120.
- Lefebvre D, Van Reeth K, Vangroenweghe F, Castryk F, Maes D, Laitat M, Nauwynck H (2008): Serosurvey for viruses associated with reproductive failure in newly introduced gilts and in multiparous sows in Belgian sow herds. Proceedings of the 20th IPVS Congress, South Africa, Durban, p. 93.
- Lipej Z, Segales J, Toplak I, Sostaric B, Roic B, Lojkic M, Hostnik P, Grom J, Barlic-Maganja D, Zarkovic K, Oraic D (2005): Postweaning multisystemic wasting syndrome (PMWS) in pigs in Croatia: Detection and characterisation of porcine circovirus type 2 (PCV2). *Acta Vet. Hungarica* 53, 385–396. doi.org/10.1556/AVet.53.2005.3.11
- Liu Q, Wang L, Willson P, O'Connor B, Keenliside J, Chirino-Trejo M, Melendez R, Babiuk L (2002): Seroprevalence of porcine circovirus type 2 in swine populations in Canada and Costa Rica. *Can. J. Vet. Res. Revue Canadienne De Recherche Veterinaire* 66, 225–231.
- Mankertz A, Domingo M, Folch JM, LeCann P, Jestin A, Segales J, Chmielewicz B, Plana-Duran J, Soike D (2000): Genetic characterisation of PCV-2 isolates from Spain, Germany and France. *Virus Res.* 66, 65–77. [doi.org/10.1016/S0168-1702\(99\)00122-7](https://doi.org/10.1016/S0168-1702(99)00122-7)
- McIntosh KA, Harding JCS, Ellis JA, Appleyard GD (2006): Detection of Porcine circovirus type 2 viremia and seroconversion in naturally infected pigs in a farrow-to-finish

- barn. Can. J. Vet. Res. Revue Canadienne De Recherche Veterinaire 70, 58–61.
- Meerts P, Misinzo G, Lefebvre D, Nielsen J, Botner O, Kristensen CS, Nauwynck HJ (2006): Correlation between the presence of neutralizing antibodies against porcine circovirus 2 (PCV2) and protection against replication of the virus and development of PCV2-associated disease. BMC Vet. Res. 2, 6.
- Nawagigitgil P, Harms PA, Morozov I, Thacker BJ, Sorden SD, Leckcharoensuk C, Paul PS (2002): Modified indirect porcine circovirus (PCV) type 2-based and recombinant capsid protein (ORF2)-based enzyme-linked Immunosorbent assays for detection of antibodies to PCV. Clin. Diagn. Lab. Immunol. 9, 33–40.
- Opriessnig T, Yu S, Thacker EL, Halbur PG (2004): Derivation of porcine circovirus type 2-negative pigs from positive breeding herds. J. Swine Health Prod. 12, 186–191.
- Ouardani M, Wilson L, Jette R, Montpetit C, Dea S (1999): Multiplex PCR for detection and typing of porcine circoviruses. J. Clin. Microbiol. 37, 3917–3924.
- Pistl J, Novackova M, Jackova A, Pollakova J, Levkut M, Vilcek S (2009): First evidence of Porcine Circovirus 2 (PCV2) in Slovakia. Deutsche Tierarztliche Wochenschrift 116, 19–23.
- Rodriguez-Arrioja GM, Segales J, Rosell C, Rovira A, Pujols J, Plana-Duran J, Domingo M (2003): Retrospective study on porcine circovirus type 2 infection in pigs from 1985 to 1997 in Spain. J. Vet. Med. Ser. B Infect. Dis. Vet. Public Health 50, 99–101.
- Salmon H, Berri M, Gerdts V, Meurens F (2009): Humoral and cellular factors of maternal immunity in swine. Develop. Comp. Immunol. 33, 384–393. doi.org/10.1016/j.dci.2008.07.007
- Sedlak K, Bartova E, Machova J (2008): Antibodies to selected viral disease agents in wild boars from the Czech republic. J. Wildl. Dis. 44, 777–780.
- Segales J (2007): Porcine circovirus disease (PCVD)- Have we won the war in Europe? Adv. Pork Prod. 18, 49–56.
- Segales J, Allan GM, Domingo M (2005): Porcine circovirus diseases. Anim. Health Res. Rev. 6, 119–42. doi.org/10.1079/AHR2005106
- Segales J, Cortey M (2010): Postweaning multisystemic wasting syndrome (PMWS) age-shift presentation is not supported by an 11-year retrospective study in Spain. 21st International Pig Veterinary Society (IPVS) Congress, p. 286.
- Schmoll F, Lang C, Steinrigl AS, Schulze K, Kauffold J (2008): Prevalence of PCV2 in Austrian and German boars and semen used for artificial insemination. Theriogenology 69, 814–821. doi.org/10.1016/j.theriogenology.2007.12.009
- Schmoll F, Opriessnig T, Schilcher F, Leeb B, Bauder B, Schuh M (2002): First description of postweaning multisystemic wasting syndrome (PMWS) in Austria. Wien. Tierarztl. Monatsschr. 89, 50–56.
- Schmoll F, Sipos W, Weissenbock H, Schilcher F, Schuh M (2003): First report of porcine dermatitis and nephropathy syndrome (PDNS) in Austria. Wien. Tierarztl. Monatsschr. 90, 23–27.
- Sibila M, Calsamiglia M, Segales J, Blanchard P, Badiella L, Le Dimna M, Jestin A, Domingo M (2004): Use of a polymerase chain reaction assay and an ELISA to monitor porcine circovirus type 2 infection in pigs from farms with and without postweaning multisystemic wasting syndrome. Am. J. Vet. Res. 65, 88–92. doi.org/10.2460/ajvr.2004.65.88
- Sofia M, Billinis C, Psychas V, Birtsas P, Sofianidis G, Leontides L, Knowles N, Spyrou V (2008): Detection and genetic characterization of porcine circivirus 2 isolates from the first cases of postweaning multisystemic and wasting syndrome in wild boars in Greece. J. Wildl. Dis. 44, 864–870.
- Stadejek T, Podgorska K, Kolodziejczyk P, Bogusz R, Kozaczynski W, Pejsak Z (2006): First report of postweaning multisystemic wasting syndrome in pigs in Poland. Medycyna Weterynaryjna 62, 297–301.
- Tibor S (2004): Histopathological lesions observed in disease (postweaning multisystemic wasting syndrome) caused by porcine circovirus type 2 (PCV-2) and their diagnostic, pathogenic and clinical evaluation. Magyar Allatorvosok Lapja 126, 465–481.
- Toplak I, Grom J, Hostnik P, Barlic-Maganja D (2004): Phylogenetic analysis of type 2 porcine circoviruses identified in wild boar in Slovenia. Vet. Rec. 155, 178–80. doi.org/10.1136/vr.155.6.178

Evidence of conserved epitopes in variable region of VP8^{*} subunit of VP4 protein of rotaviruses of P[8]-1 and P[8]-3 lineages

J.F. CONTRERAS¹, G.E. MENCHACA¹, R. INFANTE², C. E. HERNÁNDEZ¹, C. RODRÍGUEZ¹, R.S. TAMEZ¹

¹Facultad de Ciencias Biológicas, Universidad Autónoma de Nuevo León. Cd. Universitaria, San Nicolás de los Garza, N.L. 66451 México;

²Facultad de Ciencias Químicas, Universidad Autónoma de Chihuahua. Nuevo Campus Universitario, Chihuahua, Chih. 31125 México

Received February 15, 2011; accepted July 27, 2011

Summary. – Although antibody responses to the human rotavirus VP4 protein have been reported, few studies have analyzed the specificity of these responses to the VP8^{*} subunit. This study investigated antibody responses generated against the variable region of the VP4 protein (VP8^{*} subunit) in children infected with rotavirus genotype P[8]. Recombinant VP8^{*} subunit (rVP8^{*}) and truncations corresponding aa 1–102 (peptide A) and 84–180 (peptide B) of rotavirus strains P[8]-1 and P[8]-3 lineages were expressed in *Escherichia coli* and examined for antibody reactivity using ELISA and Western blot assays. Sera from infected children had IgG antibodies that reacted with full-length rVP8^{*}, peptide A and B of both lineages, with stronger reactivity observed against peptide B. In addition, anti-strain Wa (P[8]-1) and anti-rVP8^{*} (P[8]-3) rabbit polyclonal antiserum reacted against peptide B sequences of both lineages. These data indicate that the VP8^{*} variable region of rotavirus belonging to P[8]-1 and P[8]-3 lineages have conserved epitopes recognized by antibodies elicited during natural infections.

Keywords: antibodies; conserved epitopes; VP8^{*} subunit; VP4 protein; P[8] lineage; rotaviruses

Introduction

Rotaviruses (the species *Rotavirus A*, the genus *Rotavirus*, the subfamily *Sedoreovirinae*, and the family *Reoviridae*) express two outer proteins (VP4 and VP7) encoded by genes 4 and 9, respectively, which elicit the production of neutralizing antibodies (NtAb) that confer protection against subsequent infectious in children (Jiang *et al.*, 2002). Nucleotide sequences of these two genes are used to classify rotavirus strains into genotypes. To date, 23 G genotypes (VP7) and 32 P genotypes (VP4) have been identified in humans and different animal species (Collins *et al.*, 2010; Okitsu *et al.*, 2011). Worldwide, 80% of human rotavirus

strains result from infections with the P[8] genotype (Santos and Hoshino, 2005).

VP4 is an 88 kDa protein necessary for rotavirus penetration into target cells. During this process, VP4 is cleaved by trypsin, producing peptides VP8^{*} and VP5^{*}. Phylogenetic analysis of the VP8^{*} region revealed four P[8] lineages. The amino acid sequence comparisons between lineages revealed 87–91% identity (Maunula and von Bonsdorff, 1998; Cunliffe *et al.*, 2001; Arista *et al.*, 2005). Each P[8] lineage contains a variable region between aa 71–204 that has serotype-specific epitopes (Larralde and Gorziglia, 1992). However, the relationship between serotype and the variable sequences in this region for different lineages is not clear. Therefore, determining the lineage-specificity of antibodies to this region might improve our understanding of humoral responses elicited against P[8] genotypes following natural infections.

To study the antibody response to the VP8^{*} variable region of P[8]-1 and P[8]-3 lineages, truncated peptides corresponding to the VP8^{*} subunit of each lineage were produced, and

E-mail: juan.contrerascr@uanl.edu.mx; contrerasjfc@gmail.com; fax: +52-8183524212.

Abbreviations: NtAb = neutralizing antibodies; rVP8^{*} = recombinant VP8^{*} subunit

antibody specificity present in the sera of rotavirus infected children was assessed by ELISA and Western blot analyses.

Materials and Methods

Stool and serum specimens. Fecal and serum samples ($n = 10$) were collected from patients <2-years of age during the acute phase of disease, admitted with gastroenteritis to hospitals in Chihuahua City, North Mexico between 2007–2008.

Titration of neutralizing antibodies. Human rotavirus strain Wa (kindly provided by Carlos F. Arias, IBT-UNAM, Mexico) was propagated in MA104 cell as described (Taniguchi *et al.*, 1998). The presence of NtAb to rotavirus strain Wa in the sera of children was determined using the immunochemical focus reduction neutralization test (Arias *et al.*, 1987). The NtAb titer for each serum sample examined was defined as the highest serum dilution where the number of infected cells was reduced by at least 60% compared to infected cells not incubated in the presence of serum.

RT-PCR. RNA was extracted from rotavirus Wa-infected cells and from 20% fecal suspensions obtained from 10 field isolates using the TRI-REAGENT (MRS). A 762 bp amplicon corresponding to the gene 4 product encoding the VP8* subunit of the VP4 protein was amplified by RT-PCR. The primers used were PA1 (5'-CACGGATCCGGCTATAAAATGGCTTCACTC-3', nt 1–21) and PC2 (5'-CACGTCGACTTCATTAACTTGTGCTCT-3', nt 745–762) (Larralde and Gorziglia, 1992). To obtain VP8* cDNA, viral RNA and 0.1 μ mol/l PC2 primer were denatured at 94°C for 5 mins and then added to the reaction mixture containing 1X RT buffer (Bioline), 2.5 mmol/l MgCl₂, 0.8 mmol/l of each dNTP and 40 U of MMLV Reverse Transcriptase* (Bioline). Reverse transcription was conducted at 42°C for 30 mins. The PCR reaction mixture (12.5 μ l) contained 1 μ l cDNA-VP8*, 1X NH₄ buffer (Bioline), 1.5 mmol/l MgCl₂, 0.4 mmol/l of each dNTP, 0.5 μ mol/l of each primer and 250 U of Red™ DNA Polymerase (Bioline). The reaction conditions were as follows: 95°C/2 mins followed by 30 cycles at 95°C/30 secs, 42°C/30 secs, and 72°C/40 secs with a final extension at 72°C/15 mins.

Cloning and sequencing of the VP8* subunit. VP8* amplicons (762 bp) of strain Wa and the 10 field isolates were purified from agarose gel using the Wizard® SV Gel and PCR Clean-Up System (Promega) and cloned into the pGEM-T plasmid using the pGEM®-T Vector System I Kit (Promega). The nucleotide sequence was determined at IBT-UNAM, Mexico using an automated system (Perkin Elmer, Applied Biosystems). Sequencing and phylogenetic analysis of the VP8* subunit was performed using CLUSTAL W/BioEdit v7.0 (Hall, 1999) and the neighbor-joining method using the MEGA v4.1 software, respectively (Tamura *et al.*, 2007). The sequences were deposited at GenBank database under Acc. Nos. FJ665385 to FJ665391 and HQ585864 to HQ585866.

Cloning, expression, and purification of His-tagged VP8* peptides A and B. The primers used to generate full-length rVP8*, peptide

A (aa 1–102) and peptide B (aa 84–180) of rotavirus strain Wa (P[8]-1 lineage) and isolate MX08-659 (P[8]-3 lineage) were modified to match strain Wa (Larralde and Gorziglia, 1992). Each PCR product was cloned into the pGEM-T plasmid (Promega) according to the manufacturer's instructions and later subcloned into the BamHI and SalI sites of the pET28a(+) vector (Novagen). Protein expression was performed in *Escherichia coli* BL21(DE3) induced with 1 mmol/l IPTG (isopropyl-beta-D-thiogalactopyranoside) (Dowling *et al.*, 2005). The His-tagged recombinant proteins were purified using HisTrap FF Crude columns (GE Healthcare) under denaturing conditions. Each recombinant protein was characterized by SDS-PAGE and Western blot.

ELISA assays. We used a modification of the procedure previously described (Hyer *et al.*, 2008). Briefly, 96-well microtiter plates were coated with 10 μ g/ml of P[8]-1 and P[8]-3 rVP8* in carbonate-bicarbonate buffer (pH 9.6) and incubated overnight at 4°C. After washing with PBS-0.1% Tween 20 the plates were blocked with 5% nonfat dry milk in PBS at 4°C for 12 hrs. After 4 washes, 2-fold serial dilutions of respective serum samples were added and incubated at 37°C for 1 hr. FCS was used as a negative control. After washing four times, peroxidase-conjugated protein A (Amersham) was added and incubated at 37°C for 1 hr. After 4 washes, ABTS peroxidase substrate (Zymed) was added at 37°C for 30 mins. Absorbance at 405 nm was measured using an automatic plate reader (Digital and Analog Systems S.R.L.). The IgG-titer was defined as the highest dilution of serum giving the absorbance at least two SD greater than the negative control.

Western blot analysis. Full-length rVP8*, peptide A and B of rotavirus P[8]-1 and P[8]-3 lineages were subjected to 12.5% SDS-PAGE and blotted at 20 volts for 2 hrs onto 0.45 μ m nitrocellulose membranes (Sigma-Aldrich). The membranes were then blocked with 2% Tween in TBS (Tris Buffered Saline) and then incubated overnight at 4°C in the presence of respective serum samples. Antibody reactivity was detected using the ProtoBlot® II AP System with the Stabilizing Substrate Kit (Promega).

Results

VP8* subunit sequencing analysis

Amplicons (762 bp) corresponding to the VP8* subunit encoded by gene 4 of prototype rotavirus strain Wa and 10 rotavirus strains collected from infected children were cloned and sequenced. Alignment of the VP8* amino acid sequences of the field isolates showed that they shared 97.2–100% identity and belonged to the P[8] genotype. These isolates, compared to rotavirus strain Wa, had 19–22 amino acid substitutions (91.2–92.4% identity). Sixteen substitutions were localized in the variable region (aa 71–204). Phylogenetic analysis revealed that all field strains clustered to the P[8]-3 lineage whereas rotavirus Wa clustered to the P[8]-1 lineage (Fig. 1).

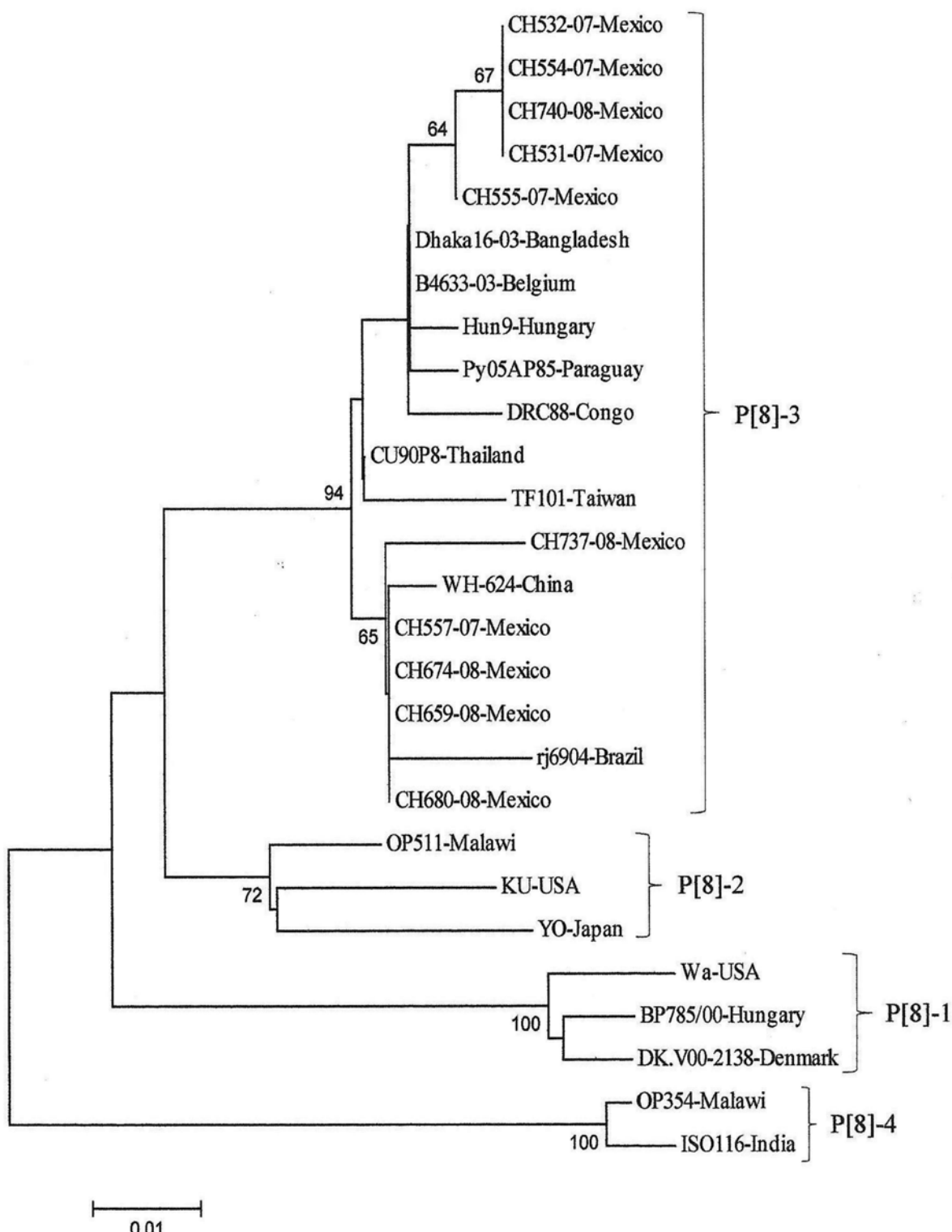


Fig. 1

Phylogenetic analysis of the deduced VP8* subunit amino acid sequences of P[8] human rotavirus strains

The tree was constructed using the neighbor joining method; bootstrap of 1,000 replications (MEGA v4.1).

Assessment of the antibody responses to the VP8 variable region*

To measure the antibody response to the VP8* subunit, sera from infected children were first screened for neutralization activity against rotavirus strain Wa followed by ELISA and Western blot analyses to detect reactivity against the VP8* His-tagged recombinant constructs. We found that 9/10 serum samples examined had detectable levels of NtAb. Specific IgG antibodies reactive against the full-length rVP8* of P[8]-1 and P[8]-3 lineages were also detected in sera with titers ranging between 100-1,600 (Table 1).

Based on these binding data, we focused our analyses to antibody responses recognizing the VP8* variable region (peptide B) and then compared this response to peptide A reactivity (which is the most conserved VP8* subunit). Each serum sample was then analyzed by Western blot for reactivity against peptides A and B of rotavirus strain Wa (P[8]-1 lineage) and rotavirus strain MX08-659 (P[8]-3 lineage). Although peptides from both lineages were detected in all serum samples tested, the reactivity with peptide B was higher than reactivity observed against peptide A (Fig. 2).

Finally, to determine if the serum reactivity observed against peptide B was lineage specific, rabbit hyperimmune antiserum raised against rotavirus strain Wa or against MX08-659 full-length rVP8* was tested by Western blot. These experiments demonstrated that rabbit anti-sera recognized both peptide B of P[8]-1 and P[8]-3 lineages (Fig. 2).

Discussion

Previous studies have described the world-wide circulation of four lineages corresponding to P[8] genotype rotavirus strains. There is an 8.6–13% amino acid sequence divergence

between lineages (Maunula and von Bonsdorff, 1998; Cunliffe *et al.*, 2001). Therefore, it is important to determine if amino acid differences between lineages can affect the reactivity of antibodies generated following natural rotavirus infections. In this report, all field isolates grouped to the P[8]-3 lineage, which is considered the most prominent lineage throughout the world (Ansaldi *et al.*, 2007; Araujo *et al.*, 2007; Rahman *et al.*, 2007; Espínola *et al.*, 2008). We also tested serum from rotavirus-infected children for reactivity against the VP8* subunit of the prototype human rotavirus strain Wa (P[8]-1 lineage) that is similar to the Rotarix vaccine licensed in Mexico since 2004 (Cheuvart *et al.*, 2009). To determine the genetic relationship between these two strains, we analyzed the amino acid sequence of the VP8* subunit of VP4 of the Rotarix vaccine (data not shown). Five substitutions were detected following comparison of the vaccine strain sequence to the non-vaccine Wa strain sequence. This analysis revealed three substitutions, in addition to those reported by Ward *et al.* (2006). For this reason, we used full-length rVP8* corresponding to the P[8]-1 and P[8]-3 lineages to determine if the antibodies elicited following natural infections reacted against these recombinant proteins.

We detected comparable IgG-titers against both P[8]-1 and P[8]-3 rVP8*, and titers were similar to those reported by Padilla-Noriega *et al.*, who measured the antibody responses to rVP8* from the rhesus rotavirus (RRV) strain using sera from children vaccinated with RRV (Padilla-Noriega *et al.*, 1992). Our results suggested that children infected with P[8] rotavirus strains mounted a homologous immune response to this genotype. In addition, these results were in agreement with our previous findings that demonstrated that a homologous antibody response could be mounted to the P1A serotype VP4 protein following natural infection (Menchaca *et al.*, 1998).

A previous report described that the variable region within the VP8* subunit had serotype-specific epitopes and that this region could be recognized by rabbit antibodies specific to whole human rotavirus (Larralde and Gorziglia, 1992). Therefore, we determined if the sera from infected children contained antibodies specific to the VP8* variable region. This was carried out by examining the reactivity against rVP8* truncated peptides (peptides A and B) of rotavirus strain Wa (P[8]-1 lineage) and MX08-659 isolate (P[8]-3 lineage). Western blot results showed that sera from the infected children examined in this report recognized epitopes present in peptides of both lineages, but that the reactivity against peptide B was stronger than reactivity against peptide A. These results suggested that during a natural rotavirus infection, an immune response against the immunodominant epitopes in the variable region of VP8* subunit is mounted.

To verify that the reactivity against peptide B corresponding to P[8]-1 and P[8]-3 lineages was to conserved epitopes, rabbit polyclonal antiserum generated against either whole

Table 1. ELISA and neutralizing antibody titers of sera from rotavirus-infected children

Children serum samples	IgG ELISA titers to the VP8* subunit		NtAb titers to strain Wa
	Strain Wa P[8]-1 lineage	MX08-659 isolate P[8]-3 lineage	
MX07-531	200	400	200
MX07-532	100	100	50
MX07-554	200	400	50
MX07-555	200	400	50
MX07-557	200	800	50
MX08-659	200	200	200
MX08-674	>1,600	>1,600	100
MX08-680	>1,600	>1,600	>3,200
MX08-737	>1,600	>1,600	25
MX08-740	400	800	<25

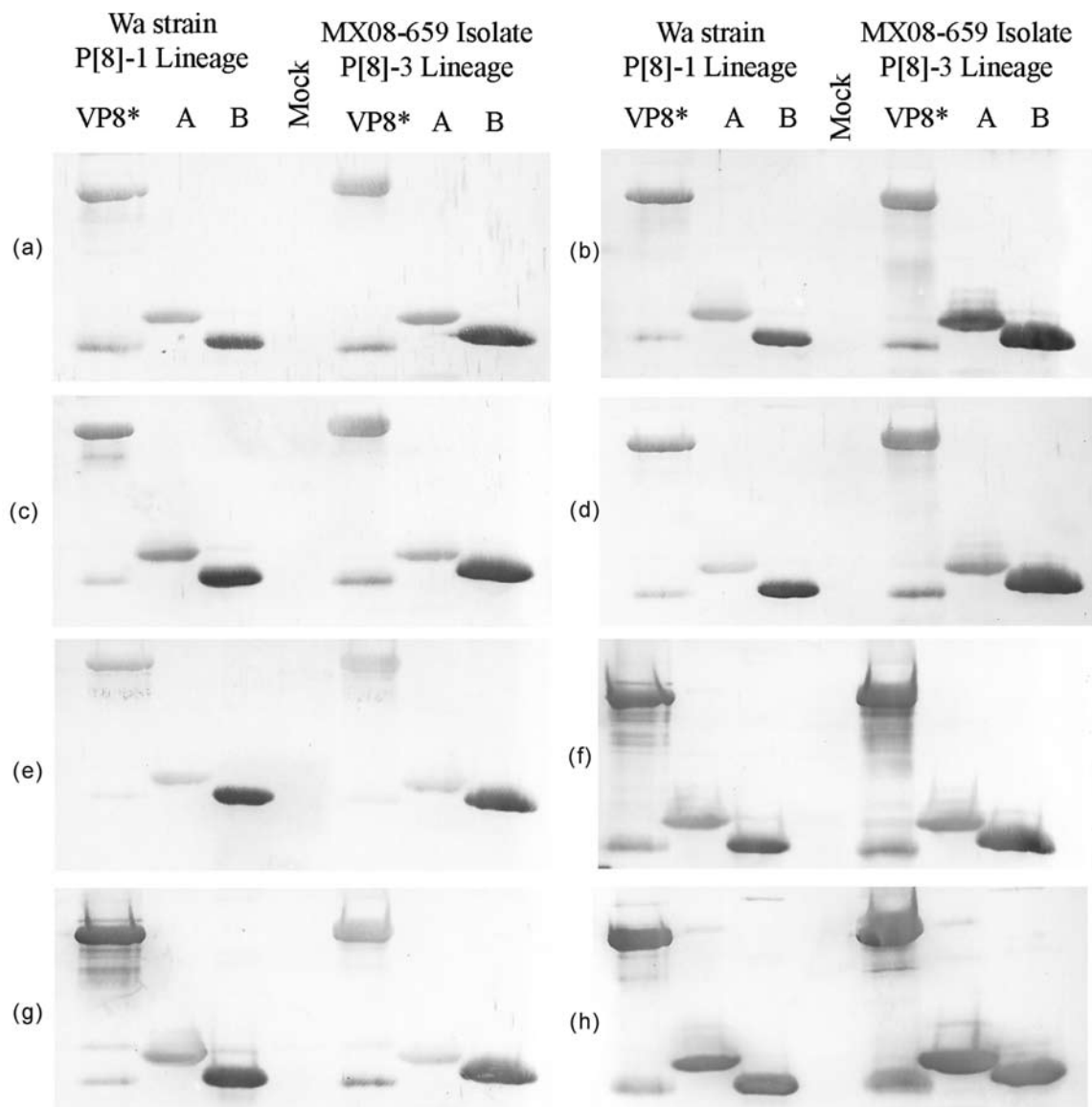


Fig. 2

Reactivities of IgG antibodies in the sera from rotavirus-infected children with VP8* and peptides A and B of P[8]-1 and P[8]-3 lineages

Western blot analysis. The blotted antigens were reacted with the children's sera (a-f), antiserum to Wa strain (P[8]-1) (g) and antiserum to VP8 of isolate MX08-659 (P[8]-3) (h), respectively.

rotavirus Wa (P[8]-1 lineage) or against recombinant MX08-659 VP8* (P[8]-3 lineage) were tested in Western blot analyses. Both rabbit serum samples recognized peptide B of P[8]-1 and P[8]-3 lineages, confirming the presence of conserved epitopes in the VP8* variable region across lineages. A possible explanation for the reactivity of the rabbit antisera is that within peptide B (aa 84-180), we found 13 amino acid substitutions between lineages P[8]-1 and P[8]-3, but the positions 106 (V/I), 108 (I/V), 120 (T/N), 121 (I/V),

150 (E/D) and 173 (V/I) had similar biochemical characteristics, suggesting that the antigenicity was not likely to have been significantly altered in the VP8* variable region.

To our knowledge, this is the first report describing the reactivity of antibodies present in the serum from infected children against the variable VP8* region corresponding to different P[8] human rotavirus lineages. Extended studies using recombinant proteins of the four P[8] lineages may be of value in monitoring vaccine efficacy against circulating rotavirus strains.

Acknowledgements. This work was supported in part by grant No. 52036 from the National Council for Science and Technology, Mexico (CONACYT) and grant SA1683-07-PAICYT from the Universidad Autónoma de Nuevo León, México. Griselda E. Menchaca was recipient of a fellowship from the CONACYT, México.

References

- Ansaldi F, Pastorino B, Valle L, Durando P, Sticchi L, Tucci P, Biasci P, Lai P, Gasparini R, Icardi G (2007): Molecular characterization of a new variant of rotavirus P[8]G9 predominant in a sentinel-based survey in central Italy. *J. Clin. Microbiol.* 45, 1011–1015. doi.org/10.1128/JCM.02054-06
- Araujo IT, Assis RM, Fialho AM, Mascarenhas JD, Heinemann MB, Leite JP (2007): Brazilian P[8], G1, P[8], G5, P[8], G9, and P[4], G2 rotavirus strains: nucleotide sequence and phylogenetic analysis. *J. Med. Virol.* 79, 995–1001. doi.org/10.1002/jmv.20918
- Arias CF, Lizano M, López S (1987): Synthesis in Escherichia coli and immunological characterization of a polypeptide containing the cleavage sites associated with trypsin enhancement of rotavirus SA11 infectivity. *J. Gen. Virol.* 68, 633–642. doi.org/10.1099/0022-1317-68-3-633
- Arista S, Giannanco GM, De Grazia S, Colombo C, Martella V (2005): Genetic variability among serotype G4 Italian human rotaviruses. *J. Clin. Microbiol.* 43, 1420–1425. doi.org/10.1128/JCM.43.3.1420-1425.2005
- Cheuvart B, Friedland LR, Abu-Elyazeed R, Han HH, Guerra Y, Verstraeten T (2009): The Human Rotavirus Vaccine RIX4414 in Infants A Review of Safety and Tolerability. *Pediatr. Infect. Dis. J.* 28, 225–232. doi.org/10.1097/INF.0b013e31819715fa
- Collins PJ, Martella V, Buonavoglia C, O'Shea H (2010): Identification of a G2-like porcine rotavirus bearing a novel VP4 type, P[32]. *Vet. Res.* 41, 73–84. doi.org/10.1051/vetres/2010045
- Cunliffe NA, Gondwe JS, Graham SM, Thindwa BDM, Dove W, Broadhead RL, Molyneux ME, Hart CA (2001): Rotavirus strain diversity in Blantyre, Malawi, from 1997 to 1999. *J. Clin. Microbiol.* 39, 836–843. doi.org/10.1128/JCM.39.3.836-843.2001
- Dowling W, Denisova E, LaMonica R, Mackow ER (2005): Selective membrane permeabilization by the rotavirus VP5* protein is abrogated by mutations in an internal hydrophobic domain. *J. Virol.* 74, 6368–6376. doi.org/10.1128/JVI.74.14.6368-6376.2000
- Espínola E, Amarilla E, Arbiza J, Parra GI (2008): Sequence and phylogenetic analysis of the VP4 gene of human rotaviruses isolated in Paraguay. *Arch. Virol.* 153, 1067–1073. doi.org/10.1007/s00705-008-0096-8
- Hall TA (1999): BioEdit: a user-friendly biological sequence alignment editor and analysis program for Windows 95/98/NT. *Nucleic Acids Symp. Ser.* 41, 95–98.
- Hyser JM, Zeng CQY, Beharry Z, Palzkill T, Estes MK (2008): Epitope mapping and use of epitope-specific antisera to characterize the VP5* binding site in rotavirus SA11 NSP4. *Virology* 373, 211–228. doi.org/10.1016/j.virol.2007.11.021
- Jiang B, Gentsch JR, Glass RI (2002): The role of serum antibodies in the protection against rotavirus disease: an overview. *Clin. Infect. Dis.* 34, 1351–1361. doi.org/10.1086/340103
- Larralde G, Gorziglia M (1992): Distribution of conserved and specific epitopes on the VP8 subunit of rotavirus VP4. *J. Virol.* 66, 7438–7443.
- Maunula L, Von Bonsdorff CH (1998): Short sequences define genetic lineages: phylogenetic analysis of group A rotaviruses based on partial sequences of genome segments 4 and 9. *J. Gen. Virol.* 79, 321–332.
- Menchaca G, Padilla-Noriega L, Méndez-Toss M, Contreras JE, Puerto FI, Guiscafré H, Mota F, Herrera I, Cedillo R, Muñoz O, Ward R, Hoshino Y, López S, Arias CF (1998): Serotype specificity of the neutralizing antibody response induced by the individual surface proteins of rotavirus in natural infections of young children. *Clin. Diagn. Lab. Immunol.* 5, 328–334.
- Okitsu S, Khamrin P, Thongprachum A, Maneekarn N, Mizuguchi M, Ushijima H (2011): Predominance of porcine P[23] genotype rotaviruses in piglets with diarrhea in Northern Thailand. *J. Clin. Microbiol.* 49, 442–445. doi.org/10.1128/JCM.02263-10
- Padilla-Noriega L, Fiore L, Rennels MB, Losonsky GA, Mackow ER, Greenberg HB (1992): Humoral immune responses to VP4 and its cleavage products VP5* and VP8* in infants vaccinated with rhesus rotavirus. *J. Clin. Microbiol.* 30, 1392–1397.
- Rahman M, Matthijnssens J, Yang X, Delbeke T, Arijs I, Taniguchi K, Iturriza-Gomara M, Iftekharuddin N, Azim T, Van Ranst M (2007): Evolutionary history and global spread of the emerging G12 human rotaviruses. *J. Virol.* 81, 2382–2390. doi.org/10.1128/JVI.01622-06
- Santos N, Hoshino Y (2005): Global distribution of rotavirus serotypes/genotypes and its implication for the development and implementation of an effective rotavirus vaccine. *Rev. Med. Virol.* 15, 29–56. doi.org/10.1002/rmv.448
- Tamura K, Dudley J, Nei M, Kumar S (2007): MEGA 4: Molecular evolutionary genetics analysis (MEGA) software version 4.0. *Mol. Biol. Evol.* 24, 1596–1599. doi.org/10.1093/molbev/msm092
- Taniguchi K, Maloy WL, Nishikawa K, Green KY, Hoshino H, Urasawa S, Kapikian AZ, Chanock RM, Gorziglia M (1998): Identification of cross-reactive and serotype 2-specific neutralization epitopes on VP3 of human rotavirus. *J. Virol.* 62, 2421–2426.
- Ward RL, Kirkwood CD, Sander DS, Smith VE, Shao M, Bean JA, Sack DA, Bernstein DI (2006): Reductions in cross-neutralizing antibody responses in infants after attenuation of the human rotavirus vaccine candidate 89–12. *J. Infect. Dis.* 194, 1729–1736. doi.org/10.1086/509623

Small interfering RNAs targeting viral structural envelope protein genes and the 5'-UTR inhibit replication of bovine viral diarrhea virus in MDBK cells

N. MISHRA, K. RAJUKUMAR, S. KALAIYARASU, S.P. BEHERA, R.K. NEMA, S.C. DUBEY

High Security Animal Disease Laboratory, Indian Veterinary Research Institute, Anand Nagar, Bhopal, Madhya Pradesh, 462021, India

Received January 2, 2011; accepted August 25, 2011

Summary. – Bovine viral diarrhea viruses (BVDVs) are important pathogens of cattle that occur worldwide, and for which no antiviral therapy is available. In the present study, the inhibitory effect of small interfering (si) RNAs on bovine viral diarrhea virus 1 (BVDV-1) replication in cultured bovine cells was explored. Four synthetic siRNAs were designed to target structural envelope region genes (E^{ms} , E1, and E2) and one cocktail of siRNA was generated to target the 5'-UTR of the BVDV-1 genome. The inhibitory effects of siRNAs were assessed by determination of infectious viral titer, viral antigen and viral RNA. The siRNA cocktail and three of the synthetic siRNAs produced moderate anti-BVDV-1 effect *in vitro* as shown by 25%–40% reduction in BVDV-1 antigen production, 7.9–19.9-fold reduction in viral titer and 21–48-fold reduction in BVDV-1 RNA copy number. Our findings suggest that siRNA cocktail targeted at the 5'-UTR is a stronger inhibitor of BVDV-1 replication and the targets for siRNA inhibition can be extended to BVDV-1 structural envelope protein genes.

Keywords: bovine viral diarrhea virus; RNA interference; small interfering RNA

Introduction

BVDVs are economically important pathogens of cattle, which cause significant respiratory and reproductive disease worldwide. Despite several control measures, such as selective test and slaughter, eradication, vaccination or in various combinations, have been adopted, the disease is still endemic in many countries. Hence, the development of effective antiviral therapies may be useful in the future. BVDV-1, BVDV-2 along with the border disease virus (BDV) and classical swine fever virus (CSFV) belong to the genus *Pestivirus* in the family *Flaviviridae* (Fauquet *et al.*, 2005). Within *Flaviviridae*, BVDV-1 and BVDV-2 are more related to human hepatitis C virus (HCV) than flaviviruses. Due to the similarities in genome structure,

organization, replication strategies and the ability to cause long-term infection, BVDV-1 has often been used as a surrogate model for HCV infection. The genome of both BVDV-1 and BVDV-2 consists of a single-stranded RNA of about 12.3 kb in length. A long ORF flanked by 5'-UTR and 3'-UTR is translated into a poly-protein of about 4000 amino acids and is cleaved into four structural (capsid (C) and three envelope (E^{ms} , E1, and E2) proteins) and 7–8 nonstructural proteins (N^{pro}, p7, NS2-3 or NS2 and NS3, NS4A, NS4B, NS5A, and NS5B) by viral and host cell proteases (Meyers and Thiel, 1996).

RNA interference (RNAi), a naturally occurring cellular mechanism of gene suppression is a promising approach to develop effective antiviral drugs. Since the discovery that small interfering RNAs (siRNA) upon direct transfection *in vitro* can selectively initiate gene suppression (Elbashir *et al.*, 2001), siRNAs have been shown to suppress replication of a variety of viruses that infect humans and animals such as hepatitis C virus (Randall *et al.*, 2003), influenza A virus (Zhou *et al.*, 2007), foot-and-mouth disease virus (Chen *et al.*, 2004), porcine reproductive and respiratory syndrome virus (He *et al.*, 2007) and classical swine fever virus (Xu *et al.*, 2008).

E-mail: mishranir@rediffmail.com; fax: +91-755-2758842.

Abbreviations: BVDVs = bovine viral diarrhea viruses; BVDV-1 = bovine viral diarrhea virus 1; BVDV-2 = bovine viral diarrhea virus 2; siRNA = small interfering RNA; IRES = internal ribosome entry site; CSFV = classical swine fever virus; HCV = hepatitis C virus; MAb = monoclonal antibody; p.i. = post infection

Inhibition of BVDV-1 replication in cell culture to a variable extent has been demonstrated recently by synthetic siRNAs targeting the 5'-UTR, capsid (C), NS4B and NS5A regions of the genome with maximum inhibition achieved by siRNAs targeting capsid and NS5A regions (Lambeth *et al.*, 2007). However, no effort has been made to study the inhibitory potential of siRNAs targeted at envelope protein genes, although the effect of siRNAs may take place during the viral progeny production and BVDVs envelope proteins play crucial roles in viral assembly and entry (Krey *et al.*, 2005). Additionally, since the 5'-UTR contains an internal ribosome entry site (IRES) that mediates translation of the ORF (Poole *et al.*, 1995), BVDV-1 replication inhibition by a cocktail of siRNAs targeting this region may be possible. Hence, the aim of this work was to determine the inhibitory effect of siRNAs targeting envelope protein genes and the 5'-UTR on the replication of BVDV-1 in MDBK cells.

Materials and Methods

Virus and cells. Pestivirus free MDBK cells (Cell Culture Collection of Veterinary Medicine, Friedrich-Loeffler Institute, Island of Riems, Germany) were grown in Eagle's MEM (Sigma) supplemented with 10% FCS (Invitrogen) in a humidified atmosphere containing 5% CO₂ at 37°C. Indian cattle BVDV-1 noncytopathic strain Ind S-1449 (Mishra *et al.*, 2004) was propagated on MDBK cells using EMEM containing 5% FCS and the titer of the virus stock was determined following a standard method.

siRNAs. Four siRNA duplexes targeting E^{rns}, E1, and E2 regions of the Indian cattle BVDV-1 isolate Ind S-1449 genome (GenBank Acc. No. AY911670, Mishra *et al.*, 2006) were designed using the Hi Performance Design Algorithm (Novartis AG) and synthesized commercially (Qiagen). The oligonucleotide sequences used for siRNA synthesis and their target regions are shown in Table 1. The negative control siRNA was synthesized (Qiagen) using previously reported sequences (Lambeth *et al.*, 2007). To generate siRNA cocktails, the

5'-UTR of BVDV-1 strain Ind S-1449 was targeted. The templates for *in vitro* transcription were obtained by amplification of a 288 bp fragment (nt 108–395 of BVDV-1 strain NADL) using primers 324 and 326 (Vilcek *et al.*, 1994) appended to the T7 promoter sequence and Access RT-PCR kit (Promega). The siRNA cocktails were produced using the Silencer siRNA cocktail kit RNase III (Ambion). The negative control siRNA was labeled with Cy3 using silencer siRNA labeling kit (Ambion) for optimization of transfection.

Testing of siRNAs. The transfection protocol and quantity of siRNAs (5 to 150 nmoles) that inhibit BVDV-1 replication without visible cytotoxicity were optimized using Cy3-labelled control siRNA, MDBK cells (90% confluence) and siPORT Amine agent (Ambion). Briefly, the transfection agent and siRNA complex was formed in serum-free Optimem 1 medium (Invitrogen). Transfection was carried out for 16 hrs in the presence of BVDV-1-specific synthetic and cocktail siRNAs at a concentration of 100 nmoles per well in 96-well plates. Following removal of the mixture and washing, the cells were infected with 100 TCID₅₀ BVDV-1 per well and incubated at 37°C for 48 hrs before testing for siRNA inhibitory effects. Healthy MDBK cells, negative control siRNA-transfected cells, BVDV-1-specific siRNA-transfected but not infected cells, and cells with only transfection agent added were kept as controls. All the experiments were conducted thrice in triplicates.

Virus titration. The infected cell supernatants collected at 48 hrs post infection (p.i.) following freezing and thawing were subjected to virus titration on MDBK cells to determine the reduction in virus titer under siRNA effect. The replication of BVDV-1 was demonstrated by immunochemistry and the virus titer was expressed as log₁₀ TCID₅₀/ml.

Immunochemistry. The effect of siRNAs on viral antigen expression was assayed by immunochemistry using BVDV-1 E2-specific monoclonal antibody (MAb) 157. Briefly, the cells at 48 hrs p.i. were washed, heat fixed and incubated with 50 µl of MAb 157 for 1 hr at 37°C. After washing, the cells were reacted with 50 µl of horseradish-conjugated anti-mouse IgG (Sigma) for 1 hr at 37°C followed by exposure to 3-amino-9-ethylcarbazole (AEC) substrate. The amount of viral antigen production (% of antigen positive cells) in cells transfected with BVDV-1 specific siRNAs was calculated by considering the value obtained by negative control siRNA as 100%.

Real-time RT-PCR. For assaying viral RNA, real-time RT-PCR was performed using Mx 3000 (Stratagene), SuperScript III quantitative real time RT-PCR system (Invitrogen), BVDV-1-specific primers and TaqMan probes as described earlier (Baxi *et al.*, 2006). The total RNA of cells transfected with various siRNAs and challenged with BVDV-1 for 48 hrs was extracted using the QIAamp viral RNA purification kit (Qiagen) and was used as template. Data analysis was performed using the Mx 3000 software to obtain log BVDV-1 RNA copy numbers.

Results

We used four synthetic siRNAs targeting E^{rns}, E1, and E2 regions and a cocktail siRNA preparation targeting 5'-UTR of BVDV-1 genome. An optimal level of transfection was observed

Table 1. Characteristics of BVDV-1 specific siRNAs

siRNA (target)	Target	
	Sequence	Location (nt) ^a
si821 (E ^{rns})	sense 5'-CAAUGGAACUUACGAGAU-3' antisense 5'-UAUCUCGUAGUCCAUUG-3'	823–841
si1518 (E1)	sense 5'-GGCUUGGUACGUCGAUUA-3' antisense -UAAUCGACGUAACCAAGCC-3'	1520–1538
si1921 (E1)	sense 5'-AGUAUUAAGAUUGUCUUA-3' antisense 5'-UAAGACAUCUUAUACU-3'	1923–1941
si2527 (E2)	sense 5'-GGCCGUUGUUCGAACGUAU-3' antisense 5'-AUACGUUCGAACAACGGCC-3'	2529–2545
si-cocktail (5'-UTR)		108–395 ^b

^aLocation corresponding to BVDV-1 isolate Ind S-1449 (GenBank Acc. No. AY911670). ^bLocation corresponding to BVDV-1 strain NADL.

at 16 hrs post transfection onwards (data not shown). MDBK cells were transfected with BVDV-1-specific siRNAs and the inhibitory effects of siRNAs on BVDV-1 replication were studied by assaying the viral antigen, infectious virus and viral RNA.

The results of viral antigen expression (% of antigen-positive cells) by immunochemistry (Table 2) showed that the level of suppression of BVDV-1 antigen production by synthetic and cocktail siRNAs was variable. The highest suppression was achieved by si-cocktail(5'-UTR) (40%), followed by si2527(E2) (35%), si821(E^{rns}) (30%) and si1518(E1) (25%). However, only marginal suppression was evident with si1921(E1).

The influence of various siRNAs on the level of infectious virus titer (TCID₅₀/ml) was determined and the results (Table 2) showed that si-cocktail(5'-UTR), si2527(E2), si821(E^{rns}) and si1518(E1) reduced the virus titer by 7.9- to 19.9-fold, while no reduction in virus titer was achieved by si1921(E1). Similar to the results of suppression of BVDV antigen production, the highest reduction in virus titer was obtained with si-cocktail(5'-UTR), followed by si2527(E2).

To further test the inhibitory potential of these siRNAs, BVDV-1 viral RNA (log RNA copy number) levels were assessed and the results are shown in Table 2. The maximum inhibition of BVDV-1 RNA was again obtained with si-cocktail(5'-UTR) (48-fold), followed by si2527(E2) (31-fold), si821(E^{rns}) (27-fold) and si1518(E1) (21-fold), while no inhibition was evident with si1921(E1). Taken together, our results demonstrated that moderate anti-BVDV-1 effect on MDBK cells was achieved by si-cocktail(5'-UTR), si821(E^{rns}), si1518(E1) and si2527(E2).

Discussion

As conventional therapies for treating viral diseases of human and livestock have their limitations, and alternate treatments are urgently needed, RNAi technology can have potential applications in this regard. As a plus-strand RNA virus, BVDV-1 appears to be an attractive target for siRNA, since its genome functions as both replication template and mRNA. In this study, we determined antiviral effects of siRNAs against the non-cytopathic biotype of BVDV-1, as this biotype is preponderant in nature and responsible for development of persistently infected immunotolerant animals, which are considered to be the main source of BVDV transmission.

We used a siRNA cocktail instead of specific siRNAs targeting the 5'-UTR of BVDV-1 genome, since a previous study has shown the failure of IRES-directed siRNAs to induce marked anti-BVDV-1 response (Lambeth *et al.*, 2007). Our results demonstrated that siRNA cocktail is a better BVDV-1 inhibitor than the individual siRNAs targeting 5'-UTR. We hypothesize that a pool of siRNAs targeted at different regions within 5'-UTR including IRES might have been effective against BVDV replication. It is surprising that although the IRES sequence shares features among pestiviruses and distantly related hepatitis C virus in humans, siRNA targeted to HCV IRES exerted significant antiviral effect (Kanda *et al.*, 2007), while siRNAs targeted to BVDV IRES had little antiviral effect (Lambeth *et al.*, 2007). Further screening of siRNAs directed to IRES extending to N^{pro} coding region may be taken up in the future for obtaining a more efficient anti BVDV-1 response.

With the exception of the nucleocapsid protein (C), all the other structural proteins E^{rns}, E1, and E2 are glycoproteins and are part of the BVDV envelope. E2 is responsible for virus attachment, entry and generation of neutralizing antibodies (Donis and Dubovi, 1987; Krey *et al.*, 2005), while E^{rns} has the ability to bind to glycosaminoglycans, and E1 is assumed to be a membrane anchor for E2 (Rumenapf *et al.*, 1993). Our results demonstrated that moderate inhibition of BVDV-1 RNA replication in MDBK cells was achieved by si821(E^{rns}), si1518(E1) and si2527(E2). Although highly variable regions are poor targets of gene silencing, the results indicate that it is possible to target siRNAs at the conserved regions within the variable envelope region for obtaining a moderate anti-BVDV-1 effect. Our results also get support from an earlier study showing efficient inhibition of hepatitis C virus in human cells by siRNA targeting the E2 envelope region (Liu *et al.*, 2006). Although the causes of non-inhibitory effect of si1921(E1) have not been ascertained, the possible reasons include inaccessibility of the target RNA region to the RNA-induced silencing complex (RISC) or inability of siRNA to form RISC essential for gene silencing. Similarly, whether induction of interferon by single or cocktail siRNAs may play a role in the observed inhibition of viral replication cannot be fully excluded.

Efficient *in vitro* inhibition of BVDV-1 replication has been achieved by siRNAs targeting structural capsid region and nonstructural NS4B and NS5A regions (Lambeth *et al.*, 2007).

Table 2. Antiviral effects of siRNAs

Virus infection parameter ^a	siRNA					
	si821(E ^{rns})	si1518(E1)	si1921(E1)	si2527(E2)	si-cocktail (5'-UTR)	Negative control
Viral antigen-positive cells (%)	70	75	95	65	60	100
Infectious virus titer (log TCID ₅₀ /ml)	4.0	4.1	5.0	3.8	3.7	5.0
Viral RNA (log copy number)	4.2	4.3	5.6	4.1	3.9	5.6

^aThe values are shown as means of three replicates of three independent experiments.

A more efficient inhibition of the closely related classical swine fever virus replication *in vitro* has recently been obtained by siRNAs targeting N^{pro} and NS5B genes (Xu *et al.*, 2008). Our results provide evidence that the siRNA cocktail targeting 5'-UTR is a stronger inhibitor of BVDV-1 replication and extends the targets for siRNA inhibition to BVDV-1 envelope protein genes. Study of the inhibitory potential of siRNAs targeting various other regions of BVDV-1 genome should, however, continue to obtain a more effective antiviral therapeutic.

Acknowledgements. N. Mishra was supported by a project grant (BT/PR4415/AAQ/01/165/2003) from Department of Biotechnology, Govt. of India.

References

- Baxi M, McRae D, Baxi S, Greiser-Wilke I, Vilcek S, Amoako K, Deregt D (2006): A one-step multiplex real time RT-PCR for detection and typing of bovine viral diarrhoea viruses. *Vet. Microbiol.* 116, 37–44. doi.org/10.1016/j.vetmic.2006.03.026
- Chen W, Yan W, Du Q, Fei L, Liu M, Ni Z, Sheng Z, Zheng Z (2004): RNA interference targeting VP1 inhibits foot and mouth disease virus replication in BHK-21 cells and suckling mice. *J. Virol.* 78, 6900–6907. doi.org/10.1128/JVI.78.13.6900-6907.2004
- Donis RO, Dubovi E J (1987): Characterization of bovine viral diarrhoea-mucosal disease virus-specific proteins in bovine cells. *J. Gen. Virol.* 68, 1597–1605. doi.org/10.1099/0022-1317-68-6-1597
- Elbashir SM, Harborth J, Lendeckel W, Yalcin A, Weber K, Tuschl T (2001): Duplexes of 21-nucleotide RNAs mediate RNA interference in cultured mammalian cells. *Nature* 411, 494–498. doi.org/10.1038/35078107
- Fauquet CM, Mayo MA, Maniloff J, Desselberger U, Ball LA (Eds) (2005): Virus Taxonomy. Eighth Report of the International Committee on Taxonomy of Viruses. Elsevier Academic Press, Amsterdam, pp. 981–998.
- He YY, Hua RH, Zhou YJ, Qiu HJ, Tong GZ (2007): Interference of porcine reproductive and respiratory syndrome virus replication on MARC-145 cells using DNA based short interfering RNAs. *Antiviral Res.* 74, 83–91. doi.org/10.1016/j.antiviral.2006.04.013
- Kanda T, Steele R, Ray R, Ray RB (2007): Small interfering RNA targeted to hepatitis C virus 5' non translated region exerts potent antiviral effect. *J. Virol.* 81, 669–676. doi.org/10.1128/JVI.01496-06
- Krey T, Thiel HJ, Rumenapf T (2005): Acid-resistant bovine pestivirus requires activation for pH-triggered fusion during entry. *J. Virol.* 79, 4191–4200. doi.org/10.1128/JVI.79.7.4191-4200.2005
- Lambeth LS, Moore RJ, Muralitharan MS, Doran TJ (2007): Suppression of bovine viral diarrhea virus replication by small interfering RNA and short hairpin RNA-mediated RNA interference. *Vet. Microbiol.* 119, 132–143. doi.org/10.1016/j.vetmic.2006.09.008
- Liu M, Ding H, Zhao P, Qin ZL, Gao J, Cao MM, Luan J, Wu WB, Qi ZT (2006): RNA interference effectively inhibits mRNA accumulation and protein expression of hepatitis C virus core and E2 genes in human cells. *Biosci. Biotech. Biochem.* 70, 2049–2055. doi.org/10.1271/bbb.60001
- Meyers G, Thiel HJ (1996): Molecular characterization of pestiviruses. *Adv. Virus Res.* 47, 53–118. [doi.org/10.1016/S0065-3527\(08\)60734-4](https://doi.org/10.1016/S0065-3527(08)60734-4)
- Mishra N, Pattnaik B, Vilcek S, Patil SS, Jain P, Swamy N, Bhatia S, Pradhan HK (2004): Genetic typing of bovine viral diarrhoea virus isolates from India. *Vet. Microbiol.* 104, 207–212. doi.org/10.1016/j.vetmic.2004.08.003
- Mishra N, Vilcek S, Jain P, Pitale SS, Pradhan HK (2006): Genetic analysis of Indian Bovine viral diarrhoea virus isolates in Npro and entire structural region genes. *Acta Virol.* 50, 39–44.
- Poole TL, Wang CY, Popp RA, Potgieter LND, Siddiqui A, Collett MS (1995): Pestivirus translation initiation occurs by internal ribosome entry. *Virology* 206, 750–754. [doi.org/10.1016/S0042-6822\(95\)80003-4](https://doi.org/10.1016/S0042-6822(95)80003-4)
- Randall G, Grakoui A, Rice CM (2003): Clearance of replicating hepatitis C virus replicon RNAs in cell culture by small interfering RNAs. *Proc. Natl. Acad. Sci. USA* 100, 235–240. doi.org/10.1073/pnas.0235524100
- Rumenapf T, Unger G, Strauss JH, Thiel HJ (1993): Processing of the envelop glycoproteins of pestiviruses. *J. Virol.* 67, 3288–3294.
- Vilcek S, Herring AJ, Herring JA, Nettleton PF, Lowings JP, Paton DJ (1994): Pestiviruses isolated from pigs, cattle and sheep can be allocated into at least three genogroups using polymerase chain reaction and restriction endonuclease analysis. *Arch. Virol.* 136, 309–323. doi.org/10.1007/BF01321060
- Xu X, Guo H, Xiao C, Zha Y, Shi Z, Xia X, Tu C (2008): In vitro inhibition of classical swine fever virus replication by siRNAs targeting Npro and NS5B genes. *Antiviral Res.* 78, 188–193. doi.org/10.1016/j.antiviral.2007.12.012
- Zhou H, Jin M, Yu Z, Xu X, Pong Y, Wu H, Liu J, Liu H, Cao S, Chen H (2007): Effective small interfering RNAs targeting matrix and nucleocapsid protein gene inhibit influenza A virus replication in cells and mice. *Antiviral Res.* 76, 186–193. doi.org/10.1016/j.antiviral.2007.07.002

LETTER TO THE EDITOR

Nucleocapsid protein gene mediated resistance against groundnut bud necrosis virus in tomato using sense and antisense constructs

P. RAJA^{1,2}, R.K. JAIN¹

¹Unit of Plant Virology, Division of Plant Pathology, Indian Agricultural Research Institute, New Delhi, 110012, India; ²Department of Plant Pathology, College of Horticulture and Forestry, Central Agricultural University, Pasighat 791 102, India

Received September 13, 2010; accepted August 22, 2011

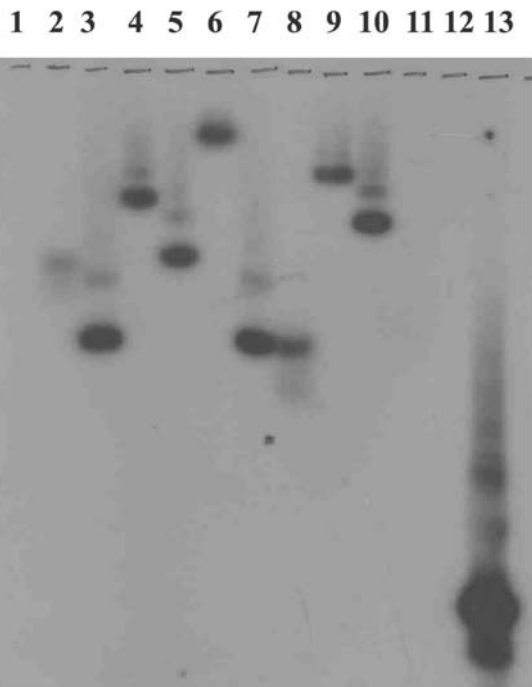
Keywords: GBNV; N gene; sense; antisense; transgenic tomato; resistance

Spotted wilt (also known as bud blight) is caused by groundnut bud necrosis virus (GBNV) and is emerging as a serious problem affecting tomato (*Lycopersicon esculentum* Mill) cultivation in the Indian subcontinent. Field symptoms of the disease include extensive necrosis of buds and petioles, necrotic spots on leaves and concentric rings on fruits. The incidence of 19–34% was recorded (1). N gene as a transgene has been reported to confer a broad-spectrum resistance against Tospoviruses (8, 12). In the absence of natural resistance against GBNV in widely grown tomato varieties, the strategy of N gene-mediated resistance could be worth attempting against GBNV. N gene (831 bp) derived from GBNV isolate of Tamil Nadu (TN-Co) was amplified using a set of specific primers (HRP26: 5'-ATGTCTAACGT(C/T) AAGCA (A/G) CTC-3' and HRP28: 5'-TTACAATTCCAGCGA AGGACC-3') derived from first and last 21 bases of the coding region of N gene of GBNV (10) and watermelon silver mottle virus (13). The amplified and confirmed full length N gene was initially cloned into pDrive vector (Qiagen, Germany) and then sub-cloned in both sense and antisense orientation into pBI121 (Clonetech laboratories, USA) and pBinAR (16) binary vectors respectively using *Xba*I and *Bam*H I sites. Then it was mobilized into the disarmed *Agrobacterium tumefaciens* strain LBA 4404 (6) separately by triparental mating procedure (5), using the helper plasmid pRK2013 (3). Presence of N gene construct was confirmed by

colony PCR and sequencing. Three popular tomato varieties viz., Co3, Pusa Early Dwarf and Pusa Ruby and the explants viz., cotyledons (7 days old) and leaves (35 days old) explants were used for *Agrobacterium*-mediated transformation. Regeneration protocol was initially standardized for three varieties (data not shown). For callusing and shootings, the effective plant growth regulator combination such as IAA (0.0002 mg/ml) and kinetin (0.0002 mg/ml) for Co3, and indole butric acid (0.002 mg/ml) and 6-benzylaminopurine (0.002 mg/ml) were used for Pusa Early Dwarf and Pusa Ruby varieties, and IAA 0.0002 mg/ml was used for rooting of all varieties. The explants were co-cultivated with 48 hr-grown *Agrobacterium* culture ($OD_{600} = 0.4$) (with and without construct) and incubated for two days in the dark at 25°C (4). After co-cultivation, tomato explants were washed gently by half strength MS medium (17) and air dried on sterile filter paper. The explants were transferred to selection callusing medium containing augmentin (0.5 mg/ml) and kanamycin (0.1 mg/ml) and incubated at 25°C in 16hrs photoperiod. Well developed calli were after two weeks transferred to selection shoot medium with augmentin (0.4 mg/ml) and kanamycin (0.1 mg/ml). After another two weeks, when regenerated plantlets reached 2–3cm in height, they were cut off and placed on a selection rooting medium (4) with augmentin (0.1 mg/ml) and kanamycin (0.05 mg/ml). The plantlets were removed from the culture and transferred to sterilized soil mix (vermiculite and sand 1:1 ratio) in pot (size 95 × 100cm) and 100 ml of half strength MS media was poured in to the soil mix (4). After 10 days, the plants were transferred to a large size (195 × 180cm) pot and maintained in phytotron at 25°C in 12 hrs day/12 hrs night photoperiod. Southern hybridization

E-mail: prajachf@gmail.com; fax: +91-3682225066.

Abbreviations: GBNV = groundnut bud necrosis virus; IAA = 3-indole acetic acid; N gene = nucleocapsid gene



Figure

BamHI restricted genomic Southern blot analysis of transgenic lines
Lanes 1 and 11: untransformed plants; Lane 2: Co3S1; Lane 3: Co3S2; Lane 4: Co3S12; Lane 5: PRS1; Lane 6: PRS3; Lane 7: PRA1; Lane 8: PRA2; Lane 9: PRA4; Lane 10: PRA5; Lane 13: Positive control.

(15) was performed after isolation of genomic DNA (7) and restriction digestion with *Bam*HI. For Northern blot analysis, total RNA was isolated from Southern-positive plants using TRIZOL reagent (Invitrogen, USA). Purified total RNA (20 µg) was separated by formaldehyde gel electrophoresis, blotted, and hybridized to an N gene probe following standard procedure (9). Direct antigen coated enzyme linked immunosorbent assay was used to detect expression of N protein in putative transformants using polyclonal antiserum to GBNV (2). Southern-positive T0-plants were evaluated for resistance to GBNV by three-fold mechanical inoculation with sap from GBNV-infected tomato plants using 0.01 M potassium phosphate buffer pH 7.0 and carborundum (600 meshes) as an abrasive (11). Untransformed plants were used as control and inoculated plants were examined for symptom development.

PCR product of expected size (ca. 800 bp) was observed, cloned and sequenced (GenBank Acc. No. AY463968). N gene constructs in *sense* and *antisense* orientation were mobilized separately into *Agrobacterium* strain LBA4404 and then transferred into tomato. Of the 35 PCR-positive transformants, only nine were Southern-positive. Transgenic lines Co3S2, PRA1, PRA5 possessed single insert of the transgene, whereas Co3S1, Co3S12, PRS1, PR S3, PRA2, and PRA4 possessed double inserts of the transgene (the figure lane 2, 4, 5, 6, 8, and 9). In

Northern blot analysis and ELISA, all transformants except for Co3S2, PRA2 and PRA4 were positive. (data not shown). These results are in agreement with earlier findings (14, 15). Transgenic lines with a single insertion of the N gene would be useful in breeding program because it is easier to breed for a trait controlled by a single dominant gene. Putative Southern-positive transgenic lines were highly resistant to GBNV infection, showing no symptoms upon inoculation with the TN-Co isolate. The usefulness of N gene mediated resistance against GBNV in tomato would depend on the stability of the gene through generations and evaluation of the transgenic lines against GBNV isolates from different locations.

Acknowledgements. This work was supported by the grant no 8827 Indian Agricultural Research Institute, New Delhi and Council of Scientific and Industrial Research, New Delhi.

References

- Anonymous, Annual report, All India coordinated research project (vegetable crops) crop meeting, Hyderabad, India 135–310, 2004.
- Clark MF, Bar J, In Marmorash K, Korowski H (Eds): Methods in Virology, vol VII, New York, Academic Press, 51–85, 1984.
- Comoi L, Schilling, Cordero C, Megia A, Houck CM, Plasmid. 10, 21–30, 1983.
- Cortina, M, Plant Cell Tiss. Org. Cult. 76, 269, 2004. doi.org/10.1023/B:TICU.0000009249.14051.77
- Ditta G, Stanfield S, Corbin D, Helsinki DR, PNAS 77, 7344–7351, 1980. doi.org/10.1073/pnas.77.12.7347
- Hoekema A, Hirsch PR, Hooykaas PJJ, Schiperoof RA, Nature 303, 179–190, 1983. doi.org/10.1038/303179a0
- Koundal, Rekha K, Laboratory Manual, National Research Centre on Plant Biotechnology, IARI, New Delhi, 2000.
- Pang SZ, Jerry L, Slightom L, Gonsalves D, Biotechnology 11, 819–824, 1993. doi.org/10.1038/nbt0793-819
- Sambrook J, Russell DW, Molecular Cloning: A Laboratory Manual. Cold Spring Harbour Laboratory, New York, USA, 2001.
- Satyanarayana, T, Mitchell SE, Reddy DVR, Brown S, Kresovich S, Jarret R, Naidu RA, Demski JW, Arch. Virol. 141, 85–96, 1996. doi.org/10.1007/BF01718590
- Umamaheswaran K, Jain RK, Bhat AI, Ahlawat YS, Indian Phytopathol. 56, 168–173, 2003.
- Vaira AM, Semeria L, Crespi S, Lisa V, Allavena A, Accotto GP, Mol. Plant Microb. Interact. 8, 66–73, 1995. doi.org/10.1094/MPMI-8-0066
- Yeh SD, Chang TF, Phytopathology 85, 58–64, 1995. doi.org/10.1094/Phyto-85-58
- Jan FJ, Fagoaga C, Pang SZ, Gonsalves D, J. Gen. Virol. 81, 2103–2109, 2000.
- Sonoda S, Plant Science 164, 717–725, 2003. [doi.org/10.1016/S0168-9452\(03\)00028-1](https://doi.org/10.1016/S0168-9452(03)00028-1)
- Arrillaga I, Gisbert C, Sales E, Roig L, Moreno V, J. Horticulture Sci. Biotechnol. 76, 413–418, 2001.
- Sreevidya CS, Manoharan M, Kumar CTR, Savithri HS, Sita GL, J. Plant Physiol. 156, 106–110, 2000.

LETTER TO THE EDITOR

Development of real-time RT-PCR for human metapneumovirus

P. XUE¹, W. ZHENG¹, M. ZHANG², L.ZHENG^{1*}

¹State Key Laboratory for Molecular Virology and Genetic Engineering, National Institute for Viral Disease Control and Prevention, China CDC, Beijing 100052, P.R. China; ²College of Veterinary Medicine, Northwest A&F University, Yangling, Shannxi 712100, P.R. China

Received November 10, 2010; accepted September 2, 2011

Key words: real-time RT-PCR; human metapneumovirus

Human metapneumovirus (HMPV) is a recently discovered pathogen identified as a cause of respiratory tract infection in human (1). HMPV is a single-strand negative RNA virus belonging to the family of Paramyxoviridae, subfamily Pneumovirinae, genus Metapneumovirus and the total length of its genome is about 13.4 kb (2). Since its discovery in 2001, subsequent studies have reported the presence of HMPV in respiratory tract samples in many countries (3–7), suggesting that this virus is a ubiquitous respiratory pathogen. In 2003, Chinese scientists (8) also discovered this virus in the hospitalized children with respiratory tract infections in the Beijing area. It is well known that there are two major methods for us to diagnose the virus infections: serological detection and nucleic acid detection. Compared with conventional RT-PCR, real-time quantitative RT-PCR is more sensitive, specific, and has a larger detection range. Besides, the potential contamination is lower than that of the conventional RT-PCR (9). To further understand the prevalence of HMPV, the aim of our study was to develop and validate a TaqMan-based real-time RT-PCR assay for detection and quantification of HMPV.

We developed a real-time RT-PCR assay for HMPV with primers and a TaqMan probe targeting the F gene of HMPV conservative sequence. Primers and the probe were designed using Primer Express 3.0 (ABI), sense: 5'-ATACACCAC-CAGCAGTTC-3', antisense: 5'-ATACCCTACCATAGTTC-3', probe: FAM-TCTGTATGCTGCATC ACAAAAGTGGTCCA-

TAMRA. At the 5'-end the probe was labeled with fluorescent dye FAM and 3'-end with a non-fluorescent quencher TAMRA. All the primers and probes were synthesized by Invitrogen. One-step QuantiTect Probe RT-PCR Kit (Qiagen) was used for the real-time RT-PCR assay. Using 2×QuantiTect Probe RT-PCR Master Mix 10 µl; Final concentration of each primer was 1.0 µmol/l and the Probe 0.2 µmol/l; Template RNA 1 pg–1 µg/reaction; QuantiTect Probe RT Mix 0.2 µl/reaction. The total volume was 20 µl, filled with RNase-free water. The amplification conditions were as follows: 50°C 20 mins, 95°C 15 mins; 55 cycles of 95°C 0 sec, 60°C 1 min with Roter Gene 3000 (Corbett Robotics). Primers for real-time RT-PCR were used to amplify part of F gene fragment from the HMPV nucleic acid. Subsequently, the PCR products were cleaned by Gel/PCR DNA fragment Extraction Kit (Geneaid), cloned into pGEM T-easy Vector Systems (Promega), and then transformed into competent *E. coli* DH5α cells (BioMed). Following a white-blue colony selection and cultivation, plasmid DNA carrying the insert was extracted and sequenced. The plasmid DNA was subsequently linearized using restriction enzyme NdeI (Takara) and cleaned by QIAamp DNA Mini Kit (Qiagen), the DNA was transcribed using the RiboMax Large scale RNA Production System-T7 (Promega) to synthesize HMPV RNA in vitro. The RNA was cleaned by RNeasy Mini Kit (Qiagen), and the transcribed RNA was spectrophotometrically quantified by measuring the absorbance at 260 nm using BioPhotometer Plus (Eppendorf). The absorbance value (µg/ml) was used to calculate the number of copies per mL of transcribed RNA using the formula: $(6.02 \times 10^{23} \text{copies/mol}) \times (\mu\text{g/ml}) / (\text{MW g/mol}) = \text{copies/ml}$. Ten-fold serial dilutions containing 10^9 – 10^0 copies of RNA transcript were added to real-time

*Corresponding authors. E-mail: zmt6371@yahoo.com.cn; zhenglishu2000@sina.com; fax: +86-10-63541221.

Abbreviations: HMPV = human metapneumovirus

RT-PCR reactions in duplicate. The results were used to generate the standard curve of HMPV. The specificity was assessed by testing the mixed samples for other common respiratory viruses, including: respiratory syncytial virus, influenza virus types A and B, rhinovirus, enterovirus 71, coxsackie B virus, adenovirus. As for the reproducibility, we added 10^8 – 10^5 copies/ml of RNA to each reaction respectively and each concentration of RNA repeated five times. From December 2008 to September 2009, 78 nasopharyngeal specimens were collected from children younger than 14 years of age with acute respiratory infection, who had been admitted to the 8th Hospital of Shenyang, Liaoning Province, China. All samples were processed by the established real-time RT-PCR assay.

With the standard curve derived from RNA serial dilutions, the dynamic range of the assay was from 10^0 – 10^6 copies/reaction and the limit of detection was 4.95 copies, while there are no amplification curves in the negative control. Coefficient of determination ($R^2 = 0.99667$) shows a good linear correlation. The TaqMan-based real-time RT-PCR assay for HMPV detection did not amplify any other mixed viral respiratory pathogens, showing excellent specificity of the assay. Four different RNA concentrations (from 10^8 to 10^5 copies per reaction) were repeated five times in each run. The maximum coefficient of variation (CV) was 3.94%, which suggest a good precision. HMPV was detected in 5 (6.4%) of 78 respiratory specimens by conventional RT-PCR, but 7 (8.9%) were positive by real-time RT-PCR. Moreover, the 5 samples detected by conventional RT-PCR were included in the 7 samples detected by real-time RT-PCR.

Conventional methods for detection of PCR-amplified DNA can be classified into three categories, agarose gel electrophoresis-based methods, southern blot methods and the enzyme-linked immunosorbent assay. All three methods require multiple steps and increase the risk of false-positive results due to the nucleic acid contamination (10). However, the real-time RT-PCR has advantages, such as wide dynamic range of quantification, high technique sensitivity, high precision, no post PCR step, and a high throughput, so it was used as the exclusive detection method since its invention by Mullis in 1983. Several studies have indicated that HMPV has been circulating in humans for at least 50 years. But until now there are only few reports about it in our country. The major obstacle was the difficulty in establishing a rapid and valid laboratory diagnosis technology, without which it was impossible for us to prevent and control this virus.

Nucleic acid amplification-based protocols for the detection of HMPV have been published based on the nucleoprotein, fusion protein and polymerase genes (11–14). In accordance with the sequence comparison, we selected the conservative F gene fragments of HMPV, designed the TaqMan probe and primers to establish a real-time RT-PCR assay for HMPV detection in clinical respiratory specimens. The result suggested that the assay was specific, it can amplify the HMPV F gene fragments, but not the gene fragments of other respiratory viruses. As for reproducibility, CV <5% suggests a good reproducibility; The

limit of detection of the assay is 4.95 copies/reaction and the span ranging is 4.0×10^0 – 4.0×10^6 copies/reaction, which is equivalent or much better than the other reports (12).

Among the 78 clinical nasopharyngeal swab specimens, 7 specimens were identified as HMPV positive by real-time RT-PCR, but 5 were positive by conventional RT-PCR. We can deduce that the sensitivity of the two methods is similar, because the number of clinical specimens is not large enough to evaluate statistical significance. Moreover, the final conclusion needs to be further investigated. In summary, we have established a sensitive, rapid and valid TaqMan-based real-time RT-PCR assay, which has many advantages in comparison with the conventional RT-PCR and we have an initial proof that it may have a better prospect in the clinical application.

Acknowledgements. This work was supported by the China Mega-Project for Infectious Disease (2008ZX10004-001, 2009ZX10004-101).

References

1. van den Hoogen BG, de Jong JC, Groen J, Kuiken T, de Groot R, Fouchier RA, Osterhaus AD, Nat. Med. 7, 719–724, 2001. doi.org/10.1038/89098
2. Biacchesi S, Skiadopoulos MH, Boivin G, Hanson G, Hanson CT, Murphy BR, Collin PL, Buchholz UJ, Virology 315, 1–9, 2003. [doi.org/10.1016/S0042-6822\(03\)00528-2](https://doi.org/10.1016/S0042-6822(03)00528-2)
3. Hamelin ME, Abed Y, Boivin G, Clin. Infect. Dis. 38, 983–990, 2004. doi.org/10.1086/382536
4. Galiano M, Videla C, Puch SS, Martinez A, Echavarria M, Carballal G, J. Med. Virol. 72, 299–303, 2004. doi.org/10.1002/jmv.10536
5. Wolf DG, Zakay-Rones Z, Fadeela A, Greenberg D, Dagan R, J. Infect. Dis. 188, 1865–1867, 2003. doi.org/10.1086/380100
6. Madhi SA, Ludewick H, Abed Y, Klugman KP, Boivin G, Clin. Infect. Dis. 37, 1705–1710, 2003. doi.org/10.1086/379771
7. Druce J, Tran T, Kelly H, Kaye M, Chibo D, Kostecki R, Amiri A, Catton M, Birch C, J. Med. Virol. 75, 122–129, 2005. doi.org/10.1002/jmv.20246
8. Zhu RN, Qian Y, Deng J, Wang F, Hu AZ, Lu J, Cao L, Yuan Y, Cheng HZ, Chin. J. Pediatr. 41, 441–444, 2003.
9. Heid CA, Stevens J, Livak KJ, Williams PM, Genome Res. 6, 986–994, 1996. doi.org/10.1101/gr.6.10.986
10. Mikael Kubista, Jose Manuel Andrade, Martin Bengtsson, Amin Forootan, Jiri Jonak, Kristina Lind, Radek Sindelka, Robert Sjöback, Björn Sjögren, Linda Strombom, Anders Stahlberg, Neven Zoric, Mol. Aspects Med. 27, 95–125, 2006. doi.org/10.1016/j.mam.2005.12.007
11. Kuypers J, Wright N, Corey L, Morrow R, J. Clin. Virol. 33, 299–305, 2005. doi.org/10.1016/j.jcv.2004.11.023
12. Chan PC, Wang CY, Wu PS, Chang PY, Yang TT, Chiang YP, Kao CL, Chang LY, Lu CY, Lee PI, Chen JM, Shao PL, Huang FY, Lee CY, Huang LM, J. Formos. Med. Assoc. 106, 16–24, 2007. [doi.org/10.1016/S0929-6646\(09\)60211-4](https://doi.org/10.1016/S0929-6646(09)60211-4)
13. Pabbaraju K, Wong S, McMillan T, Lee BE, Fox JD, J. Clin. Virol. 40, 186–192, 2007. doi.org/10.1016/j.jcv.2007.08.004
14. Xing JM, Weng XJ, Zhang S, Yuan XH, Shen CF, Zhang YQ, Cheng HL, Li G, Yao LH, Chinese J. Exp. Clin. Virol. 22, 510–512, 2008.